PNL--8169

DE93 005120

SLURRY GROWTH, GAS RETENTION, AND FLAMMABLE GAS GENERATION BY HANFORD RADIOACTIVE WASTE TANKS: SYNTHETIC WASTE STUDIES, FY 1991

S. A. Bryan
L. R. Pederson
J. L. Ryan
R. D. Scheele
J. M. Tingey

August 1992

Prepared for
the U.S. Department of Energy
under Contract DE-AC06-76RLO 1830

Pacific Northwest Laboratory
Richland, Washington 99352

SUMMARY AND CONCLUSIONS

This report summarizes the results of studies conducted in FY 1991 to help establish the causes of generation, retention, and episodic release of flammable gases from Tank 241-SY-101 (Tank 101-SY). Tank 101-SY is one of the 23 waste tanks on the watch list for flammable gas generation, and its cycle has exhibited the largest growth/collapse of waste volume.

This report critically reviews available waste composition data for double-shell and single-shell waste tanks on the watch list. Physical and chemical properties of layers formed in laboratory tests using synthetic Tank 101-SY wastes are summarized, as are the results of gas generation measurements using these synthetic wastes. Microscopic-scale phenomena responsible for the retention of gases within the wastes are also discussed.

Information on the composition of wastes on the flammable gas generation watch list was reviewed. It is clear from the data that composition varies from tank to tank and that composition within each tank also varies. Despite uncertainties and inconsistencies identified in some of the data, the major component concentrations of wastes in double-shell tanks are quite similar. Double-shell waste slurries consist of 1.8 to 4.0 molar sodium nitrate, 1.3 to 3.0 molar sodium nitrite, 1.9 to 5.6 molar sodium hydroxide, 0.9 to 2.7 molar sodium aluminate, and 0.15 to 0.65 molar sodium carbonate. Variations in compositions of the solution phase are small because of saturation with respect to certain major components.

Crust growth studies were performed on a laboratory scale using synthetic waste compositions based on actual Tank 101-SY analyses. Five different waste compositions were used in these experiments. A reference composition most closely matching that of the inorganic components of the actual waste was chosen as a control, and contained HEDTA and EDTA as the organic components. Four variant compositions were prepared by changing sodium aluminate and organic concentrations by 50% above and 50% below the reference composition. The synthetic wastes were aged at 60°C for 6 weeks, and the resulting solid and liquid products were characterized. Chemical analyses included ion chromatography for anion detection, inductively coupled

plasma for element detection, total inorganic carbon detection, and total organic carbon detection. Physical characterization included weight and volume percent of solids versus time, density, shear strength, viscosity, crust penetration resistance, x-ray diffraction, differential scanning calorimetry, and scanning thermogravimetry.

Synthetic reaction mixtures held at 60°C separated into a floating crust, a relatively clear aqueous supernate, and solids within a few days, depending on the waste composition. No sharp distinctions in the concentrations of major inorganic components were noted among the separated layers. Total organic carbon analyses were highest for the supernate, but substantial quantities were found in the floating crust and solids. The total solids volume was clearly affected by the concentration ratio of organics to sodium aluminate: high organic to sodium aluminate ratios favored high solids volumes.

A series of experiments was performed on synthetic waste samples to determine the thermal sensitivity of selected oxidant and complexant mixtures and the potential thermal releases from potential reactions. Differential scanning calorimetry and a modified Henkin test were used to evaluate these sensitivities. Exothermic reactions were not observed below 200°C during a period of at least 30 minutes. At no time was an explosive reaction observed in the small-scale explosion test. Nonviolent, charring reactions were occasionally observed when waste mixtures were heated to 380°C. Thus, solids formed in synthetic 101-SY wastes are thermally quite stable and are unlikely to combust under any foreseeable circumstances.

The stoichiometry and rate of gas generation from the five synthetic waste compositions were assessed at 90°C (in the absence of radiation). Principal gases produced, in order of decreasing abundance, were nitrogen, nitrous oxide, and hydrogen. Nitrous oxide yields were typically 5 to 10 times higher than yields of hydrogen. Using an activation energy of 25 kcal/mole (Delegard 1980) to adjust gas production rates measured at 90°C to the approximate tank temperature of 60°C, and tank volume, we estimate that 20 moles per day of hydrogen and 100 moles per day of nitrous oxide are produced by the reference synthetic waste. Hydrogen production from the reference synthetic waste is

roughly one-third of that estimated to be produced by Tank 101-SY, while nitrous oxide production is twice that estimated to be produced by Tank 101-SY waste. Reasons for these differences are not well understood at this time, but are probably influenced by the choice of organic constituents used in synthetic waste formulations.

The formation of a floating crust composed of solids whose densities exceed that of the liquid phase has been shown to be the result of interfacial tension forces. When solid surfaces are incompletely wetted at equilibrium, the surface energy of the system can be minimized if the solid particle positions itself at the gas/liquid interface. The result is that solid particles will capture gas bubbles and, if sufficiently buoyant, will rise to the surface of the waste. Organic components were shown to significantly decrease the wettability of the solid particulates in synthetic waste slurries. When such slurries were sparged with nitrogen and other gases, those containing organic constituents formed a floating crust that was stable indefinitely, whereas those without organics did not form a crust.

The studies at PNL have shown that synthetic wastes representative of and similar to the waste present in Tank 101-SY behave similarly to the 101-SY waste, although some differences exist. The synthetic wastes formed three distinct layers--a floating crust, an aqueous phase, and a layer of bottom solids. These synthetic wastes thermally produced nitrogen, nitrous oxide, and hydrogen, although the ratio of the latter two gases differed from that produced by the actual 101-SY waste. The similarity in behavior between real and synthetic wastes lend credence to the fact that the synthetic studies are suitable models for helping to identify the mechanism whereby periodic releases of flammable gas mixtures occur.

ACKNOWLEDGMENTS

We would like to thank S. R. Adami, G. M. Richardson, and R. L. Sell for their work in performing many of the experiments reported here. We are also grateful to G. J. Lumetta for peer reviewing this report.

CONTENTS

FIGURES

1.0 INTRODUCTION

Of 177 high-level waste storage tanks on the Hanford Site, 23 have been placed on a safety watch list because they are suspected of producing flammable gases in flammable or explosive concentrate. One tank in particular, Tank 241-SY-101 (Tank 101-SY), has exhibited slow increases in waste volume followed by a rapid decrease accompanied by venting of large quantities of gases. Such cycles have occurred every 8-15 weeks beginning in the early 1980s and continuing to the present time. The concentration of hydrogen in the space above the waste slurry has approached its lower flammability limit during some of the gas release episodes. Other tanks have also been observed to periodically vent flammable gases, but to a lesser degree (Tank 241-SY-103 and 241-AN-104, in particular).

The purpose of this study is to help determine the processes by which flammable gases are produced, retained, and eventually released from Tank 101-SY. This report documents progress made during FY 1991 to these ends. Waste composition data for single- and double-shell waste tanks on the flammable gas watch list are critically reviewed. The results of laboratory studies using synthetic double-shell wastes are summarized, including physical and chemical properties of crusts that are formed, the stoichiometry and rate of gas generation, and mechanisms responsible for formation of a floating crust. It is hoped that this information will be useful in developing strategies to mitigate safety hazards associated with the operation of this tank and other tanks having similar behavior.

This report is organized as follows: Section 2 critically reviews the available data on waste composition for tanks on the flammable gas generation watch list. Section 3 describes selection of the compositions of the synthetic waste formulations. Section 4 describes preliminary safety studies. Section 5 describes experimental design and methods used and the results of chemical, physical, and thermal characterization of synthetic wastes aged at the temperature of Tank 101-SY. Section 6 gives the results of gas generation studies, and relates these results to those estimated to occur in the actual tank. Section 7 discusses mechanisms for forming a floating crust that is

composed of solids whose density exceeds that of the liquid phase on which it floats. A report on possible gas generation by microbial action is included as Appendix A. Appendix B provides all the tables cited in this report, and Appendices C, D, and E provide raw data for differential scanning calorimetry and scanning thermogravimetric analyses, shear stress versus shear rate analyses, and x-ray diffraction analyses, respectively.

2.0 REVIEW OF WASTE COMPOSITIONS IN TANKS ON THE HYDROGEN AND FLAMMABLE GAS GENERATION WATCH LIST

The purpose of this section is to bring together and review available information on the composition of wastes in those waste tanks on the watch list for hydrogen or other flammable gas generation. The information reported here is based on data obtainable from a variety of sources such as letters, letter reports, analytical laboratory reports, etc. It is clear from these data, especially for cases of multiple samples from the same tank, that there is variability in composition within each tank and that the values presented here cannot exactly represent the true average composition of the tanks in question.

There are currently 23 tanks on the watch list for producing potentially flammable concentrations of hydrogen or for flammable gas generation. These are listed in Table B.1 (all tables are in Appendix B) (Hanlon 1990a and 1990b). Measurable flammable gas (normally H_2) generation or measured slurry growth are apparently criteria for such listing, although at least one single-shell tank is listed because other tanks on the list vent through it. Of these 23 tanks, 18 are single-shell tanks.

Apparently all of the single-shell tanks are on the watch list for at best marginal reasons and none have apparently been shown to be clearly hydrogen or other flammable gas generators to anywhere near the extent of double-shell Tank 101-SY. As an example, single-shell Tank 110-T is on the watch list because of slurry growth. This growth amounts to a clearly seasonal fluctuation in tank level (high in late summer, low in late winter) of about 1 inch. This seasonal change has occurred very consistently over at least a 7-year period and, over those 7 years, the average level has increased by about 1 inch (data shown to the author by D. A. Reynolds, WHC). This can be contrasted to an approximately 8-inch slurry growth in double-shell Tank 101-SY occurring with an approximately 3-4 month frequency, with each growth cycle usually followed by a rapid collapse and definite release of gases enriched in H_2. In some of these releases in Tank 101-SY, the hydrogen content of the tank gas space has exceeded 4% for several minutes during the slurry growth

collapse. This value is less than the lower flammability limit for hydrogen in air but greater than the lower flammability limit of hydrogen in nitrous oxide. However, in the tank, air is believed to be the primary oxidant.

The single-shell tanks have passive ventilation and the vapor space in several of these tanks, when sampled, has been found to contain 0.1% H_2 as measured using a hydrogen detection instrument. Apparently this is the lowest possible instrument scale reading above zero. It is not even certain that such readings are real, but it is the reason for several of the single-shell tanks being on the watch list for H_2 generation (D. A. Reynolds, WHC, private communications with the author, November 1990).

For tanks containing very large fractions of solids, as most of these or the watch list do, and with additions of different wastes at different times, it should be clear that it is difficult to obtain samples that reflect the average tank contents. Two sampling methods have been used, a dip or bottle-on-a-pole method and core drilling. The bottle-on-a-pole method does not accurately reflect variability in composition of this material with depth, but it probably can, if properly used and if the sample is not too viscous, produce a fairly good sample for the composition at the sampling point. Core drilling gives a better continuous representation with depth and is capable of sampling very semi-solid to solid material and thus, in theory, gives a better picture of the total tank contents. If care is not taken in core drilling, however, the solids/liquid ratio in the sample can be altered from that in the tank. In practice, a normal paraffin hydrocarbon drilling fluid (hydrostatic pressure compensating fluid) has normally been used, and this renders total organic carbon (TOC) analyses on such samples extremely suspect.

Unlike double-shell tanks, analytical data, except for total organic carbon (TOC) content of any of the single-shell tanks on the watch list, were not found. Internal memos containing references to such data were located, however. As a result, this section emphasizes principally the double-shell tanks for which slurry growth and flammable gas generation are much more firmly established and for which analytical data are much more available.

2.1 MEASURED TANK COMPOSITIONS

This section presents composition data for the double-shell tanks 101-SY, 103-AN, 103-SY, 104-AN, and 105-AN and the TOC analyses available for the single-shell tanks. The presented compositions represent the authors' assessment of the available data and analyses.

2.1.1 Tank 101-SY

This double-shell tank is the most notorious of the tanks on the watch list for hydrogen or flammable gas generation. It is well-established that slurry growth occurs in this tank with a surface level increase of typically 8 to 9 inches occurring over a 3 to 4-month time frame. This slow growth of slurry is usually followed by a rapid collapse (Hanlon 1990b). Significant hydrogen and nitrous oxide release, in some cases approaching the lower flammable limit for hydrogen in air, has been measured in the tank head space during these rapid collapses of slurry.

The contents of Tank 101-SY consist of five separate additions made over an approximately 3-1/2-year period starting in April 1977. Table B.2 shows the nature, amounts, and times of these five additions (Simpson 1984). Table B.2 also shows that the total additions should have resulted in a total tank waste depth of 386.85 inches assuming the volumes to be additive, whereas the maximum level up to August 1984 had been 414.5 inches in March 1981. This was attributed to a 27.65-inch (7.1%) slurry growth.

The total initial composition of Tank 101-SY was estimated by Simpson (1984) based on the best available information for various feeds making up the five major additions to this tank. This process is more complex than it might appear. For example, the complexant concentrate generated from the evaporator run on contents of 102-SY (Table B.2) reflects wastes from 102-U, 105-U and 111-U, which had been combined in 102-SY. Simpson noted that optimum tank analyses were unavailable for most of the transfers and almost all of the tank compositions had to be based on one sample-one-analysis data. He assumed that the one sample of evaporator feed or effluent, or in some cases a reasonable estimate when no analysis was available, was representative of the total waste

transferred at the time. This estimated total tank composition is shown in Table B.3 and has recently been cited as the composition of Tank 101-SY by Hanlon (1990b).

Three samples of the contents of Tank 101-SY were obtained on January 6, 1986 (endnote 1)[(a)] by the dip or bottle-on-a-pole method and analyzed in early 1986 (Mauss 1986). These samples were designated as top, middle, and bottom samples. The estimated distances from the tank bottom that each sample was taken are bottom, 20 inches; middle, 175 inches; and top, 380 inches (endnote 1). These samples were taken 2 weeks after a maximum level of 411.2 inches tank depth followed by a gas release event. It is estimated that the top sample was taken 27 inches below the surface, and Reynolds presumed that this was below any crust.

The analyses of these samples are shown in Table B.4. The bottom and the middle samples are rather similar in composition for most constituents, with the greatest difference for major constituents being higher TOC (total organic carbon) for the bottom sample. The top sample is more dilute in all major constituents relative to the middle and bottom samples, with the apparent dilution ratio being about the same for all major inorganic constituents except Al. Aluminum appears to be even more dilute in the top sample relative to the other inorganic constituents. The ratio of TOC to inorganic constituents such as NO_3^-, NO_2^-, OH^-, and CO_3^{2-} seems to be lowest in the middle sample. Whether these ratio differences reflect real compositional differences or analytical/sampling errors is not certain. It should also be noted that the analyzed Na contents for all these samples exceed the sum of the equivalents of all the analyzed anions by an average of about 19% (assuming all Al is present as mononegative anions). Even if the unlikely assumption were made that each mole of organic carbon constituted one equivalent of anion (such as it would if all organic carbon was present as oxalate) there would still be an average 3.8% excess of Na, which is no doubt within expected analytical uncertainty.

(a) The endnotes given in this chapter and subsequent chapters cite internal memos and letters that generally do not appear elsewhere in published form. Hence, they are acknowledged here as endnotes.

In addition to the above data for Tank 101-SY waste, an earlier tank sampling and analysis was done in about June 1980 before all the waste additions to this tank had been made (endnote 2). At this time three samples, apparently at the 3-, 6-, and 9-ft depth, were taken. The data presented by Jansky in (endnote 2) are by no means clear. Thus, the 9-ft sample is reported to be 100% solids, and in the table showing analytical results for this sample, it is indicated that the analyses are for a 3.0-g to 25-ml dilution. Molarities and a specific gravity of 1.033 are reasonable for such a dilution but a value of 38.59% H_2O given in the same table is totally inconsistent with such a dilution. Without the density of the solid sample, a concentration per unit volume cannot be determined from these data. It is noted in this letter that the 6-ft sample was analyzed directly and yet NO_3^- is only 0.66 M, NO_2^- is 0.61 M, OH^- is 0.44 M, and Al is only 0.17 M. This should be well under saturation in several components. The 3-ft depth sample was presumably diluted 1:1 and analytical results are given as NO_3^-, 2.18 M; NO_2^-, 1.61 M; OH^-, 3.02 M and; Al, 1.75 M. Doubling these numbers to account for dilution gives very high values for the concentrations of these components, and it is not clear how a high concentration solid or largely solid material could exist as a thick layer on top of a lower density undersaturated layer. These values may possibly be the result of nonequilibrium conditions in the recently filled tank and probably are of little if any value to understanding the current composition of Tank 101-SY. It can be concluded that either the calculated composition data of Table B.3 or the analytical results of Table B.4 better represent the true tank composition than other values.

2.1.2 Tank 103-SY

Tank 103-SY showed up to almost 5-inch surface level fluctuations during 1987 and has shown level increases followed by sudden drops of about 1.5 to 3 inches during 1990 (endnote 3). The contents of double-shell Tank 103-SY apparently resulted from the addition in October 1980 of 132.5 inches of double-shell slurry to 45.8 inches of heel in the tank (Simpson 1984). This double-shell slurry waste was the same material as the 84-inch double-shell slurry addition to Tank 101-SY on October 29, 1980 (see Table B.2). No description of the heel was given by Simpson other than to list in his letter

the total number of moles of major components in this heel (Simpson 1984). Peters (endnote 4) defines this heel as transuranic-bearing complexant concentrate, and Fow et al. (endnote 5) state that the tank contains double-shell slurry, complexant concentrate, and uranium sludge from ion exchange processes.

The total initial Tank 103-SY composition calculated by Simpson (1984) is shown in Table B.5. It is based on the same methods and uncertainties as those for the Tank 101-SY data calculated in the same manner and discussed in the preceding section (Table B.3). The total depth of Tank 103-SY based on the heel depth and the double-shell slurry addition is 178.3 inches, and Simpson (1984) indicates an average depth of 190 inches (Table B.5).

Fow et al. (endnote 5), in describing core samples taken by Rockwell personnel, indicate that segment #2 comprises 109-209 inches from the tank bottom, and they indicate a tank fill depth of 213 inches. Apparently "33 inches" of "uranium sludge from ion exchange processes" cited by Fow et al. was added between the time of the Simpson letter (1984) and the time of the Fow et al. work and accounts for the additional depth in this tank. Prignano (endnote 6) also states that "uranium sludge from ion exchange processing was later placed on top of the DSS." Peters (endnote 4), in discussing some of the core samples taken in the same sampling as those in the Fow et al. work, apparently did not recognize that this uranium sludge addition had occurred. The result of this sludge addition is that the data of Simpson (1984) do not accurately reflect the current contents of Tank 103-SY. Hanlon (1990b) indicates that this tank is filled to a level of 274.1 inches. This indicates that additional waste has been added since the last known tank sampling and analysis (endnote 5). Liquid level data (endnote 7) indicate such an addition in July and August 1988. Six more small additions were apparently made to this tank in late 1988, 1989, and early 1990 (endnote 8).

Results of analyses of three core samples from Tank 103-SY by Fow et al. (endnote 5) are shown in Table B.6. Table B.6 shows that the concentrations of major constituents varies very little between the top and middle of the tank except for the case of carbonate, which appears to be higher in the middle than at the top of the tank. This, along with similar densities for

the top and middle samples, would point toward the upper half of the tank possibly being reasonably well mixed. The differences between the carbonate (and also sulfate) values for the top (#2) and middle (#7) samples, if real, could result from a different amount of solids in the two samples since certain carbonates and sulfates may be precipitated. Indeed sample #7 (middle of tank) was reported by Fow et al. to be similar in appearance to sample #2 but to contain bigger particles and to be less fluid. This probably indicates a higher total solids content as would be expected anyway.

The bottom sample (#12) was reported to contain "very little liquid" and to have the consistency of "chunky peanut butter and sand" (endnote 5). This is in agreement with the high concentrations of the major constituents shown in Table B.6. Based on the (somewhat uncertain) density of this sample and the values in Table B.6, it is easy to show that the sample contains no more than about 20% and possibly only 10% water by weight. Several constituents such as $NaNO_3$ and $NaAlO_2$ are no doubt present as major solid constituents. The significantly different ratio of NO_3^- to NO_2^- in this sample relative to the middle and top of the tank is not explainable by differences in solubility alone since $NaNO_3$ and $NaNO_2$ do not differ greatly in solubility.

The total sodium content of the bottom sample (#12), as well as the other two samples, exceeds the equivalents of anions measured. In the bottom sample (#12) this excess is 6.1 M. If this is due to an analytical problem, it indicates a serious problem. If, on the other hand, the difference is attributed to organic anions (TOC was not determined), it represents 3.05 M oxalic acid if all TOC is present as such. Oxalate is a likely end product of degradation of the complexants because of its relative stability to oxidation, and it represents about the maximum anion equivalents per carbon possible. If the bottom sample had contained 3.05 M oxalate, the total mass of constituents shown in Table B.6 for sample #12 would be 1860 g/L. This does not include water, which unfortunately was apparently not determined, so it is not possible to determine whether its inclusion would produce a reasonable sample density. Prignano's (endnote 6) value for TOC in adjacent core segments (to be discussed below) is far too low to account for this anion/cation discrepancy.

Peters (endnote 4) presented limited analytical data for segments 3, 6, and 11 (each segment 19 inches) from the same core sampling for which Fow et al. presented data for segments 2, 7, and 12. Unfortunately these apparently are not total sample analyses but rather are analyses of the aqueous phases removed from the samples or from 1:1 or 2:1 dilutions of the samples with water. The fact that NO_3^- values for the supernate for all three samples are only 1.43 to 1.85 M in comparison to values of 2.43 to 7.1 in Table B.6 would indicate that this value (~1.4 to 1.9 M) is a solubility limit. The higher supernate NO_3^- value for the 2:1 dilution versus the undiluted aliquot of segment 11 would also indicate the presence of a large amount of solid $NaNO_3$. Peters' values for undiluted samples (ranging from 1.43 to 1.85 M and including 1.65 for segment 11) are lower, however, than values reported by Barney as solubility limits for solutions at these NaOH concentrations and saturated with $NaNO_3$, $NaNO_2$, $NaAlO_2$, and Na_2CO_3. The very low values of NO_2^- (<0.04 M) (endnote 4) make the analysis for this anion very suspect. The high bulk densities for the samples (up to 2.93 g/mL) are also very suspect since they are greater than any of the true densities of the pure, major component solid salts expected to crystallize from such solutions.

Prignano (endnote 6), in discussing the preparation of a composite 103-SY sample by blending aliquots of core samples from this same tank sampling, stated "Segments 1 and 4 were found to be empty and 3, 5, and 6 were liquid and not used in preparing the composites." The absence of any solids was not noted by Peters (endnote 4), nor are his densities at all reasonable for an aqueous solution. It will of course explain why Peters' 1:1 dilution of segments 3 and 6 show only about half as much NO_3^- as the undiluted sample, whereas a 2:1 dilution of segment 11 shows slightly more NO_3^- than the undiluted sample. If Peters' values do actually represent $NaNO_3$ saturated solution, it could also account for his values being significantly lower than those of Fow et al. (endnote 5).

Prignano (endnote 6) rejected segments 3, 5, and 6 in preparing a composite sample of Tank 103-SY waste for analyses. Since segments 2, 7, and 12 had been sent to PNL, she used segments 8, 9, 10, and 11, representing waste 19 to 95 inches from the tank bottom, to prepare this composite. Whether Tank

103-SY actually contains a zone with virtually no solids or whether this was a sampling artifact is not known. Limited analytical data for this composite slurry and for the supernate liquid in it are available (endnote 6). The Al value for this composite was about one-half the values shown for segment 7 in Table B.6, while the value for Na was about 68% of that for NO_3^-. The value for SO_4^{2-} was almost identical to that for segment 7 (Table B.6), and other major constituents were not determined. The higher NO_3^- in the composite is not surprising because in dissolution in strong acid as performed by Prignano, one-third of a mole of nitrate is produced per mole of NO_2^- decomposed. It appears that the lower Al and Na values represent real and large analytical differences.

Other more minor constituents reported by Prignano for this composite differ markedly from values reported by Fow et al. for either segment 9 immediately above or segment 12 immediately below the composite region. Thus, Prignano's values for Cr and Fe are much lower than those reported for segments 7 and 12 (Table B.6), and her value for PO_4^{3-} is significantly higher.

It is difficult to conclude why these differences occur, but it should be emphasized that Prignano states that this slurry composite was contacted with HCl (presumably to prepare a solution for its analysis) and that a large amount of solids (~50% by volume after centrifugation) did not dissolve. If this HCl was 12 M (as was the HNO_3 mixed with 0.1 M HF used on later samples), and particularly if such small volumes were used as indicated by the comment on centrifuged volume of solid, the Na salts would not even be dissolved since NaCl and $AlCl_3 \cdot xH_2O$ both have low solubility in strong HCl solution. If this interpretation is correct, it would explain why the Na, Al, Fe, and Cr values are so low relative to segments 2 and 12 from Table B.6, and would indicate that the Table B.6 data are more reliable.

Prignano (endnote 6) reports a value of 0.692% TOC (or about 0.9 M) for the composite slurry. Since normal paraffin hydrocarbon is apparently commonly used as a drilling fluid in core sampling, this should be considered an upper limit.

Prignano (endnote 6) also gives analyses for the interstitial liquid (separated by centrifugation) present in the core composite, and these are

shown in Table B.7. The value for NO_3^- is significantly higher than those of Peters (endnote 4), who, as noted earlier, analyzed core segments 3 and 6, which, according to Prignano (endnote 6), contained only liquid and agrees much more closely with that expected from solubility data (Barney 1976). Prignano's data, given in Table B.7, show a very good match between total Na and total equivalents of anions not including organic carbon anions.

2.1.3 Tank 103-AN

Tank 103-AN showed a gradual surface level increase from January 1987 to mid-1989 of about 10 inches where it essentially leveled off (endnotes 7 and 8). Shorter term level fluctuations have not exceeded 2 inches. According to Fow (endnote 9) Tank 103-AN was filled to 320 inches with double-shell slurry feed (DSSF) during the third evaporator campaign in 1984. This DSSF came from various tank farms:

> "During 1984 and 1985 the tank was used as a dilute receiver of approximately 86.5 inches of miscellaneous PUREX waste. In the second evaporator campaign of 1985, the slurry level in DST 103-AN was pumped from 406.5 inches down to 93.6 inches. This slurry along with 102-AW feed was concentrated in the evaporator and sent back to DST 103-AN. The tank depth at the end of this campaign was 337.6 inches. In the most recent campaign, 88 inches of waste from 103-AN and waste from 104-AW and 102-AW were pumped through the evaporator and back to 103-AN. The depth of waste in DST 103-AN at the end of the campaign was 329 inches. Core samples (core segments 2 through 18) were retrieved from DST 103-AN in January 1987."

Hanlon (1990b) indicates a tank depth at present of 345.09 inches. This increase in depth over the 329 inches is subsequent to the performance of all the analytical work reported below. Mauss (endnote 10) indicates the DSSF was removed in the second campaign (February 1986 rather than 1985).

Mauss (endnote 10) indicates that a sludge sample was taken from this (93.6 inches) heel before material was returned from the evaporator. The sample was "pea-green," with 5% supernatant, 85% settled solids, and 10% foam. It was separated by filtration and the liquid phase and filtered solids were analyzed separately. The sample was 58% filtered solids, by either volume or

mass since the densities of the two phases were almost identical (1.47-1.48 g/mL). The solids had a 39.0 wt% water content versus 48.8 wt% in the liquid. Solids were 49 wt% Na_2CO_3, 31 wt% $NaNO_3$, and 11 wt% $NaNO_2$.

Tank 103-AN was core sampled, apparently in the earlier half of 1987. A composite sample was prepared and sent (endnote 11) to PNL in May 1987 for comprehensive analysis. (It is assumed here that this is a composite of all core segments rather than a composite of only the lower 8 segments of an 18-segment core referred to by Prignano (endnote 12) in dissolution studies.) The analytical results for the core sample sent to PNL are shown in Table B.8. This tank appears to be somewhat lower in NO_3^- and CO_3^{2-} than Tanks 101-SY and 103-SY but somewhat higher in OH^-. Other major constituents (Al, NO_2^-, Na) are similar to those in Tanks 101-SY and 103-SY.

Toste (endnote 13) also reports the identification of and analyses for some of the specific organic compounds present in the waste. Of the 0.42 M total organic carbon, he found 21.9% of it to be oxalic acid, 3.2% to be succinic acid, 5.6% to be N-(Methylamine) iminodiacetic acid and no more than 1.4% of any other single organic compound identified. He identified 33.1% of the total organic carbon (all were organic acids). It should again be emphasized that the waste being analyzed here is a core sample and that a hydrocarbon (n-dodecane) was typically used as a drilling fluid; thus, the total organic carbon reported in Table B.8 must be considered an upper limit.

The analyses in Table B.8 show that total Na plus K exceeds total equivalents of anions by 3.2 M. Since total organic carbon is only 0.42 M, since drilling fluid may have contributed some to this, and since oxalic acid (at one mole acid per mole carbon) contributes only 22% of this, the discrepancy in anion-cation balance can hardly be attributed to any other source than analytical problems.

2.1.4 Tank 104-AN

Tank 104-AN has shown slow surface level increases of up to almost 8 inches followed by rapid decreases (endnote 14). The time period for these fluctuations has been much longer than those occurring in Tank 101-SY, being about 2 years in Tank 104-AN. Some hydrogen has also been detected in gas

leaving this tank. The only other data found for this tank were those tabulated in the Tank Farm Surveillance and Waste Status Reports (Hanlon 1990a and b). This tank is listed as containing 385.8 inches of waste. The principal component is DSSF, which is a more dilute solution than double-shell slurry and which is the principal component listed in the same source for Tank 103-AN discussed in the preceding section. It is not known if any other wastes have been added to this tank. No analytical data were found for this tank. The tank discussed in the following section (Tank 105-AN) is also listed as being composed of DSSF, but whereas Tank 104-AN has 25% by volume sludge, Tank 105-AN is listed as having no sludge solids volume.

2.1.5 Tank 105-AN

Tank 105-AN is on the watch list because of level changes over time and because of the correlation of these level changes to temperature fluctuations (endnote 15). This tank is also reported to have a crust, and it was estimated that it has a worse slurry growth problem than Tank 103-AN (endnote 15). Tank 105-AN is reported to contain DSSF as at least the principal waste type that has been placed in this tank (Hanlon 1990b). The waste depth is 410.6 inches and the solids volume is reported as zero. Sludge, double-shell slurry, and salt cake are the types of solids normally reported, if present, by Hanlon. These two references, thus, raise some question regarding the nature of the solids content of this tank.

No information about when the tank was filled was recovered in this survey. The tank was presumably sampled in 1984 since analyses were reported in November 1984 (endnote 16). No detail about the sampling procedure was found, but it is presumed that the sample was a dip sample, since this type of sampling would be logical for a low solids content tank. It is presumed that, if there was no significant solids layer and if the tank was filled an adequate time before sampling, the tank would have been fairly homogeneous. No information was obtained about the waste depth at the time of sampling or about the tank history after sampling to ascertain whether this sampling is representative of the current tank contents.

Results of analyses of Tank 105-AN samples are shown in Table B.9 (endnote 16). Comparison of these data with those for Tanks 101-SY, 103-SY, and

103-AN presented earlier (Tables B.4, B.6, and B.8) shows that this tank contains waste that is more dilute in the major constituents. Comparison of these values to the solubility data of Barney (1976) indicates that this waste is undersaturated in $NaNO_3$, $NaNO_2$, $NaAlO_2$, and NaOH. This is consistent with this waste being DSSF instead of double-shell slurry or complexant concentrate, which are the principal materials in the other three tanks. This would indicate that the only solids expected in these tanks would be the relatively minor constituents forming insoluble carbonates, phosphates, sulphates, etc.

The total organic carbon content for Tank 105-AN is 3.36 M, as shown in Table B.9. It should be noted that in reported analyses of other tanks, Mauss (endnote 16) has shown total organic carbon in a table column whose units were designated M but with a footnote on the total organic carbon value to indicate that it alone was being reported as g/L. Since 3.36 M total organic carbon seems a high value for this tank, and since in the same letter Mauss shows a value for Tank 104-AW (listed by Hanlon 1990b as dilute non-complexed waste at present) of 4.675 M total organic carbon, it is quite possible that such a footnote was inadvertently left off. If this interpretation is correct, the true value of total organic carbon for Tank 105-AN would be 0.28 M carbon.

The data in Table B.9 show a close correspondence between total anion equivalents (neglecting total organic carbon) and total cations (mostly Na). It seems that, in the tank waste analyses given in this document, samples having little or no solids have shown a much closer match between cation and anion charge balance than have samples containing large amounts of solids. Whether this is because of random chance or a more fundamental reason is not clear.

2.1.6 Single-Shell Tanks

As shown in Table B.1, there are 18 single-shell waste tanks on the watch list for hydrogen or flammable gas generation. As discussed above, there seems to be far less solid evidence for these tanks being significant hydrogen producers and retainers than are the double-shell tanks. For this reason, less effort has been put into locating analytical data for the single-shell tanks on the watch list, although analytical data for these tanks are currently being collected. References (all but two of which are from 1980 or

earlier) containing analytical data for nine of these tanks have recently been obtained and review is underway. Until these references can be reviewed, the thoroughness of the data, the methods of sampling, or the degree to which the data is representative of the total tank contents cannot even be speculated on.

Of the 18 single-shell tanks on the watch list, 10 are described as containing non-complexed waste, 6 are listed as containing DSSF, and the other 2 are listed as containing complexed waste (Hanlon 1990a and 1990b). The referenced analytical data described above represents all three waste types. Hanlon (1990a and 1990b) describes these tanks as being mostly solids with no more than 11.3 vol% (mostly 0 to 5%) supernatant liquids.

Klem (endnote 17) has recently collected available data on total organic carbon analyses for single-shell tanks. This includes nine of the tanks on the hydrogen and flammable gas generation watch list. The total organic carbon values for these nine tanks are shown in Table B.10 along with the phase (liquid, solid, or both) that the sample represents and the type of waste (Hanlon 1990a and 1990b) present in that tank. How reliable these total organic carbon data are is not certain. It is apparent that the highest value in Table B.10 is for Tank 105-U at 3.71 M C (presumably non-complexed waste) and the lowest is for Tank 101-SX at 0.033 M C (presumably for complexed waste). It is known that at least some of these samples were taken by core sampling. These may be highly contaminated by the organic drilling fluid usually used during drilling operations.

---

1. Reynolds, D. A. 1990. "Additional Information on the 1986 Sample of 101-SY." Westinghouse Hanford Company Internal Memo No. 86434-90-089 to N. W. Kirch, September 17.

2. Jansky, M. T. 1980. "Tank 101-SY Samples." Rockwell International Internal Letter No. 65453-080-193 to D. E. Bowers, July 14.

3. Husa, E. I. 1990. "Surface Level Data Plots for Tanks 241-SY-103 and 241-AN-103." Don't Say It Write It to Distribution, August 22.

4. Peters, B. B. 1988. "Dissolution Study of Tank 103-SY Core Sample-Scoping Study Results." Westinghouse Hanford Company Internal Memo No. 12221-PCL 88-128 to C. E. Sowa, May 10.

5. Fow, C. L., R. D. Scheele, D. McCarthy, G. T. Thornton, W. O. Heath, and P. A. Scott. September 1986. "Characterization of Waste from Double-Shell Tank 103-SY." Pacific Northwest Laboratory letter report for Rockwell Hanford Operations.

6. Prignano, A. L. 1988. "Tank 103-SY Dissolution Study-Results of Chemical Analyses." Westinghouse Hanford Company Internal Memo No. 12712-PCL88-037 to K. E. Schull, December 30.

7. Husa, E. I. 1990. "Surface Level Data Plots for Tanks 241-SY-103 and 241-AN-103." Don't Say It Write It to Distribution, August 22.

8. Husa, E. I. 1990. "Refined Surface Level Plots for SY-101, SY-103 and AN-103." Don't Say It Write It to H. R. Brager, August 29.

9. Fow, C. L. July 1987. "Characterization of Waste from Double-Shell Tank 103-AN." Pacific Northwest Laboratory letter report for Westinghouse Hanford Company.

10. Mauss, B. M. 1986. The 86-2 Evaporators Campaign: Laboratory Results on the Production of Double-Shell Slurry." Rockwell International Internal Letter No. 65453-86-038 to M. G. Kelly, March 28.

11. Richmond, W. G. 1987. "Analysis of Composite Samples from Tank 103-AN." Rockwell International Letter No. R87-2114 to A. P. Toste, May 14.

12. Prignano, A. L. 1988. "Dissolution Study of Composite from Tank 103-AN." Westinghouse Hanford Company Internal Memo to Distribution, January 13.

13. Toste, A. P. 1987. Pacific Northwest Laboratory Letter to W. G. Richmond, Westinghouse Hanford Company. September 25, 1987.

14. Harris, J. P. 1990. "Tank 104-AN Level Fluctuations Due to Slurry Growth." Westinghouse Hanford Company Internal Memo No. 82331-90-259 to D. G. Baide.

15. Harris, J. P. 1990. "Determination of Possibility of Slurry Growth in AW/AN Tank Farms." Westinghouse Hanford Company Internal Memo No. 82331-90-153 to K. G. Carothers.

16. Mauss, B. M. 1984. "Chemical Compositions of 102-AY, 101-AW, 105-AN, and 104-AW." Rockwell International Internal Letter No. 65453-84-348 to E. G. Grathy, November 9.

17. Klem, M. J. 1990. "Total Organic Carbon Concentration of Single-Shell Tank Waste." Westinghouse Hanford Company Internal memo No. 82316-90-032 to R. E. Raymond.

3.0 SELECTION OF SYNTHETIC WASTE COMPOSITION

The concentrations of inorganic materials in the reference formulation are based on a letter from Mauss (1986a) that summarizes analyses of the compositions of various layers in Tank 101-SY. We chose not to use the concentrations of EDTA and HEDTA from the Mauss report in our formulation because these values represent the amount of these materials present in 1986, after years of potential decomposition, and probably do not reflect the initial or current concentrations of these complexants nor the total organic carbon in the waste. Instead, we chose to use the concentrations of EDTA and HEDTA given by Delegard (1980), which are estimated to be the concentrations in the waste actually put into the tank. This would bound the maximum possible concentration of organics in the tank. The concentration values for these two organics, as outlined in Delegard's report, are based on total organic carbon analysis of the Tank 101-SY waste and on B Plant process flowsheets.

Four other variant formulations were chosen to determine the effects of different concentrations of AlO_2^- and the organics (i.e., EDTA and HEDTA). In two of the four variant compositions, the AlO_2^- and organic concentrations were both changed by a factor of 50% above and below the test formulation concentrations. In the remaining two variant formulations, the concentrations of AlO_2^- and organics were alternately changed to 50% higher and lower, respectively, and 50% lower and higher, respectively. The variant formulations were arbitrarily chosen to provide a great enough change in concentration from the reference to ensure observation of the effects of these changes and to allow use of statistical analytical methods.

Table B.11 presents the concentrations for the constituents for the reference and four variant formulations. The anions in this table were added as the sodium salts, and the transition metal ions were added as the nitrate salts.

For this study, noble metals were not included in the formulation because there is no information on their concentrations in the wastes. Several of these elements (e.g., Pd, Rh, Ru, Pt, Ir, etc.), which are produced as fission products at potentially catalytically significant levels, are known

to thermally catalyze reactions involving the decomposition of alcohols and organic acids. For this reason, these elements should be considered for inclusion in formulations for future crust and gas formation studies. In future synthetic waste studies, the actinide elements, which may also act as catalysts, should also be considered.

4.0 PRELIMINARY SAFETY STUDIES

Martin (1985) completed an in-depth review of explosive reaction potential for Hanford organic-containing wastes similar to those described in this report. The potential for organic-bearing wastes to react explosively was found to be remote. The maintenance of several conditions would reduce the likelihood of producing hazardous explosive conditions: 1) an aqueous environment, 2) an alkaline solution, and 3) controlled temperatures (below 300°C).

To evaluate the safety of working with organic complexant and nitrate/nitrite slurries at elevated temperatures, we performed a series of experiments to determine the thermal sensitivity of selected oxidant and complexant mixtures and the potential enthalpy releases from potential reactions.

4.1 EXPERIMENTAL EVALUATION

To ensure that testing of large batches of the synthetic waste formulations would not lead to an explosion, an experimental safety study was undertaken, and thermodynamic calculations were made. Small batches of mixtures containing organics, nitrate, and nitrite were produced and tested using differential scanning calorimetry (DSC) and a modified Henkin test analysis (Burger and Scheele 1991). The components and amounts used are listed in Table B.12. The purpose of the DSC and Henkin testing was to get a general idea of the thermal behavior and sensitivity of the test mixtures.

DSC measures enthalpy change as the temperature is increased at a constant controlled rate. The DSC provides information on the temperature at which a thermal event occurs, such as an observed minimum reaction temperature for an exothermic reaction. However, the observation of an event is dependent on sample size and the heating rate.

A modified Henkin test is a thermal shock test which consists of placing small amounts (~100 mg) of sample into a pre-heated sample holder and measuring the time until an audible report or visible flame is observed. The Henkin test measures the stability of reaction mixtures when they are exposed to elevated temperatures and thus caused to heat up very rapidly. Results from

Henkin tests are dependent on sample size and geometry. Henkin tests are commonly used to evaluate explosive materials to determine the effect of a severe thermal shock to the materials.

In order to bound the experimental conditions used in the full-scale tests, which were to consist of 1-L batches, the mixtures chosen for this safety-related preliminary study had higher and lower concentrations of organics than those used in the full-scale experiments. Six of the mixtures (identified as mixtures 1-6 in Table B.12) included only the organic fuel (HEDTA and EDTA) and oxidant (nitrate and nitrite) components of the synthetic waste formulation. Also included were mixtures containing the transition metal salts that are part of the reference synthetic waste formulation. These mixtures, identified as mixtures 7-12 in Table B.12, were tested because the transition metals may catalyze one or more of the reactions and perhaps lower the temperature at which an exothermic reaction occurs.

Each test mixture was mixed with water and then dried overnight in an oven at 70°C. The mixtures containing transition metals were dried at this temperature for 2 days. No reaction from the drying was observed in these samples.

Using the DSC, exothermic reactions were not observed below 200°C. Using the modified Henkin analysis, reactions were not observed at 200°C over a period of 30 minutes. In no Henkin experiment was an explosive reaction observed. At 380°C, the Henkin experiment yielded a charring reaction but not an explosive one. Occasionally at 380°C, mixtures with high HEDTA and EDTA concentrations would flame after the charring reaction. These same mixtures were stable for more than 4 hours at 200°C.

Because of the observed reactions at 380°C, we tested a mixture containing the high HEDTA and EDTA concentrations along with the other components found in the "high $NaAlO_2$/high organic" composition (sample #13, Table B.12). The DSC did not reveal an exothermic reaction below 200°C. The Henkin analysis did not show a reaction at 200°C, but a nonviolent charring reaction occurred at 380°C.

It is worth noting that the DSC and Henkin analyses were run on dried material. The large batches used in this work all contained water, which acted as a heat sink for energy released by any reaction.

4.2 THERMODYNAMIC CONSIDERATIONS

Based on balanced chemical reactions between HEDTA and EDTA with NO_2^- and NO_3^-(assuming N_2, CO_2, and H_2O as products), heats of reactions (ΔH_{rxn}) were calculated using appropriate standard thermodynamic tables. Heats of formation for HEDTA and EDTA were calculated from standard bond dissociation energies. The protonated forms of HEDTA and EDTA were used in the calculations rather than the sodium salts in order to permit calculation of the heats of formation from molecular species. Table B.13 provides the balanced chemical equations. The total heat that theoretically could be produced per liter of solution was calculated based on these equations and the concentrations of the expected ingredients (HEDTA, EDTA, NO_3^- and NO_2^-) in each of the test formulations given in Table B.11. The calculated heats are also included in Table B.13.

The calculations show that in the "worst case" mixtures (high organic), the total energy thermodynamically available is ~50% of the energy available in an equivalent mass of TNT, or alternatively for the air oxidation of an equivalent mass of sugar. Although the reaction of HEDTA and EDTA with nitrate and nitrites results in significant releases of energy, for the test mixtures used here a reaction is not expected without an initiating event (Martin 1985).

5.0 AGING STUDIES

5.1 EXPERIMENTAL METHODS

In order to simulate the chemistry of the aged radioactive waste within Tank 101-SY, it was necessary to heat treat the synthetic waste at tank temperatures (~60°C) for several weeks. Chemical and physical samples were taken periodically to assess the effect of aging on the synthetic waste. The total aging time for these solutions was 66 days. This doesn't compare with the resident time for the actual waste currently in Tank 101-SY, which was filled more than 10 years ago. We believe, however, that important information about the gas retention and crust growth phenomena can be obtained from such a short aging study because Tank 101-SY has manifested these characteristics since the initial waste addition in 1977 (Delegard 1980).

A typical preparation of synthetic waste was made by adding each ingredient from each respective formulation in Table B.11 in the order of its appearance in the table (except for $NaAlO_2$, which was always added last) to approximately 80% of the total H_2O required for the desired composition, while maintaining vigorous mechanical stirring. After all the solid ingredients were added, the amount of water was brought to the required level. Batches were stirred at room temperature for several days to ensure mixing prior to use.

Approximately 900 mL of each of the five formulations were placed into five separate 1-L polymethylpentene (PMP) containers. Each formulation was prepared in quadruplicate in the PMP containers. Samples were taken from two containers throughout the aging experiment for chemical analyses. Two containers were left intact until the end of the experiment so that uninterrupted phase volume and weight measurements could be taken. Each container was equipped with a lid with a gas escape tube filled with glass wool to reduce air mixing and water evaporation.

An additional amount of the reference formulation was also placed in two 500-mL graduated borosilicate cylinders. Graduated cylinder glassware was used for the reference formulation to assess the difference between synthetic waste aging behavior in various container geometries. PMP was chosen as the

standard because of its resistance to alkaline solutions and moderate heat. The use of borosilicate glass in one experiment resulted in a measurable dissolution of the glass, almost to the point of failure. Figure 1 shows the five synthetic waste formulations in PMP containers after approximately 6 weeks of aging.

All reaction vessels were placed in a heating oven maintained at 60°C for the duration of the experiment. Reaction vessels were taken out of the oven only for the time required for recording weight and phase volume measurements or for taking the chemical samples to be analyzed.

Extensive chemical, thermal, and physical characterizations were performed on the synthetic waste samples from the initial production, periodically throughout, and at the termination of the aging studies. This section details the methods used and results of the characterization of the synthetic waste samples.

5.2 CHEMICAL ANALYSES AND BEHAVIOR

The chemical characterizations performed on the synthetic waste samples include ion chromatography (IC) for anion detection, inductively coupled plasma (ICP) for element detection, total carbon, (TC), total inorganic carbon, (TIC), and total organic carbon (TOC).

High-performance liquid chromatography (HPLC) for EDTA and HEDTA analysis was initially scheduled for these samples, but unforeseen delays in acquiring the appropriate methodologies made it impossible to include results from that analysis in this report. Archive samples have been preserved for analysis at a later date.

Samples used for analyses of the five formulations were taken before heating (day 0), twice during heating (day 16 and day 41), and at the end of the heating period (day 66). The samples taken at day 0 were centrifuged to create a supernate and a solids layer. With the exception of the low aluminate-high organic formulation, three definite layers formed very quickly with each formulation. In each formulation, solids had formed a thin top layer; this layer was labeled "crust layer." The body of the reaction vessels

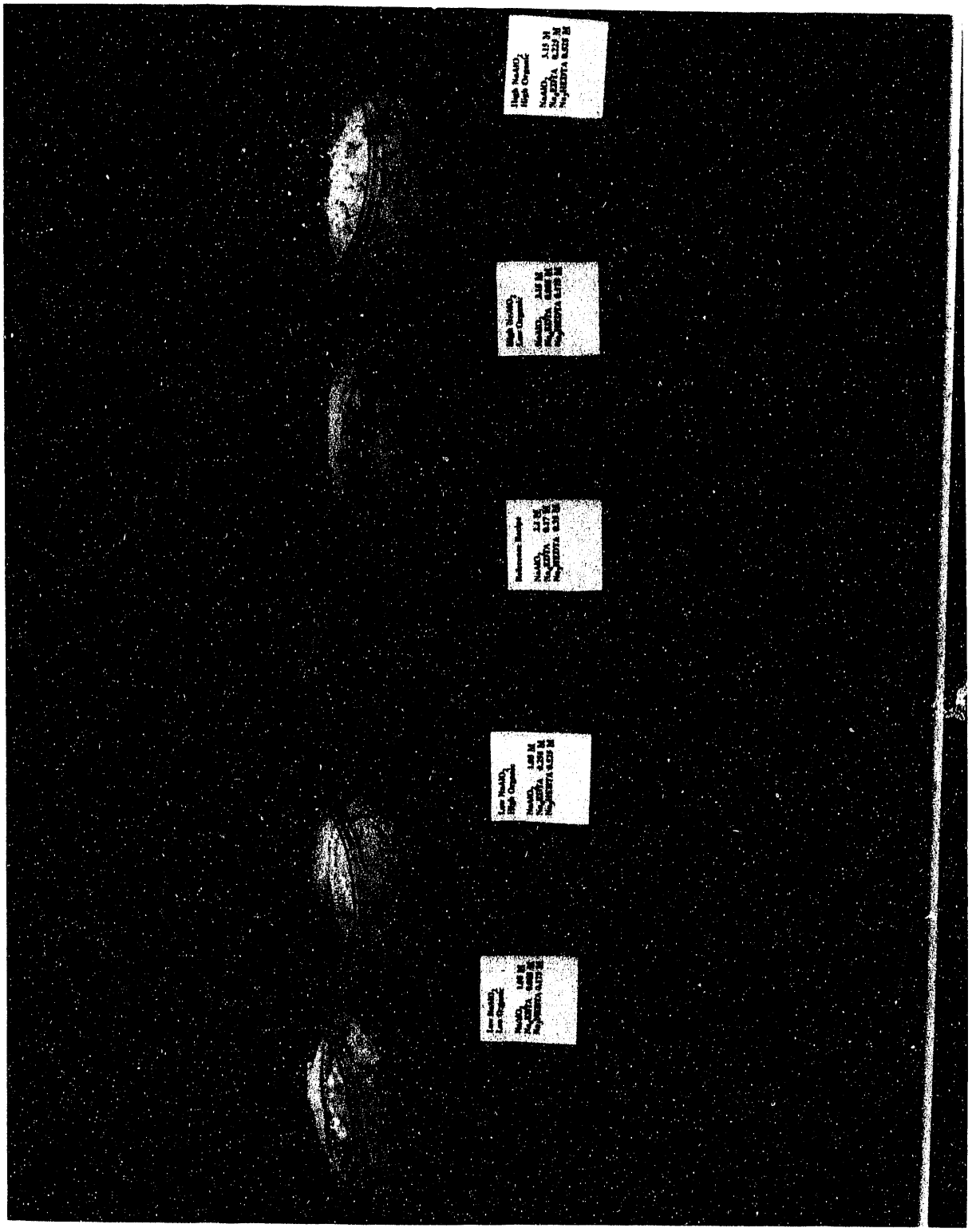

FIGURE 1. Various Formulations After ~6 Weeks of Aging at 60°C

contained a solids layer labeled "solids" and a liquid layer labeled "supernate." Samples used for analyses were taken from each well-defined layer of each aged formulation.

5.2.1 Ion Chromatography

The IC analyses were performed to determine specific analytes including fluoride, chloride, nitrite, nitrate, and phosphate. These were specifically requested because they are all present within the synthetic waste matrix. All samples were analyzed in duplicate and the reported values are the average determined concentration. The IC data are recorded in Tables B.14-B.18.

Table B.14 contains IC data for unheated samples from each formulation at day 0. A supernate and solid fraction of each formulation was generated by centrifuging the unheated sample. The supernate and solid samples were both analyzed, and results are included in these tables.

Tables B.15, B.16, and B.17 contain IC data for synthetic waste samples aged at 60°C for 16, 41, and 66 days, respectively. Samples were taken from the crust, supernate, and solids layers of the two reaction vessels for each formulation used for chemical sampling throughout the experiment. For the instances in which the solid phase present was layered into more than one facies, a combined solid sample was taken and homogenized before it was submitted for analysis. The results are listed in these tables as "crust," "supernate," or "solids," according to the phase from which it was taken.

Table B.18 contains IC data obtained from samples taken from the reference formulation on day 66. The source for these samples differed from other samples taken for chemical analyses. These samples were taken from the two reaction vessels reserved for physical testing and left undisturbed throughout the experiment. In the case of the solid phase, three distinct layers were observed. Each of these layers was sampled separately. They are labeled as Solid-1, Solid-2, and Solid-3, which coincide to the top, middle, and bottom layer, respectively, of the solid phase.

The IC results indicate that there does not appear to be a universal tendency for concentration, of the nitrate and nitrite ions in the crust.

There were two exceptions: on day 16 and day 41 (Tables B.15 and B.16, respectively), the low aluminate, low organic formulation showed an increase in the crust concentration of nitrate ion (approximately 30 wt%) compared to the average concentration for nitrate added to the synthetic waste, approximately 10 wt%. A similar increase in nitrate and nitrite was also observed for the high aluminate, high organic formulation on day 41 (Table B.16); there was an increase in the nitrate concentration in the crust above the average concentration in the synthetic waste.

The reference formulation samples, which were analyzed by each individual strata on day 66 of testing (Table B.18), did not show an increase of nitrate or nitrite in the crust. There does, however, appear to be a concentration of nitrate and nitrite in the Solid-3 layer of the reference formulation at day 66.

Figure 2 is a plot of the measured concentration of anions as a function of phase location and shows a large increase in nitrate and nitrite ion concentrations in the Solid-3 sample. These observations are consistent with the fact that the sodium nitrate and sodium nitrite were added in concentrations

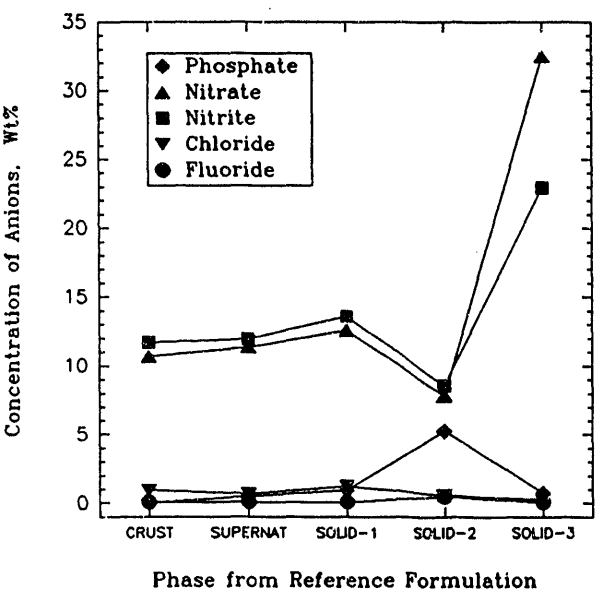

FIGURE 2. Concentration of Anions from Various Phases of the Reference Formulation (Day 66)

greater than their solubility limits (Reynolds and Herting 1984). The solid phase of these salts presumably has settled to the bottom of the reference formulation reaction vessel.

The phosphate ion concentration in the solids layer of the reference formulation is approximately twice the average concentration of the other formulations throughout the entire experiment (days 16, 41, and 66; Tables B.15 through B.18). In Figure 2, it can be seen that it is concentrated in the middle strata (Solid-2) of the bottom solids (Table B.18), where it is approximately a factor of five times more concentrated than it is in the strata above or below. It is interesting to point out that the transition metals which form insoluble phosphate salts are enriched in this Solids-2 facies of the reference formulation. The information on the metals concentration is provided within the discussion of the ICP data below.

5.2.2 Inductively Coupled Plasma (ICP)

Specific elements analyzed by ICP include Al, Cr, Cu, Fe, Na, Ni, and P. The TCP analysis was requested because these elements are present in the synthetic waste feed. All samples were analyzed in duplicate, and the reported values are the average determined concentration. The ICP data are recorded in Tables B.19-B.23.

Table B.19 contains ICP data for unheated samples from each formulation at day 0. A supernate and solid fraction of each formulation was generated by centrifuging the unheated sample. The supernate and solid samples were both analyzed and the data are included in these tables.

Tables B.20, B.21, and B.22 contain ICP data for synthetic waste samples aged at 60°C for 16, 41, and 66 days, respectively. Samples were taken from the crust, supernate, and solids layers of the two reaction vessels for each formulation set aside for chemical sampling throughout the experiment. For the instances in which the solid phase present was layered into more than one facies, a combined solid sample was taken and homogenized before it was submitted for analysis. The results are listed in these tables as "crust," "supernate," or "solids," according to the phases from which they were taken.

Table B.23 contains ICP data obtained from samples taken from the reference formulation on day 66. The samples were taken from the two reaction vessels reserved for physical testing and left undisturbed throughout the experiment. Chemical samples were taken after all other needs for physical testing were satisfied. In the case of the solid phase, three distinct layers were observed. Each of these layers was sampled separately. These layers are labeled as Solid-1, Solid-2, and Solid-3 as before to designate their relative vertical placement within the reaction container. It can be seen from Figure 3 that the concentration of sodium (Na) is the highest in the solid phases, and in particular, the Solid-3 phase. The high level of sodium in this phase corresponds to the high concentration of nitrate and nitrite observed by the IC analyses above and is due to the settled sodium nitrate and sodium nitrite salts.

The ICP analysis for phosphorus corresponds well with the IC analysis for phosphorus. The phosphate level in the reference formulation on day 66 (shown as phosphate in Figure 2 and phosphorous in Figure 3) indicate an increase in facies Solid-2. There is a concurrent increase in the transition metal concentration in the Solid-2 facies of the reference formulation on day 66 (Figure 4). It is expected that low solubilities of the transition metal phosphates are responsible for the coincidental concentration of the transition metals with phosphate.

All other elemental concentrations appear to be independent of the day of aging of the formulation, the layer analyzed, or the makeup of the formulation, except for aluminum. The aluminum concentrations in the solid phases present on each day of testing were dependent on the total amount of $NaAlO_2$ added to each formulation. Figure 5 summarizes the aluminum concentration in the bottom solids throughout the aging of the synthetic waste. In all cases, the higher the $NaAlO_2$ concentration in the formulation, the higher the analyzed concentration of aluminum in the solid phase, as shown in Figure 5.

This same relationship exists for aluminum in the crust. The aluminum concentration data listed for the crust in Tables 20, 21, and 22 are

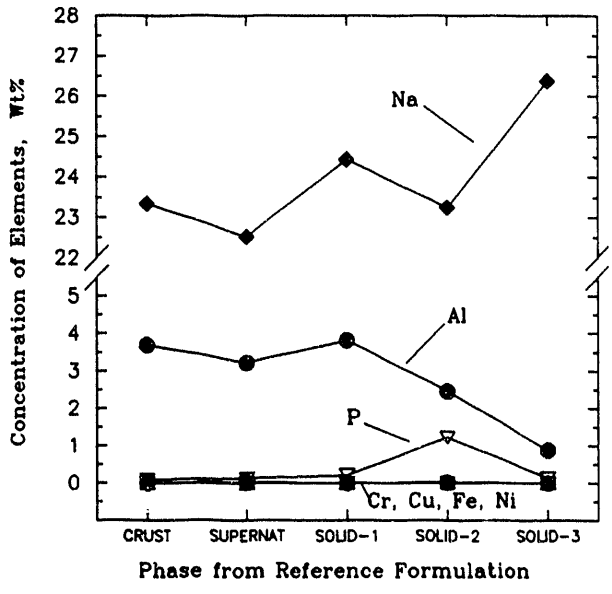

FIGURE 3. Concentration of Elements Analyzed by ICP for the Various Phases Present in the Reference Formulation (Day 66)

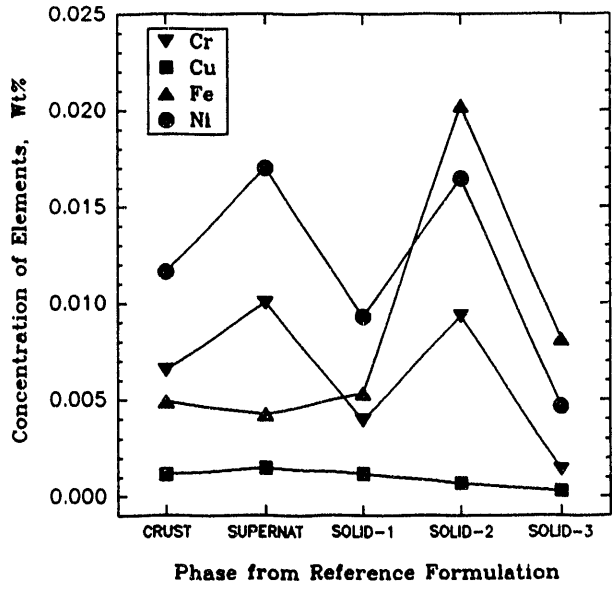

FIGURE 4. Concentrations of the Transition Metals Measured by ICP in the Various Phases of the Reference Formulation (Day 66)

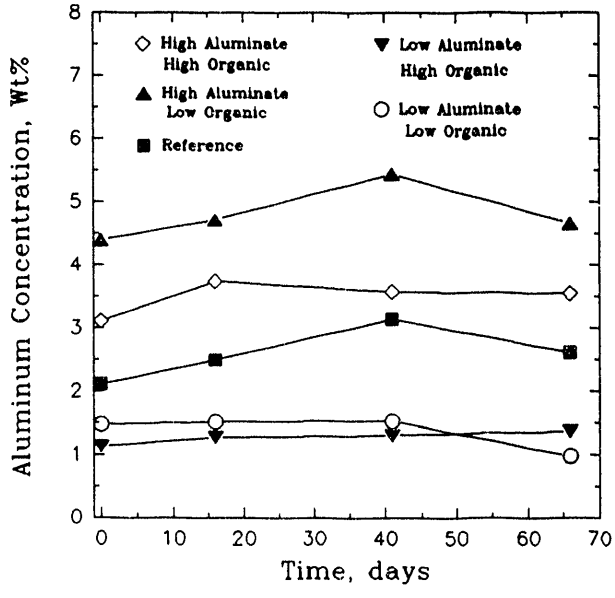

FIGURE 5. Measured Aluminum Concentration in Solids for the Various Formulations as a Function of Time

summarized in Figure 6. As shown by Figure 6, the relationship of increasing aluminum concentration in the crust with added aluminum in the formulation is not as definitive as it is for the bottom solids (Figure 5).

The supernate concentration of aluminum for all days of testing for all formulations is summarized in Figure 7 (data taken from Tables 19 through 22). This figure shows that for all formulations with the same added concentrations of $NaAlO_2$, the amount of aluminum species dissolved in solution is not dependent on how long the solutions are aged. Otherwise, the concentrations of measured aluminum in the supernate would not be grouped together so tightly for formulations with differing $NaAlO_2$ concentrations. A plateau or solubility limit of aluminum concentration appears to be reached in Figure 7 at approximately 3.5 wt% measured aluminum. This agrees with the predicted phase diagram data and calculations by Reynolds and Herting (1984) based on $NaAlO_2$ solubility in a system containing only $NaNO_3$, $NaNO_2$, $NaAlO_2$, NaOH, and water at 60°C. Actual measured aluminum concentrations slightly above the calculated solubility limit of 3.5 wt% Al may be due to the effects of added organics and other material in our system and not accounted for in the solubility equations.

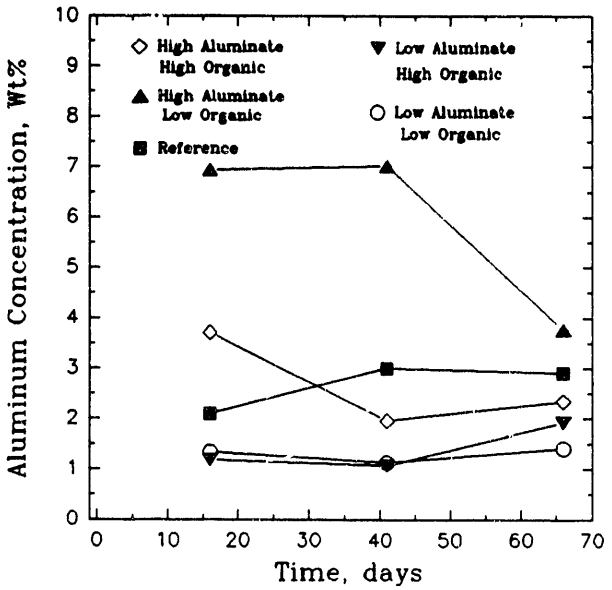

FIGURE 6. Measured Aluminum Concentration in Crust Samples for Various Formulations as a Function of Time

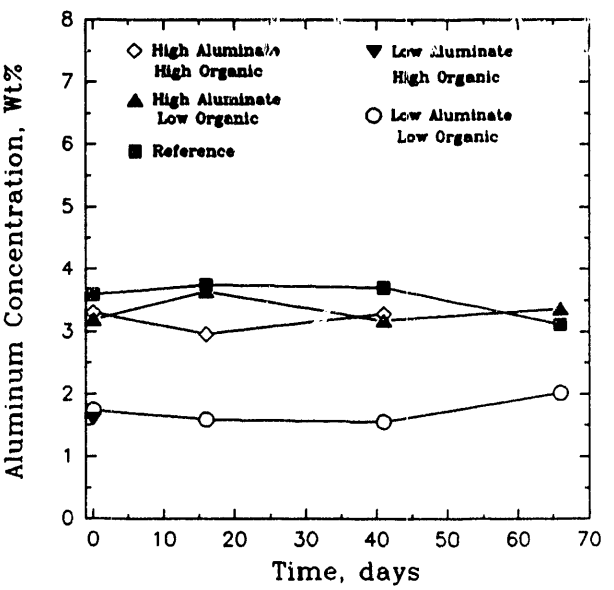

FIGURE 7. Measured Aluminum Concentration in Supernate for the Various Formulations as a Functions of Time

5.2.3 Total Carbon, Total Organic Carbon, and Total Inorganic Carbon Analyses

Analyses of TC, TOC, and TIC were performed on each solid phase of each formulation during the aging of the waste. This was done to see what effect, if any, aging the waste would have on the distribution of organic and inorganic carbon within the sample. The concern is that the organic carbon could possibly be concentrated within one layer and increase the fuel load of that layer.

Table B.24 contains TC, TIC, and TOC data from unheated solid samples of each formulation on day 0. Each sample was centrifuged to provide a solid sample for analysis. The analysis was of solids with interstitial solution.

Tables B.25, B.26, and B.27 contain TC, TIC, and TOC data for synthetic waste samples aged at 60°C for 16, 41, and 66 days, respectively. Samples were taken from the crust and solids layers of two reaction vessels for each formulation. For the instances in which the solid phase present was layered into more than one facies, a combined solid sample was taken and homogenized before it was analyzed. The results are listed in these tables as "crust" or "solids," according to the phase from which each sample was taken.

Table B.28 contains TC, TIC, and TOC data obtained from samples taken from the reference formulation on day 66. Three distinct layers were observed in the solid phase. Each of these layers was sampled separately. They are labeled as Solid-1, Solid-2, and Solid-3 to designate their relative vertical placement within the reaction container. The TOC data from the reference formulation on day 66 is presented in Figure 8. It is apparent from Figure 8 that the wt% TOC is considerably higher in the supernate than in any of the solid facies. Of the solid facies, the Solid-1 phase had the highest measured concentration of TOC.

Figures 9 and 10 detail the wt% TOC versus the relative organic concentration for crust and solids, respectively. By inspection of these figures, there appears to be a correlation between the organic concentration added to the formulation and the measured TOC in the crust and bottom solids. For example, for the bottom solid samples in Figure 10, the high organic formulations and the reference have much higher TOC values than the corresponding low

the formulations. For the bottom solids in Figure 12, the high organic and reference formulations, in general, have considerably higher TIC values than the low organic formulations.

It is not surprising that there would be higher measured TOC in the solid samples with higher added organic constituents. The relationship between the higher measured TIC in the solids with higher added organics may be explained by higher concentrations of carbonates, which is the final carbon decomposition product of the organic constituents in those systems with higher added organic.

5.3 THERMAL ANALYSES

Differential scanning calorimetry (DSC) and scanning thermogravimetric analysis (STG) of each solid phase of each formulation was carried out at the end of the aging studies (day 66). The DSC results yield endotherms and exotherms. STG analysis gives weight loss information as a function of temperature. This information is important for determining the amount of heat generated or absorbed due to chemical reactions during heating of the waste. The mass loss can be correlated to water loss or loss of other gaseous products of reaction.

Table B.29 contains DSC data for the crust and homogenized solid samples from reaction vessels for each formulation. Table B.30 contains data for the crust and a separate sample from each of the three distinct solid facies from the reference formulation. The original DSC thermograms are compiled in Appendix C.

The DSC data from Tables B.29 and B.30 are represented in Figures 13 and 14. In Figure 13, the magnitude of the endotherms and exotherms for crust samples of the various formulations are plotted as a function of the relative concentration of organic and as a function of the relative concentration of $NaAlO_2$ added to the formulation. There does not appear to be any relationship between the endothermic or exothermic characteristics of the crust samples and the added organic or sodium aluminate concentrations.

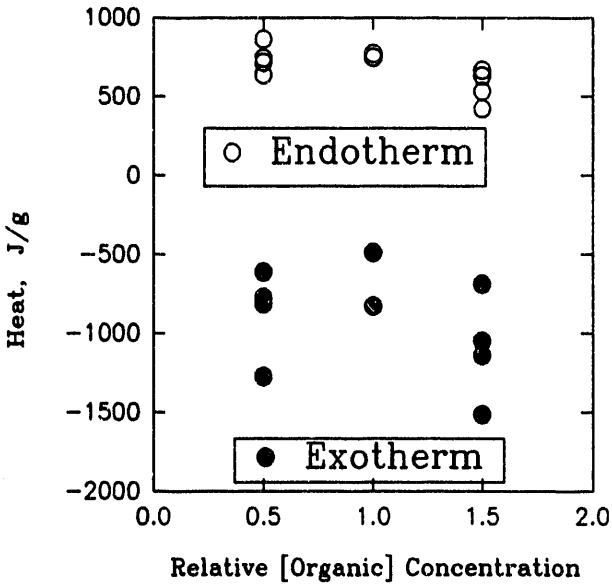

FIGURE 13. DSC Results of Crust Samples

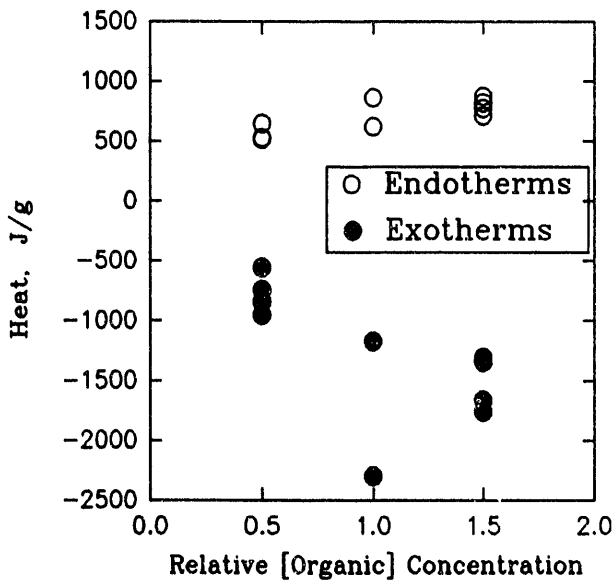

FIGURE 14. DSC Results of Bottom Solid Samples

Figure 14 shows DSC data from bottom solids samples. Plots of the observed endotherms and exotherms versus the relative organic concentration added to the formulations show definite relationships between the intensity of the endotherm or exotherm and the amount of organic present. The increase in the endotherm with added organic in the formulation is real but slight, and is difficult to rationalize since off gases were not analyzed in the DSC.

The observed increase in the exotherm portion of the DSC with increased organic concentration is very pronounced, probably because of the oxidation of increased amounts of organics in these bottom solids. Since the sodium nitrate and sodium nitrite are above their solubility limits in these mixtures, the solid phase would most likely be fuel (organic) deficient. It makes sense, then, that an increase in organic concentration has an increased effect on the observed exothermic characteristics of the reaction. There does not appear to be any relationship between the intensity of the endotherms or exotherms and the relative $NaAlO_2$ concentration added to the formulation.

Tables B.31 and B.32 present STG data for the various synthetic waste formulations. These tables give percent weight loss during heating of the sample. The weight loss is broken down between that lost during an exothermic

event and that lost during an endothermic event. A weight loss measured by STG was identified as arising from an endotherm or an exotherm by comparison with data taken by DSC of the same sample. The temperature between endotherm and exotherm listed in these tables was determined by judging at what temperature the reaction went from endothermic to exothermic according to DSC results. The endothermic weight loss is that loss below this transition temperature, and the exothermic weight loss is that loss above the transition temperature. Mass loss during the endothermic process is thought to involve water loss primarily; mass loss during the exothermic process is believed to be due to loss from gases released from combustion processes. The original STG thermograms are compiled in Appendix C.

The STG data are summarized in Figures 15 and 16 (data taken from Tables B.31 and B.32). Figure 15 includes plots of wt% mass loss of crust samples as a function of added relative organic concentration, and wt% mass loss of crust samples versus the added relative aluminate concentration. There does not seem to be a clear trend for the STG crust data.

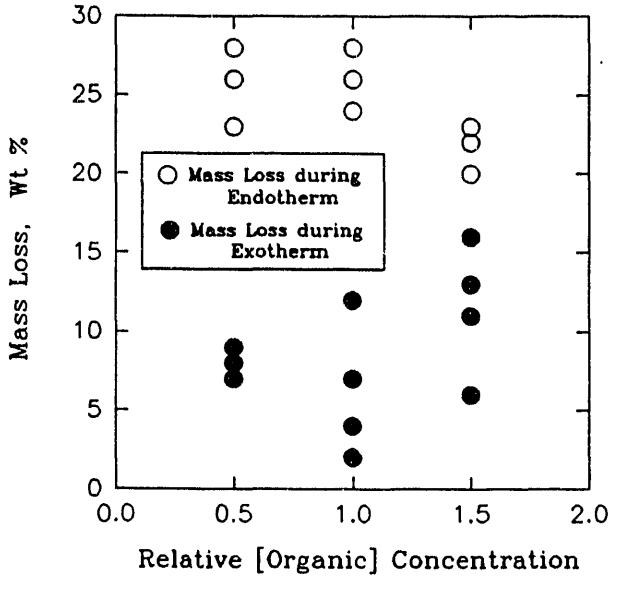

FIGURE 15. STG Results of Crust Samples (Day 66)

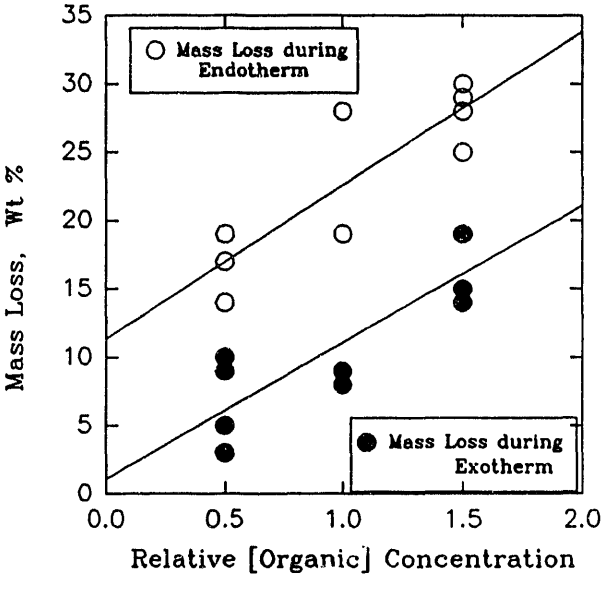

FIGURE 16. STG Results of Solid Samples (Day 66)

Figure 16 contains plots of the wt% loss of bottom solids samples versus relative organic concentrations in the formulations and wt% loss of the same sample versus relative aluminate concentration added to the formulation. Clear trends are observed for the wt% loss during the endotherms and exotherms as a function of added organic to these formulations.

The higher the concentration of added organic to these formulations, the larger the mass loss tends to be during the endotherm and exotherm. This observation can be explained if increasing the free organic in solution incorporates an increased concentration of bound organic in the solid phase. The increased concentration of the organic will directly increase the mass loss during the exotherm because of loss of combustion product gases.

However, the observed increase in mass loss during the endotherm with an increase in the organic concentration is not easily explained, but the reason may be related to an increased ability of the solid to hold solvent since the organics tend to disperse the solid phase (see the following discussion). The mass loss of water with heating would be expected during the endotherm portion of the STG.

5.4 PHYSICAL CHARACTERIZATIONS

Extensive physical and rheological characterizations were performed on the day 0 samples and on the samples heated at 60°C for 66 days. These characterizations were performed for each formulation on duplicate samples. The physical and rheological characterizations included density, settling rate, volume percent settled solids, volume percent and weight percent centrifuged solids, weight percent total solids, weight percent dissolved solids, weight percent total oxide, pH, shear stress versus shear rate (apparent viscosity), shear strength, and penetration resistance.

5.4.1 Crust, Supernate, and Bottom Solids Phase Volumes

Crust, supernate, and bottom solids volumes, as well as mass of reaction contents, of each reaction container were measured periodically (approximately twice each week). This was done to assess the settling behavior of the solids within the aging waste.

Tables B.33 through B.37 provide the data from the phase volume and weight measurements. Approximately 1 L of each formulation was added to four PMP containers. All four containers for each formulation were monitored for phase volume and mass changes during heating. On day 16 of heating, two containers from each formulation were sampled to obtain material for chemical analysis, thereby disrupting the mass and phase volume measurements for these containers. Phase volume and mass data collection was continued for the remaining two vessels until the termination of heating on day 66.

The data in Tables B.33 through B.37 have been normalized to a 1000-mL total volume for the day 0 (initial state) measurement. The weight loss with time is represented as wt% remaining. The density of the total reaction contents is also included in these tables.

The phase volumes for crust, supernate, and solids are shown in Figures 17 through 21 for all five formulations (data taken from Tables B.33 through B.37, respectively). In all stages of the experiment the crust volume

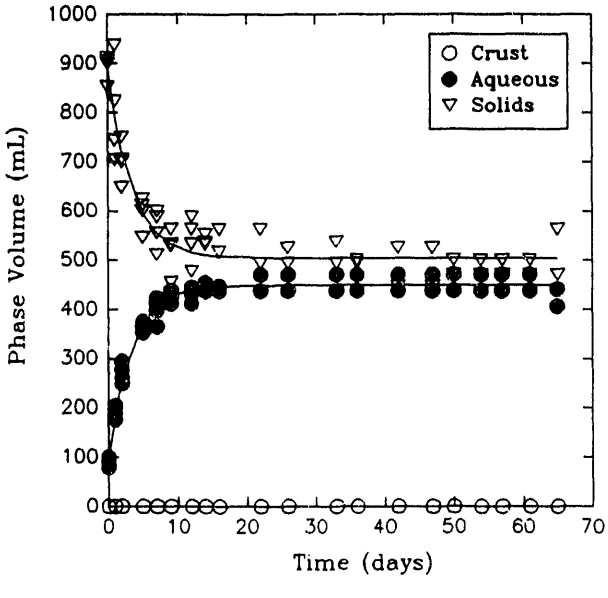

FIGURE 17. Plot of Phase Volumes Versus Time of Aging for Low Aluminate/Low Organic Formulation

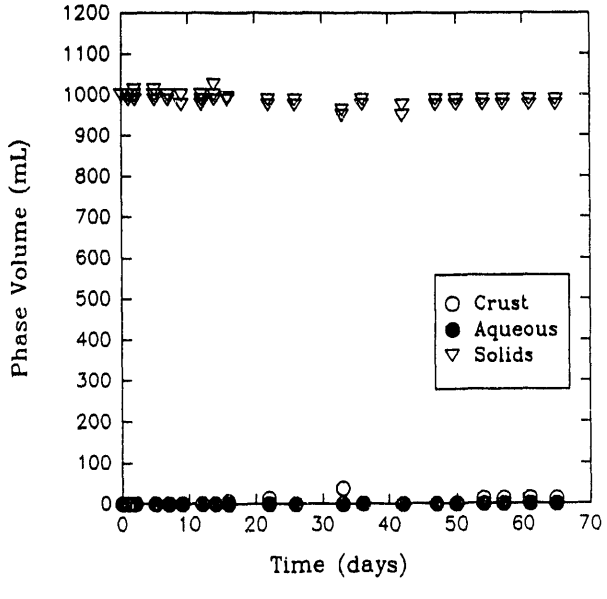

FIGURE 18. Plot of Phase Volumes Versus Time of Aging for Low Aluminate/High Organic Formulation

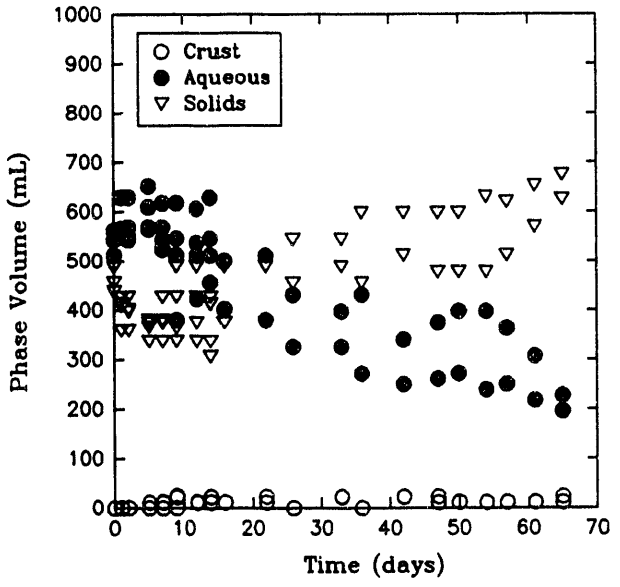

FIGURE 19. Plot of Phase Volumes Versus Time of Aging for Reference Formulation

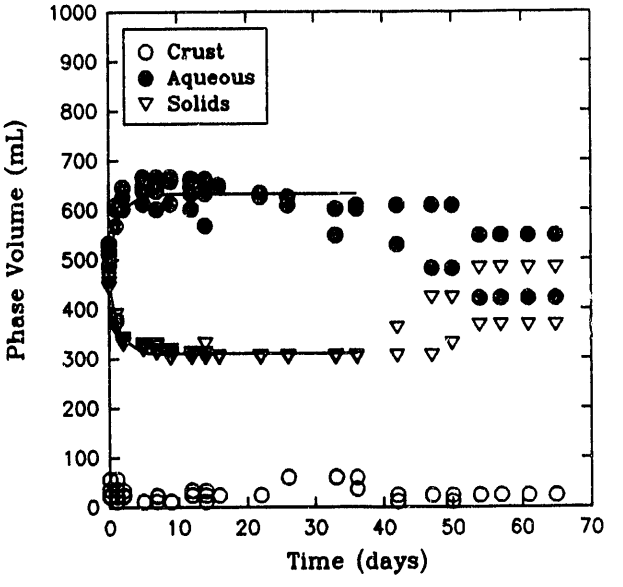

FIGURE 20. Plot of Phase Volumes Versus Time for High Aluminate/Low Organic Formulation

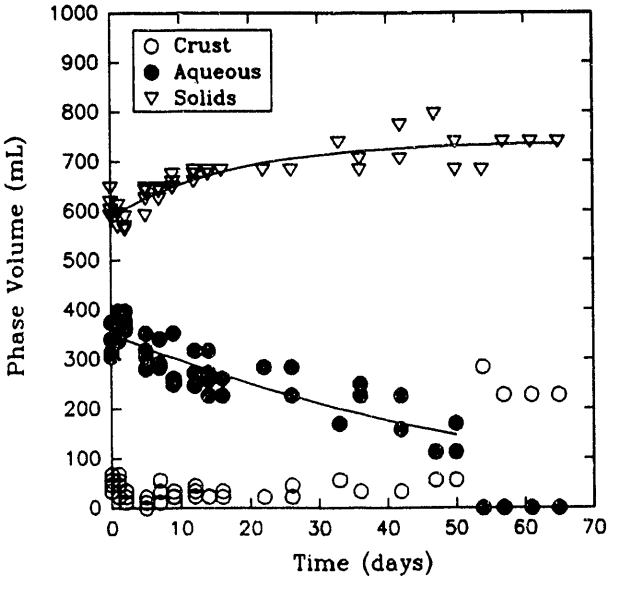

FIGURE 21. Plot of Phase Volumes Versus Time for High Aluminate/High Organic Formulations

was an insignificant contribution to the total volume of all components. The volume changes with time of aging for these formulations show quite different behavior depending on the total composition of the system.

The volume measurement of each phase present was relatively easy to make during early heating of all the formulations. However, after approximately 4 to 6 weeks of heating, the distinction between phases of several of the formulations became difficult to determine and required subjective evaluations. For this reason, only the portion of each formulation data set of solid volume data believed to be significant is compiled in Figure 18.

Figure 22 divides the solid volume data into two groups. The upper group in Figure 22 is data for the solids phase volume versus time of aging for the high and reference organic-containing compositions. The lower group in this figure is the data for solid phase volume versus time for the low organic-containing formulations. It is evident from Figure 22 that in all cases involving high or medium organic concentrations, the solid phase volume either increases throughout the aging period or is 100% of the volume of the container and remains the same throughout this period. In contrast, in both of the low organic-containing formulations, the solid phase volumes decrease and level off at a lower than initial state volume with time. In all these formulations as shown in Figure 22, a constant volume of the solid phase is eventually achieved (in the case of the high organic/low aluminate formulation, the solid phase volume was constant throughout the aging process). This constant or terminal volume of the solid phase at long aging times can easily be determined by inspection of Figure 22 (for the high organic/low aluminate formulation, this volume is essentially 1000 mL). The terminal volume of solids is shown in Figure 23 as a function of the ratio of the relative organic and aluminate concentrations for each formulation. This figure shows a strong correlation between the solids volume and the relative organic to aluminate ratio. Since the high organic/low aluminate shows the highest solids volume (most dispersed), and the low organic/high aluminate shows the smallest volume of solids (most compact), one role of the organic in this system is believed to be that of a dispersing agent.

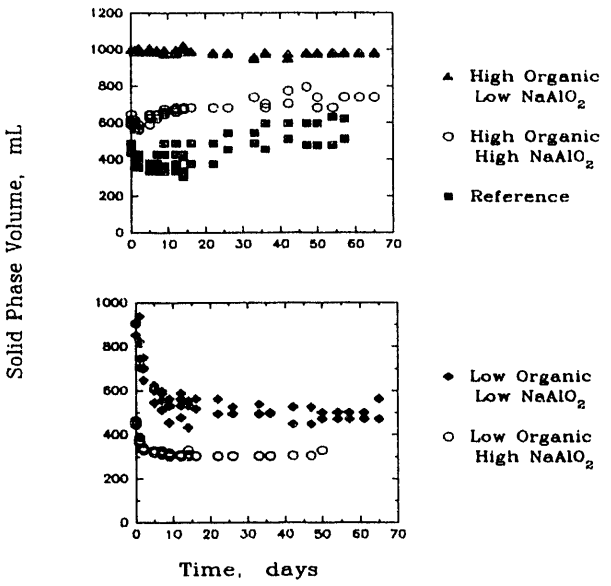

FIGURE 22. Plot of Solid Phase Volume Versus Time of Aging for All Formulations

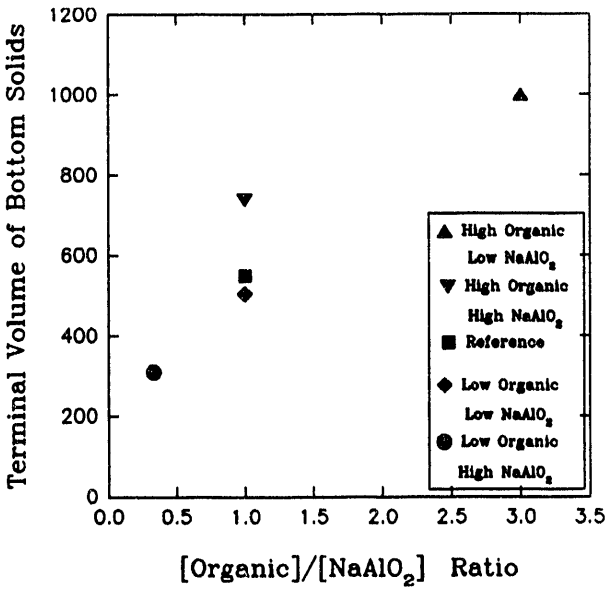

FIGURE 23. Terminal Volume (Settled Solids) of Solids Versus Relative [Organic]/[Sodium Aluminate] Ratio

Additionally, the high aluminate mixture also has the highest sodium ion concentration. The common ion effect would cause more sodium nitrate and nitrite salts to precipitate. Despite this, the high aluminate/low organic mixture has the smallest observed volume of settled solids and reinforces the role of the organic as a dispersing agent.

Figure 23 shows similar amounts of terminal solids for the high organic/high aluminate, reference, and low organic/low aluminate formulations. Each of these systems has the same ratio of organic to aluminate concentrations. This suggests that EDTA and HEDTA are serving as dispersive agents for the aluminate solids. The role of the organics that coat the solid phases is important not only for the dispersion of the solids, but can be shown in the next section to play an integral role in allowing gas bubbles to attach themselves to the surface of the solids.

Table B.38 contains crust, supernate, and bottom solids data for the reference formulation aged in two 500-mL borosilicate graduated cylinders. This experiment was undertaken to determine if there would be a large effect of container geometry on the measured phase volumes. The data are normalized

to an initial volume of 1 L in order to directly compare the phase volume versus time behavior with the reference formulation aged in 1-L PMP containers. Figure 24 is a plot of the phase volumes versus time. The terminal phase achieved by the reference in the graduated cylinder for the aqueous and solids phases is similar to that found for the same phases for the reference in the PMP containers (Figure 19). There appears to be an increase in the crust volume of the graduated cylinder reaction container over that of the PMP reaction container, but these differences are small.

5.4.2 Density

A sample of waste was placed in a preweighed graduated centrifuge tube and sealed. The total sample weight was determined. Often the waste from the settling rate and volume percent centrifuged solids was used for the density measurements. The sample centrifuged for 1 hour at greater than 1000 gravities to remove any voids in the samples so that an accurate volume could be measured. The total volume of sample was measured using the graduations of the commercially available centrifuge tube. The sample density was calculated

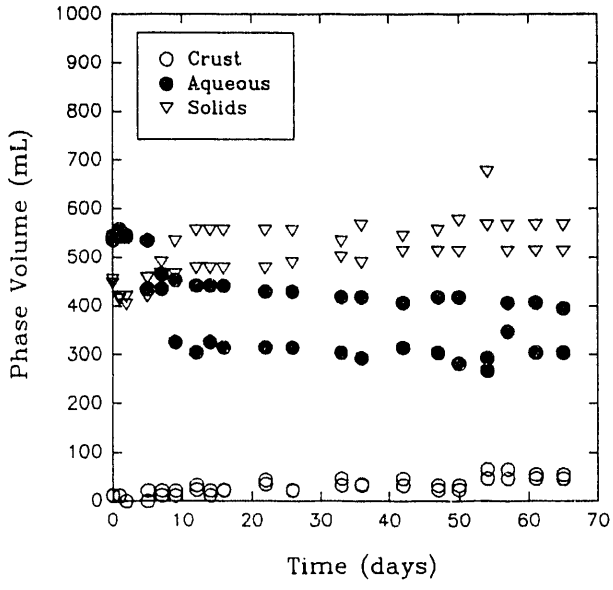

FIGURE 24. Plot of Phase Volumes Versus Time of Aging for Reference Formulation in Graduated Cylinder

by dividing the sample mass by the sample volume. It should be noted that the centrifuged solids contained an unknown amount of interstitial solution.

The densities of the centrifuged solids and centrifuged supernate were determined after the sample was centrifuged for 1 hour at greater than 1000 gravities. The total sample volume and centrifuged solids volume were determined using the graduations on the centrifuge tube. The supernate was removed from the centrifuge tube and placed in a preweighed container. The mass of solids and interstitial solution in the centrifuge tube and the mass of supernate in the container were determined. The centrifuged solids density was calculated by dividing the mass of the sample by the sample volume. The centrifuged supernate density was calculated by dividing the mass of supernate by the supernate volume.

As shown in Tables B.39 and B.40, the densities of the centrifuged supernate and solids are essentially constant for all the formulations at both day 0 and day 66. The densities for the centrifuged supernate and solids are 1.48 ± 0.03 and 1.78 ± 0.08 g/mL, respectively. The densities for the slurry are essentially constant for all the formulations at day 0 (1.61 ± 0.03 g/mL) but increase for most of the formulations on day 66. This increase appears to be due to the loss of water, and corresponds to an increase of approximately 7% for the reference and high aluminate feeds. The low aluminate formulations did not appear to change significantly.

5.4.3 Solids Settling Rates

The settling rate and volume percent settled solids measurements were determined in a centrifuge tube. The sample was placed in the centrifuge tube, and the weight of the sample was determined. Volumes of the total sample, solids, and liquid were determined using the graduations on the centrifuge tube. The solids in the sample were allowed to settle with minimal disturbance. The total sample volume and the volume at the solid-liquid interface were recorded at appropriate intervals (approximately every 2 hours). Volumes were measured until no change was observed among three successive measurements.

The settling rate data are presented as the vol% settled solids versus time. The settling rate data for the reference and the high aluminate/low organic formulations at day 0 are given in Figures 25 and 26. The settling rate appears to be first order with a settling rate constant for the reference and high aluminate/low organic formulations of -0.08 and -0.02 hr^{-1}, respectively. The other formulations showed no significant settling over a period of 3 days. This data is consistent with the phase volume studies with the exception of the low organic/low aluminate formulation. The phase volume data indicates that this formulation settles at 60°C. The settling rate was measured at room temperature and it appears that temperature has a significant effect upon the settling behavior of this formulation.

The volume percent settled solids was determined by dividing the final settled solids volume by the total sample volume and multiplying by 100%.

5.4.4 Volume Percent and Weight Percent Centrifuged Solids and Supernate

The sample used for the settling rate measurements was also used to determine the volume percent and weight percent centrifuged solids and

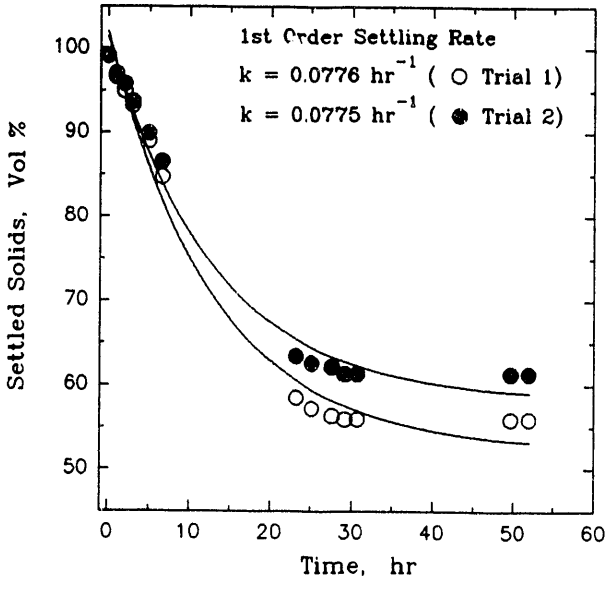

FIGURE 25. Settling Rate Data for the Reference Formulation for Day 0 of Aging

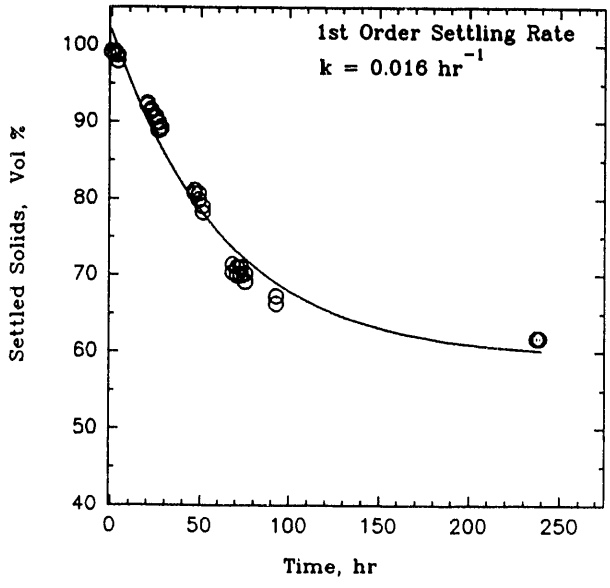

FIGURE 26. Settling Rate Data for the High Aluminate/Low Organic Formulation for Day 0

supernate. The sample was put into a preweighed centrifuged tube and the total mass of sample was determined. The sample was centrifuged for 1 hour at greater than 1000 gravities. The total sample volume and solids volume were determined using the graduations on the centrifuge tube. The supernate volume was calculated by subtracting the solids volume from the total sample volume.

The volume percent centrifuged solids was the solids volume divided by the total sample volume multiplied by 100%. The volume percent centrifuged supernate was 100% minus the volume percent centrifuged solids.

To determine the weight percent centrifuged solids, the centrifuged supernate was decanted or transferred using a pipet into a preweighed graduated cylinder. The mass of the solids remaining in the centrifuge tube was determined, and the mass of the decanted supernate was determined. The weight percent centrifuged solids was the mass of the centrifuged solids divided by the total sample mass multiplied by 100%. The weight percent centrifuged supernate was the mass of the decanted supernate divided by the total sample mass multiplied by 100%.

The volume and weight percent centrifuged solids for each formulation are reported in Table B.39 and B.40. Table B.39 lists the physical properties of the raw formulations (day 0), and Table B.40 lists the physical properties of the formulations after heating at 60°C for 66 days. All the measurements were performed at ambient temperature (~24°C). The volume and weight percent solids in each formulation after heating is larger than in the raw formulation. This is expected due to water losses during the heating process, but the increase in the weight percent centrifuged solids for the reference and high aluminate formulations is much greater than can be described by water losses (see Table B.33-B.37). It appears that at ambient temperature the solubility of aluminate is higher in the unheated formulations.

5.4.5 Weight Percent Total Solids, Dissolved Solids and Total Oxides

The sample of synthetic waste was placed into either a preweighed crucible or vial. The crucible was used for the weight percent measurements of total oxides. The mass of sample was determined. The sample was allowed to air-dry overnight to remove any free liquid and thus prevent splattering of

the sample in the oven. After the free liquid was evaporated, the sample was transferred to a drying oven or furnace at 105 ± 5°C, where it was dried for 24 hours. The dried samples were then removed from the oven and placed in a desiccator to cool to room temperature. The weight of the dried solids was determined. The weight percent total solids was the dried solids weight divided by the initial sample weight multiplied by 100%.

The weight percent dissolved solids was determined for supernate samples and for the interstitial solution or centrifuged supernate from slurry or sludge samples. The samples of the supernate and the interstitial solution were dried using the same procedure as the weight percent total solids measurement. For solutions, the weight percent dissolved solids was the dried weight of material divided by the initial sample mass multiplied by 100%. For slurries or sludges, the weight percent dissolved solids was the weight percent dissolved solids in the supernate or interstitial solution multiplied by the weight percent centrifuged supernate in the slurry or sludge divided by 100.

The weight percent total oxides was measured using the dried solids from the weight percent total solids measurement. The dried solids were placed in a furnace at 1025 ± 25°C for 30 minutes, which converted the chemicals in the sample to their stable oxide form. The sample was then allowed to cool to about 150°C and then transferred to a desiccator and cooled to room temperature. After it had cooled, the sample was weighed. The weight percent total oxide was the final mass of the sample divided by the initial sample mass prior to drying multiplied by 100%. During the weight percent total oxide measurement, volatile elements in the sample may have been lost.

The wt% solids and oxides for each of the raw formulations (day 0 prior to heating) and their centrifuged solids are given in Table B.39. As is expected, the weight percent solids of the raw formulations increases as the amount of organic plus aluminate increases. Based on previous measurements, the lower wt% solids value (71.6%) reported for the high aluminate/low organic formulation appears to be in error; therefore, the wt% solids for this formulation appears to be approximately 80%. The wt% oxides for the uncentrifuged formulations increases with increasing aluminate concentration, and additional

organic appears to have minimal effect as can be seen in Figure 27. For the centrifuged solids, the wt% oxides are essentially constant for each formulation except for the low organic/high aluminate (Figure 28). It appears that the presence of the organic tends to increase the solubility of the aluminate in the supernate, causing a lower wt% oxides in the centrifuged solids of the high aluminate/high organic formulation. The wt% oxides in the other formulations are limited by the solubility of the aluminate in the supernate.

The wt% solids and oxides for the crust, supernate, solids, and the centrifuged solids of the composite for each formulation after 66 days of heating at 60°C are shown in Table B.40. The data indicate that the wt% solids and oxides increases with increasing aluminate. The organic concentrations in the formulation did not significantly affect the wt% solids and oxides except for the bottom solids in the high organic/high aluminate formulation. The high organic decreased the wt% solids and oxides in the bottom solids as was observed in the centrifuged solids of the raw formulation (day 0).

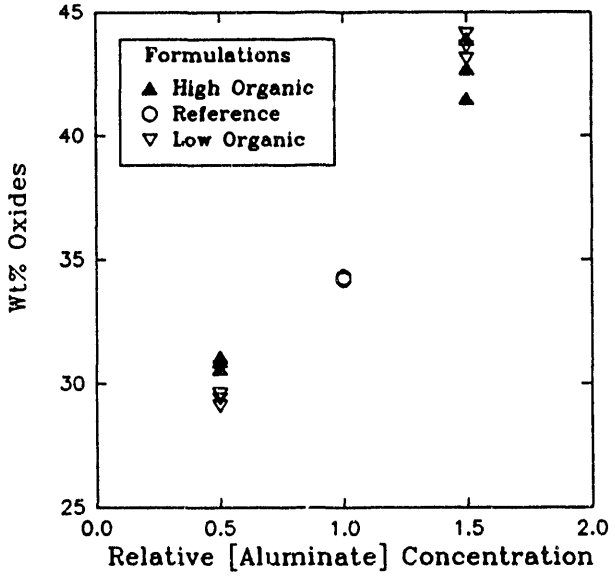

FIGURE 27. Wt% Total Oxides Measured for the Various Formulations Prior to Heat Treatment (Day 0)

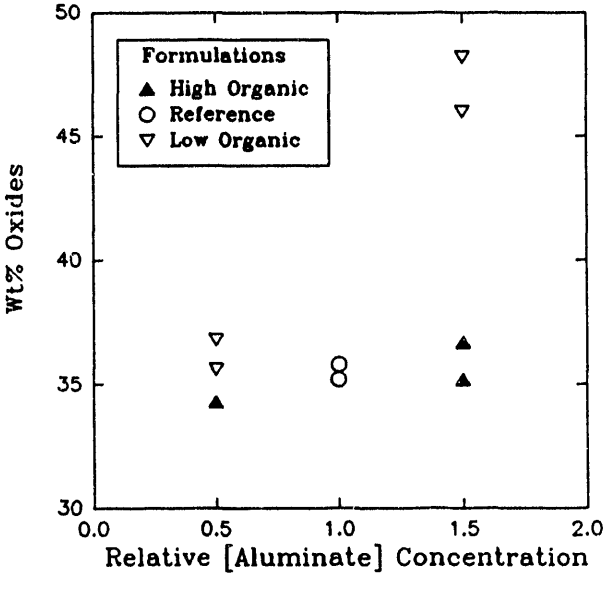

FIGURE 28. Wt% Oxides Measured on the Centrifuged Solids from the Various Formulations before Heat Treatment (Day 0)

5.4.6 pH

Standard laboratory procedures were used to measure the pH of solutions and slurries. Before it was used, the pH electrode was calibrated by a two-standard method that takes into account the temperatures of the standards and samples. The pH for the raw formulations was >14 (see Table B.39). After heating the formulations for 66 days, the pH lowered slightly to ~13.8 for each of the formulations except the reference, whose pH remained >14 (see Table B.40).

5.4.7 Rheological Properties

Shear Stress Versus Shear Rate

The data regarding shear stress versus shear rate are used to evaluate the viscosity of a fluid. The data were generated in the form of a rheogram or flow curve, which is a plot of shear stress as a function of shear rate. The rheograms were obtained using a Haake RV 100® viscometer equipped with an M5 measuring-drive head and the MV1 sensor system. The measurement of viscosity with this instrument requires that the sample be placed in the gap between two coaxial cylinders.

About 40 mL of sample was thoroughly agitated and transferred into the cylinders. When the system was set in motion, a viscosity-related torque, caused by the sample's resistance to shearing, acted on the inner cylinder. This torque deflected a calibrated measuring spring placed between the motor and the inner cylinder. The magnitude of the spring deflection correlated linearly with the torque. This torque is a measure of the shear stress of the material. The spring deflection was transformed into an electrical signal, and the spring deflection and tachometer signals were recorded as shear stress and shear rate, respectively.

The apparent viscosity of the sample was then calculated by dividing the stress at a given shear rate by that shear rate. The viscosity of the sample can then be plotted as a function of shear rate. In Appendix D, the viscosity of a composite of each of the formulations is plotted as a function of shear rate. These composites are non-Newtonian fluids and exhibit a yield stress.

A slurry with a yield stress will "clamp" the rotor to the cup until the applied torque exceeds the yield stress. While the rotor is still "clamped" and remains motionless, the motor rotation will cause some spring deflection and consequently a torque signal which is recorded on the ordinate.

The measured yield stresses for each of the formulations are given in Table B.42. The yield stress for all the formulations except the high aluminate/high organic are ~10 Pa. The yield stress for the high aluminate/high organic is about double the yield stress of the other formulations (21 ± 5 Pa). The viscosity at high shear rates (~480 s^{-1}) ranged from 100 to 250 cP with the low aluminate/low organic exhibiting the lowest viscosity (100 cP) and the high aluminate/high organic exhibiting the highest viscosity (250 cP). The viscosity appears to increase with increasing aluminate concentration. The addition of organic also tended to increase the viscosity of the sample.

Shear Strength

Shear strength is a semiquantitative, primarily qualitative, measure of the force that is required to move the material. The Haake RV 100 viscometer with the M5 measuring-drive head and a shear vane were used for this measurement. The shear vane was 0.80 cm in diameter and 1.588 cm in height.

Shear strength is dependent on sample history. Exhibited during transient "start-up" shear, it marks the transition from a solid to a viscous slurry. The value of the shear strength was determined by using a shear vane to generate a plot of torque versus time at a constant shear rate. A shear vane rotational speed of 50 rpm was used during this evaluation. The plot will show a peak at the beginning; then it will level off and finally drop off. The shear strength was calculated from the peak torque. The shear strengths for the crust, bottom solids, and composite are reported in Table B.41. The shear strength for the crust and bottom solids are generally >25,000 dyne/cm^2, and the shear strength for the composite is generally <25,000 dyne/cm^2 except for the high aluminate/high organic formulation which has a shear strength of ~40,000 dyne/cm^2.

Penetration Resistance

The measurement of the penetration resistance of the sludge was used as a qualitative indicator of a sludge's cohesive or dilatant behavior. Knowledge of the cohesive or dilatant properties of a sludge is useful for 1) interpreting shear strength data, 2) applying pilot-scale sludge mobilization equations, and 3) determining full-scale mixer-pump performance for sludge retrieval. A dilatant sludge will tend to be eroded by the mixer pump, whereas a cohesive sludge will be broken down into large chunks of sludge by the mixer pump. Retrieval of a sludge by erosion action would require a smaller mixer pump than the retrieval of a sludge that breaks into large chunks.

The difference between the penetration resistance of a dilatant material and a cohesive material is large (a factor of 10), making the penetration resistance a good indicator of this sludge property. A low penetration resistance (0 to 10 psi) indicates that a sludge is cohesive. A high penetration resistance (100 psi or greater) suggests that a sludge is dilatant, but it must be known whether the sludge is composed of finely divided material and not some other type of material such as a solid crystal mass. The penetration for all the samples was >10 psi; therefore, the solids are classified as dialatent (see Tables B.39 and B.40).

The CT-421A penetrometer supplied by Soil Test, Inc., was used for these measurements. The measurement was made in the center of the sample and to a depth of 1.0 in.

5.4.8 X-ray Diffraction

X-ray diffraction (XRD) analysis of each solid phase of each formulation was performed on day 66 samples. The relative intensities for identified crystalline phases present for each solid phase in each formulation are presented in Table B.43. The relative intensities of the identified crystalline phases in the crust and the three distinct bottom solids phases for the reference formulation are listed in Table B.43. The original XRD data is compiled in Appendix E.

The XRD data in Tables B.43 and B.44 indicate that sodium nitrate and sodium nitrite are the two most abundant crystalline phases present in the crust and solid phases of all the formulations (the high reading for sodium butyrate is not believable as discussed below). It is worth noting that decomposition products of EDTA and HEDTA, such as sodium hydrogen oxalate, sodium acetate, glycine, and valine, were identified in all the formulations. Sodium butyrate was also identified, but its presence is suspect because of the unlikely event that a four-carbon chain would form. The identification of the acid form of glycine acid as well as $NaHCO_3$ is also suspect in these mixtures even though they are plausible breakdown products of EDTA and HEDTA. The high pH of these mixtures would most likely preclude the formation of a significant amount of a crystalline phase of these acids.

The XRD results for each solid strata for the reference formulation indicate the lower bottom solid layer has been enriched in sodium nitrate relative to the bulk concentration. This is consistent with the IC results reported earlier. It is also worth noting that only in the reference and high aluminates formulations were crystalline phases of $NaAlO_2$ observed by XRD (Tables B.43 and B.44). This is consistent with the expected solubility behavior for $NaAlO_2$ in these mixtures (see Figure 7 and accompanying text), which predicts that $NaAlO_2$ is below its solubility limit in the low aluminate formulations but exceeds this limit in the reference and high aluminate formulations.

6.0 GAS GENERATION STUDIES

6.1 EXPERIMENTAL METHODS

For each of the five formulations, approximately 500 mL was placed inside a separate borosilicate glass gas generation and gas collection apparatus. Glass dissolution was observed for these vessels but was not a problem during these experiments. A photo of the reaction assembly is shown in Figure 29. The temperature of the reaction vessel was maintained at approximately 90°C throughout the experiment by temperature controllers connected to heating mantles around the round bottom flask containing the synthetic waste.

Periodically during the course of the reaction, gas samples were taken from the vapor space of the apparatus and analyzed using mass spectroscopy (MS). The MS data for each formulation versus time is presented in Table B.45. Total moles of each gas found in the vapor space of each formulation are given in Table B.46. This represents moles of gas in the system corrected for samples taken for MS analysis. This also includes the initial gas within the system at time 0. No attempt was made to subtract the initial moles of gas in the system from each subsequent analysis.

6.2 RATE AND STOICHIOMETRY OF GAS PRODUCTION

Figure 30 summarizes the gas generation data for gases produced for all the formulations. The relative amounts of the gases produced were observed to be in the order $N_2 > N_2O > H_2$. It was also observed that formulations containing high organic concentrations generated more of each gas than formulations containing moderate or low organic concentrations. It was also apparent the high aluminate formulations were better at producing gases than their low aluminate counterpart. Figures 31 through 35 contain the data from Table B.46, which lists the contributions of each gas measured in the reaction vessel for each formulation. It is possible to calculate the rate of gas generation for each of these reaction mixtures expressed in terms of change in the moles of nitrogen gas with respect to time. Using the slope of the initial portion of each of the plots for nitrogen, the rate data contained in

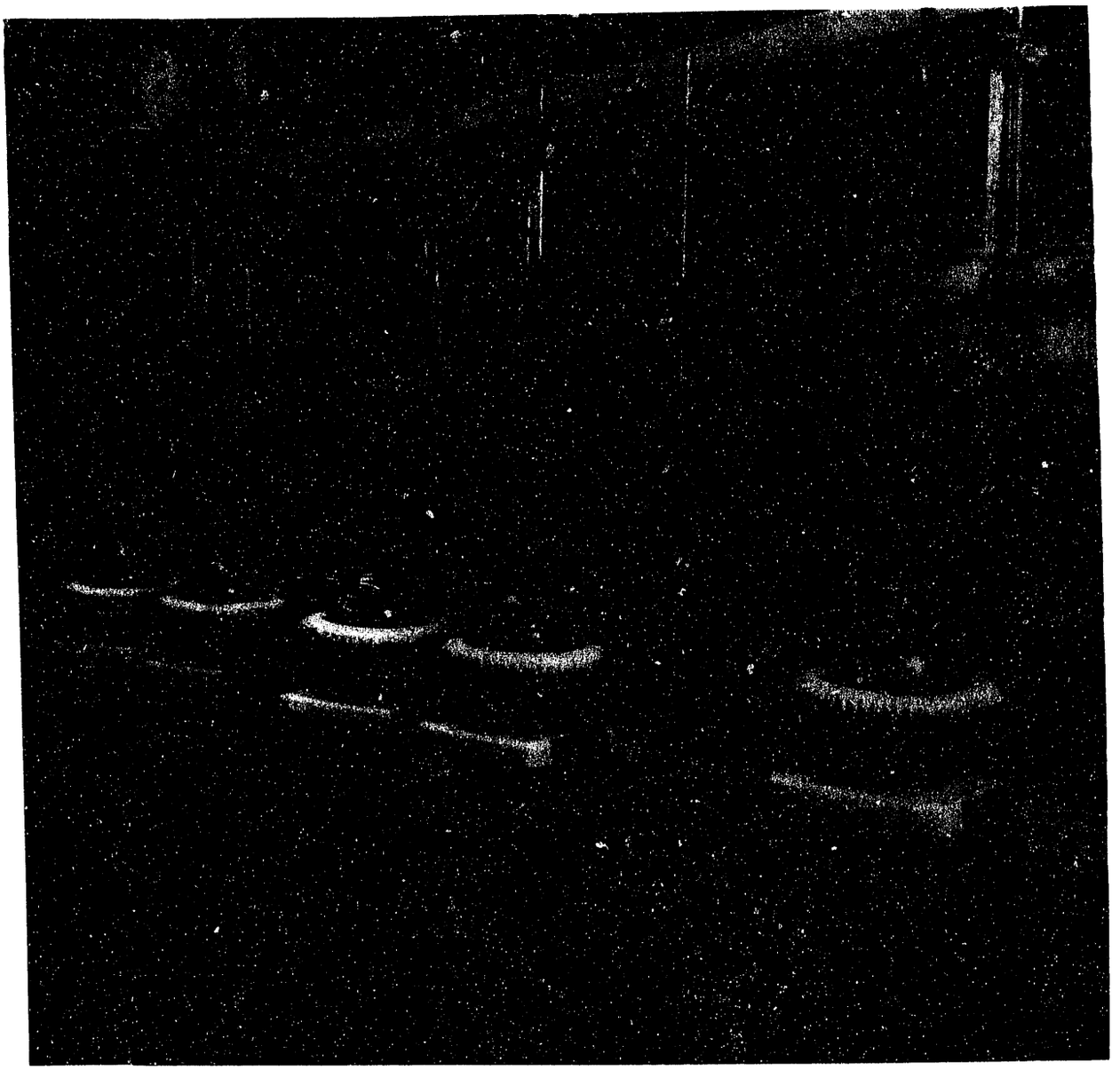

FIGURE 29. Gas Generation Experimental Apparatus

Figure 36 was obtained. These data (expressed as d(moles N_2)/dt versus relative organic concentration) show a general trend that the more total organic available, the faster the reaction.

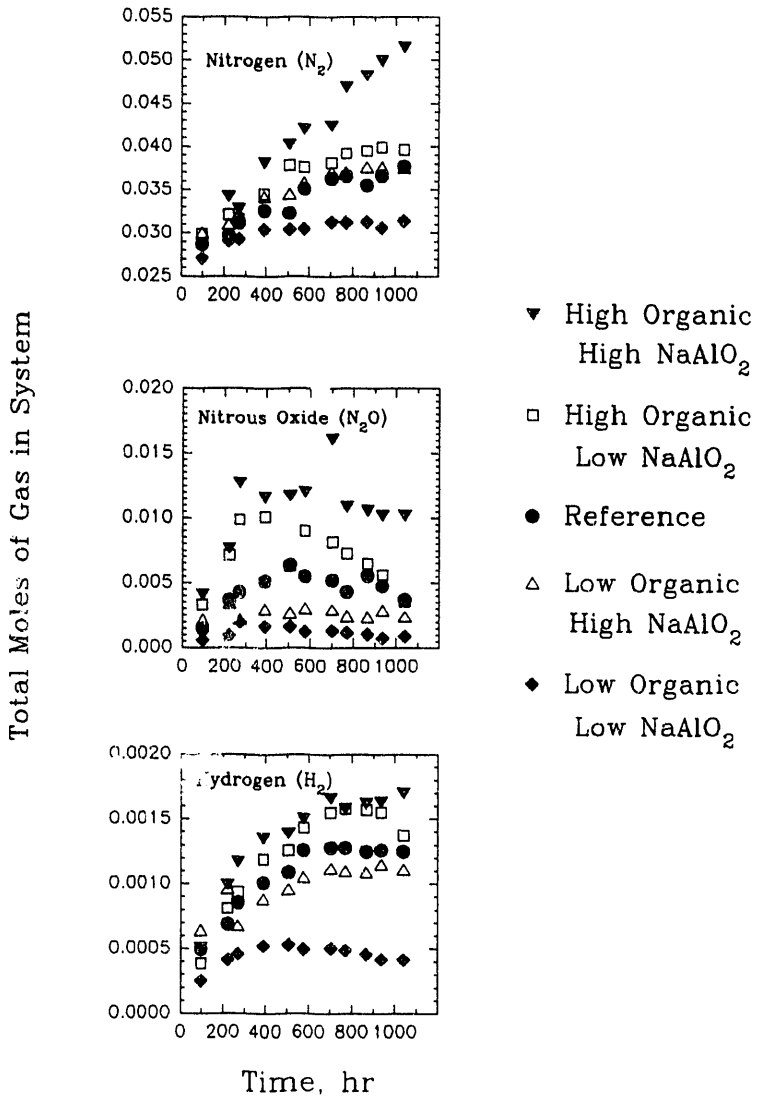

FIGURE 30. Plot of Moles of Nitrogen, Nitrous Oxide, and Hydrogen Gases in Reaction Vessel Versus Time for All the Formulations

The slope of the moles of N_2O produced versus time is essentially zero for most of the reaction period for these reactions. This can be rationalized by at least two possibilities. It is possible that the production of the N_2O gas establishes a steady state concentration with the rate of loss of this gas through transport through the water used as a hydrostatic head. A second possibility may be the rate of N_2O formation is balanced by the rate of the decomposition of this gas to produce N_2 as well as other products.

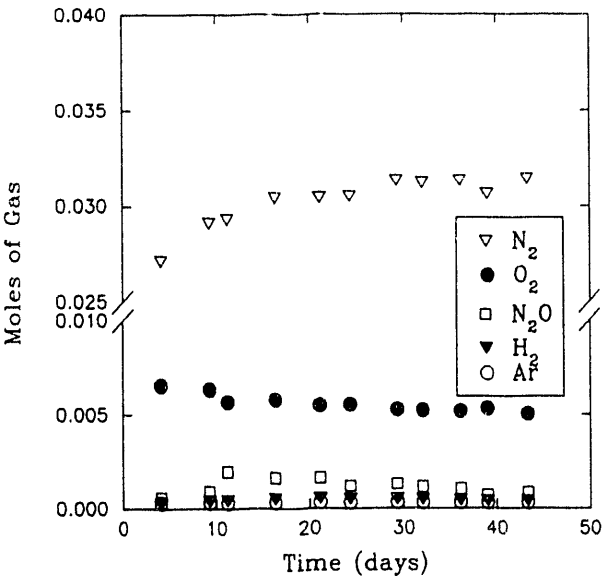

FIGURE 31. Plot of Measured Gases Present in Reaction Vessel Versus Time for Low Aluminate/Low Organic Formulation

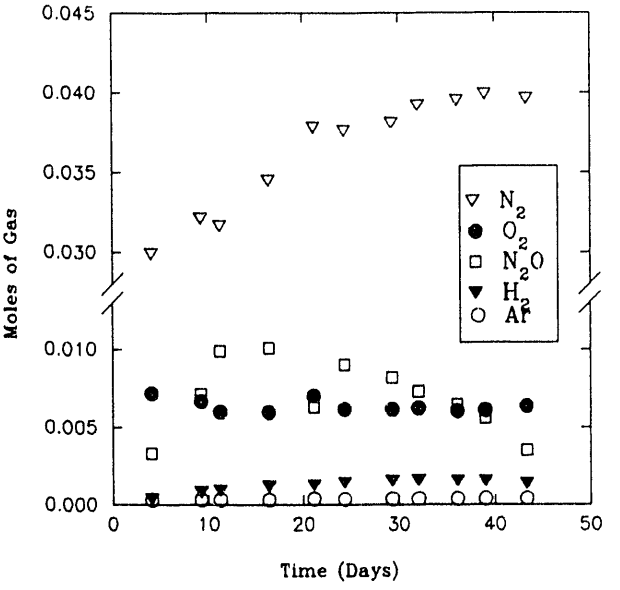

FIGURE 32. Plot of Measured Gases Present in Reaction Vessel Versus Time for Low Aluminate/High Organic Formulation

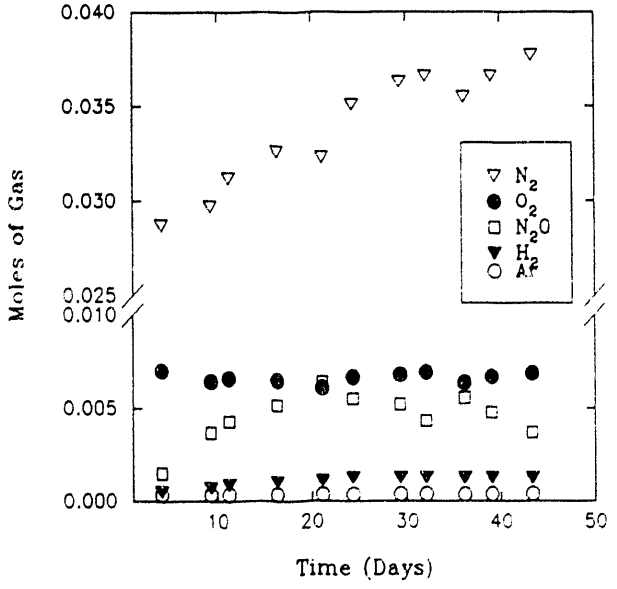

FIGURE 33. Plot of Measured Gases Present in Reaction Vessel Versus Time for Reference Formulation

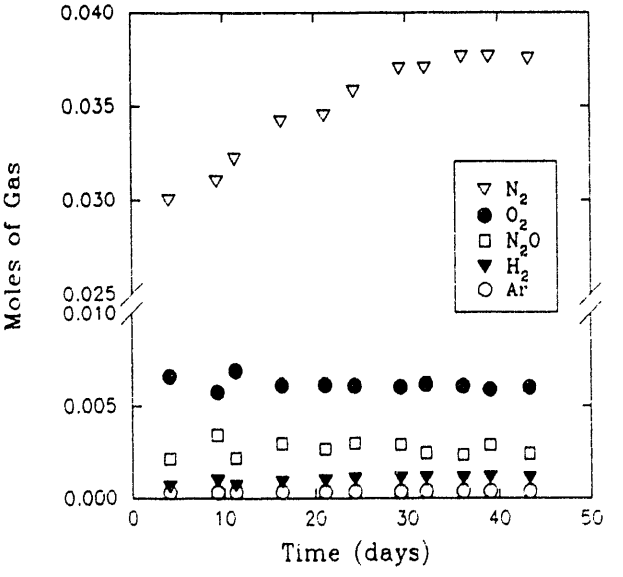

FIGURE 34. Plot of Measured Gases Present in Reaction Vessel Versus Time for High Aluminate/Low Organic Formulation

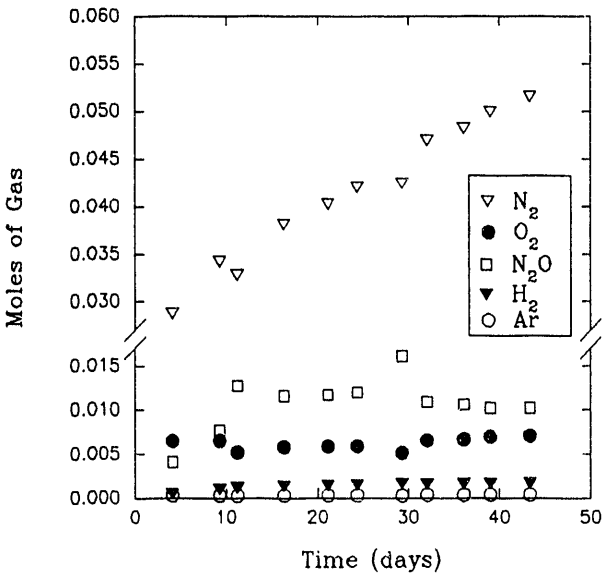

FIGURE 35. Plot of Measured Gases Present in Reaction Vessel Versus Time for High Aluminate/High Organic Formulation

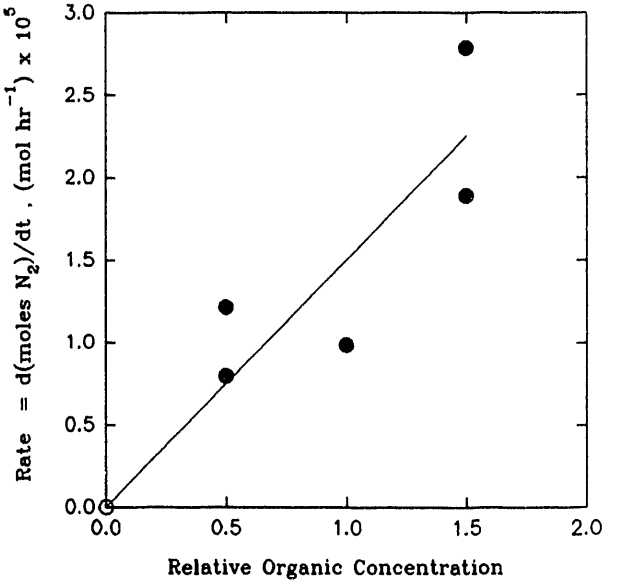

FIGURE 36. Least Squares Fit of Rate Data for Nitrogen Generation Versus Relative Organic Concentration Added to Each Formulation

This data shows that N_2, H_2, and N_2O are generated by reactions of an unknown mechanism. To better understand the reaction pathway of the reactions involved, studies are being performed by personnel at Georgia Institute of Technology on simpler systems. Such studies can provide information on how to treat the waste to eliminate the gas production problem.

6.3 COMPARISON OF GAS GENERATION TO TANK 101-SY

As in the actual tank, the predominant gases produced by synthetic wastes are nitrogen, nitrous oxide, and hydrogen. However, the relative abundance of these gases in synthetic waste studies does not agree particularly well with observations from the actual waste tank. Gases vented from the actual tank are nearly equimolar with respect to nitrogen, nitrous oxide, and hydrogen (Barker et al. 1991). In the present study, nitrous oxide production exceeded that of hydrogen by a factor of five for the reference waste composition. Larger excesses of nitrous oxide were found for certain of the variant waste compositions.

The quantity of hydrogen generated by thermally driven chemical degradation reactions accounts for perhaps one-third of that generated by the actual tank. In this study, the reference waste composition at 90°C yielded 1.3 millimoles of hydrogen gas over a 500-hour period for a 500-mL waste volume (see Figure 30). This corresponds to 500 moles of hydrogen per day per million gallons of waste. The activation energy for gas generation has been determined in previous studies to be 25 kcal/mole (Delegard 1980; Siemers, in Strachan 1991), which can be used to estimate gas production rates at other temperatures. At 60°C, which is approximately the actual tank temperature, a rate of 20 moles of hydrogen per day per million gallons of waste is calculated from synthetic waste studies. Hydrogen generation rates for Tank 101-SY are estimated to be 64 moles per day per million gallons of waste (Strachan 1991), approximately three times the value based on synthetic waste results. The hydrogen generation rate for the actual tank given above assumes that gases are generated throughout the tank but are retained only in the nonconvecting layer (Strachan 1991).

A similar treatment of nitrous oxide production data from reference synthetic waste compositions leads to an estimate of 100 moles nitrous oxide per day per million gallons of waste. This quantity is approximately twice that estimated to be produced in the actual tank, again assuming that gases are produced throughout the tank but are retained only in the nonconvecting layer (Strachan 1991).

The reasons for the apparent lack of agreement between quantities of gases produced using synthetic wastes and those estimated to be produced by the actual tank are not well understood. Of course, in the present tests using synthetic wastes, radiolytic processes, which will produce additional hydrogen, were excluded (Meisel et al. 1991). Obviously, the absence of radiolysis does not explain the apparently too high values for nitrous oxide obtained using synthetic wastes, as nitrous oxide also is a radiolytic product. Nitrous oxide is considerably more soluble in water than either nitrogen or hydrogen, so that component may be selectively retained in the actual

wastes. Solubilities of these gases in solutions of high ionic strength, such as the waste in Tank 101-SY, have not been measured, however, nor are they easily calculated.

Perhaps the most important factor in determining quantities of gaseous products may be the choice of organic waste components. A mixture of HEDTA and EDTA was used in the present tests. However, based on results obtained from Tank 107-AN, a much more complex mixture is expected to be present in the actual waste tank (Strachan 1991). These chelators constitute only a small fraction of the total organic carbon in that tank. Thus, a number of factors may contribute to differences in the quantities of product gases observed in synthetic waste tests compared to actual tank estimates, but the choice of organic components in synthetic wastes is likely to be the most important.

7.0 MECHANISM OF GAS RETENTION AND CRUST FORMATION

7.1 WETTING BEHAVIOR AND FLOTATION

Flotation of solid particles with densities greater than the liquid phase in which they were originally immersed has been widely used by the mining industry. Solid particle buoyancy is gained by attachment of the particles to air bubbles. The tendency for particles to attach to air bubbles is largely controlled by the surface energy of the solid. The principles underlying mineral flotation technology provide some insight into the mechanism of crust formation in Tank 101-SY.

A solid particle immersed in a liquid will tend to become attached to an air bubble if the equilibrium contact angle between the solid and the liquid is greater than zero (or, at equilibrium, the solid is incompletely wetted by the liquid). The Young-Dupre′ equation, Equation 1 (Huh and Mason 1974), describes expected trends in wetting behavior as a function of the interfacial tensions between the solid, liquid, and gas phases:

$$\cos\Theta = [\sigma_{SV}-\sigma_{SL}]/\sigma_{LV} \qquad (1)$$

The contact angle, Θ, is measured between the solid and liquid phases. A value of $\Theta=0°$ is indicative of completely wetted solids and no tendency for gas bubble retention, while a value of $\Theta = 180°$ is indicative of the absence of wetting and a great tendency for gas bubble retention. The terms σ_{SV}, σ_{SL}, and σ_{LV} refer to interfacial tensions at the solid/vapor, solid/liquid, and liquid/vapor interfaces, respectively.

The contact angle between a gas, solid, and liquid interface is demonstrated in Figure 37 for a surface that resists wetting (Figure 37, part A) and a surface that favors wetting (Figure 37, part B). To minimize the surface energy of the system, a solid will seek a position at a liquid-gas interface so that the equilibrium contact angle Θ is achieved. Or, for any value of $\Theta > 0$, a stable position for a solid particle is at the liquid-gas interface.

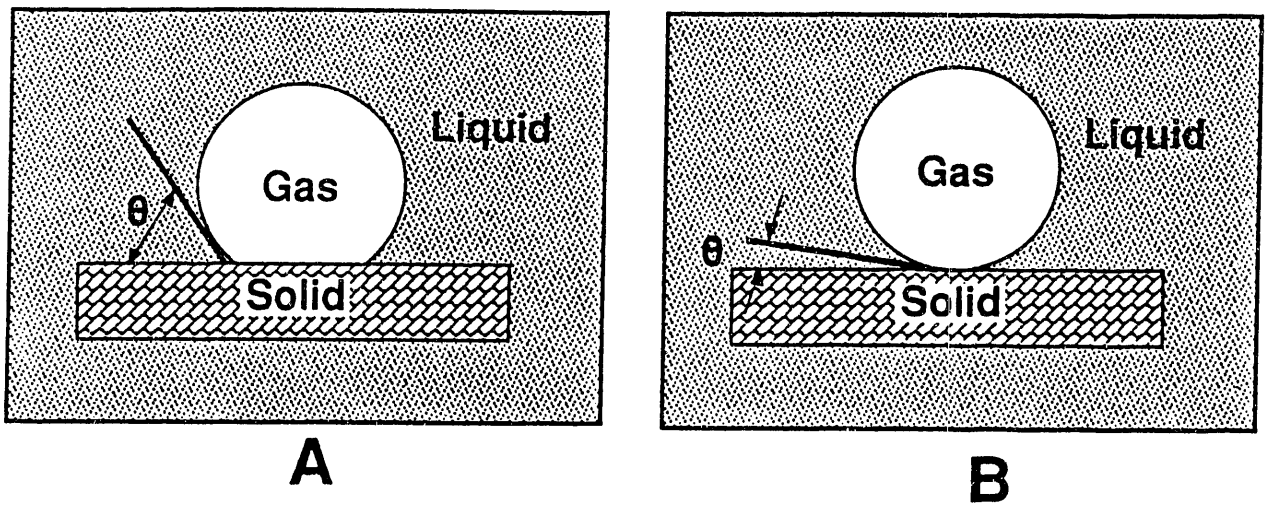

FIGURE 37. Adsorption of Organic Waste Components Lowers the Wettability of Solids, and Enhances Gas Bubble-Particle Adhesion. (A) A large contact angle is the result of reduced solids wettability with organics present. (B) Nearly complete wetting with organics absent results in a small equilibrium contact angle.

Critical conditions for the flotation of solid particles in a less dense liquid phase have been calculated by Huh and Mason (1974). Flotation is favored by a high value of the equilibrium contact angle θ, or an increasing degree of solid surface hydrophobicity. Flotation is diminished by high solid/liquid density ratios, large particle sizes, and decreases in the surface tension of the liquid phase.

7.2 FLOTATION OF PMMA BEADS

Flotation of solid particles that are more dense than the liquid phase in which they are immersed is demonstrated quite simply in Figures 38 and 39. Polymethylmethacrylate (PMMA) cylinders [typically 0.2-cm-diameter, 0.4-cm-length, density = 1.2 $g(cm)^{-3}$] were submerged in deionized water, as shown in Figure 38. Although the equilibrium contact angle was not measured, it was clear that θ was greater than zero because of the tendency of water droplets to form "beads" on the PMMA surfaces. The liquid was then sparged with

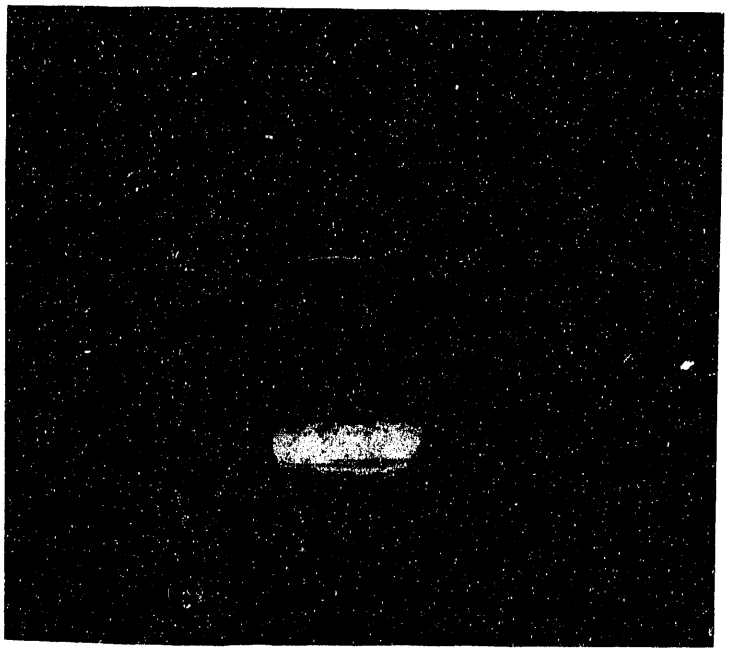

FIGURE 38. Polymethylmethacrylate (PMMA) Beads Submerged in Deionized Water Before Sparging with Gas

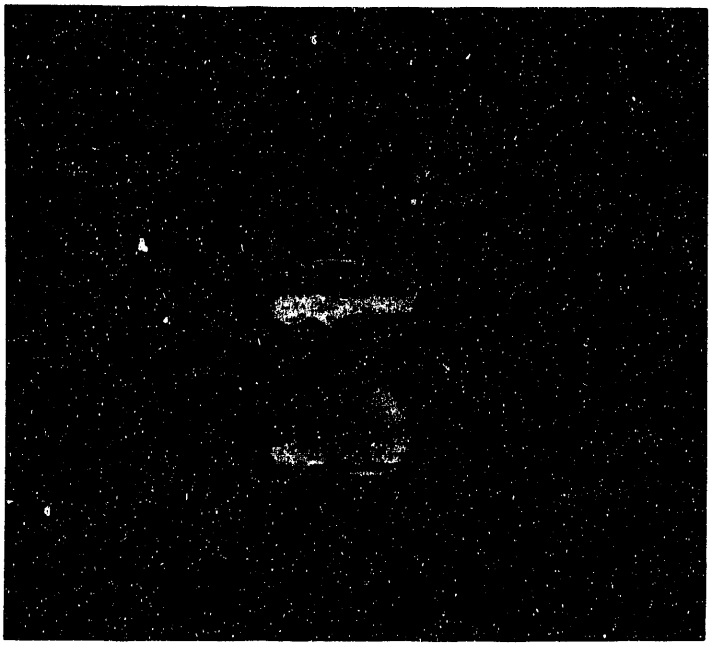

FIGURE 39. Flotation of Polymethylmethacrylate (PMMA) Beads by Attachment of Gas Bubbles from Nitrogen Sparge.

nitrogen through a glass frit. As shown in Figure 39, gas bubbles became attached to the surfaces of the PMMA beads, causing the solids to rise to the surface of the liquid.

Those PMMA beads that reached the surface were indefinitely stable in that position following the cessation of nitrogen sparging. However, those beads attached to nitrogen bubbles that were unable to reach the liquid-air interface were not indefinitely stable. Eventually, the nitrogen bubbles coalesced and were released to the atmosphere, and the PMMA beads, no longer buoyant, sank to the bottom of the beaker.

7.3 CRUST FLOTATION IN SYNTHETIC WASTE

Flotation of precipitated solids by nitrogen sparging of Tank 101-SY synthetic wastes was also demonstrated, as shown in Figures 40 and 41. Table B.11 contains the details of the components and concentrations used in this

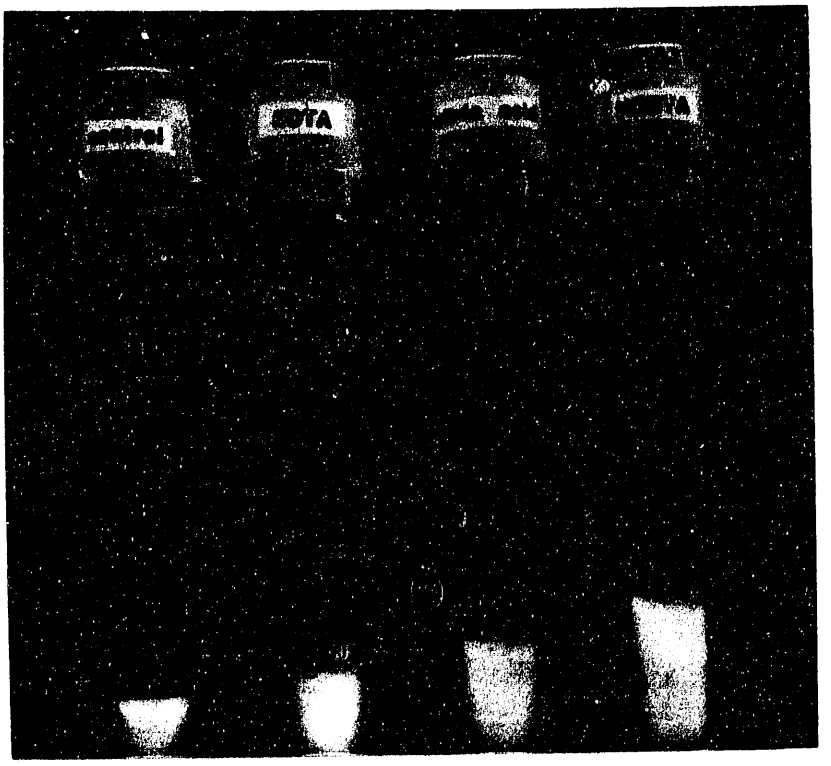

FIGURE 40. Synthetic Waste Formulations Before Sparging with Nitrogen Gas

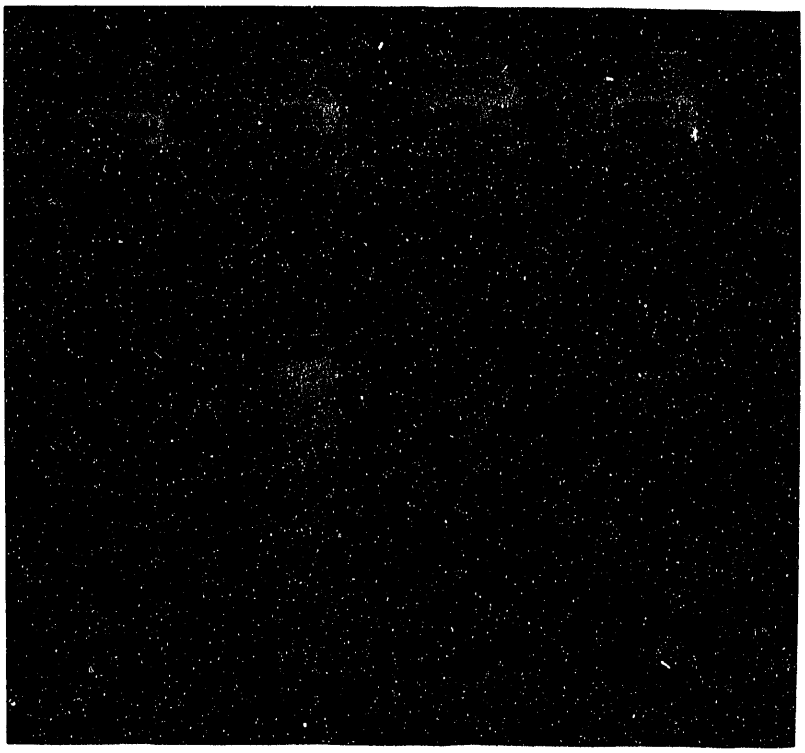

FIGURE 41. Synthetic Waste Formulations 30 Minutes After Sparging with Nitrogen Gas

formulation. This reference formulation was originally proposed by D. Herting of WHC. One solution, labeled the control in Figures 40 and 41, contained only the inorganic components. Three other solutions contained either EDTA, citric acid, or HEDTA, so that the final solution was 3.0 M in total organic carbon.

As is shown in Figure 40, the apparent volume of solids prior to nitrogen sparging was greatest for the sample containing HEDTA and least for the control (containing no organic carbon). The control gave a relatively hard monolithic solid that could be broken up only with difficulty. The other three solutions yielded solids that were easily dispersed by stirring.

The four solutions were then sparged with nitrogen gas through a glass frit and allowed to stand at room temperature for 30 minutes. A considerable quantity of precipitated solids remained in suspension in the synthetic waste containing EDTA and HEDTA, as is shown in Figure 41. Both of these samples

also produced a stable crust composed of solid particles and adhering gas bubbles. Neither the control nor the sample containing citric acid yielded a floating crust. The phenomena of bubble attachment to solids is shown dramatically in Figure 42, which shows several bubbles attached to a single particle in the organic-containing synthetic waste.

The believed role of organic constituents in the waste is to adsorb into the solid surfaces, rendering them more hydrophobic than the clean surfaces. This surface alteration enhances the tendency for gas bubbles to adhere to the

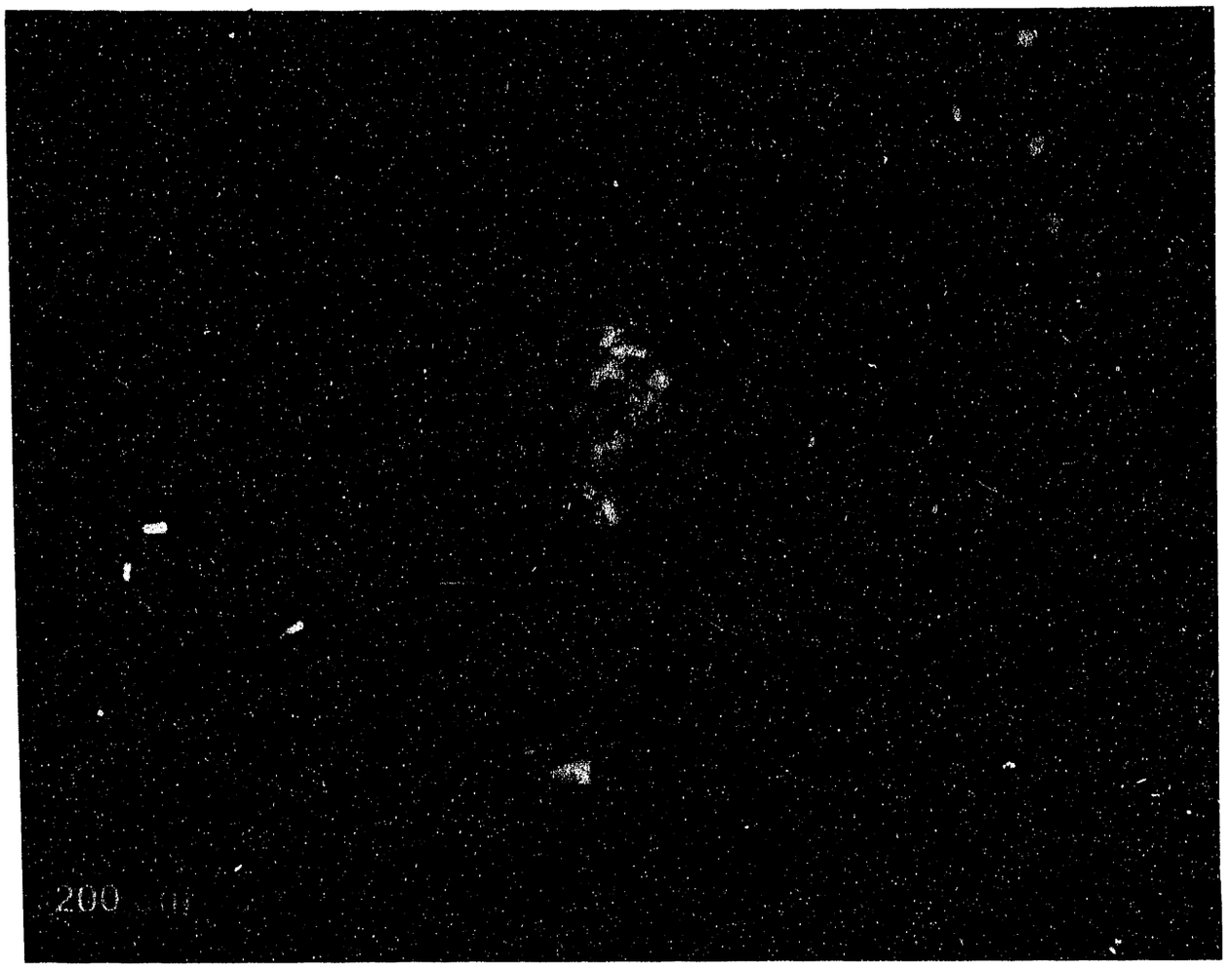

FIGURE 42. Light Micrograph of Synthetic Waste Showing the Attachment of Gas Bubbles to Solid Particles

solid particles, and may cause the solid particles to rise to the surface of the liquid. The exact nature of the solid-adsorbate bonds in strongly alkaline solutions is not known but probably involves linkage through carboxylate and/or alcohol groups for EDTA and HEDTA. The situation is, of course, complicated by the decomposition of organic chelators into other fragments in the actual waste.

It is somewhat surprising to us that citric acid was ineffective in promoting crust growth in synthetic waste, given the presence of carboxylate and alcohol groups that should form surface adsorbate bonds. It was noted, however, that NO_x was evolved when synthetic wastes containing citric acid were concentrated by heating. When citric acid was added as a solid to a solution containing only the inorganic components at 80 - 100°C, NO_x was evolved vigorously, indicating extensive oxidation of the organic molecules. Thus, the finding that citric acid did not promote crust growth may be more a result of extensive decomposition under conditions of these experiments than the ability of the citric acid to increase the hydrophobicity of solid particles through adsorption.

8.0 REFERENCES

Barker, J. J., T. M. Burke, K. G. Carothers, and D. A. Reynolds. 1991. Evaluation of October 24, 1990, Tank 241-SY-101 Gas Release Event. WHC-SD-WM-PE-041, Westinghouse Hanford Company, Richland, Washington.

Barney, G. S. 1976. Vapor-Liquid-Solid Phase Equilibria of Radioactive Sodium Salt Wastes at Hanford. ARH-ST-133, Atlantic Richfield Hanford Co., Richland, Washington.

Burger, L. L., and R. D. Scheele. 1991. The Reactivity of Cesium Nickel Ferrocyanide Toward Nitrate and Nitrite Salts. PNL-7550, Pacific Northwest Laboratory, Richland, Washington.

CRC, 1969. Handbook of Chemistry and Physics, Chemical Rubber Co., Cleveland, Ohio, p. F28-29.

Delegard, C. 1980. Laboratory Studies of Complexed Waste Slurry Volume Growth in Tank 241-SY-101. RHO-LD-124, Rockwell Hanford Operations, Richland, Washington.

Hanlon, B. M. 1990a. Tank Farm Surveillance and Waste Summary Report for June 1990. WHC-EP-0182-27, Westinghouse Hanford Company, Richland, Washington.

Hanlon, B. M. 1990b. Tank Farm Surveillance and Waste Summary Report for July 1990. WHC-EP-0182-28, Westinghouse Hanford Company, Richland, Washington.

Huh, C., and S. G. Mason. 1974. J. Colloid Interface Science 47:271.

Martin, E. C. 1985. Complexant Stability Investigation: Task 2 - Organic Complexants. PNL-5453, Pacific Northwest Laboratory, Richland, Washington.

Mauss, B. M. 1986. "101-SY Samples: Laboratory Analysis and Results." Rockwell International Internal Letter No. 65453-86-079 to L. M. Sasaki, May 30.

Meisel, D., H. Diamond, E. P. Horwitz, C. D. Jonah, M. S. Matheson, M. C. Sauer, Jr., J. C. Sullivan, F. Barnabas, E. Cerny, and Y. D. Cheng. 1991. Radiolytic Generation of Gases from Synthetic Waste. ANL-91/41, Argonne National Laboratory, Argonne, Illinois.

Pajunen, A. L. S. M. Joyce, K. G. Carothers, and T. M. Burke. 1990. Evaluation of April 19, 1990 Tank 241-SY-101 Release Event. WHC-SD-WM-DE-039, Westinghouse Hanford Company, Richland, Washington.

Reynolds, D. A., and D. L. Herting. 1984. Solubilities of Sodium Nitrate, Sodium Nitrite, and Sodium Aluminate in Simulated Nuclear Waste. RHO-RE-ST-14P, Rockwell Hanford Operations, Richland, Washington.

Strachan, D. M. 1991. Minutes of the Tank Waste Science Panel Meeting, February 7-8, 1991. PNL-7709, Pacific Northwest Laboratory, Richland, Washington.

APPENDIX A

POTENTIAL FOR MICROBIAL GAS GENERATION IN HIGH-LEVEL RADIOACTIVE WASTE STORAGE TANKS

Potential for Microbial Gas Generation in High-Level Radioactive Waste Storage Tanks

TO Stevens
JK Fredrickson
Environmental Sciences Department

December, 1990

Informal Report
Prepared for
Westinghouse Hanford Company

DSTSS91:0007

Pacific Northwest Laboratory
Richland, Washington 99352

Introduction

Generation of potentially explosive gases within high-level radioactive waste tanks at the Hanford reservation has recently become a major safety and health concern. Because the tanks contain considerable amounts of organic matter, and because the gases being produced are common microbial metabolites, this report addresses the possibility that that gas production in these waste tanks, specifically tank 101-SY, is mediated by microorganisms. We briefly review what is known about the environmental conditions within tank 101-SY, then discuss the ability of microorganisms to tolerate such conditions, especially the current knowledge of microbial resistance to radiation doses. Assuming that the production of various gases in the waste tanks represents a metabolic signature, we discuss which types of organisms which might be expected to produce them, and finally suggest some experiments which should confirm or reject microorganisms as a cause of gas generation in the high-level waste.

Conclusions and recommendations

Although many of the tank 101-SY wastes are attractive substrates for microorganisms, conditions within the tank appear to present a severe challenge to the tenacity of life. An extended adaptation period is usually required before microbial proliferation in such an extreme habitat. The quick onset of gas production, as well as it's occurrence above 100°C, in simulated waste mixtures, appears to rule out any need to invoke bacterial fermentation as a cause.

However, until samples of actual waste can be examined for the presence of microorganisms, it is not possible to completely rule out the possibility of active microbial fermentation. Three logical postulates must be fulfilled to prove that microorganisms are responsible for a given activity: microorganisms must always be present when the activity occurs, the activity must not occur in the absence of microorganisms, and transfer of microorganisms from active to inactive samples must produce activity in the previously inactive sample. If any of these postulates is not fulfilled, the activity cannot be attributed to microorganisms. Simple experiments to test these postulates in the double-shelled tank wastes are briefly outlined below. If the first test is positive, the remaining experiments should be done, otherwise microorganisms can be discounted as a cause of chemical reactions in the high-level waste tanks.

I. **Microscopic examination of waste samples**. If microorganisms do exist in the double shell waste tanks, it is likely to be in zones where they might be protected from extreme conditions. Such zones might be expected where the waste has separated into phases, such as in the upper crust, bottom sediments, or any less saline layers which may have resulted from water injection. Films along the walls of the tanks could also be potential refugia for microorganisms. Samples obtained from such zones in tank 101-SY, or similar tanks, should be examined by high-power phase-contrast and epifluorescence microscopy. Phase contrast microscopy is simple, and allows observation of living cells, but in the presence of many bacteria-sized particles, interpretation can be difficult. Epifluorescent microscopy allows the use of various fluorescent reagents that bind specifically to living cells.

II. **Sterilization of active waste samples**. If microorganisms are responsible for some component of gas production in active waste subsamples, the gas production rate or its composition should change after sterilizing treatments. An example of such a treatment would be autoclaving three times, on three successive days, with incubation at ambient temperature in between, however other methods are possible. Sterilized and non-sterilized samples should be analyzed for differences in gas composition and production.

III. **Transfer of activity by inoculation.** If some microbially-mediated reaction is eliminated by the sterilization treatment, it should be possible to transfer this activity from active samples to sterile, inactive waste samples of similar composition. Inactive samples could be obtained from experiment number 2, described above, or from preparation of sterilized "synthetic waste." A small volume (e.g. 5%) of the active sample should be transfered into the inactive sample. After a suitable incubation period, any microbiological activity present in the first sample, should be observed in the second sample. The rate of gas production and the gas composition of inoculated and uninoculated samples should be compared over time.

Environmental conditions within tank 101-SY

Information on conditions within tank 101-SY are limited, and we have based our analysis on information provided by the members of the Tank Waste Science Panel. Major waste constituents are listed in Table 1. The high organic content is composed primarily of the chelating agents citrate, HEDTA, EDTA, NTA, and breakdown products of these compounds. Significant quantities of various carboxylic acids, alkanes, and phthalates have also been detected. The temperature distribution within the tank is unclear, but average temperatures are probably near 55° C. The major obstacles to life in this slurry appear to be the extreme high pH, extreme osmotic pressure, heavy metal concentrations, and high radioactivity levels. We currently have little information on the absorptive radiation dose expected at various locations within the tank.

Gases produced in tank 101-SY include N_2O and H_2 and, based on analysis from similar tanks, presumeably CO, N_2, CO_2, CH_4, and NH_3 as well, although an exact analysis of the relative quantities is not available. This gas production began shortly after the initial addition of waste to the tank, and has continued to the present. Oxygen is consumed by the reactions in the waste slurry. Waste in the tank does not appear to be homogeneous, but the exact location of gas generation is not known.

A 1980 study using non-radioactive simulated waste mixtures demonstrated non-biological chemical evolution of N_2, N_2O, and H_2 due to oxidative degradation of HEDTA and reduction of NO_3 and NO_2. The reaction depended on high concentrations of $NaAlO_2$ and NaOH. Although these experiments appear to explain gas production in the waste mixture, the reaction rates and stoichiometry predicted by this model do not conform well to the observed phenomena in tank 101-SY.

Suitability of waste components as microbiological substrates

Components of the waste in tank 101-SY include many compounds which, under milder conditions, would unquestionably be metabolized by microorganisms. Citrate is a central metabolite in one of the most common metabolic pathways on Earth; it is an excellent substrate for most modes of life. The chelating agents EDTA and NTA are readily metabolized in aerobic environments, and their metabolism has also been demonstrated under anaerobic conditions, although it was less rapid. Long-chain carboxylic acids, alkanes, and phthalates are all potential microbial substrates. Nitrate, nitrite, ferric iron, sulfate, and bicarbonate all serve as metabolic electron acceptors under anoxic conditions, where they serve as alternatives to molecular oxygen. There is no question that, in the absence of inhibitory conditions noted above, this mixture would result in profuse fermentation resulting in large quantities of CO_2, N_2, N_2O, NH_3, H_2, H_2S, and CH_4.

Table 1. Principle Components of Tank 101-SY Samples

Total Organic Carbon	11 - 25 g/l
$NaAlO_2$	2.1 M
Cl^-	0.35 M
PO_4	0.2 M
NO_2^-	3.1 M
NO_3^-	3.1 M
$CO_3^=$	0.4 M
F^-	0.1 M
Na^+	14 M
Cr (III)	1.5 mM
Cu (II)	0.2 mM
Fe (III)	2.0 mM
Ni (II)	3.1 mM
OH^-	2.7 M

Microbial resistance to extremes of temperature, pH, and osmotic pressure

Microorganisms have adapted to almost all the extremes of environmental conditions found on Earth, although the diversity of physiological types is usually restricted under extreme conditions. Even microorganisms which are restricted to milder conditions can often colonize extreme habitats by formation of biofilms. In a biofilm, microorganisms are embedded in a polysaccharide layer (produced by one or more of the organisms) which generally becomes acidic and anoxic by the action of microbial metabolism. As long as the metabolic reactions are faster than diffusion from the bulk phase, the biofilm provides a refuge from the outer environment. In a similar manner, soils, sediments, and sludges contain microenvironments which vary widely from overall ambient conditions.

Bacteria have been observed to grow over a wide temperature range, from - 10° to well over 100°C, however growth at the extremes of this range appears to require high pressures, such as are found on the ocean floor. At atmospheric pressure, growth of thermophillic microorganisms can occur up to 90° - 95° C. Because of the changing conformation of enzymes with temperature changes, these thermophiles usually do not grow below 40° - 50°C, while most common "mesophillic" bacteria do not grow above 40°C.

The pH range of microorganisms is also quite wide. Some acidophiles can grow at pH as low as 1 - 2, while alkaliphillic bacteria can grow above pH 11. These organisms use metabolic energy to drive ion pumps which keep the cytoplasmic pH relatively neutral to outside conditions. Many organisms growing above pH 10 are restricted to high pH environments. Because many naturally existing high-pH environments are also hypersaline, many alkaliphillic bacteria are also extremely salt-tolerant (halophillic). Aerobic and anaerobic microorganisms have been observed growing in saturated salt solutions.

Relevance to Hanford waste tanks: The temperatures within tank 101-SY appear to be well within the range of microbial growth. The high concentrations of bases and salts are outside the range found in nature, and it is doubtful that microorganisms can grow in them, however heterogeneities within the waste and colonization via biofilms are mechanisms which might provide refugia where microorganisms could survive and function.

Microbial resistance to radioactivity

Nature of previous studies: Although considerable literature exists on microbial resistance to ionizing radiation, it is mostly concerned with food sterilization applications. These studies have largely consisted of treating a bacterial culture with a short, high-level radiation treatment (usually from a ^{60}Co source), then measuring recovery of the culture under subsequent radiation-free growth conditions. In addition, these studies have focused on pathogenic and food-borne organisms, and were often conducted in culture media and other artificial suspensions. Thus, although previous studies document considerable information on bacterial responses to radiation exposure, the full range of microbial responses and the effects of soil/sediment matrices on radiation dose remain unknown. Little or nothing is known about the ability of bacteria to grow during exposure to radiation, or the possibility that such conditions might select for increased radiation resistance in subsequent generations.

Range of microbial resistance: Radiation resistance of bacteria is typically measured by the D_{10} value, which is the dose required to reduce the viable population by 90%. The ability of different bacterial strains to withstand radiation exposure varies widely, even within a single genus. Many common gram-negative bacteria have D_{10} values as low as 20 Gy, in solution at room temperature, while some gram-positive bacteria can withstand several thousand Gy. Food products are irradiated at a dose of 1.5 - 3.0 kGy, which has been determined to kill most potential food-borne pathogens, without eliminating the normal bacterial flora of the food. In general, gram-positive bacteria are more resistant than gram-negative bacteria, but not as resistant as yeasts and molds (D_{10} = 3 - 10 kGy). Bacterial spores exhibit the highest radiation resistance (D_{10} = 9 - 20 kGy) under normal conditions.

Effect of environmental parameters on resistance: A number of factors appear to affect radiation-resistance in bacteria. Actively growing cultures are more resistant in some genera, while static cultures are more resistant in others. Denser cultures are more resistant than dilute cultures. Lower temperatures lead to greater resistance. In frozen foods, for example, at -80° C, *Deinococcus* sp. have a D_{10} of 24 kGy, while even enteric bacteria have a D_{10} of 3 - 6 kGy. Higher oxygen levels lead to increased sensitivity, while cells cultivated under a nitrogen atmosphere have D_{10} values 2 - 3 times lower. Water content also affects radiation resistance in different ways; aerobic cells are more resistant at higher water contents, while anaerobic cells are less resistant. Obviously association of bacterial cells with solid matter will change the effect of radiation, most likely by providing shielding, however the extent of this protection for different matrices, such as soil or sludge, is largely unknown.

Mechanism of radiation damage to microorganisms: The main lethal effect of ionizing radiation on bacteria appears to be DNA damage. Experimental evidence indicates that DNA damage is directly proportional to the radiation dose between 0.5 and 7 kGy. Calculations show that, under standard atmospheric conditions, single-strand DNA breakage occurs with an efficiency of 1 break per krad in 4 x 10^8 daltons, and double-strand breakage occurs at about 1 break per krad in 5 x 10^9 daltons. Thus survival of a targeted cell largely depends upon the size and number of copies of its genome, and the efficiency of its DNA repair mechanisms. Other cellular components, such as cell walls, structural proteins, and vital enzymes can be damaged by ionizing radiation, but since these structures can be replenished using information stored in the DNA, their loss probably does not become critical until after fatal DNA damage has already occurred.

Characteristics of radiation-resistant bacteria: The bacteria known to be most resistant to ionizing radiation have been classified in the gram-positive genus *Deinococcus* ("strange berry"), and have D_{10} values on the order of 5 kGy. A number of studies have examined the unique features of these organisms that may be responsible for their hardiness. The members of this genus produce a number of bright red carotenoid pigments, once thought to be involved in possible energy-transfer mechanisms, however nonpigmented mutants have been obtained with the same D_{10} as the parent strain. High levels of sulfhydryl compounds are produced by some strains, which may be involved in radical-trapping mechanisms. These organisms also have

complex, multi-layered cell walls and unusual lipid composition. Interestingly, some gram-negative bacteria which exhibit high radiation resistance have similar cell-wall structures and lipids. Deinococcus species posses a number of DNA repair mechanisms, however they do not possess the error-prone "SOS" system described in many common bacteria. There is evidence that they contain many copies of their chromosome, thus reducing the potential damage per radiation hit, and that the chromosomes are bound to the cell membrane by many points, thereby holding the two ends of any double-stranded DNA breaks close together to ease repair. One might expect that other organisms which share these traits might also be resistant to ionizing radiation.

Significance to Hanford waste tanks: It is clear that some bacteria can tolerate very high one-time doses of radiation, however nothing is known about how microorganisms might respond to prolonged incubation with lower doses. The absence of dosimetry data for tank 101-SY makes conclusions difficult. Little is known about what sorts of matrix effects could be expected from the waste slurry, although some degree of shielding is likely.

Microbial generation of hydrogen

Role of hydrogen in microbial metabolism: Hydrogen, as an electron sink, plays a central role in microbial metabolism. Obviously the total mass of substrates, including all atoms and electrons, absorbed by bacteria must equal the total mass converted to cell material plus the mass excreted. The excess electrons generated by oxidation of substrates must be excreted by reducing some electron-accepting compound. Generally protons (H^+) are added to some electron acceptor characteristic of the particular bacterium (e.g. O_2, NO_3, SO_4, CO_2, Fe(III)) in such a way that metabolic energy is generated. The availability of these electron acceptors largely determines which bacterial groups are active in a particular environment. Some bacteria, under appropriate conditions, can reduce these excess protons and excrete them as molecular hydrogen (H_2).

Hydrogen production by heterotrophs: A number of fermentative bacteria produce hydrogen gas as a product of organic matter fermentations under anaerobic conditions. In fermentation processes, a single substrate serves as both the carbon and electron donor and the electron acceptor. Evolution of hydrogen gas allows a more complete oxidation of the substrate, and thus more energy is derived. Compounds such as carbohydrates, amino acids, organic acids, and alcohols are fermented with subsequent production of H_2. Some recently discovered extreme thermophiles can ferment complex organic compounds completely to CO_2 and H_2 at 98°C. In most natural systems, if appropriate electron acceptors are present, other bacteria usually consume this hydrogen gas to gain additional energy. For some substrates, thermodynamic considerations prohibit production of large concentrations of hydrogen. In these cases the fermenting organism must be associated with a hydrogen consuming organism, which allows the fermentation to proceed and prevents the buildup of hydrogen. These hydrogen consuming organisms are usually methanogens, which combine acetate or CO_2 with H_2 to form methane gas. If sulfate is present, sulfate reducing bacteria are the dominant hydrogen sink, combining hydrogen and sulfate to produce sulfide.

Hydrogen production by phototrophs: Hydrogen gas can also be produced by phototrophic microorganisms; those which gain energy from light. Bacterial photosystems absorb light in the near-infra red range, however they possess numerous carotenoid pigments that can transduce energy from other wavelength ranges. Considerable study has been made of the potential of these organisms for commercial hydrogen production. Phototrophic microorganisms produce protons from water, hydrogen sulfide, or organic acids using light energy, however these reducing equivalents are usually used to fix CO_2 to organic compounds with no release of H_2 gas. Many phototrophic microorganisms however, also are able to fix atmospheric N_2 using photoproduced protons. When this nitrogenase system is induced in the absence of molecular N_2, the protons are excreted as H_2 gas. The greatest amounts of hydrogen production have been observed with the photoheterotrophic bacterium *Rhodospirillum* growing on organic acids such as acetate or lactate with amino acids as the sole nitrogen source. Phototrophic bacteria are able to grow in numerous extreme environments. In

fact, the most productive biological systems on earth are strongly alkaline brines populated by dense mats of phototrophic and other bacteria. Hydrogen production by cyanobacteria using only water as the electron donor has also been demonstrated, however at much lower levels than those observed with the photoheterotrophic bacteria.

Relevance to Hanford waste tanks: If bacteria can grow enough to produce anaerobic zones in the tanks, hydrogen production from fermentation of the organic waste is likely. Generally, higher methane and sulfide concentrations would be expected, but if methanogens and sulfate reducers are especially sensitive to conditions within the waste, it is conceivable that hydrogen-producing fermenters could dominate. Photoproduction of hydrogen is unlikely within closed tanks, unless light is produced by radioactive decay or radioactivity-induced fluorescence.

Microbial generation of N_2O, NH_4, and N_2 gases

Biological denitrification, the reduction of NO_3- and NO_2-, is the second most common mode of respiration on Earth, yielding the most metabolic energy of any common electron acceptor except oxygen. Depending on the organism, the products are N_2 gas, N_2O, or NH_4. Complete dissimilatory nitrate reduction proceeds as:

$$NO_3^- \rightarrow NO_2^- \rightarrow N_2O \rightarrow N_2$$

with various enzyme-bound intermediates not shown. Numerous organisms lack one or more enzymes of this system, and consequently excrete N_2O or NO_2^- as the major product. Because only minimal energy is available from such a reaction, N_2O generation is usually considered to be a NO_2^- detoxification mechanism, rather than an energy yielding reaction. Denitrification is an anaerobic process, but denitrifying microorganisms are facultative aerobes, and the denitrifying enzymes are strongly regulated by both the presence of the appropriate substrate and the absence of oxygen. The three major steps of denitrification have different oxygen repression thresholds. Generally, increasing oxygen leads to nitrite accumulation, and an increase in the N_2O/N_2 ratio.

In contrast to this system, assimilatory nitrate reduction incorporates the nitrogen into cell organic matter rather than producing energy. Nitrogen must enter metabolic systems at the oxidation level of NH_4^+, and assimilatory nitrate reduction usually produces glutamate.

Significant denitrification can readily be observed even in well-aerated environments such as top soils and streams, because oxygen consumption by other organisms leads to anoxic microsites within soil particles, or biofilms on surfaces. Oxygen gradients have been observed that are steep enough that air-saturated fluids are separated from denitrifying zones by 1mm or less.

Relevance to Hanford Waste tanks: All of the nitrogenous gases produced in tank 101-SY could be produced by microorganisms in well-characterized reactions. A high N_2O/N_2 ratio could be explained by several mechanisms. Extreme nitrite concentrations could drive N_2O production solely as a detoxification mechanism. The limited microbial diversity to be expected under extreme conditions could restrict the denitrifier population to a group of organisms which lack the terminal enzymes of denitrification. The extreme conditions inhibit microbial metabolism in general, leading to higher than normal oxygen concentrations (due to reduced oxygen consumption) which boosts the N_2O/N_2 ratio. Finally, some component of the waste may be an inhibitor of the final N_2O reducing enzyme, leading to N_2O accumulation.

Bibliography

Anellis, A.; Berkowitz, D.; Kemper, D. Comparative resistance of nonsporogenic bacteria to low-temperature gamma irradiation. Applied and Environmental microbiology.; 1973; 25(4): 517-523.

Buranakarl, L.; Fan, C.Y.; Ito, K.; Izaki, K.; Takahashi, H. Production of molecular hydrogen by photosynthetic bacteria with raw starch. Agricultural and biological chemistry; 1985; 49(11): 3339-3341.

Delegard, Calvin. Laboratory studies of complexed waste slurry volume growth in tank 241-SY-101; Dec 1980 Rockwell International; RHO-LD-124. 21 pp.

Dickson, J.S; Maxcy, R.B. Enumeration of radiation-resistant, nonsporeforming bacteria. Journal of food science.; Jan/Feb 1985; 50(1): 268-269

Edwards, R.B; Peterson, L.J.; Cummings, D.G. The effect of cathode rays on bacteria. Food technology.; June 1954; 8(6): 284-290

Embley, T.M.; O'Donnell, A.G.; Wait, R.; Rostron, J. Lipid and cell wall amino acid composition in the classification of members of the genus Deinococcus Syst. Appl. Microbiol.; 1987; 64: 20-27.

Francou, N.; Vigais, P.M. Hydrogen production by Rhodopseudomonas capsulata cells entrapped in carrageenan beads. Biotechnology Letters; 1984; 6(10): 639-644

Grant, I.R; Patterson, M.F. A novel radiation-resistant Deinobacter sp. isolated from irradiated pork. Letters in applied microbiology.; 1989; 8(1): 21-24

Hastings, J.W., W.H. Holzapfel, and J.G. Niemand. Radiation resistance of lactobacilli isolated from radurized meat relative to growth and environment. Appl. Environ. Microbiol.; 1986; 52(4): 898-901.

Keller, L.C; Maxcy, R.B. Effect of physiological age on radiation resistance of some bacteria that are highly radiation resistant. Applied and environmental microbiology.; 1984; 47(5): 915-918.

Kim, J.H; Stegeman, H.; Farkas, J. Preliminary studies on radiation resistance of thermophilic anaerobic spores and the effect of gamma radiation on their heat resistance. International journal of food microbiology.; 1987; 5(2): 129-136;

Koh, Won Young; Morehouse, Catherine T.; Chandler, Velma L. Relative resistances of microorganisms to cathode rays I. Nonsporeforming bacteria. Applied and Environmental Microbiology; 1956; 4(3): 143-146.

Kuwada, Y., M. Nakatsukasa, Y. Ohta. Isolation and characterization of a nonheterocystous cyanobacterium, Lyngbya sp. isolate no. 108 for large-quantity hydrogen production. Agr. Biol. Chem.; 1988; 52(8): 1923.

Lambert, J.D; Maxcy, R.B. Effect of gamma radiation on Campylobacter jejuni. Journal of food science.; 1984; 49(3): 665-674.

Lancy, Pl; Murray, R.G.E. The envolopc of Micrococcus radiodurans: isolation, purification, and preliminary analysis of the wall layers . Can. J. Microbiol.; 1977 24: 162-176.

Liuzzo, J.A; Novak, A.F.; Ortego, J.R. Physiological changes induced by gamma irradiation of bacteria from shrimp. Journal of food science.; 1965; 30(4): 710-713

Ma, K.; Maxcy, R.B. Factors influencing radiation resistance of vegetative bacteria and spores associated with radappertization of meat. Journal of food science.; 1981; 46(2): 612-616.

Macler, B.A., J.A. Bassham. Carbon allocation in wild-type and Glc+ Rhodobacter sphaeroides under photoheterotrophic conditions. Appl. Environ. Microbiol.; 1988; 54: 2727-2741.

Madigan, Michael T. Microbiology, physiology, and ecology of phototrophic bacteria. 1988. in A.J.B. Zehnder (ed) Biology of anaerobic microorganisms. John Wiley & Sons, Inc.

Maxcy, R.B. Irradiation of food for public health protection. Journal of food protection.; 1982; 45(4): 363-366.

Moseley, B.E.B. Photobiology and radiobiology of Micrococcus (Deinococcus) radiodurans. Photochem. Photobiol. Rev.; 1982; 7: 233-274.

Nishimura, Y.; Ino, T.; Iizuka, H. Acinetobacter radioresistens sp. no.v isolated from cotton and soil [research paper]. Int. J. Syst. Bacteriol.; 1988; 38: 209-211.

Oyaizu, H.; Stackebrandt, E.; Schleifer, K.H.; Ludwig, W.; Pohla, H.; Ito, H.; Hirata, A.; Oyaizu, Y.; Komagata, K. A radiation-resistant rod-shaped bacterium, Deinobacter grandis gen. nov. sp. nov., with peptidoglycan containing ornithine Int. J. Syst. Bacteriol.; 1987; 37: 62-67.

Palumbo, S.A; Jenkins, R.K.; Buchanan, R.L.; Thayer, D.W. Determination of irradiation D-values for Aeromonas hydrophila. Journal of food protection.; 1986; 49(3): 189-191

Pepper, Rollin E.; Buffa, Nancy T.; Chandler, Velma L. Relative resistances of microorganisms to cathode rays III. Bacterial spores. Applied and Environmental Microbiology; 1956; 4(3): 149-152.

Raghavendra, A.S.; Vallejos, R.H. Photobiological production of hydrogen (Bacteria, algae). Gnanam, A.; Krishnaswamy, S.; Kahn, Joseph S. Proceedings of the International Symposium on Biological Applications of Solar Energy; 1978: S.G. Wasani for the Macmillan Co. of India; 1980: 193-195.

Sasaki, L.M.; Mauss, B.M. 101-SY Samples: Laboratory analysis and results Rockwell International Internal Letter 65453-86-079

Sleytr, U.B.; Silva, M.T.; Kocur, M.; Lewis, N.F. The fine structure of Micrococcus radiophilus and Micrococcus radioproteolyticus. Arch. Microbiol; 1976; 107: 313-320.

Strachan, D.M.; Reynolds, D.A.; Siemer, D.D.; Wallace, R.W.. A survey of available information on gas generation in tank 241-SY-101: Pacific Northwest Laboratory; Sep 1990; contract DE-AC06-76RLO 1830.

Stouthamer, Adriaan H. Dissimilatory reduction of oxidized nitrogen compounds. 1988. in A.J.B. Zehnder (ed) Biology of anaerobic microorganisms. John Wiley & Sons, Inc.

Tallentire, A. The spectrum of microbial radiation-sensitivity.Radiat. Phys. Chem.; 1980; 15: 83-89.

Thayer, D.W.; Boyd, G.; Muller, W.S.; Lipson, C.A.; Hayne, W.C.; Baer, S.H. Radiation Resistance of Salmonella. Journal of Industrial Microbiology; 1990 Aug; 5(6): 383-390.

Tiedje, James M. Ecology of denitrification and dissimilatory nitrate reduction to ammonium. 1988. in A.J.B. Zehnder (ed) Biology of Anaerobic Microorganisms. John Wiley & Sons, Inc.

Vatsala, T.M.; Seshadri, C.V. Microbial production of hydrogen: a review. Proceedings of the Indian National Science Academy. Part B: Biological sciences; 1985; 51(2): 282-295;.

Weaver, P.F. Photoconversion of organic substrates into hydrogen using photosynthetic bacteria (Production of fuel gas). Energy from biomass and wastes symposium papers.; Apr 1981; 5: 489-497.

Welch, Ardyce B.; Maxcy, R.B. Characteristics of some radiation-resistant hemolytic micrococci isolated from chicken. Journal of food science; 1979; 44(3): 673-675.

APPENDIX B

TABLES CITED

APPENDIX B

TABLES CITED

TABLE B.1. Tanks with Potential for Hydrogen or Flammable Gas Generation[a]

Tank Number	Maximum Temperature (°F)	Probe Position	Date
101-A	158	TC	06/04/90
101-AX	145	TC	01/01/90
103-AX	117	TC	06/09/90
102-S	104	TC	06/04/90
111-S	100	TC	02/05/88
112-S	93	TC	02/05/88
101-SX	137	TC	06/04/90
102-SX	147	TC	06/04/90
103-SX	164	TC	06/04/90
104-SX	161	TC	06/04/90
105-SX	173	TC	06/04/90
106-SX	98	TC	06/04/90
109-SX[b]	150	TC	06/07/90
110-T	64	TC	07/03/89
103-U	87	TC	07/01/89
105-U	89	TC	07/01/89
108-U	87	TC	07/01/89
109-U	85	TC	07/01/89
103-AN[c]	111	TC	06/25/90
104-AN[c]	112	TC	06/25/90
105-AN[c]	109	TC	06/25/90
101-SY[c]	137	TC	06/07/90
103-SY[c]	107	TC	06/26/90
23 Tanks			

(a) From Hanlon 1990.
(b) On list because other tanks on list vent through it.
(c) Double-shell tanks.

TABLE B.2. Tank 101-SY Fill Record[a]

Fill Type	Date	Inches Added
Double Shell Slurry	April 25, 1977	100.1
Evaporator Run From 102-SY, Complexant Concentrate	November 1, 1977	132.75
Transfer From 106-SX	June 25, 1978	48.4
Transfer From 111-U	August 14, 1978	21.6
Double Shell Slurry	October 29, 1980	84.0
Total inches		386.85
Maximum Height (inches)		414.5 (March 1981)
Maximum Growth (inches)		27.65 (7.1%)

(a) From Simpson 1984.

TABLE B.3. Tank 101-SY Total Initial Composition[a]

Component	Concentration, M
NaOH	3.22
$NaAlO_2$	1.90
$NaNO_2$	3.28
$NaNO_3$	4.23
Na_2CO_3	0.62
Na_2SO_4	0.12
Na_3PO_4	0.19
TOC	2.19
Pu	713 (g)
Sr	2.187×11^{11} (μCi)
Cs	3.102×10^{12} (μCi)
H_2O	594,600 (gal)

(a) From Simpson 1984.
Note: The concentrations are based on an average tank volume of 408 inches in 1984.

TABLE B.4. Analyses of Tank 101-SY Samples[a]

	Top Sample Molarity	Middle Sample Molarity	Bottom Sample Molarity
NO_3^-	1.46	3.09	3.07
NO_2^-	1.34	3.06	2.96
OH^-	1.17	2.66	2.33
Al	0.71	2.09	2.24
Na	7.35	14.30	16.16
CO_3^{2-}	0.45	0.39	0.90
SO_4^{2-}	0.03	<0.07	<0.13
PO_4^{3-}	0.06	0.17	0.13
F^-	<0.08	<0.16	<0.16
Cl^-	0.15	0.34	0.34
K	0.0565	0.14	0.13
NH_3	NA[b]	NA	NA
TOC	0.93	1.59	2.11
HEDTA	0.0176	0.0230	<0.0162
EDTA	<0.00905	<0.0181	0.043
^{137}Cs (μCi/L)	2.88×10^5	1.20×10^6	6.66×10^5
^{90}Sr (μCi/L)	6.05×10^3	7.20×10^3	1.35×10^4
SpG	1.33	1.29	1.69
B	0.00334	0.0081	0.00755
Ca	0.00314	0.00515	0.00711
Cr	0.00189	0.000925	0.00066
Fe	NA[b]	NA	NA
La	NA	NA	NA
Mg	NA	NA	NA
Mn	NA	NA	NA
Mo	NA	NA	NA
Ni	0.00257	0.00235	0.000654
Si	NA	NA	NA
Zn	NA	NA	NA
Zr	NA	NA	NA

(a) From Mauss 1986.
(b) NA = not analyzed.

TABLE B.5. Tank 103-SY Total Initial Composition[a]

Component	Concentration, M
NaOH	2.78
$NaAlO_2$	2.65
$NaNO_2$	4.22
$NaNO_3$	4.22
Na_2CO_3	0.283
TOC	2.46
H_2O	266,130 gal

(a) From Simpson 1984.
Note: The concentrations are based on a 1984 average tank depth of 109 inches.

TABLE B.6. Analyses of Tank 103-SY Samples[a]

Component	#2 (M)[b]	#7 (M)[c]	#12 (M)[d]
NO_3^-	2.45	2.48	7.10
NO_2^-	2.76	2.65	2.80
OH^-	2.10	2.06	1.55
Al	2.51	2.37	3.11
Na	14.3	13.9	22.7
CO_3^{2-}	0.415	0.693	0.716
SO_4^{2-}	0.038	0.074	0.070
PO_4^{3-}	0.050	0.062	0.078
F^-	<0.12	<0.12	<0.10
Cl^-	0.313	0.295	0.263
K	0.148	0.134	0.117
NH_3	NA[e]	NA	NA
TOC	NA	NA	NA
HEDTA	NA	NA	NA
EDTA	NA	NA	NA
^{137}Cs (μCi/L)	7.52×10^5	7.36×10^5	6.09×10^5
^{90}Sr (μCi/L)	NR[f]	NR	NR
ρ, (g/ml)	1.52	1.54	1.76 ± 0.16
B	0.021	0.017	0.014
Ca	0.0076	0.010	0.0070
Cr	0.088	0.175	0.196
Fe	0.026	0.044	0.063
La	0.0002	0.0005	0.0002
Mg	0.0006	0.0019	0.0007
Mn	0.0064	0.013	0.016
Mo	0.0021	0.0019	0.0016
Ni	0.002	0.003	0.004
Si	0.0087	0.019	0.038
Zn	ND[g]	0.0009	0.011
Zr	0.0003	0.0005	0.0004

(a) From Fow et al. 1984.
(b) #2 is upper (190-209 inch) sample.
(c) #7 is middle (95-114 inch) sample.
(d) #12 is a bottom (0-19 inch sample.
(e) NA = not analyzed.
(f) NR = not reported.
(g) ND = not detectable.

TABLE B.7. Analysis of Interstitial Liquid in Tank 103-SY Composite Slurry[a]

Component	Molarity
NO_3^-	2.34
NO_2^-	3.27
OH^-	2.26
Al	2.30
Na	11.3
CO_3^{2-}	0.235
SO_4^{2-}	<0.0145
PO_4^{3-}	0.0221
F^-	0.200
Cl^-	0.503
TOC	1.31
Cr	0.0143
Fe	$<1.19 \times 10^{-3}$
ρ (g/mL)	1.54

(a) From Prignano (1988). This is a composite of core samples from the 19 to 95 inch level.

TABLE B.8. Analysis of Tank 103-AN Composite Slurry[a]

Component	Molarity
NO_3^-	1.84
NO_2^-	2.54
OH^-	5.6
Al	2.61
Na	16.1
CO_3^{2-}	0.145
SO_4^{2-}	0.029
PO_4^{3-}	0.0148
F^-	0.0172
Cl^-	0.236
K	0.36
NH_3	0.020
TOC	0.42
HEDTA	NA
EDTA	NA
^{137}Cs (μCi/L)	7.55×10^5
^{90}Sr (μCi/L)	2.44×10^4
ρ (g/ml)	1.56
B	NA[b]
Ca	0.0037
Cr	0.018
Fe	0.0022
La	NA
Mg	0.0016
Mn	0.00070
Mo	0.00081
Ni	0.00053
Si	0.0162
Zn	0.0012
Zr	0.00034
Cu	0.00012
V	0.0031

(a) From Toste 1987.
(b) NA = not analyzed.

TABLE B.9. Analysis of Tank 105-AN Composite Slurry[a]

Component	Molarity
NO_3^-	2.17
NO_2^-	1.36
OH^-	2.22
Al	0.94
Na	7.85
CO_3^{2-}	0.453
SO_4^{2-}	(b)
PO_4^{3-}	0.015
F^-	(a)
Cl^-	0.018
K	0.093
NH_3	0.010
TOC	3.36[c]
HEDTA	0.002
EDTA	0.003
^{137}Cs (μCi/L)	3.60×10^5
^{90}Sr (μCi/L)	2.24×10^3
Sp. Grav.	1.434
% H_2O	54.7

(a) From Mauss 1984.
(b) Below detection limit.
(c) See text.

TABLE B.10. Reported Total Organic Carbon in Single Shell Tanks on the Hydrogen Watch List

Waste Tank Number	Waste Type[a]	TOC Based on Waste Phase(s)[b]	TOC M C[b]
101-A	DSSF	liquid	1.12
101-AX	DSSF	liquid	1.03
103-AX	CPLX	liquid	0.90
111-S	NCPLX	solid and liquid	0.35
101-SX	CPLX	liquid	0.033
102-SX	DSSF	liquid	1.06
104-SX	DSSF	liquid	0.42
103-U	NCPLX	solid	0.8
105-U	NCPLX	solid	3.71

(a) From Hanlon (1990a,b). DSSF = Double-Shell Slurry Feed, CPLX = Complexed Waste, NCPLX = Non-Complexed Waste.
(b) From Klem (1990).

TABLE B.11. Compositions of Synthetic Waste Formulations

Component	Reference Formulation		WHC Formulation	
	M	Wt%	M	Wt%
$NaAlO_2$	2.1	10.7	2.2	16.5
Na_4EDTA	0.17	4.0	0.3[a]	7.6
Na_3HEDTA	0.35	8.3	--	--
NaCl	0.35	1.3	--	--
Na_3PO_4	0.20	3.3	--	--
$NaNO_2$	3.1	13.3	3.2	14.5
$NaNO_3$	3.1	16.4	3.7	20.7
Na_2CO_3	0.4	2.6	0.6	4.2
NaF	0.1	0.26	--	--
NaOH	2.9	7.2	2.3	6.1
$Cr(NO_3)_3$	$1.5x10^{-3}$	0.04	--	--
$Cu(NO_3)_2$	$2.1x10^{-4}$	0.00	--	--
$Fe(NO_3)_3$	$2.0x10^{-3}$	0.05	--	--
$Ni(NO_3)_2$	$3.1x10^{-3}$	0.06	--	--

(a) Total HEDTA and EDTA concentration is 0.3M.

TABLE B.12. Compositions of Samples used in Safety Study

Sample #	Component (g)							
	Na_4EDTA	Na_3HEDTA	$NaNO_3$	$NaNO_2$	$Cr(NO_3)_3$	$Cu(NO_3)_2$	$Fe(NO_3)_3$	$Ni(NO_3)_2$
1	0.21		0.85	0.69				
2		0.43	0.85	0.69				
3	0.10		0.85	0.69				
4		0.21	0.85	0.69				
5	0.42		0.85	0.69				
6		0.86	0.85	0.69				
7	0.21		0.85	0.69	1.9E-3	1.6E-4	2.6E-3	2.9E-3
8		0.43	0.85	0.69	1.9E-3	1.6E-4	2.6E-3	2.9E-3
9	0.10		0.85	0.69	1.9E-3	1.6E-4	2.6E-3	2.9E-3
10		0.21	0.85	0.69	1.9E-3	1.6E-4	2.6E-3	2.9E-3
11	0.42		0.85	0.69	1.9E-3	1.6E-4	2.6E-3	2.9E-3
12		0.86	0.85	0.69	1.9E-3	1.6E-4	2.6E-3	2.9E-3
13[a]	0.42	0.86	0.85	0.69	1.9E-3	1.6E-4	2.6E-3	2.9E-3

(a) Sample #13 also contains all of the inert components in their appropriate ratios as found in the "High $NaAlO_2$/High Organic" recipe in Table 11.

TABLE B.13. Thermodynamic Calculations of Reactions Between EDTA and HEDTA with Nitrite and Nitrate

$C_{10}H_{16}N_2O_8$ = EDTA

$C_{10}H_{18}N_2O_7$ = HEDTA

$C_{10}H_{16}N_2O_8 + 8\ HNO_3 \longrightarrow 10\ CO_2 + 5\ N_2 + 12\ H_2O$

ΔH_{rxn} = -1540 Kcal/mole EDTA

$C_{10}H_{18}N_2O_7 + 8.8\ HNO_3 \longrightarrow 10\ CO_2 + 5.4\ N_2 + 13.4\ H_2O$

ΔH_{rxn} = -1613 Kcal/mole HEDTA

$C_{10}H_{16}N_2O_8 + 13.33\ HNO_2 \longrightarrow 10\ CO_2 + 7.66\ N_2 + 14.66\ H_2O$

ΔH_{rxn} = -1738 Kcal/mole EDTA

$C_{10}H_{18}N_2O_7 + 14.66\ HNO_2 \longrightarrow 10\ CO_2 + 8.33\ N_2 + 16.33\ H_2O$

ΔH_{rxn} = -1830 Kcal/mole HEDTA

For "High Organic" compositions from Table 1, the total heat released per liter of solution is calculated to be 957 Kcal. This takes into account that the nitrate and nitrite are the limiting reagents and are based on the heats of reaction within the Table.

For the "Reference Recipe" from Table 1, the total heat released per liter of solution is calculated to be 872 Kcal. The HEDTA and the EDTA are the limiting reagents.

For the "Low Organics" compositions from Table 1, the total heat generated per liter of solution is 459 Kcal. The EDTA and HEDTA are the limiting reagents in this case.

TABLE B.14. Analyzed Concentration of Anions in Sample, Day 0

Relative Concentration in Initial Formulation		Fluoride, Wt%	Chloride, Wt%	Nitrite, Wt%	Nitrate, Wt%	Phosphate, Wt%
$NaAlO_2$	Organic					
Supernate						
0.5	0.5	0.1	1.2	10.8	9.6	0.5
0.5	1.5	0.1	1.2	9.2	8.9	0.9
1	1	0.1	1	9.3	8.4	0.5
1.5	0.5	0.1	1.2	9.2	8.5	0.7
1.5	1.5	0.1	1	9.6	8.6	0.6
Solids						
0.5	0.5	0.2	1	10.6	9.6	1.7
0.5	1.5	0.3	0.8	11.2	17	2
1	1	0.1	0.7	9.4	16.5	0.6
1.5	0.5	0.3	1	8.9	8.3	2.3
1.5	1.5	0.1	0.7	15.5	13	1

TABLE B.15. Analyzed Concentration of Anions in Sample, Day 16

Relative Concentration in Initial Formulation		Fluoride, Wt%	Chloride, Wt%	Nitrite, Wt%	Nitrate, Wt%	Phosphate, Wt%
$NaAlO_2$	Organic					
Crust						
0.5	0.5	0.2	0.7	8.2	30.5	1.2
0.5	0.5	0.2	0.7	8.8	32	1.6
0.5	1.5	0.3	1.4	8.8	11.3	0.9
0.5	1.5	0.1	1.4	9	13.1	0.9
1	1	0.1	3	6.8	4.8	0.9
1.5	0.5	0.1	1	8.2	7.9	3.4
1.5	0.5	0.1	1	8.4	8.5	0.9
1.5	1.5	0.1	1.7	9.7	11.1	1.9
1.5	1.5	0.1	1.2	9.4	12	1.5
Supernate						
0.5	0.5	0.1	1	11.4	15.3	1.1
0.5	0.5	0.1	1	11.2	14.7	1.1
1	1	0.1	1.1	9.4	8.2	0.8
1	1	0.1	0.9	11.2	10.1	0.9
1.5	0.5	0.1	1.2	10.4	10	1.3
1.5	0.5	0.1	1.2	10.2	9.8	1.3
1.5	1.5	0.1	1	10.9	12.2	0.6
1.5	1.5	0.1	1	11.6	13.2	0.7
Solids						
0.5	0.5	0.4	0.9	10.5	13.6	2.3
0.5	0.5	0.4	1	10.8	14.2	2.2
0.5	1.5	0.1	0.9	10	13	1.3
0.5	1.5	0.1	1	9.7	12.5	1.7
1	1	0.5	0.6	6.9	6.1	4.8
1	1	0.5	0.8	9.1	7.4	4.4
1.5	0.5	0.3	0.7	13.5	27	1.7
1.5	0.5	0.3	0.9	9.1	9.3	2.6
1.5	1.5	0.1	0.9	8.9	10.8	1.2
1.5	1.5	0.2	0.9	9.1	11.4	1.4

TABLE B.16. Analyzed Concentration of Anions in Sample, Day 41

Relative Concentration in Initial Formulation		Fluoride,	Chloride,	Nitrite,	Nitrate,	Phosphate,
$NaAlO_2$	Organic	Wt%	Wt%	Wt%	Wt%	Wt%
Crust						
0.5	0.5	0.1	0.6	7.9	34	1.5
0.5	0.5	0.1	0.8	8.6	32	2.7
0.5	1.5	0.1	1.5	9	14.5	8.5
0.5	1.5	0.15	1.6	9	12	0.5
1	1	0.05	3	6.5	4.2	0.5
1	1	0.05	0.95	20.5	9	0.3
1.5	0.5	0.1	1.1	8	7.5	1.2
1.5	0.5	0.1	2.9	8.6	8.5	3
1.5	1.5	0.05	0.95	11.5	26	0.3
1.5	1.5	0.05	0.6	11	30.5	0.3
Supernate						
0.5	0.5	0.1	1	11.7	15	1.1
0.5	0.5	0.1	1	11.3	14.5	1.1
1	1	0.05	0.9	12	9	0.3
1	1	0.05	0.85	12	10.5	0.6
1.5	0.5	0.1	1.1	11.5	10.8	ND
1.5	0.5	0.1	0.9	12.1	11.3	ND
1.5	1.5	0.05	0.9	13.5	11.5	0.3
1.5	1.5	0.05	0.95	13.5	11	0.4
Solids						
0.5	0.5	0.4	0.9	10.9	12.7	2.2
0.5	0.5	0.4	0.9	11.3	13	2.3
0.5	1.5	0.1	0.95	10	11	1.1
0.5	1.5	0.1	0.8	9.3	12.3	1.5
1	1	0.35	0.95	8	6.6	3.6
1	1	0.25	0.85	10.5	9	2.5
1.5	0.5	0.5	0.7	8.4	8.4	2.8
1.5	0.5	0.1	0.9	10.1	10.1	2
1.5	1.5	0.1	0.75	7	18	1.1
1.5	1.5	0.1	0.8	8	11.5	1.3

TABLE B.17. Analyzed Concentration of Anions in Sample, Day 66

Relative Concentration in Initial Formulation		Fluoride, Wt%	Chloride, Wt%	Nitrite, Wt%	Nitrate, Wt%	Phosphate, Wt%
$NaAlO_2$	Organic					
Crust						
0.5	0.5	0.3	0.9	10	14	3
0.5	0.5	0.3	1	11.5	16	2
0.5	1.5	0.1	1	17	19	0.6
0.5	1.5	0.1	0.8	8	9	1
1	1	0.1	2.5	9.1	8.1	1
1	1	0.1	1	15.1	13.7	0.6
1.5	0.5	0.1	1.3	11.8	13.9	0.7
1.5	0.5	0.1	1.9	14.9	12.8	0.7
1.5	1.5	0.1	1.2	15	21	0.4
1.5	1.5	0.1	0.9	15	21	0.8
Supernate						
0.5	0.5	0.1	1.3	8.2	7.7	0.6
0.5	0.5	0.1	1.4	8.7	8	0.4
1	1	0.1	0.8	5.9	5.6	0.5
1	1	0.1	0.8	7.4	6.9	0.5
1.5	0.5	0.1	0.9	6.7	6.6	0.4
1.5	0.5	0.1	0.9	6.8	6.4	0.5
Solids						
0.5	0.5	0.2	0.5	9.9	36	1.1
0.5	0.5	0.2	0.6	11.5	25	3.3
0.5	1.5	0.1	0.9	9.2	11	1.2
0.5	1.5	0.1	1.4	22	26	1.1
1	1	0.5	1.1	10.1	9.2	5.5
1	1	0.4	0.8	9.2	8.9	4.2
1.5	0.5	0.1	0.8	9.2	13	2.8
1.5	0.5	0.6	0.5	7.5	17	3.7
1.5	1.5	0.1	0.9	9.1	10	1.2
1.5	1.5	0.1	0.9	9.3	10	1.3

TABLE B.18. Analyzed Concentration of Anions in Facies of Reference Formulation, Day 66

Relative Concentration in Initial Formulation		Fluoride,	Chloride,	Nitrite,	Nitrate,	Phosphate,
$NaAlO_2$	Organic	Wt%	Wt%	Wt%	Wt%	Wt%
Crust						
1	1	0.1	1	12.4	12.7	ND
1	1	0.1	0.9	11	8.7	0.5
Supernate						
1	1	0.1	0.7	11.9	11.4	0.5
1	1	0.1	0.7	12	11.3	0.5
Upper Solids						
1	1	0.1	1.2	14.5	12.5	1
1	1	0.1	1.3	12.7	12.7	0.9
Mid Solids						
1	1	0.5	0.5	8.8	8.2	5.2
1	1	0.5	0.7	8.4	7.5	5.3
Lower Solids						
1	1	0.1	0.2	20.8	35	0.8
1	1	0.1	0.3	25.1	30	0.7

TABLE B.19. Analyzed Concentration of Elements in Sample, Day 0

Relative Concentration in Initial Formulation		Aluminum,	Chromium,	Copper,	Iron,	Sodium,	Nickel,	Phosphorus,
$NaAlO_2$	Organic	Wt%	Wt%	Wt%	Wt%	Wt%	Wt%	Wt%
Unheated Cetrifuged Supernate								
0.5	0.5	1.738	0.0019	0.0013	0.0033	17.62	0.01619	0.0714
0.5	1.5	1.595	0.0055	0.0014	0.006	18	0.0145	0.0445
1	1	3.595	0.00579	0.0014	0.0063	18.42	0.006842	0.0205
1.5	0.5	3.195	0.0007	0.0013	0.0059	18.64	0.015909	0.0841
1.5	1.5	3.305	0.005	0.0015	0.0065	18	0.0055	0.039
Unheated Cetrifuged Solids								
0.5	0.5	1.474	0.00579	0.0011	0.0105	19.47	0.013684	0.4716
0.5	1.5	1.131	0.00462	0.0008	0.0085	19.62	0.010385	0.5038
1	1	2.111	0.00421	0.0009	0.01	21.58	0.009474	0.3437
1.5	0.5	4.394	0.005	0.0012	0.0119	19.38	0.014375	0.3931
1.5	1.5	3.109	0.00364	0.001	0.0136	22.73	0.015	0.5364

TABLE B.20. Analyzed Concentrations of Elements in Sample, Day 16

Relative Concentration in Initial Formulation		Aluminum, Wt%	Chromium, Wt%	Copper, Wt%	Iron, Wt%	Sodium, Wt%	Nickel, Wt%	Phosphorus, Wt%
$NaAlO_2$	Organic							
Crust Samples								
0.5	0.5	1.247	0.00418	0.0009	0.0071	26.06	0.010588	0.3824
0.5	0.5	1.432	0.00384	0.0009	0.0079	26.21	0.013158	0.4421
0.5	1.5	1.191	0.00415	0.0011	0.0071	22.95	0.011067	0.308
0.5	1.5	1.17	0.00437	0.001	0.0061	22.28	0.010591	0.3095
1	1	2.088	0.00294	0.0009	0.0047	21.18	0.005882	0.0694
1.5	0.5	6.75	0.00491	0.0011	0.0167	22.16	0.012692	0.5042
1.5	0.5	7.129	0.00473	0.0012	0.017	24.41	0.013524	0.2935
1.5	1.5	3.778	0.00326	0.0007	0.0097	22.17	0.005722	0.1511
1.5	1.5	3.626	0.00364	0.0009	0.008	22.05	0.006971	0.2152
Supernate Samples								
0.5	0.5	1.583	0.00506	0.0012	0.0033	21	0.013889	0.2889
0.5	0.5	1.6	0.00483	0.0008	0.005	21.33	0.013333	0.3056
1	1	3.714	0.00591	0.0013	0.0055	19.55	0.009091	0.
1	1	3.773	0.00654	0.0016	0.0058	20.38	0.010385	0.1615
1.5	0.5	3.663	0.00597	0.0012	0.0071	22.03	0.015533	0.3224
1.5	0.5	3.614	0.0059	0.0013	0.0073	21.71	0.015374	0.3417
1.5	1.5	2.922	0.00482	0.001	0.0048	21.29	0.00922	0.221
1.5	1.5	2.996	0.00552	0.0012	0.005	22.22	0.010705	0.21
Solid Samples								
0.5	0.5	1.567	0.0068	0.0012	0.0193	24.2	0.013333	0.7267
0.5	0.5	1.469	0.0065	0.0006	0.0156	22.81	0.011875	0.6438
0.5	1.5	1.288	0.00454	0.0007	0.0047	19.91	0.01133	0.2615
0.5	1.5	1.243	0.00476	0.0009	0.009	19.57	0.010781	0.3963
1	1	1.931	0.00552	0.0008	0.0245	22.76	0.027586	1.1172
1	1	3.059	0.00593	0.0013	0.013	21.48	0.015556	0.7296
1.5	0.5	4.302	0.00422	0.0009	0.014	19.17	0.009477	0.4727
1.5	0.5	5.12	0.00368	0.0006	0.0208	22.72	0.0072	1.06
1.5	1.5	3.933	0.00386	0.0007	0.0111	22.7	0.112	0.4105
1.5	1.5	3.544	0.00436	0.0008	0.0101	20.54	0.010147	0.4028

TABLE B.21. Analyzed Concentration of Elements in Sample, Day 41

Relative Concentration in Initial Formulation		Aluminum, Wt%	Chromium, Wt%	Copper, Wt%	Iron, Wt%	Sodium, Wt%	Nickel, Wt%	Phosphorus, Wt%
$NaAlO_2$	Organic							
Crust Samples								
0.5	0.5	1.128	0.00356	0.001	0.005	25.33	0.009444	0.5944
0.5	0.5	1.129	0.00342	0.0012	0.0033	23.5	0.01	0.7417
0.5	1.5	1.017	0.00358	0.0019	0.005	23.92	0.009167	0.2542
0.5	1.5	1.13	0.00335	0.0028	0.0043	24.87	0.009565	0.1957
1	1	2.855	0.0024	0.0009	0.0035	22.3	0.0055	0.07
1	1	3.153	0.00559	0.0013	0.01	24.88	0.011765	0.0941
1.5	0.5	6.792	0.00367	0.0009	0.015	24.25	0.010417	0.5542
1.5	0.5	7.25	0.00271	0.0008	0.0108	24.92	0.007917	1.5125
1.5	1.5	1.996	0.00313	0.0007	0.003	24.13	0.006087	0.2304
1.5	1.5	1.922	0.00344	0.0004	0.0028	25.33	0.006667	0.0833
Supernate Samples								
0.5	0.5	1.514	0.00464	0.0011	0.0032	20.59	0.013182	0.2818
0.5	0.5	1.6	0.0048	0.0014	0.003	21.25	0.0135	0.295
1	1	4.018	0.00671	0.0013	0.0059	22.18	0.011765	0.1824
1	1	3.395	0.00805	0.0015	0.0053	22.58	0.015789	0.1105
1.5	0.5	3.24	0.006	0.0012	0.006	21.2	0.0155	0.17
1.5	0.5	3.117	0.00633	0.0013	0.0061	21.72	0.016667	0.1556
1.5	1.5	3.519	0.00714	0.0009	0.0052	23.1	0.012381	0.1333
1.5	1.5	3.05	0.00577	0.0012	0.005	21.41	0.012273	0.1273
Solids Samples								
0.5	0.5	1.558	0.0075	0.0011	0.02	22.38	0.013333	0.7333
0.5	0.5	1.5	0.00741	0.0015	0.0188	21.76	0.012353	0.6529
0.5	1.5	1.293	0.00467	0.0009	0.008	21.07	0.010667	0.3933
0.5	1.5	1.318	0.00512	0.0012	0.0071	21.88	0.011176	0.3941
1	1	2.963	0.00533	0.0013	0.0179	23.54	0.012917	0.9792
1	1	3.321	0.00613	0.0012	0.0125	24.17	0.014583	0.6167
1.5	0.5	4.933	0.00423	0.0011	0.016	22.8	0.010333	0.7233
1.5	0.5	5.955	0.00468	0.0015	0.0191	23.36	0.012273	0.8727
1.5	1.5	4.053	0.003	0.0007	0.012	23.8	0.01	0.4
1.5	1.5	3.1	0.0043	0.001	0.0083	23.3	0.010435	0.2826

TABLE B.22. Analyzed Concentration of Elements in Sample, Day 66

Relative Concentration in Initial Formulation		Aluminum, Wt%	Chromium, Wt%	Copper, Wt%	Iron, Wt%	Sodium, Wt%	Nickel, Wt%	Phosphorus, Wt%
$NaAlO_2$	Organic							
Crust Samples								
0.5	0.5	1.435	0.00769	0.0008	0.0192	21.19	0.012692	0.75
0.5	0.5	1.387	0.00667	0.0007	0.0153	20.33	0.012333	0.4867
0.5	1.5	2.155	0.005	0.0004	0.0035	22.8	0.02	0.155
0.5	1.5	1.69	0.00476	0.0005	0.0038	26.43	0.014762	0.319
1	1	3.368	0.00323	0.001	0.0013	19.35	0.006452	0.1871
1	1	2.443	0.00476	0.0014	0.0038	25.24	0.014286	0.0905
1.5	0.5	4.179	0.00714	0.0011	0.0082	21.96	0.015714	0.0786
1.5	0.5	3.344	0.00389	0.0011	0.0056	23.5	0.011111	0.1556
1.5	1.5	2.114	0.00409	0.0009	0.0032	24.14	0.009091	0.0864
1.5	1.5	2.573	0.0027	0.0008	0.0046	22.54	0.008108	0.1432
Supernate Samples								
0.5	0.5	1.905	0.00526	0.0011	0.0037	18.16	0.016842	0.1526
0.5	0.5	2.125	0.005	0.001	0.004	20	0.0185	0.135
1	1	3.439	0.00556	0.0017	0.0044	18	0.017222	0.0167
1	1	2.793	0.01107	0.002	0.0046	20	0.025357	0.0357
1.5	0.5	3.418	0.00893	0.0014	0.0068	182.8	0.023929	0.0321
1.5	0.5	3.316	0.01053	0.0016	0.0068	19.89	0.025263	0.0368
Solids Samples								
0.5	0.5	0.996	0.00261	0.0009	0.0026	21.87	0.008696	0.313
0.5	0.5	0.948	0.00238	0.0004	0.0019	23.76	0.009524	0.4476
0.5	1.5	1.429	0.00588	0.0012	0.0112	23.06	0.11765	0.4353
0.5	1.5	1.303	0.00303	0.0009	0.0082	21.33	0.011212	0.4212
1	1	2.375	0.00714	0.0011	0.0154	18.36	0.010714	0.6179
1	1	2.857	0.00952	0.001	0.0162	23.24	0.015238	1.0619
1.5	0.5	3.053	0.00211	0.0008	0.0066	24.32	0.007895	0.0842
1.5	0.5	6.261	0.00435	0.0004	0.0222	25.52	0.008696	1.0348
1.5	1.5	3.647	0.00294	0.0009	0.0118	20.62	0.01	0.4353
1.5	1.5	3.452	0.00323	0.0006	0.0113	19.61	0.01	0.4097

TABLE B.23. Analyzed Concentration of Elements in Various Facies of Reference Formulation, Day 66

Relative Concentration in Initial Formulation		Aluminum, Wt%	Chromium, Wt%	Copper, Wt%	Iron, Wt%	Sodium, Wt%	Nickel, Wt%	Phosphorus, Wt%
$NaAlO_2$	Organic							
Crust Samples								
1	1	3.604	0.00833	0.0013	0.0046	22.88	0.01375	0.075
1	1	3.781	0.00476	0.001	0.0052	23.81	0.009524	0.119
Supernate Samples								
1	1	3.563	0.01053	0.0016	0.0047	22.37	0.017368	0.1316
1	1	2.871	0.00952	0.0014	0.0038	22.67	0.016667	0.1286
Middle Solids								
1	1	3.652	0.00333	0.001	0.0052	25.43	0.009524	0.1714
1	1	3.995	0.00455	0.0014	0.0055	23.45	0.009091	0.2636
Upper Middle Solids								
1	1	2.285	0.01	0.0005	0.0205	23.4	0.016	1.205
1	1	2.626	0.0087	0.0009	0.02	23.09	0.016957	1.2348
Lower Samples								
1	1	0.857	0.0013	0.0003	0.0083	26.96	0.004348	0.1217
1	1	0.905	0.0015	0.0003	0.008	25.8	0.005	0.145

TABLE B.24. Total Carbon, Total Organic Carbon, and Total Inorganic Carbon, Day 0--Unheated Centrifuged Solids

Relative Concentration				
$NaAlO_2$	Organic	TC, Wt%	TOC, Wt%	TIC, Wt%
0.5	0.5	2.48	0.099	2.39
0.5	0.5	3.11	0.41	2.7
0.5	1.5	5.5	2.11	3.39
0.5	1.5	5.22	1.52	4.7
1	1	2.86	1.5	1.36
1	1	5.08	1.32	3.76
1.5	0.5	2.34	0.382	1.96
1.5	0.5	2.42	0.486	1.93
1.5	1.5	4.96	2.45	2.51
1.5	1.5	5.33	2.93	2.4

TABLE B.25. Total Carbon, Total Organic Carbon, and Total Inorganic Carbon, Day 16

Relative Concentration				
$NaAlO_2$	Organic	TC, Wt%	TOC, Wt%	TIC, Wt%
Crust Samples				
0.5	0.5	2.73	0.51	2.22
0.5	0.5	2.47	0.85	1.62
0.5	1.5	9.16	4.55	4.61
0.5	1.5	6.67	5.19	1.48
1	1	17.2	15.2	2
1.5	0.5	2.82	0.86	1.96
1.5	0.5	3.36	1.04	2.32
1.5	1.5	10.1	5.1	5
1.5	1.5	7.05	4.11	2.94
Below Crust Solid Samples				
0.5	0.5	2.66	0.305	2.36
0.5	0.5	2.75	0.538	2.21
0.5	1.5	6.14	1.88	4.26
0.5	1.5	6.74	2.38	4.36
1	1	7.06	3.01	4.05
1	1	4.1	0.9	3.2
1.5	0.5	2.34	0.171	2.17
1.5	0.5	2.76	0.33	2.43
1.5	1.5	5.82	2.82	3
1.5	1.5	5.31	1.48	3.83

TABLE B.26. Total Carbon, Total Organic Carbon, and Total Inorganic Carbon, Day 41

Relative Concentration				
$NaAlO_2$	Organic	TC, Wt%	TOC, Wt%	TIC, Wt%
Crust Samples				
0.5	0.5	2.43	1.19	1.24
0.5	0.5	2.58	1.06	1.52
0.5	1.5	12.5	5.76	6.74
0.5	1.5	9.72	4.6	5.12
1	1	6.09	3	3.09
1	1	3.97	1.78	2.19
1.5	0.5	2.44	0.55	1.89
1.5	0.5	2.59	1.03	1.56
1.5	1.5	4.09	1.63	2.46
1.5	1.5	3.31	0.92	2.39
Below Crust Solid Samples				
0.5	0.5	2.86	0.83	2.03
0.5	0.5	3.05	1.29	1.76
0.5	1.5	6.72	2.8	3.92
0.5	1.5	5.97	2.62	3.35
1	1	3.22	1.78	1.44
1	1	3.09	1.35	1.74
1.5	0.5	2.04	0.91	1.13
1.5	0.5	1.7	0.52	1.18
1.5	1.5	6.28	2.33	3.95
1.5	1.5	6.14	2.56	3.58

TABLE B.27. Total Carbon, Total Organic Carbon, and Total Inorganic Carbon, Day 66

Relative Concentration		TC, Wt%	TOC, Wt%	TIC, Wt%
$NaAlO_2$	Organic			
Crust Samples				
0.5	0.5	3.28	0.58	2.7
0.5	0.5	3.12	0.46	2.66
0.5	1.5	4.52	2.17	2.35
0.5	1.5	6.87	2.88	3.99
1	1	2.85	2.24	0.61
1	1	3.19	1.32	1.87
1	1	2.32	0.3	2.02
1	1	3.97	1.27	2.7
1.5	0.5	2.93	0.55	2.38
1.5	0.5	3.6	0.9	2.7
1.5	1.5	4.19	1.42	2.77
1.5	1.5	3.62	2.17	1.45
Below Crust Solid Samples				
0.5	0.5	2.18	0.33	1.85
0.5	0.5	2.3	1.2	1.1
0.5	1.5	5.84	2	3.84
0.5	1.5	6.49	3.23	3.26
1	1	6.26	3.76	2.5
1	1	6.48	1.55	4.93
1.5	0.5	2.26	0.23	2.03
1.5	0.5	2.08	0.34	1.64
1.5	1.5	6.47	2.41	4.06
1.5	1.5	5.72	2.85	2.87

TABLE B.28. Total Carbon, Total Organic Carbon, and Total Inorganic Carbon, Various Layers of the Reference Formulation, Day 66

Relative Concentration		TC, Wt%	TOC, Wt%	TIC, Wt%
$NaAlO_2$	Organic			
Crust				
1	1	2.32	0.3	2.02
1	1	3.97	1.27	2.7
Middle Waste				
1	1	4.36	1.07	3.29
1	1	3.7	1.45	2.25
Upper Bottom				
1	1	3.87	0.79	3.08
1	1	6.24	1.07	5.17
Lower Bottom				
1	1	1.17	1.34	NC[(a)]
1	1	1.04	0.82	0.22

(a) NC = not calculated.

TABLE B.29. Differential Scanning Calorimetry Analysis, Day 66

Relative Concentration in Initial Formulation		Sample Type	Endotherm J/g	Exotherm J/g
$NaAlO_2$	Organic			
0.5	0.5	Crust	742	-772
0.5	0.5	Crust	863	-611
0.5	0.5	Bottom	529	-554
0.5	0.5	Bottom	520	-842
0.5	1.5	Crust	667	-1049
0.5	1.5	Crust	424	-687
0.5	1.5	Bottom	876	-1343
0.5	1.5	Bottom	822	-1760
1	1	Crust	772	-488
1	1	Crust	747	-827
1	1	Bottom	624	-2296
1	1	Bottom	865	-1170
1.5	0.5	Crust	716	-813
1.5	0.5	Crust	638	-1273
1.5	0.5	Bottom	647	-742
1.5	0.5	Bottom	647	-951
1.5	1.5	Crust	632	-1139
1.5	1.5	Crust	534	-1514
1.5	1.5	Bottom	774	-1303
1.5	1.5	Bottom	712	-1662

TABLE B.30. Differential Scanning Calorimetry Analysis for the Solid Phase of the Reference Formulation, Day 66

Relative Concentration in Initial Formulation		Sample Type	Endotherm J/g	Exotherm J/g
$NaAlO_2$	Organic			
1	1	Crust	793	-974
1	1	Crust	690	-916
1	1	Upper Solid	442	-1763
1	1	Upper Solid	654	-1127
1	1	Middle Solid	593	-1515
1	1	Middle Solid	565	-3417
1	1	Lower Solid	301	-444
1	1	Lower Solid	256	-289

TABLE B.31. Scanning Thermal Gravimetry Analysis, Day 66

Relative Concentration in Initial Formulation		Sample Type	Endotherm Wt% Loss	Exotherm Wt% Loss	Temperature Between Endotherm and Exotherm, °C
$NaAlO_2$	Organic				
0.5	0.5	Crust	26	8	200
0.5	0.5	Crust	28	7	206
0.5	0.5	Bottom	17	3	206
0.5	0.5	Bottom	19	5	205
0.5	1.5	Crust	20	13	190
0.5	1.5	Crust	16	6	200
0.5	1.5	Bottom	29	15	200
0.5	1.5	Bottom	28	19	185
1	1	Crust	26	4	215
1	1	Crust	24	2	225
1	1	Bottom	19	9	200
1	1	Bottom	28	8	210
1.5	0.5	Crust	23	8	200
1.5	0.5	Crust	26	9	210
1.5	0.5	Bottom	14	10	165
1.5	0.5	Bottom	17	9	184
1.5	1.5	Crust	22	11	210
1.5	1.5	Crust	23	16	190
1.5	1.5	Bottom	30	14	205
1.5	1.5	Bottom	25	19	200

TABLE B.32. Scanning Thermal Gravimetry Analysis of the Solid Phases of the Reference Formulation, Day 66

Relative Concentration in Initial Formulation		Sample Type	Endotherm Wt% Loss	Exotherm Wt% Loss	Temperature Between Endotherm and Exotherm, °C
$NaAlO_2$	Organic				
1	1	Crust	28	7	205
1	1	Crust	26	12	210
1	1	Upper Solid	19	8	200
1	1	Upper Solid	20	13	200
1	1	Middle Solid	29	9	200
1	1	Middle Solid	32	6	185
1	1	Lower Bottom	9	1.5	235
1	1	Lower Bottom	10	1	230

TABLE B.33. Phase Volume Data: Low Aluminate, Low Organic Formulation

Time (days)	Normalized Volumes (mL) Crust	Aqueous	Solids	Wt% Remaining	Total Density
0	0	88	911	100.00	1.39
0	0	79	852	100.00	1.42
0	0	94	905	100.00	1.42
0	0	100	900	100.00	1.42
1	0	200	744	99.76	1.47
1	0	204	704	99.70	1.46
1	0	176	823	99.64	1.41
1	0	187	937	99.65	1.42
2	0	277	700	99.75	1.42
2	0	261	647	99.61	1.45
2	0	294	705	99.48	1.41
2	0	250	750	99.49	1.42
5	0	366	600	99.33	1.43
5	0	363	545	99.35	1.45
5	0	352	611	98.93	1.45
5	0	375	625	99.10	1.41
7	0	422	555	99.24	1.41
7	0	397	511	99.12	1.45
7	0	364	600	98.73	1.45
7	0	412	587	98.86	1.41
9	0	422	533	99.15	1.44
9	0	431	454	98.90	1.48
9	0	411	529	98.59	1.48
9	0	437	562	98.65	1.40
12	0	444	533	98.79	1.40
12	0	431	477	98.48	1.44
12	0	411	588	98.42	1.39
12	0	437	562	98.30	1.40
14	0	444	533	98.53	1.40
14	0	454	431	98.05	1.46
14	0	447	552	98.10	1.39
14	0	437	537	98.02	1.43
16	0	447	517	97.98	1.43
16	0	437	562	97.85	1.39
22	0	470	494	97.75	1.43
22	0	437	562	97.28	1.38

TABLE B.33. (contd)

Time (days)	Normalized Volumes (mL)			Wt% Remaining	Total Density
	Crust	Aqueous	Solids		
26	0	470	494	97.60	1.43
26	0	437	525	96.91	1.43
33	0	470	494	97.22	1.42
33	0	437	537	96.47	1.40
36	0	470	494	96.92	1.42
36	0	437	5C0	96.23	1.45
42	0	470	447	96.37	1.48
42	0	437	525	95.75	1.41
47	0	470	447	95.83	1.47
47	0	437	525	95.39	1.40
50	0	470	470	95.60	1.43
50	0	437	500	95.17	1.44
54	0	470	470	95.34	1.43
54	0	437	500	94.87	1.43
57	0	470	470	95.12	1.42
57	0	437	500	94.62	1.43
61	0	470	470	94.58	1.41
61	0	437	500	94.40	1.42
65	0	441	470	94.34	1.46
65	0	406	562	94.16	1.37

TABLE B.34. Phase Volume Data: Low Aluminate-High Organic Formulation

Time (days)	Normalized Volumes (mL) Crust	Aqueous	Solids	Wt% Remaining	Total Density
0	0	0	1000	100.00	1.54
0	0	0	1000	100.00	1.56
0	0	0	1000	100.00	1.51
0	0	0	1000	100.00	1.48
1	0	0	1000	99.72	1.54
1	0	0	1000	99.78	1.55
1	0	0	1000	99.76	1.51
1	0	0	987	99.70	1.50
2	0	0	1000	99.80	1.54
2	0	0	1012	99.75	1.53
2	0	0	1000	99.74	1.51
2	0	0	987	99.79	1.50
5	0	0	1000	99.45	1.53
5	0	0	1012	99.44	1.53
5	0	0	1000	99.28	1.50
5	0	0	987	99.71	1.50
7	0	0	1000	99.31	1.53
7	0	0	1000	99.35	1.54
7	0	0	1000	99.12	1.50
7	0	0	987	99.67	1.50
9	0	0	1000	99.23	1.53
9	0	0	975	99.26	1.58
9	0	0	1000	98.95	1.49
9	0	0	1000	99.62	1.48
12	0	0	1000	99.11	1.53
12	0	0	975	99.08	1.58
12	0	0	975	98.68	1.53
12	0	0	987	99.54	1.49
14	0	0	1025	99.04	1.49
14	0	0	1000	98.76	1.53
14	0	0	1000	98.52	1.49
14	0	0	987	99.50	1.49
16	6	0	993	98.31	1.48
16	0	0	987	99.44	1.49
22	12	0	975	97.81	1.49
22	0	0	987	99.29	1.49

TABLE B.34. (contd)

Time (days)	Normalized Volumes (mL)			Wt% Remaining	Total Density
	Crust	Aqueous	Solids		
26	0	0	975	97.49	1.51
26	0	0	987	99.19	1.49
33	37	0	962	97.02	1.46
33	37	0	949	99.02	1.49
36	0	0	975	96.86	1.50
36	0	0	987	98.95	1.48
42	0	0	975	96.55	1.49
42	0	0	949	98.82	1.54
47	0	0	975	96.27	1.48
47	0	0	987	98.70	1.48
50	0	0	975	96.13	1.48
50	0	0	987	98.63	1.48
54	12	0	975	95.97	1.46
54	0	0	987	98.54	1.48
57	12	0	975	95.86	1.46
57	0	0	987	98.46	1.48
61	12	0	975	95.71	1.46
61	0	0	987	98.37	1.47
65	12	0	975	95.49	1.45
65	0	0	987	98.28	1.47

TABLE B.35. Phase Volume Data: Reference Formulation

Time (days)	Normalized Volumes (mL)			Wt% Remaining	Total Density
	Crust	Aqueous	Solids		
0	0	561	438	100.00	1.56
0	0	512	487	100.00	1.62
0	0	543	456	100.00	1.59
0	0	511	488	100.00	1.56
1	0	629	359	98.92	1.56
1	0	548	426	97.97	1.62
1	0	565	413	99.06	1.61
1	0	556	409	99.04	1.59
2	0	629	359	98.88	1.56
2	0	548	426	97.56	1.61
2	0	543	402	96.56	1.62
2	0	568	397	99.04	1.59
5	0	651	337	98.47	1.55
5	0	609	365	97.12	1.60
5	10	565	380	95.32	1.58
5	0	568	375	98.35	1.62
7	0	617	337	98.13	1.60
7	12	524	426	96.36	1.61
7	10	543	380	95.11	1.61
7	0	568	375	97.05	1.60
9	0	617	337	97.90	1.59
9	24	512	426	95.99	1.60
9	21	380	489	94.01	1.67
9	0	545	363	96.71	1.65
12	11	606	337	97.64	1.59
12	12	536	426	95.68	1.58
12	10	423	489	93.51	1.60
12	11	511	375	94.89	1.64
14	11	629	337	97.52	1.55
14	12	512	426	94.90	1.60
14	21	456	413	93.30	1.66
14	22	545	306	94.53	1.67
16	10	402	489	92.77	1.63
16	11	500	375	94.08	1.64
22	10	380	489	92.52	1.66
22	22	511	375	93.71	1.59

TABLE B.35. (contd)

Time (days)	Normalized Volumes (mL)			Wt% Remaining	Total Density
	Crust	Aqueous	Solids		
26	0	326	543	91.86	1.67
26	0	431	454	93.40	1.63
33	21	326	543	90.80	1.61
33	22	397	488	92.54	1.57
36	0	271	597	90.62	1.64
36	0	431	454	92.29	1.61
42	21	250	597	90.21	1.64
42	22	340	511	91.79	1.62
47	10	260	597	90.05	1.63
47	22	375	477	91.27	1.61
50	10	271	597	89.98	1.61
50	11	397	477	90.99	1.58
54	10	239	630	89.66	1.60
54	11	397	477	90.68	1.58
57	10	250	619	89.72	1.61
57	11	363	511	90.21	1.57
61	10	217	652	89.30	1.60
61	11	306	568	89.68	1.56
65	10	195	673	88.61	1.58
65	22	227	625	89.22	1.57

TABLE B.36. Phase Volume Data: High Aluminate, Low Organic Formulation

Time (days)	Normalized Volumes (mL)			Wt% Remaining	Total Density
	Crust	Aqueous	Solids		
0	56	488	454	100.00	1.57
0	22	533	444	100.00	1.61
0	36	518	445	100.00	1.62
0	24	512	463	100.00	1.60
1	56	568	375	99.30	1.56
1	22	377	388	99.30	1.78
1	36	602	361	99.23	1.61
1	12	609	365	99.34	1.61
2	34	602	340	99.21	1.59
2	22	644	333	99.28	1.60
2	24	626	337	99.11	1.63
2	24	646	329	99.32	1.59
5	11	613	318	98.61	1.64
5	11	666	322	98.94	1.59
5	12	638	325	98.68	1.64
5	12	646	329	99.08	1.60
7	22	602	318	98.21	1.63
7	22	666	311	98.71	1.59
7	24	638	325	98.48	1.62
7	12	646	329	98.94	1.60
9	11	613	318	97.72	1.62
9	11	666	311	98.48	1.60
9	12	662	301	98.23	1.63
9	12	658	304	98.70	1.61
12	34	602	306	96.88	1.61
12	33	633	311	97.65	1.61
12	24	662	301	98.00	1.61
12	24	646	304	98.30	1.61
14	11	568	329	96.40	1.66
14	33	633	311	97.22	1.60
14	24	662	301	97.82	1.60
14	24	646	304	98.16	1.61
16	24	650	301	97.58	1.62
16	24	646	304	97.95	1.60
22	24	626	301	96.90	1.65
22	24	634	304	97.55	1.61

TABLE B.36. (contd)

Time (days)	Normalized Volumes (mL)			Wt% Remaining	Total Density
	Crust	Aqueous	Solids		
26	60	626	301	96.38	1.58
26	60	609	304	97.35	1.59
33	60	602	301	95.40	1.60
33	60	548	304	96.26	1.57
36	60	602	301	94.82	1.59
36	36	609	304	95.70	1.60
42	12	530	361	93.64	1.67
42	24	609	304	94.85	1.58
47	24	481	421	91.99	1.60
47	24	609	304	94.33	1.60
50	24	481	421	91.25	1.58
50	12	609	329	94.17	1.57
54	24	421	481	90.96	1.58
54	24	548	365	93.46	1.58
57	24	421	481	90.55	1.57
57	24	548	365	93.07	1.57
61	24	421	481	90.24	1.56
61	24	548	365	92.86	1.57
65	24	421	481	89.95	1.56
65	24	548	365	92.60	1.56

TABLE B.37. Phase Volume Data: High Aluminate, High Organic Formulation

Time (days)	Normalized Volumes (mL)			Wt% Remaining	Total Density
	Crust	Aqueous	Solids		
0	47	305	647	100.00	1.63
0	67	314	617	100.00	1.58
0	56	340	602	100.00	1.57
0	34	375	590	100.00	1.57
1	47	352	611	99.50	1.61
1	56	337	595	99.81	1.59
1	68	363	568	99.84	1.57
1	22	397	568	99.76	1.58
2	35	376	588	99.44	1.62
2	33	359	561	99.74	1.65
2	22	363	568	99.66	1.64
2	11	397	568	99.74	1.60
5	0	352	647	99.18	1.62
5	11	280	640	99.07	1.67
5	22	306	625	98.95	1.62
5	22	318	590	99.29	1.67
7	11	341	647	98.95	1.61
7	33	292	640	98.65	1.61
7	56	284	625	98.66	1.60
7	56	284	625	99.05	1.60
9	23	352	647	98.69	1.57
9	33	258	674	98.28	1.60
9	34	250	659	98.37	1.63
9	22	261	647	98.79	1.66
12	23	317	682	98.36	1.57
12	44	247	674	97.89	1.59
12	34	272	659	98.13	1.59
12	34	272	659	98.40	1.59
14	23	317	682	98.27	1.57
14	22	258	674	97.48	1.61
14	22	227	681	97.97	1.65
14	22	272	681	98.12	1.57
16	22	227	681	97.64	1.64
16	34	261	681	97.87	1.56
	22	284	681	97.25	1.54
22					
22	22	284	681	97.41	1.54

TABLE B.37. (contd)

Time (days)	Normalized Volumes (mL)			Wt% Remaining	Total Density
	Crust	Aqueous	Solids		
26	45	227	681	96.76	1.58
26	22	284	681	96.85	1.53
33	56	170	738	95.74	1.55
33	56	170	738	96.02	1.55
36	34	250	681	95.48	1.54
36	34	227	704	95.72	1.54
42	34	227	704	94.58	1.53
42	34	159	772	95.28	1.54
47	56	113	795	94.19	1.52
47	56	113	795	94.36	1.52
50	56	170	681	93.75	1.61
50	56	113	738	93.91	1.61
54	284	0	681	93.44	1.51
54	284	0	681	93.34	1.50
57	227	0	738	93.32	1.50
57	227	0	738	92.93	1.49
61	227	0	738	93.15	1.50
61	227	0	738	92.68	1.49
65	227	0	738	92.90	1.50
65	227	0	738	92.38	1.48

TABLE B.38. Phase Volume Data: Reference Formulation in Graduated Cylinder

Time (days)	Normalized Volumes (mL)		
	Crust	Aqueous	Solids
0	10	543	445
0	11	534	453
1	10	543	413
1	11	558	418
2	0	543	402
2	0	546	418
5	21	434	456
5	0	534	418
7	21	434	489
7	11	465	465
9	21	326	532
9	11	453	465
12	32	304	554
12	23	441	476
14	21	326	554
14	11	441	476
16	21	315	554
16	23	441	476
22	43	315	554
22	34	430	476
26	21	315	554
26	23	430	488
33	32	304	532
33	46	418	500
36	32	293	565
36	34	418	488
42	32	315	543
42	46	406	511
47	32	304	554
47	23	418	511

TABLE B.38. (contd)

Time (days)	Normalized Volumes (mL)		
	Crust	Aqueous	Solids
50	32	282	576
50	23	418	511
54	65	293	565
54	46	267	674
57	65	347	565
57	46	406	511
61	54	304	565
61	46	406	511
65	54	304	565
65	46	395	511

TABLE B.39. Physical Analyses Data (Day 0)

Relative Concentration of Initial Formulation		Wt% Total				pH Centrifuged Supernate	Slurry Density	Centrifuged Samples	
$NaAlO_2$	Organic	Solids	Average	Oxides	Average			Solids Density (g/mL)	Supernate Density (g/mL)
0.5	0.5	75	75.3	29.6	29.4	14.079	1.65	1.74	1.45
0.5	0.5	75.5		29.1			1.61	1.72	1.45
0.5	1.5	78.7	79.9	30.6	30.9	14.079	2.11	1.74	1.49
0.5	1.5	81.1		31.1			2.06	1.74	1.51
1	1	82	81	34.2	34.3	14.079	1.59	1.84	1.51
1	1	80		34.3			1.63	1.85	1.491
1.5	0.5	80.4	80.4	44.1	43.6	14.079	1.68	1.9	1.43
1.5	0.5	{71.6}		43.1			1.67	1.89	1.45
1.5	1.5	82.2	82.2	43.9	42.7	14.079	1.59	1.7	1.49
1.5	1.5	82.1		41.5			1.58	1.72	1.48

{ } indicates deviation is larger than expected.

TABLE B.39. (contd)

Relative Concentration of Initial Formulation		Centrifuged Samples						Centrifuged Solids Penetration Resistance[a]
$NaAlO_2$	Organic	Vol% Solids	Wt% Solids	Wt% Dissolved Solids	Wt% Total Solid	Wt% Total Oxide	Vol% Settled Solids	
0.5	0.5	46.8	51	27.7	65.1	36.8	100	438
0.5	0.5	47.8	51.2	28.4	66.3	35.6	100	438
0.5	1.5	52.61	56.8	34.8	68.6	34.3	100	65
0.5	1.5	54.5	59.3	32.6	69.5	34.3	100	65
1	1	{29.7}	{34.5}	42.3	71.4	35.2	55.9	59
1	1	{35.6}	{40.2}	39.3	68.9	35.8	61.3	59
1.5	0.5	42.86	48.4	31.5	71.7	46	61.77	125
1.5	0.5	42.8	48.7	31	71.9	48.2	61.73	125
1.5	1.5	50.8	54.3	29.4	72.4	35.2	100	60
1.5	1.5	49.2	53.6	31.2	72.5	36.7	100	60

(a) psi for a 1 in. penetration.
{ } indicates deviation is larger than expected.

TABLE B.40. Physical Analysis Data (Day 66)

Relative Concentration of Initial Formulation		Crust		Supernate	Middle Level Sample		Bottom Sample		Penetration Resistance		
$NaALO_2$	Organic	Wt% Total Solids	Wt% Total Oxides	Wt% Total Solids	Wt% Total Solids	Wt% Total Oxides	Wt% Total Solids	Wt% Total Oxides	Top 1/8 in.	Top 3/4 in.	Top 1 in.
0.5	0.5	78.8	35.6	65.6	NS	NS	74.1	37.1	15[a]		
0.5	0.5	78.4	37.1	64.4	NS	NS	73.7	36			
0.5	0.5	76.6	36.9	66.4	NS	NS	74.8	33.3			
0.5	0.5	76.7	37.1	65.4	NS	NS	72.7	33.3			
0.5	1.5	77.9	34.5	NS	NS	NS	76	31.7	120[a]		
0.5	1.5	79	35.2	NS	NS	NS	75	32.4			
0.5	1.5	72.8	33	NS	NS	NS	71.6	12.8	40[a]		
0.5	1.5	74	33.7	NS	NS	NS	71.4	19			
1	1	81.6	35	76.4	82.1	39.3	81.1	38.7	140	200	520
1	1	84.2	40.6	73.7	81.9	39.7	80.9	39.1			
1	1	80.2	43.4	75.5	79.3	39.7	81.9	39.7	220	300	530
1	1	85.6	42.3	74.1	78.3	41.5	81.7	41.3			
1.5	0.5	83.2	56.1	72	81.6	43.9	82.5	50.5	480[a]		
1.5	0.5	83.2	54.2	71.6	81.5	43.5	81.3	50.5			
1.5	0.5	74.5	51.9	77.7	80.5	48.7	84	50.9	510[a]		
1.5	0.5	80.2	51.9	77.5	81.5	44.5	83.3	51			
1.5	1.5	83.8	45.7	0	82	36	77.6	44.9	60[a]		
1.5	1.5	84.1	47.7	0	80.6	34.3	76.5	46.1			
1.5	1.5	88.1	44.1	0	81.5	36.1	77.8	38.5	70[a]		
1.5	1.5	88.2	41.8	0	81	34.3	77.5	44.1			

(a) Only one resistance measurement taken. Depth not indicated.
NS indicates no sample was taken for analysis.

TABLE B.40. (contd)

Concentration of Initial Formulation		Slurry Density	Centifuged Samples					Wt% Dissolved Solids	Solids	
$NaAlO_2$	Organic	g/mL	pH Supernate	Solids Density g/mL	Supernate Density g/mL	Vol% Solids	Wt% Solids		Wt% Total Solids	Wt% Total Oxides
0.5	0.5	1.66	13.8	1.88	1.46	49.4	55.83	26.6	77.7	37.9
0.5	0.5	1.66	13.8	1.83	1.48	51.2	56.5	26	84.2	36.6
0.5	0.5	1.67	13.8	1.87	1.44	53.1	59.4	23.9	81.2	37.6
0.5	0.5	1.66	13.8	1.86	1.47	49.4	55.3	27.1	82	37
0.5	1.5	1.6	13.7	1.66	1.46	71.1	73.6	15.6	73.3	43.6
0.5	1.5	1.63	13.7	1.68	1.47	71.6	74.2	15.1	73.3	42.6
0.5	1.5	1.59	13.8	1.67	1.47	60.5	63.3	23.7	70.6	16.7
0.5	1.5	1.59	13.8	1.68	1.45	59.5	62.6	26	71.6	32.4
1	1	1.75	>14	1.83	1.38	82.6	86.17	8.43	75.7	43.7
1	1	1.74	>14	1.78	1.49	84.7	86.85	8.35	76.5	41.2
1	1	1.72	>14	1.78	1.41	83.8	86.52	8.21	76	48
1	1	1.71	>14	1.77	1.38	83.4	86.03	8.09	77.5	47.1
1.5	0.5	1.78	13.7	1.93	1.43	68.1	74.08	16.1	79.4	58.8
1.5	0.5	1.77	13.7	1.89	1.48	69.5	74.33	15.9	77.7	56.3
1.5	0.5	1.79	>14	2.02	1.44	60.4	68.14	18.6	80	54
1.5	0.5	1.79	>14	1.97	1.47	63.2	69.53	19	79.6	52.4
1.5	1.5	1.7	14	1.74	1.46	84.4	86.6	8.24	78.2	50.5
1.5	1.5	1.7	14	1.77	1.31	85	88.31	7.26	79.2	43.6
1.5	1.5	1.7	13.9	1.72	1.54	88.3	89.5	6.15	78.4	60
1.5	1.5	1.7	13.9	1.73	1.51	88.1	89.35	6.13	80	60

TABLE B.41. Physical Analysis Data (Day 66)

Relative Concentration in Initial Formulation		Crust Data	Bottom Data	Composite Data
$NaAlO_2$	Organic	τ(dyne/cm^2)	τ(dyne/cm^2)	τ(dyne/cm^2)
0.5	0.5	38500	12700	1360
0.5	0.5	26300	4530	680
0.5	0.5	NM	21800	NM
0.5	0.5	NM	10200	NM
0.5	0.5	46200	13800	816
0.5	0.5	29000	9520	272
0.5	0.5	NM	15400	NM
0.5	0.5	NM	13600	NM
0.5	1.5	258000	98400	18100
0.5	1.5	145000	66600	23600
0.5	1.5	NM	86100	NM
0.5	1.5	NM	65700	NM
0.5	1.5	63500	29500	20900
0.5	1.5	50300	19000	28100
0.5	1.5	NM	42600	NM
0.5	1.5	NM	20900	NM
1	1	185000	295000	19900
1	1	223000	NM	12200
1	1	NM	444000	NM
1	1	NM	NM	NM
1	1	210000	444000	16300
1	1	79800	471000	16800
1	1	NM	444000	NM
1.5	0.5	25800	159000	32600
1.5	0.5	6800	218000	6800
1.5	0.5	NM	367000	907
1.5	0.5	NM	263000	408
1.5	0.5	NM	NM	1360
1.5	1.5	444000	187000	39000
1.5	1.5	440000	254000	30400
1.5	1.5	372000	235000	NM
1.5	1.5	NM	222000	NM
1.5	1.5	480000	267000	41700
1.5	1.5	426000	235000	46200
1.5	1.5	NM	273000	NM
1.5	1.5	NM	232000	NM

NM indicates no measurement was taken.

TABLE B.42. Yield Stress Data

Relative Concentration in Initial Formulation				
$NaAlO_2$	Organic	τ(Pa = N/m^2)	Average	Temperature (°C)
0.5	0.5	4.8		60
0.5	0.5	11.6		60
0.5	0.5	8.7	8 ± 3.2	60
0.5	0.5	3.5		60
0.5	0.5	10.6		60
0.5	0.5	7.7		60
0.5	1.5	12.6		60
0.5	1.5	15.5		60
0.5	1.5	13.5	10 ± 5	60
0.5	1.5	3.8		60
0.5	1.5	4.8		60
0.5	1.5	7.7		60
1	1	16.1		60
1	1	9.7	12 ± 3.6	60
1	1	8.7		60
1	1	14.5		60
1.5	0.5	1.2		60
1.5	0.5	10.6		60
1.5	0.5	9.7	9 ± 4.8	60
1.5	0.5	5.8		60
1.5	0.5	15.5		60
1.5	0.5	9.7		60
1.5	1.5	17.7		60
1.5	1.5	20.9		60
1.5	1.5	24.2	21 ± 4.6	60
1.5	1.5	27.4		60
1.5	1.5	16.1		60

TABLE B.43. X-ray Diffraction Data for All Formulations

Relative Concentration in Initial Formulation			Relative Abundance						
$NaAlO_2$	Organic	Layer	$NaNO_3$	$NaNO_2$	$NaAlO_2$	$NaHC_2O_4$	$NaC_2H_3O_2$	$NaHCO_3$	Na_2CO_3
0.5	0.5	Crust	30	100					
0.5	0.5	Crust	100	90		90	10		20
0.5	0.5	Bottom	90	20					40
0.5	0.5	Bottom	70	100		10			
0.5	1.5	Crust	60	30		30	2		
0.5	1.5	Crust	100	30		20	3		
0.5	1.5	Bottom	30	30			10		
0.5	1.5	Bottom	40	40		20	20		10
1	1	Crust	30	20	10	40	10		50
1	1	Crust	100	20	5				
1	1	Bottom	40	40	10	10	10		
1	1	Bottom	100	60	10	10	10		
1.5	0.5	Crust	100	90					
1.5	0.5	Crust	20	60	10	5			
1.5	0.5	Bottom	100	30	50	10	5		
1.5	0.5	Bottom	100	30	30	10			2
1.5	1.5	Crust	100	10					
1.5	1.5	Crust	100	50	10	40	5		
1.5	1.5	Bottom	80	70	40		20	20	
1.5	1.5	Bottom	80	80	50	20	30		

TABLE B.43. (contd)

Relative Concentration in Initial Formulation							Number of Unmatched Strong Lines	Total Number of Strong Lines
$NaAlO_2$	Organic	Layer	Na_2Al_2O34	NaButyrate	Glycine	Valine		
0.5	0.5	Crust		10			0	4
0.5	0.5	Crust		60			2	14
0.5	0.5	Bottom		10			0	6
0.5	0.5	Bottom		10			0	6
0.5	1.5	Crust		20			2	7
0.5	1.5	Crust	10	10			0	5
0.5	1.5	Bottom		100			1	4
0.5	1.5	Bottom	10	100			1	5
1	1	Crust	20	20			8	19
1	1	Crust	5				0	2
1	1	Bottom	100	20	30	4		10
1	1	Bottom	10	10	5		3	5
1.5	0.5	Crust	10	90			7	16
1.5	0.5	Crust		100			0	7
1.5	0.5	Bottom		70			3	11
1.5	0.5	Bottom		40			2	6
1.5	1.5	Crust	2				1	3
1.5	1.5	Crust	10	20			0	5
1.5	1.5	Bottom	40	20			4	18
1.5	1.5	Bottom	40	40	20		4	23

TABLE B.44. X-ray Diffraction Data for Various Facies of Reference Formulation

Relative Concentration in Initial Formulation			Relative Abundance						
$NaAlO_2$	Organic	Layer	$NaNO_3$	$NaNO_2$	$NaAlO_2$	$NaHC_2O_4$	$NaC_2H_3O_2$	$NaHCO_3$	Na_2CO_3
1	1	Crust	70	100					
1	1	Crust	30	50	50		5		
1	1	Solid 1	90	60	40	60	30		20
1	1	Solid 1	60	30	20	30	20		
1	1	Solid 2	40	40	20	50	10		10
1	1	Solid 2	50	100	30	20	20	20	
1	1	Solid 3	100	20					
1	1	Solid 3	100	40					

Relative Concentration in Initial Formulation								
$NaAlO_2$	Organic	Layer	$Na_2Al_2O_3$	NaButyrate	Glycine	Valine	Number of Unmatched Strong Lines	Total Number of Strong Lines
1	1	Crust	10	10			4	9
1	1	Crust	50	10			3	7
1	1	Solid 1	40	70		40	11	31
1	1	Solid 1	20	100			3	12
1	1	Solid 2	30	10			8	19
1	1	Solid 2	60	20			5	20
1	1	Solid 3					0	3
1	1	Solid 3					0	3

TABLE B.45. Mass Spectral Results from Gas Generation Experiments

Reaction Time (hr)	Relative Concentrations		Component Measured in Sample (mole %)									
	$NaAlO_2$	Organic	CO_2	Ar	O_2	N_2	CO	He	H_2	CH_4	N_2O	NO_x
97.58	0.5	0.5	DL[a]	0.91	19	77.9	DL	DL	0.68	DL	1.53	
222.3	0.5	0.5	DL	0.89	17.3	78.4	DL	DL	1.05	DL	2.37	
269.9	0.5	0.5	DL	0.86	15.3	77.5	DL	DL	1.15	DL	5.15	
391.6	0.5	0.5	DL	0.86	15.2	78.5	DL	DL	1.29	DL	4.07	
506.6	0.5	0.5	DL	0.87	14.5	79.2	DL	DL	1.33	DL	4.09	
575.8	0.5	0.5	DL	0.89	14.8	80.2	DL	DL	1.24	DL	2.92	
703.1	0.5	0.5	DL	0.89	13.7	81.1	DL	DL	1.24	DL	3.16	DL
796.1	0.5	0.5	DL	0.89	13.7	81.5	DL	DL	1.20	DL	2.67	DL
866.6	0.5	0.5	DL	0.90	13.6	82.1	DL	DL	1.11	DL	2.33	DL
936.1	0.5	0.5	DL	0.92	14.5	82.3	DL	DL	1.00	DL	1.28	DL
1040	0.5	0.5	DL	0.91	13.2	83.1	DL	DL	0.97	DL	1.77	DL
97.58	0.5	1.5	DL	0.83	17.7	73.1	DL	DL	0.88	DL	7.52	
222.3	0.5	1.5	DL	0.73	14.6	68.7	DL	DL	1.63	DL	14.30	
269.9	0.5	1.5	DL	0.67	12.7	65.5	DL	DL	1.82	DL	19.30	
391.6	0.5	1.5	DL	0.67	11.9	66.8	DL	DL	2.18	DL	18.40	
506.6	0.5	1.5	DL	0.75	13.8	72.4	DL	DL	2.29	DL	10.80	
575.8	0.5	1.5	DL	0.70	11.7	69.5	DL	DL	2.54	DL	15.60	
703.1	0.5	1.5	DL	0.72	11.7	70.8	DL	DL	2.78	DL	14.00	DL
796.1	0.5	1.5	DL	0.74	11.8	72.5	DL	DL	2.81	DL	12.10	DL
866.6	0.5	1.5	DL	0.76	11.6	74.2	DL	DL	2.85	DL	10.60	DL
936.1	0.5	1.5	DL	0.78	11.8	75.8	DL	DL	2.83	DL	8.82	DL
1040	0.5	1.5	DL	0.84	13	79.2	DL	DL	2.56	DL	4.43	DL

TABLE B.45. (contd)

Reaction Time (hr)	Relative Concentrations		Compoenent Measured in Sample (mole %)									
	$NaAlO_2$	Organic	CO_2	Ar	O_2	N_2	CO	He	H_2	CH_4	N_2O	NO_x
97.58	1	1	DL	0.87	18.6	75.6	DL	DL	1.22	DL	3.64	
222.3	1	1	DL	0.80	16	73	DL	DL	1.59	DL	8.52	
269.9	1	1	DL	0.78	15.5	72.4	DL	DL	1.87	DL	9.41	
391.6	1	1	DL	0.74	14.5	71.8	DL	DL	2.11	DL	10.80	
506.6	1	1	DL	0.71	13.4	70.2	DL	DL	2.27	DL	13.40	
575.8	1	1	DL	0.74	13.9	72.2	DL	DL	2.48	DL	10.70	
703.1	1	1	DL	0.75	13.9	73.1	DL	DL	2.48	DL	9.81	DL
796.1	1	1	DL	0.77	14.3	74.6	DL	DL	2.49	DL	7.87	DL
866.6	1	1	DL	0.74	13.2	72.8	DL	DL	2.45	DL	10.90	DL
936.1	1	1	DL	0.76	13.7	74.4	DL	DL	2.43	DL	8.80	DL
1040	1	1	DL	0.79	14.1	76.5	DL	DL	2.39	DL	6.17	DL
97.58	1.5	0.5	DL	0.84	16.9	75.7	DL	DL	1.51	DL	5.04	
222.3	1.5	0.5	DL	0.77	14.3	75	DL	DL	2.18	DL	7.81	
269.9	1.5	0.5	DL	0.84	16.7	76.3	DL	DL	1.47	DL	4.73	
391.6	1.5	0.5	DL	0.78	14.4	78.7	DL	DL	1.90	DL	6.41	
506.6	1.5	0.5	DL	0.78	14.1	77.5	DL	DL	2.03	DL	5.57	
575.8	1.5	0.5	DL	0.79	13.5	77.5	DL	DL	2.17	DL	6.08	
703.1	1.5	0.5	DL	0.78	13	78.2	DL	DL	2.27	DL	5.74	DL
796.1	1.5	0.5	DL	0.79	13.4	79	DL	DL	2.24	DL	4.64	DL
866.6	1.5	0.5	DL	0.79	13.1	79.5	DL	DL	2.18	DL	4.39	DL
936.1	1.5	0.5	DL	0.78	12.5	78.8	DL	DL	2.31	DL	5.63	DL
1040	1.5	0.5	DL	0.80	12.7	80	DL	DL	2.20	DL	4.38	DL

TABLE B.45. (contd)

Reaction Time (hr)	Relative Concentrations		Component Measured in Sample (mole %)									
	$NaAlO_2$	Organic	Co_2	Ar	O_2	N_2	CO	HE	H_2	CH_4	H_2O	NO_x
97.58	1.5	1.5	DL	0.78	16.5	72.1	DL	DL	1.18	DL	9.50	
222.3	1.5	1.5	DL	0.66	13.6	69.4	DL	DL	1.88	DL	14.50	
269.9	1.5	1.5	DL	0.53	10.5	63.7	DL	DL	2.12	DL	23.20	
391.6	1.5	1.5	DL	0.55	10.7	67.4	DL	DL	2.24	DL	19.10	
506.6	1.5	1.5	DL	0.54	10.4	68.4	DL	DL	2.22	DL	18.50	
575.8	1.5	1.5	DL	0.54	10.1	68.7	DL	DL	2.30	DL	18.30	
703.1	1.5	1.5	DL	0.46	8.33	65.1	DL	DL	2.40	0.03	23.60	DL
796.1	1.5	1.5	DL	0.57	10.5	71.8	DL	DL	2.26	0.02	14.90	DL
866.6	1.5	1.5	DL	0.57	10.5	72.4	DL	DL	2.26	0.02	14.20	DL
936.1	1.5	1.5	DL	0.59	10.7	73.4	DL	DL	2.22	0.02	13.10	DL
1040	1.5	1.5	DL	0.58	10.6	73.8	DL	DL	2.27	0.02	12.70	DL
222.3	Ambient	0.03	0.93	21.1	77.9	DL	DL	DL	DL	DL		
269.9	Ambient	0.09	0.93	20.9	78	DL	DL	DL	DL	DL		
391.6	Ambient	0.04	0.92	21.5	77.6	DL	DL	DL	DL	DL		
506.6	Ambient	0.04	0.93	21.1	78	DL	DL	DL	DL	DL		
575.8	Ambient	0.03	0.94	21.1	78	DL	DL	DL	DL	DL		
703.1	Ambient	0.03	0.94	21.1	77.9	DL	DL	DL	DL	DL		DL
796.1	Ambient	0.03	0.94	21	78	DL	DL	DL	DL	DL		DL
866.6	Ambient	0.03	0.94	21.1	78	DL	DL	DL	DL	DL		DL

(a) DL signifies the measured species was at or below the detection limit. The detection limits are as follows: Gas, DL; CO_2, 0.01; CO, 0.1; He, 0.01; H_2, 0.01; CH_4, 0.01; N_2O, 0.01; NO_x, 0.01.

TABLE B.46. Moles of Gases Present in Each Reaction Vessel as a Function of Time

Time (hr)	Moles of Gas in System									
	CO_2	Ar	O_2	N_2	H_2	N_2O	CH_4	NO_x	CO	He
Low Aluminate, Low Organic										
97.58	2.70E-06	3.16E-04	6.56E-03	2.71E-02	2.53E-04	5.70E-04	3.48E-06	NA	3.48E-05	3.48E-06
222.3	2.88E-06	3.30E-04	6.35E-03	2.91E-02	4.13E-04	9.32E-04	3.71E-06	NA	3.71E-05	3.71E-06
269.9	2.93E-06	3.24E-04	5.69E-03	2.93E-02	4.58E-04	2.00E-03	3.78E-06	NA	3.78E-05	3.78E-06
391.6	3.01E-06	3.32E-04	5.80E-03	3.04E-02	5.23E-04	1.65E-03	3.88E-06	NA	3.88E-05	3.88E-06
506.6	2.98E-06	3.33E-04	5.50E-03	3.04E-02	5.32E-04	1.64E-03	3.84E-06	NA	3.84E-05	3.84E-06
575.8	2.95E-06	3.37E-04	5.55E-03	3.05E-02	4.97E-04	1.22E-03	3.81E-06	NA	3.81E-05	3.81E-06
703.1	3.00E-06	3.42E-04	5.27E-03	3.13E-02	5.05E-04	1.32E-03	3.87E-06	3.39E-06	3.87E-05	3.87E-06
769.1	2.99E-06	3.40E-04	5.24E-03	3.12E-02	4.89E-04	1.16E-03	3.85E-06	3.37E-06	3.85E-05	3.85E-06
866.6	2.97E-06	3.42E-04	5.19E-03	3.13E-02	4.59E-04	1.05E-03	3.83E-06	3.35E-06	3.83E-05	3.83E-06
936.1	2.91E-06	3.40E-04	5.34E-03	3.06E-02	4.17E-04	7.24E-04	3.75E-06	3.26E-06	3.75E-05	3.75E-06
1040	2.95E-06	3.43E-04	5.05E-03	3.14E-02	4.15E-04	8.70E-04	3.80E-06	3.32E-06	3.80E-05	3.80E-06
Low Aluminate, High Organic										
97.58	3.19E-06	3.38E-04	7.18E-03	2.99E-02	3.88E-04	3.32E-03	4.11E-06	NA	4.11E-05	4.11E-06
222.3	3.65E-06	3.38E-04	6.69E-03	3.21E-02	8.11E-04	7.12E-03	4.70E-06	NA	4.70E-05	4.70E-06
269.9	3.78E-06	3.20E-04	5.99E-03	3.16E-02	9.36E-04	9.87E-03	4.87E-06	NA	4.87E-05	4.87E-06
391.6	4.05E-06	3.42E-04	5.98E-03	3.45E-02	1.19E-03	1.01E-02	5.21E-06	NA	5.21E-05	5.21E-06
506.6	4.09E-06	3.87E-04	7.02E-03	3.78E-02	1.26E-03	6.31E-03	5.27E-06	NA	5.27E-05	5.27E-06
575.8	4.23E-06	3.75E-04	6.17E-03	3.76E-02	1.43E-03	9.02E-03	5.46E-06	NA	5.46E-05	5.46E-06
703.1	4.22E-06	3.84E-04	6.15E-03	3.81E-02	1.55E-03	8.18E-03	5.44E-06	5.07E-06	5.44E-05	5.44E-06
769.1	4.25E-06	3.96E-04	6.24E-03	3.92E-02	1.58E-03	7.29E-03	5.47E-06	5.10E-06	5.47E-05	5.47E-06
866.6	4.19E-06	4.00E-04	6.06E-03	3.95E-02	1.57E-03	6.47E-03	5.40E-06	5.02E-06	5.40E-05	5.40E-06
936.1	4.15E-06	4.06E-04	6.10E-03	3.99E-02	1.55E-03	5.61E-03	5.35E-06	4.97E-06	5.35E-05	5.35E-06
1040	3.98E-06	4.14E-04	6.37E-03	3.96E-02	1.37E-03	3.54E-03	5.13E-06	4.74E-06	5.13E-05	5.13E-06

TABLE B.46. (contd)

Time (hr)	Moles of Gas in System									
	CO_2	Ar	O_2	N_2	H_2	N_2O	CH_4	NO_x	CO	He
Reference Formulation										
97.58	2.95E-06	3.29E-04	7.00E-03	2.87E-02	4.97E-04	1.48E-03	3.80E-06	NA	3.80E-05	3.80E-06
222.3	3.17E-06	3.24E-04	6.42E-03	2.97E-02	6.91E-04	3.67E-03	4.08E-06	NA	4.08E-05	4.08E-06
269.9	3.36E-06	3.34E-04	6.59E-03	3.12E-02	8.56E-04	4.28E-03	4.33E-06	NA	4.33E-05	4.33E-06
391.6	3.54E-06	3.34E-04	6.48E-03	3.26E-02	1.01E-03	5.14E-03	4.56E-06	NA	4.56E-05	4.56E-06
506.6	3.59E-06	3.25E-04	6.08E-03	3.23E-02	1.09E-03	6.37E-03	4.62E-06	NA	4.62E-05	4.62E-06
575.8	3.79E-06	3.57E-04	6.65E-03	3.51E-02	1.26E-03	5.50E-03	4.89E-06	NA	4.89E-05	4.89E-06
703.1	3.87E-06	3.69E-04	6.79E-03	3.63E-02	1.28E-03	5.21E-03	4.99E-06	4.59E-06	4.99E-05	4.99E-06
769.1	3.84E-06	3.75E-04	6.91E-03	3.66E-02	1.28E-03	4.31E-03	4.95E-06	4.55E-06	4.95E-05	4.95E-06
866.6	3.80E-06	3.58E-04	6.37E-03	3.55E-02	1.25E-03	5.55E-03	4.90E-06	4.49E-06	4.90E-05	4.90E-06
936.1	3.85E-06	3.72E-04	6.67E-03	3.66E-02	1.26E-03	4.76E-03	4.97E-06	4.56E-06	4.97E-05	4.97E-06
1040	3.87E-06	3.86E-04	6.86E-03	3.77E-02	1.25E-03	3.70E-03	4.99E-06	4.59E-06	4.99E-05	4.99E-06
High Aluminate, Low Organic										
97.58	3.09E-06	3.31E-04	6.60E-03	3.00E-02	6.43E-04	2.15E-03	3.98E-06	NA	3.98E-05	3.98E-06
222.3	3.22E-06	3.15E-04	5.76E-03	3.10E-02	9.60E-04	3.43E-03	4.15E-06	NA	4.15E-05	4.15E-06
269.9	3.29E-06	3.52E-04	6.91E-03	3.22E-02	6.76E-04	2.19E-03	4.23E-06	NA	4.23E-05	4.23E-06
391.6	3.38E-06	3.36E-04	6.12E-03	3.42E-02	8.80E-04	2.97E-03	4.36E-06	NA	4.36E-05	4.36E-06
506.6	3.46E-06	3.44E-04	6.14E-03	3.45E-02	9.57E-04	2.68E-03	4.46E-06	NA	4.46E-05	4.46E-06
575.8	3.59E-06	3.61E-04	6.10E-03	3.58E-02	1.05E-03	3.00E-03	4.62E-06	NA	4.62E-05	4.62E-06
703.1	3.68E-06	3.66E-04	6.04E-03	3.70E-02	1.12E-03	2.93E-03	4.74E-06	4.33E-06	4.74E-05	4.74E-06
769.1	3.65E-06	3.67E-04	6.16E-03	3.70E-02	1.10E-03	2.45E-03	4.70E-06	4.29E-06	4.70E-05	4.70E-06
866.6	3.69E-06	3.71E-04	6.09E-03	3.76E-02	1.09E-03	2.37E-03	4.75E-06	4.33E-06	4.75E-05	4.75E-06
936.1	3.71E-06	3.69E-04	5.90E-03	3.76E-02	1.15E-03	2.88E-03	4.78E-06	4.37E-06	4.78E-05	4.78E-06
1040	3.73E-06	3.79E-04	6.01E-03	3.75E-02	1.11E-03	2.41E-03	4.81E-06	4.40E-06	4.81E-05	4.81E-06

TABLE B.46. (contd)

Time (hr)	Moles of Gas in System									
	CO_2	Ar	O_2	N_2	H_2	N_2O	CH_4	NO_x	CO	He
High Aluminate, High Organic										
97.58	3.11E-06	3.08E-04	6.48E-03	2.87E-02	5.06E-04	4.08E-03	4.01E-06	NA	4.01E-05	4.01E-06
222.3	3.86E-06	3.20E-04	6.53E-03	3.42E-02	9.91E-04	7.65E-03	4.97E-06	NA	4.97E-05	4.97E-06
269.9	4.04E-06	2.66E-04	5.19E-03	3.28E-02	1.17E-03	1.27E-02	5.21E-06	NA	5.21E-05	5.21E-06
391.6	4.43E-06	3.02E-04	5.80E-03	3.81E-02	1.35E-03	1.16E-02	5.71E-06	NA	5.71E-05	5.71E-06
506.6	4.61E-06	3.08E-04	5.84E-03	4.02E-02	1.39E-03	1.17E-02	5.94E-06	NA	5.94E-05	5.94E-06
575.8	4.79E-06	3.21E-04	5.90E-03	4.20E-02	1.50E-03	1.20E-02	6.18E-06	NA	6.18E-05	6.18E-06
703.1	5.10E-06	2.91E-04	5.15E-03	4.24E-02	1.66E-03	1.61E-02	1.91E-05	6.27E-06	6.57E-05	6.57E-06
769.1	5.14E-06	3.61E-04	6.54E-03	4.69E-02	1.58E-03	1.09E-02	1.31E-05	6.33E-06	6.62E-05	6.62E-06
866.6	5.24E-06	3.68E-04	6.67E-03	4.82E-02	1.62E-03	1.06E-02	1.34E-05	6.47E-06	6.76E-05	6.76E-06
936.1	5.36E-06	3.89E-04	6.94E-03	4.99E-02	1.63E-03	1.02E-02	1.37E-05	6.63E-06	6.90E-05	6.90E-06
1040	5.49E-06	3.92E-04	7.05E-03	5.15E-02	1.70E-03	1.02E-02	1.40E-05	6.82E-06	7.08E-05	7.08E-06

NA = Not analyzed for.

APPENDIX C

RAW DATA FOR DIFFERENTIAL SCANNING CALORIMETRY AND SCANNING THERMOGRAVIMETRIC ANALYSES

Low Aluminate / Low Organic

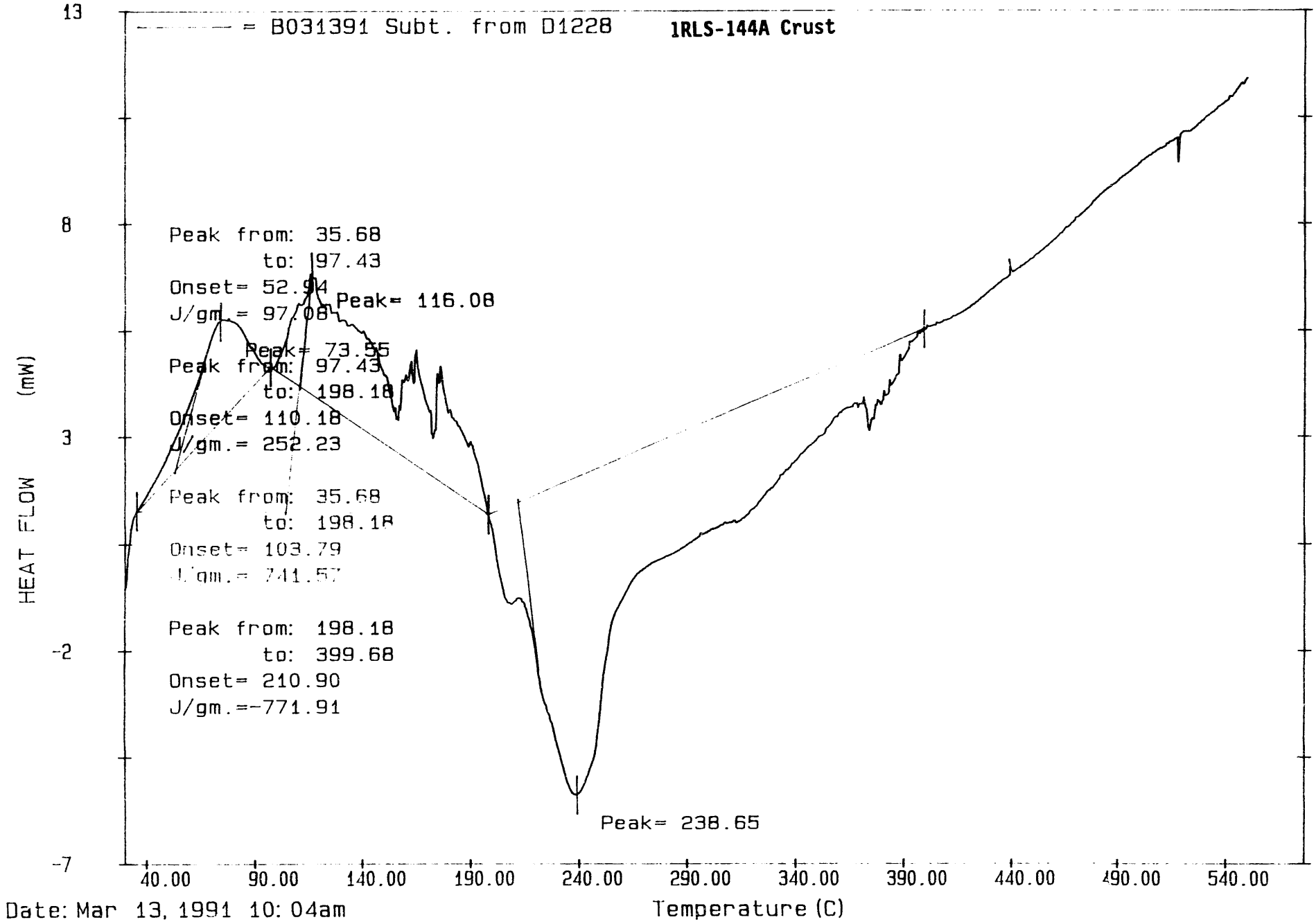

Date: Mar 13, 1991 10:04am
Scanning Rate: 5.0 C/min
Sample Wt: 8.400 mg Path: A:\
File: D1228 R L SELL

PE PC SERIES DSC7

Low Aluminate / Low Organic

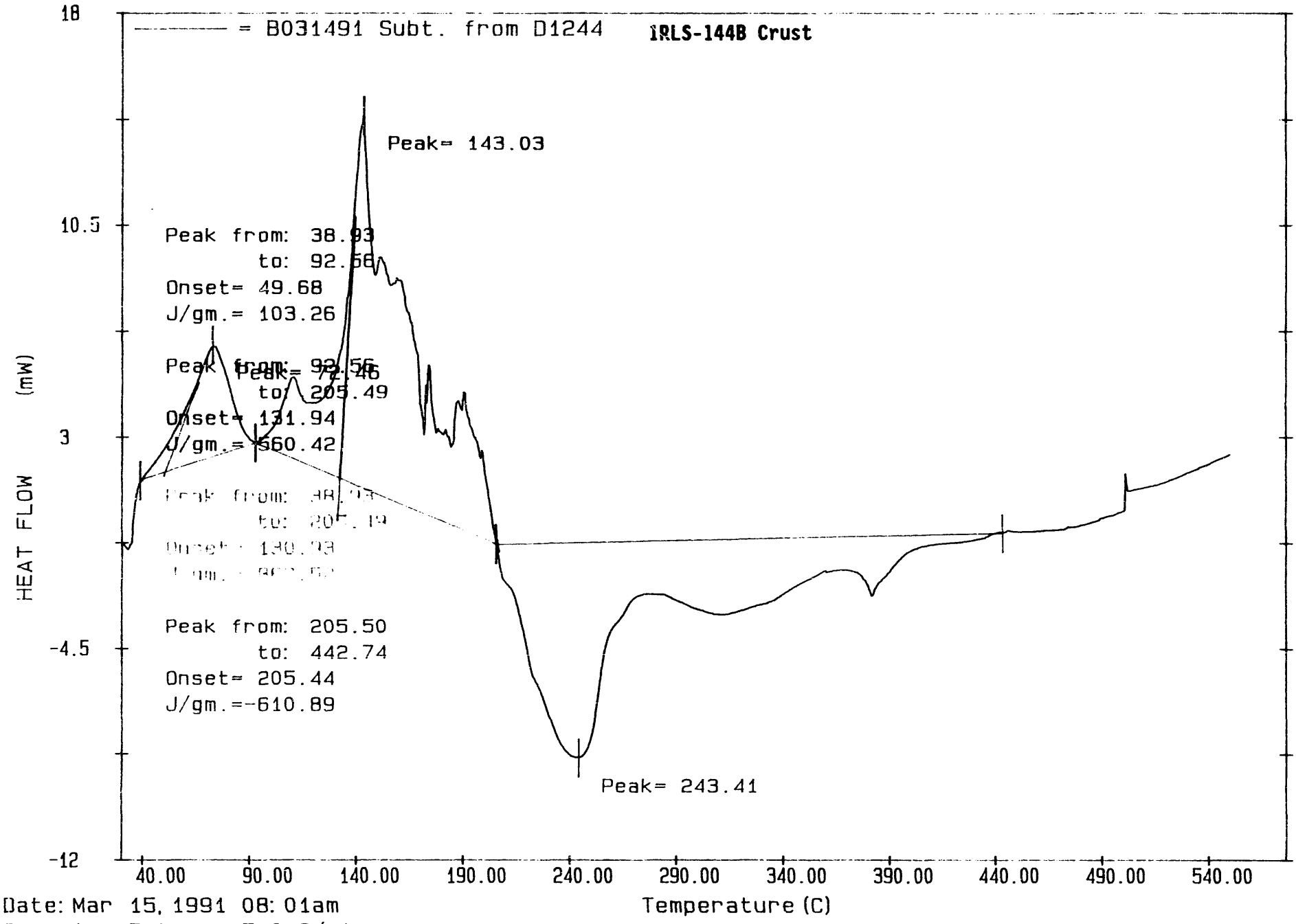

Date: Mar 15, 1991 08:01am
Scanning Rate: 5.0 C/min
Sample Wt: 10.700 mg Path: A:\

C.2

Low Aluminate / Low Organic

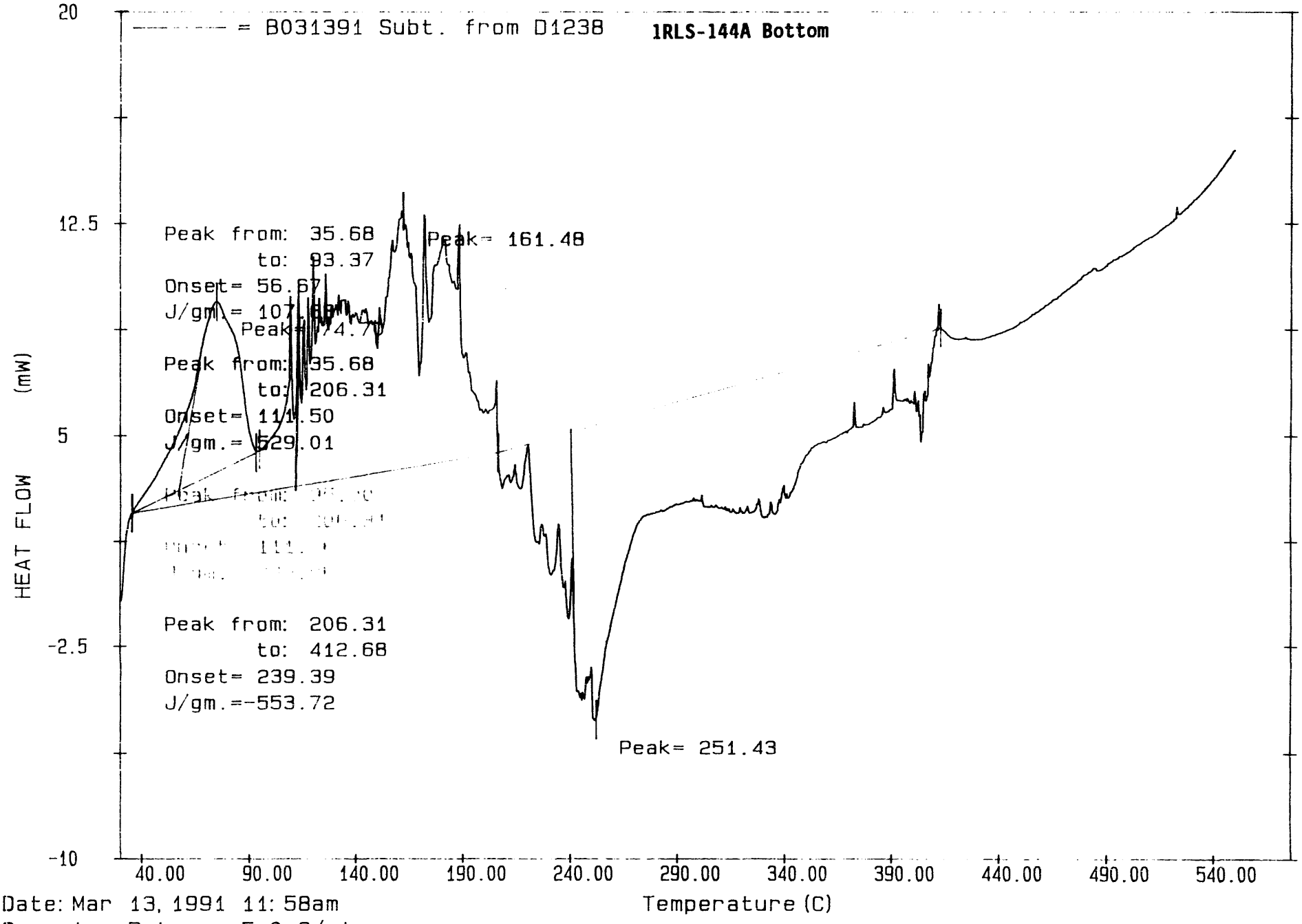

Date: Mar 13, 1991 11:58am
Scanning Rate: 5.0 C/min
Sample Wt: 17.000 mg Path: a:\
File: D1238 R L SELL

PE PC SERIES DSC7

Low Aluminate / Low Organic

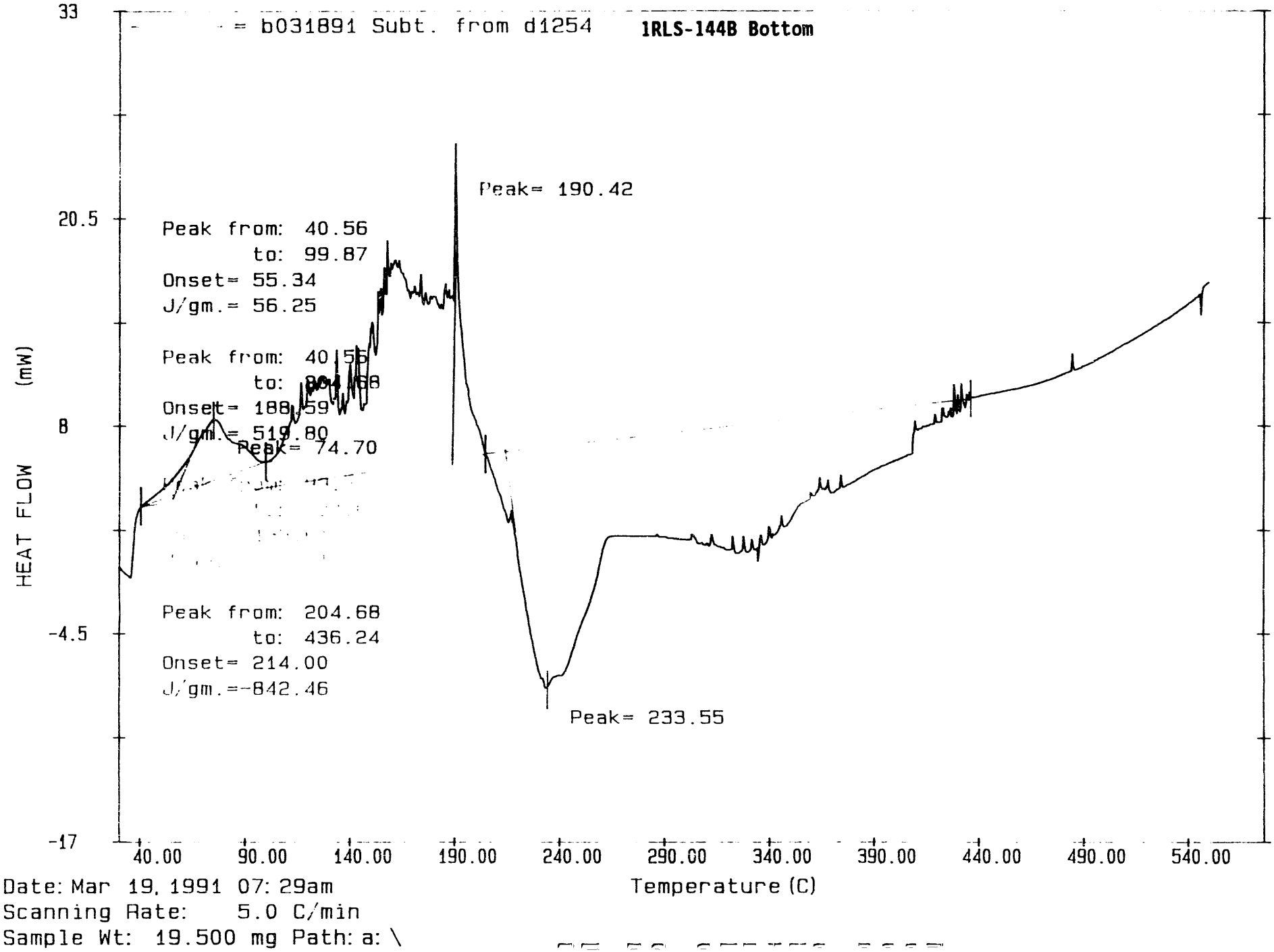

Date: Mar 19, 1991 07:29am
Scanning Rate: 5.0 C/min
Sample Wt: 19.500 mg Path: a:\

C.4

Low Aluminate / High Organic

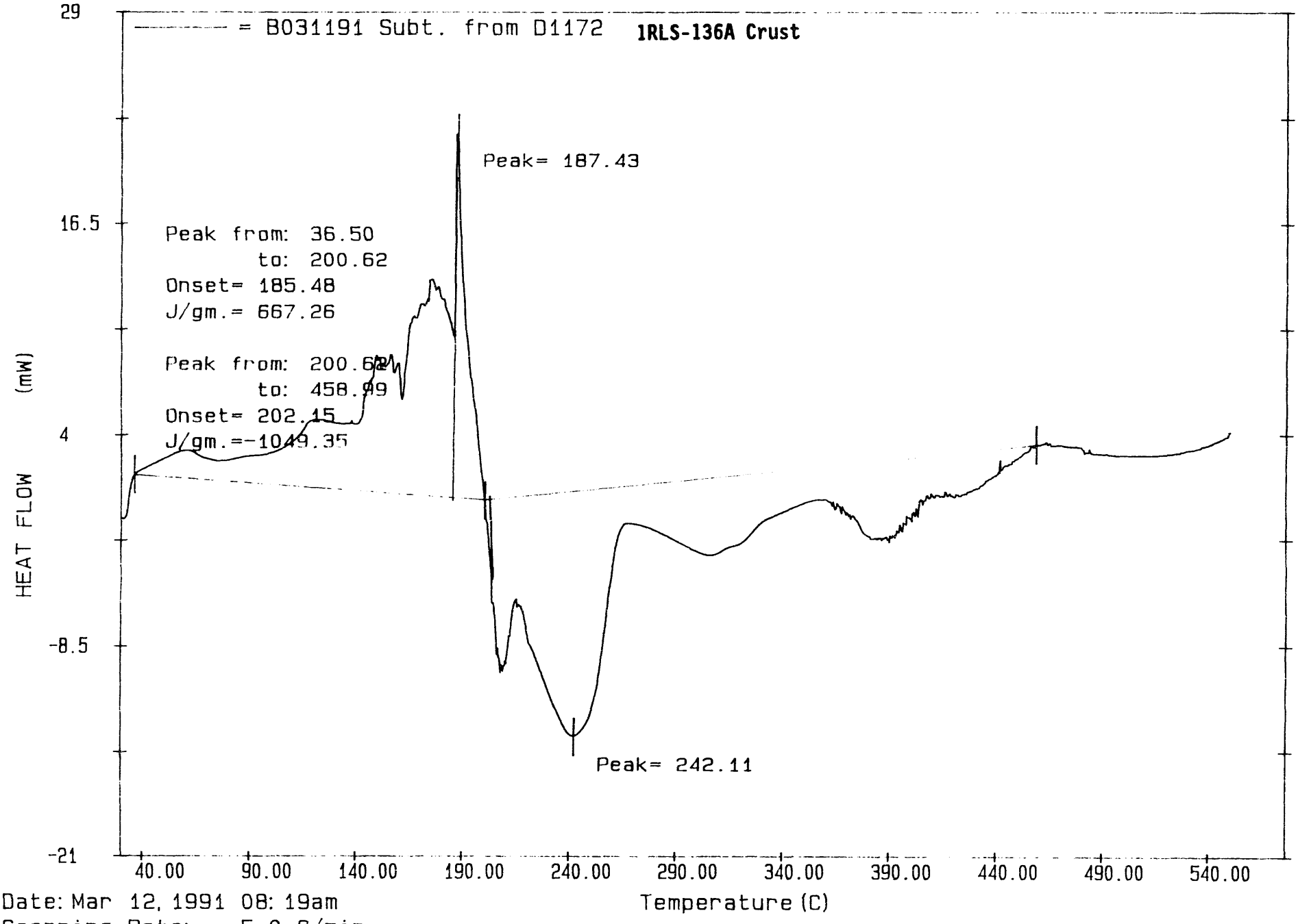

Date: Mar 12, 1991 08: 19am
Scanning Rate: 5.0 C/min
Sample Wt: 13.500 mg Path: A: \
File: D1172 R L SELL

PE PC SERIES DSC7

C.5

Low Aluminate / High Organic

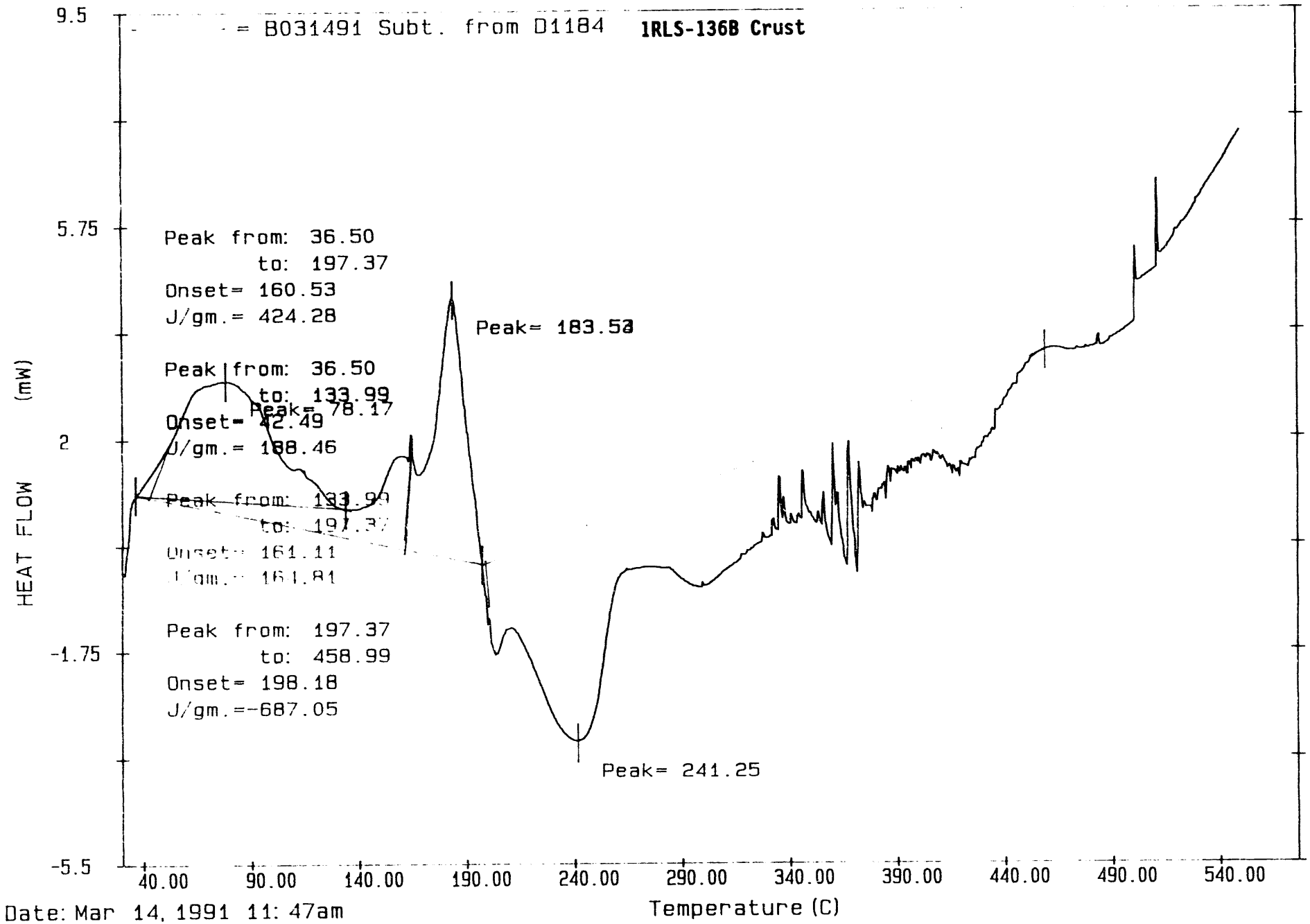

Date: Mar 14, 1991 11:47am
Scanning Rate: 5.0 C/min
Sample Wt: 6.900 mg Path: A:\

Low Aluminate / High Organic

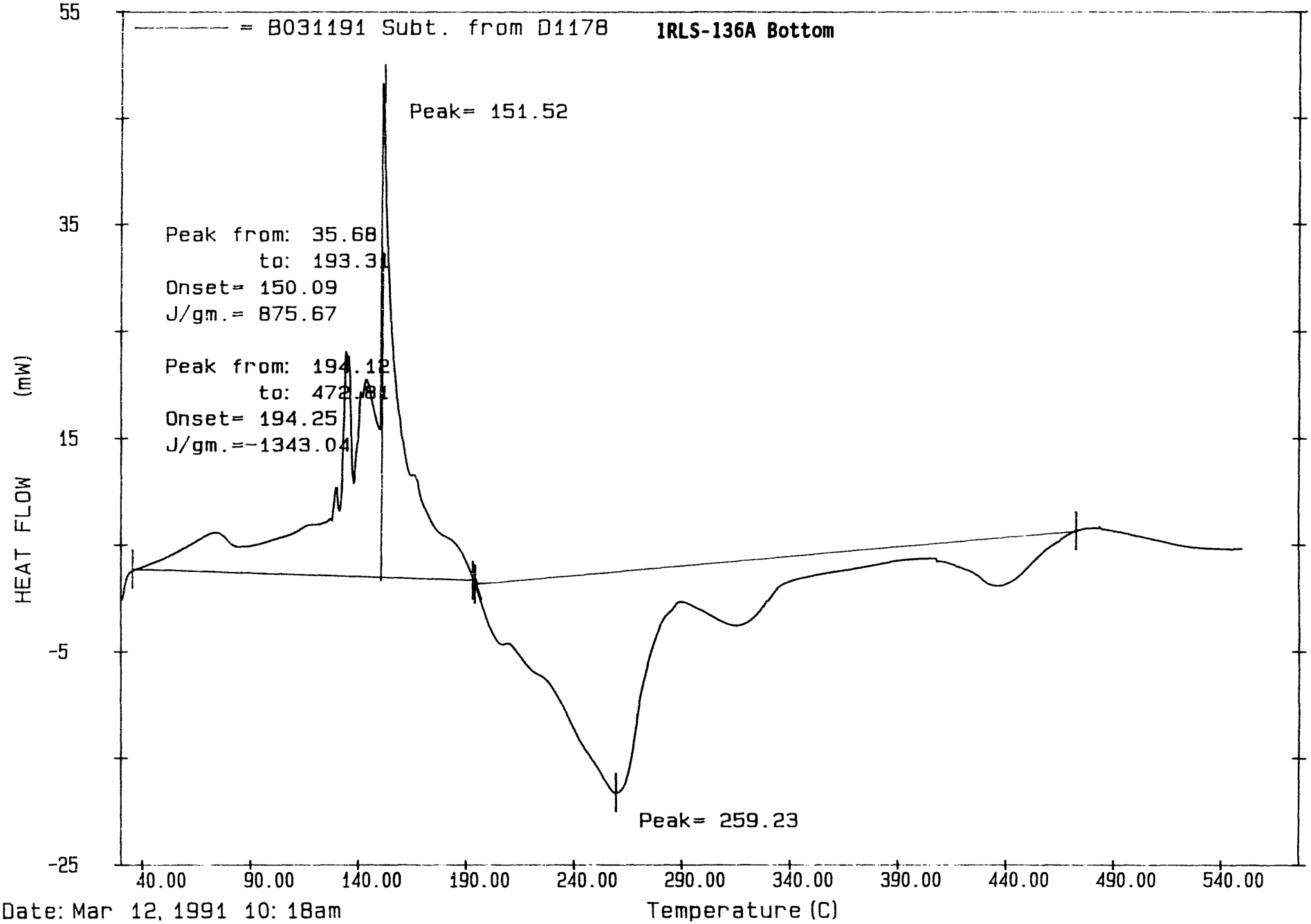

Date: Mar 12, 1991 10:18am
Scanning Rate: 5.0 C/min
Sample Wt: 13.700 mg Path: A:\
File: D1178 R L SELL

PE PC SERIES DSC7

Low Aluminate / High Organic

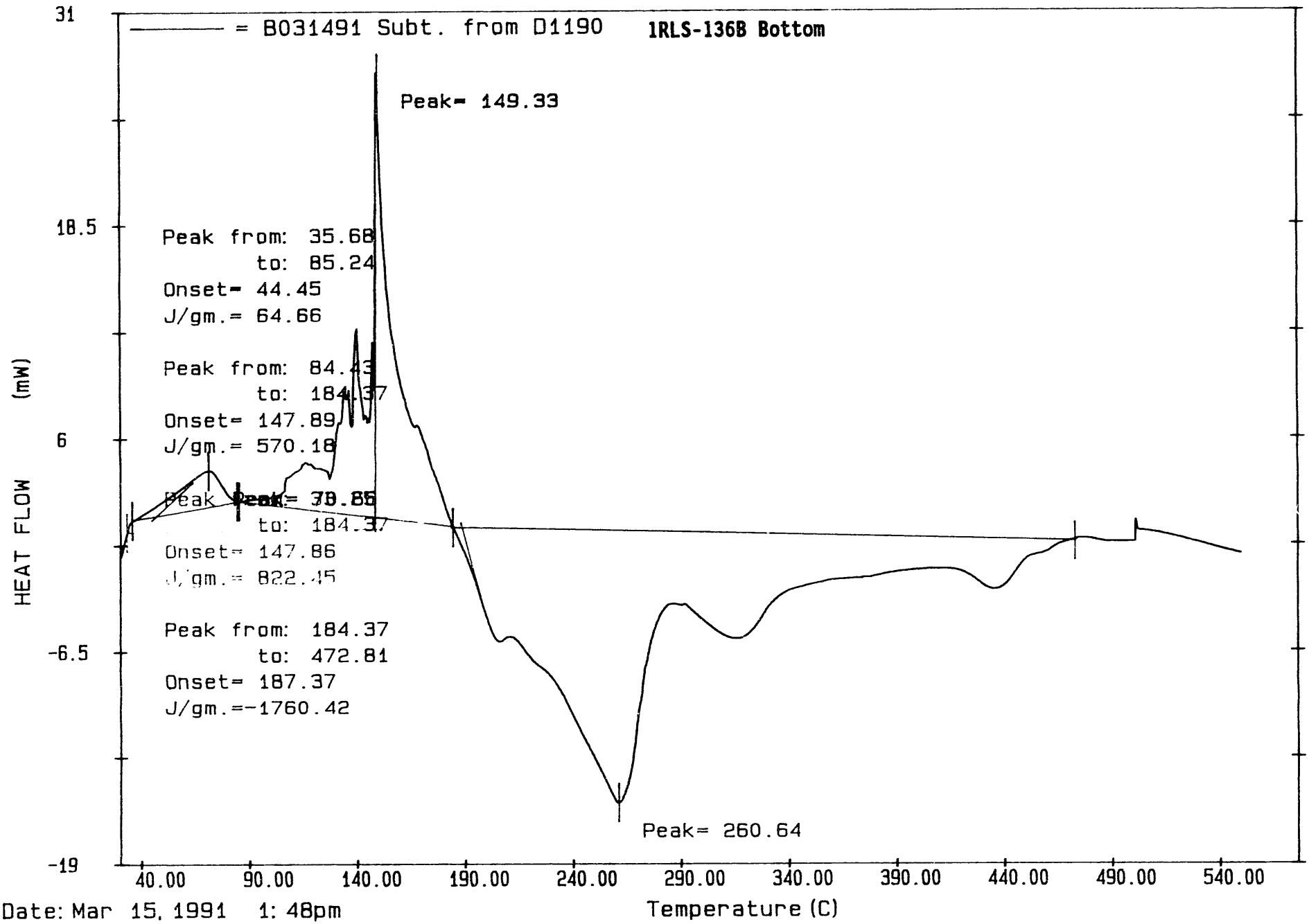

Date: Mar 15, 1991 1:48pm
Scanning Rate: 5.0 C/min
Sample Wt: [illegible] mg Pan: Al

C.8

Reference

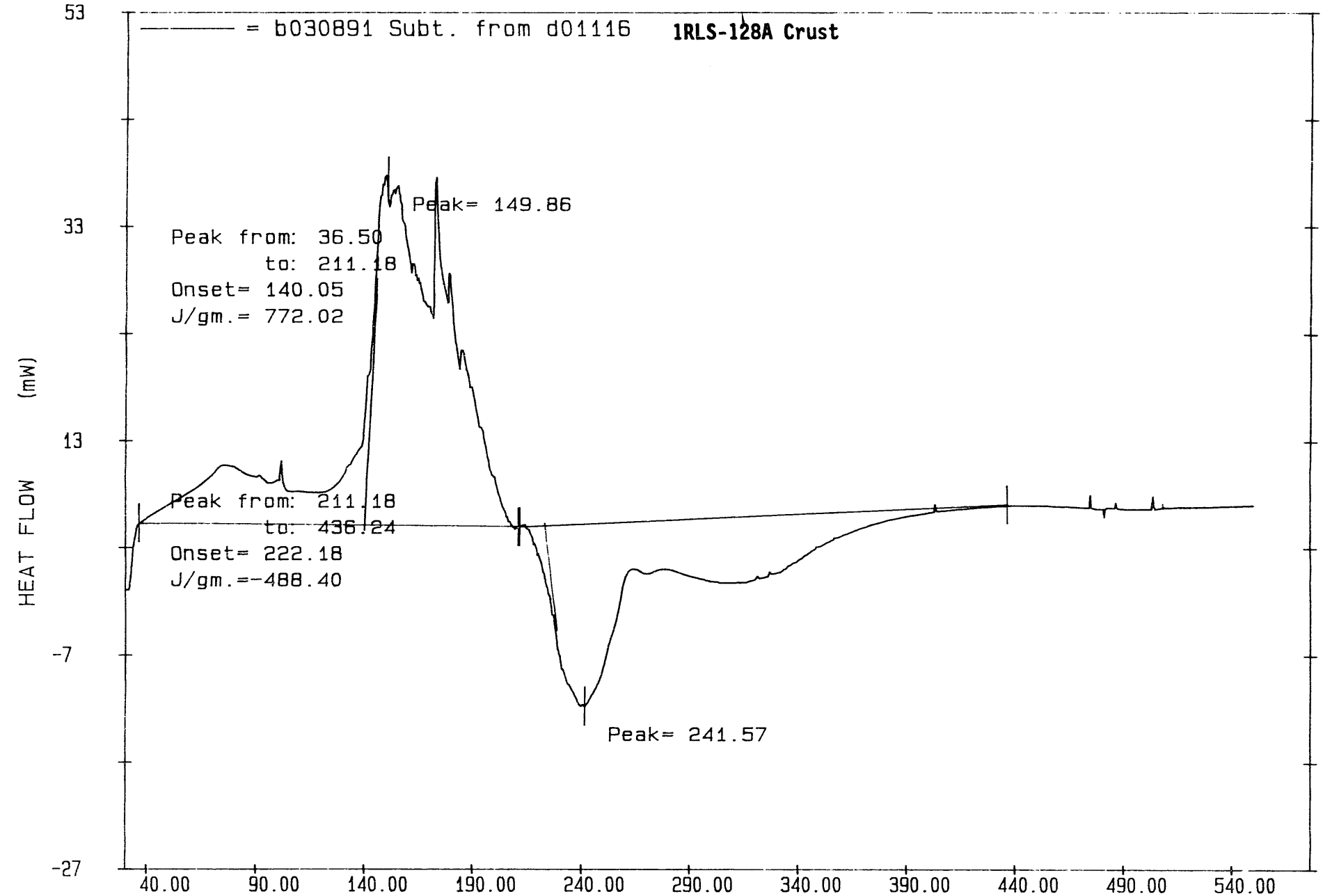

C.9

Date: Mar 08, 1991 11:57am
Scanning Rate: 5.0 C/min
Sample Wt: 25.100 mg Path: a:\
File: D01116 R L SELL

PE PC SERIES DSC7

Reference

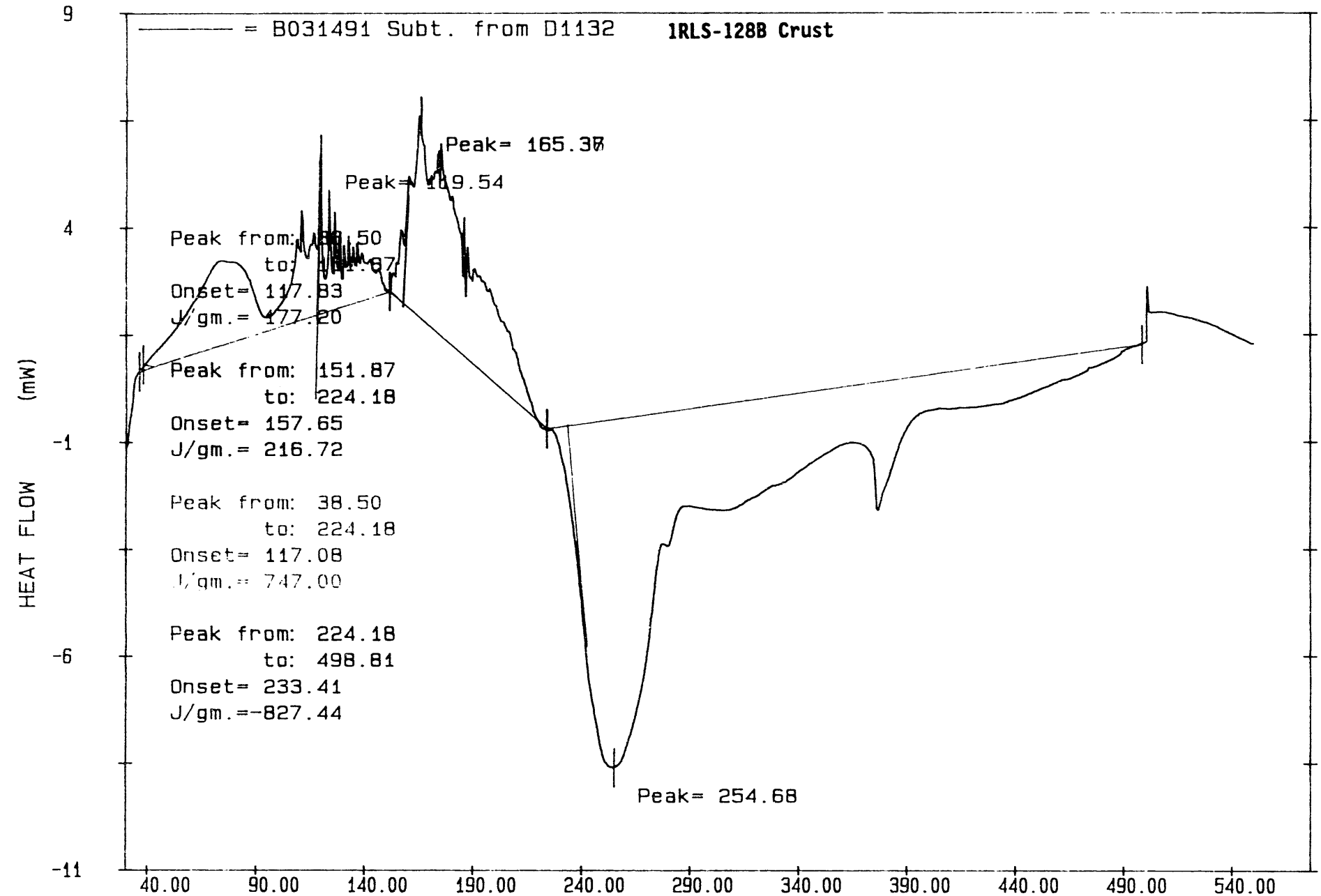

Date: Mar 13, 1991 2:15pm
Scanning Rate: 5.0 C/min
Sample Wt: 8.200 mg Path: A:\

Reference

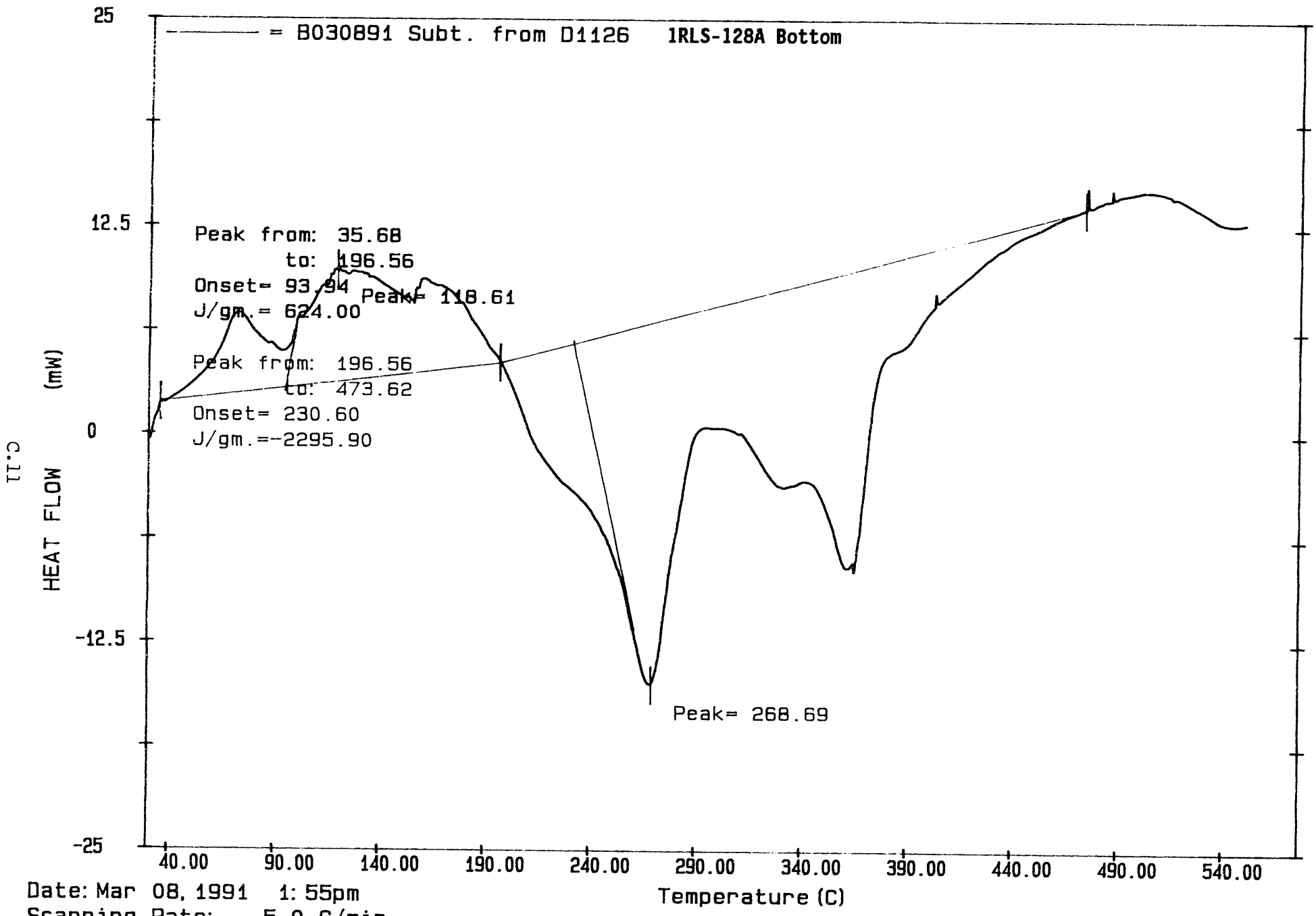

C.11

Date: Mar 08, 1991 1:55pm
Scanning Rate: 5.0 C/min
Sample Wt: 11.600 mg Path: \pe\hyd\dsc
File: D1126 R L SELL

PE PC SERIES DSC7

Reference

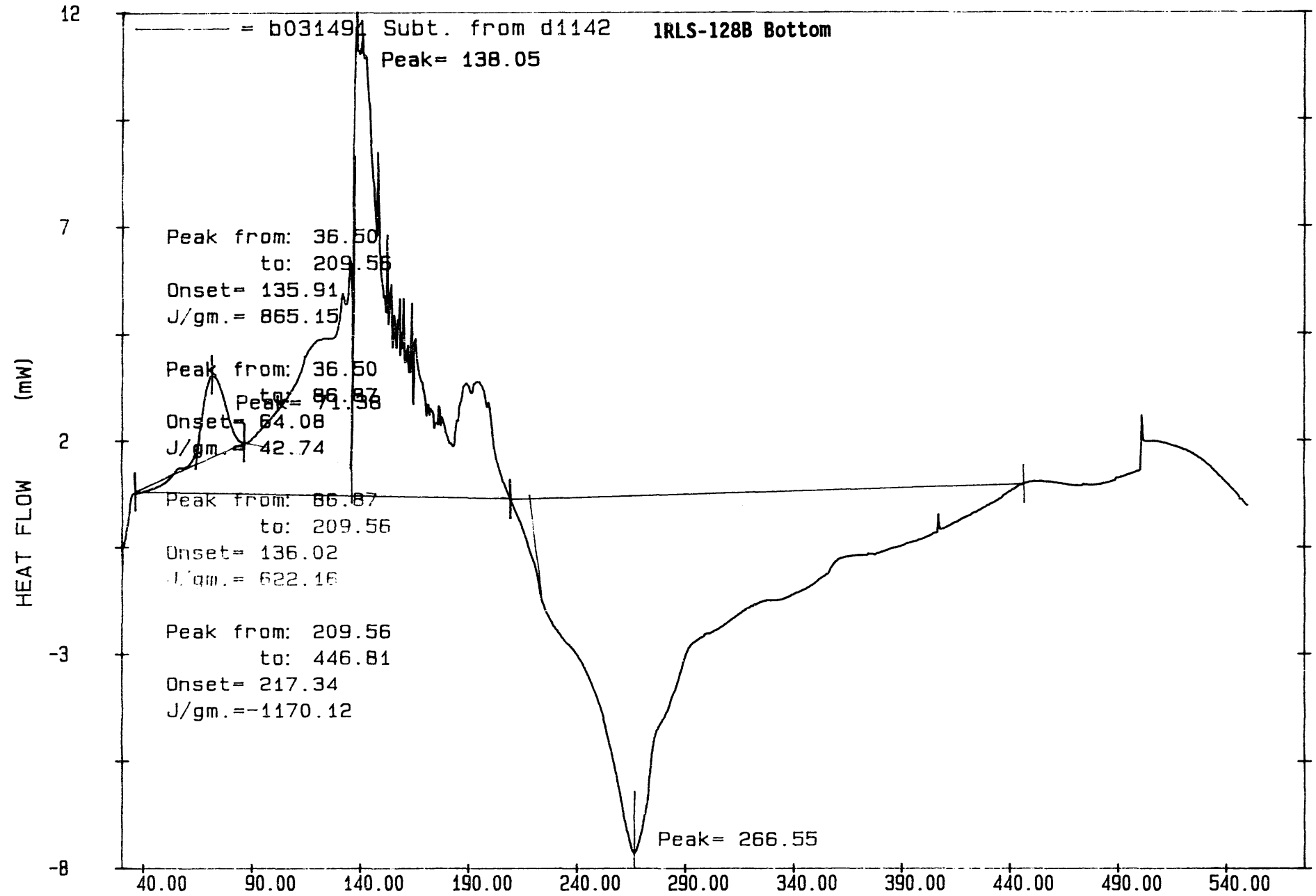

Date: Mar 15, 1991 09:55am
Scanning Rate: 5.0 C/min
Sample Wt: 6.400 mg Path: a:`

High Aluminate / Low Organic

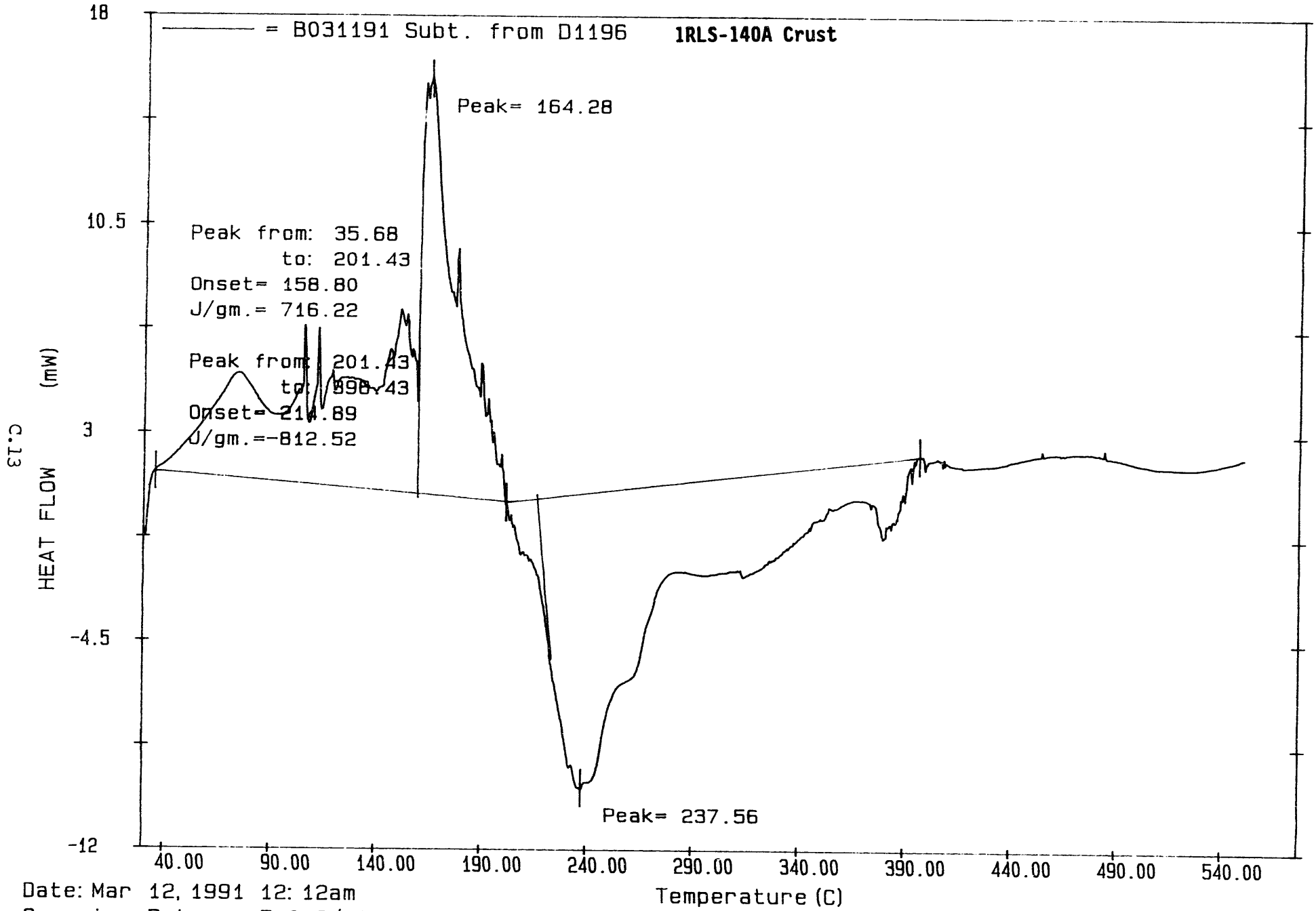

Date: Mar 12, 1991 12:12am
Scanning Rate: 5.0 C/min
Sample Wt: 11.200 mg Path: A:\
File: D1196 R L SELL

PE PC SERIES DSC7

High Aluminate / Low Organic

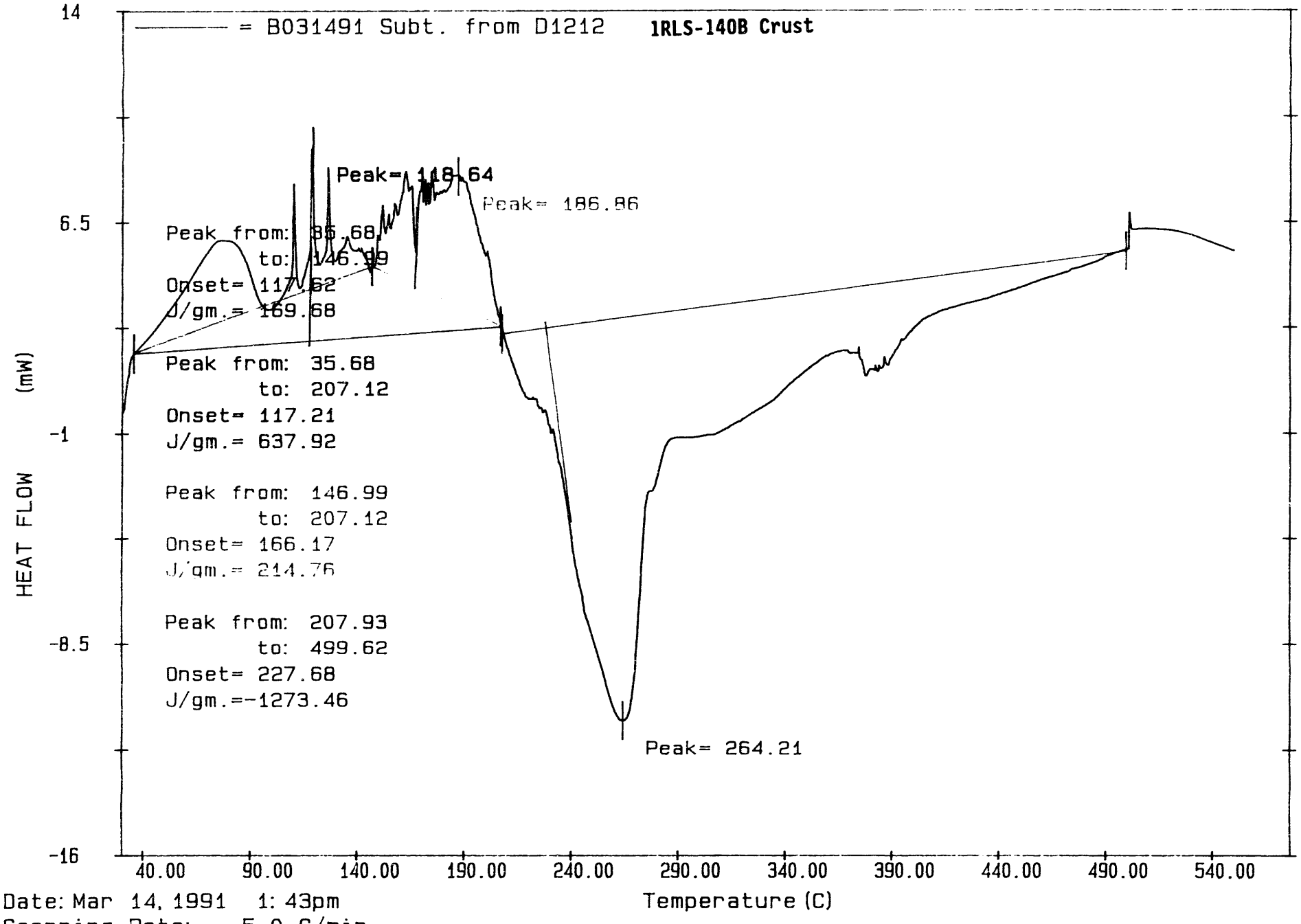

Date: Mar 14, 1991 1:43pm
Scanning Rate: 5.0 C/min
Sample Wt: 9.800 mg Path: A:\

High Aluminate/Low Organic

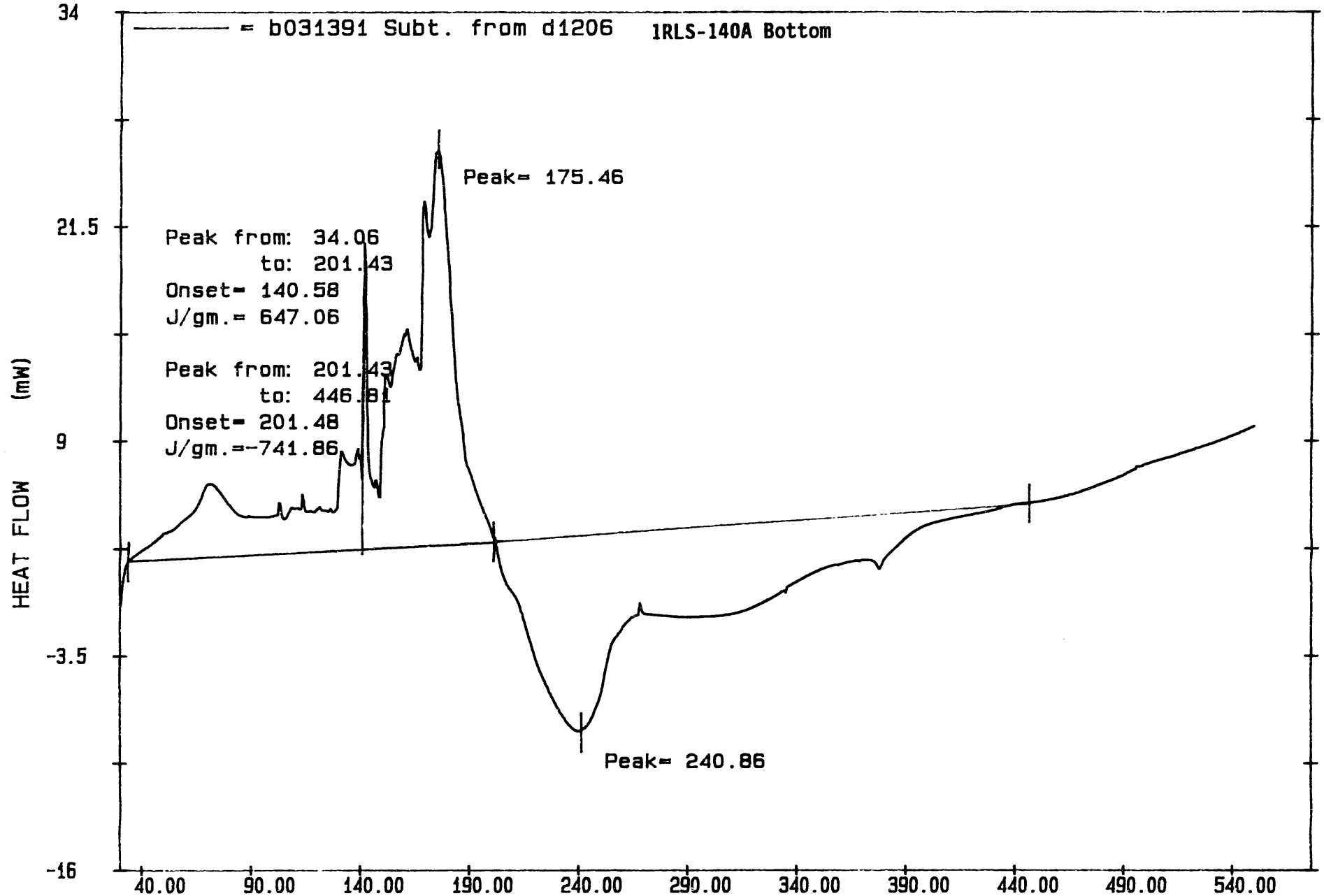

Date: Mar 13, 1991 08:03am
Scanning Rate: 5.0 C/min
Sample Wt: 16.200 mg Path: d:\archive\
File: D1206 R L SELL

PE PC SERIES DSC7

High Aluminate/Low Organic

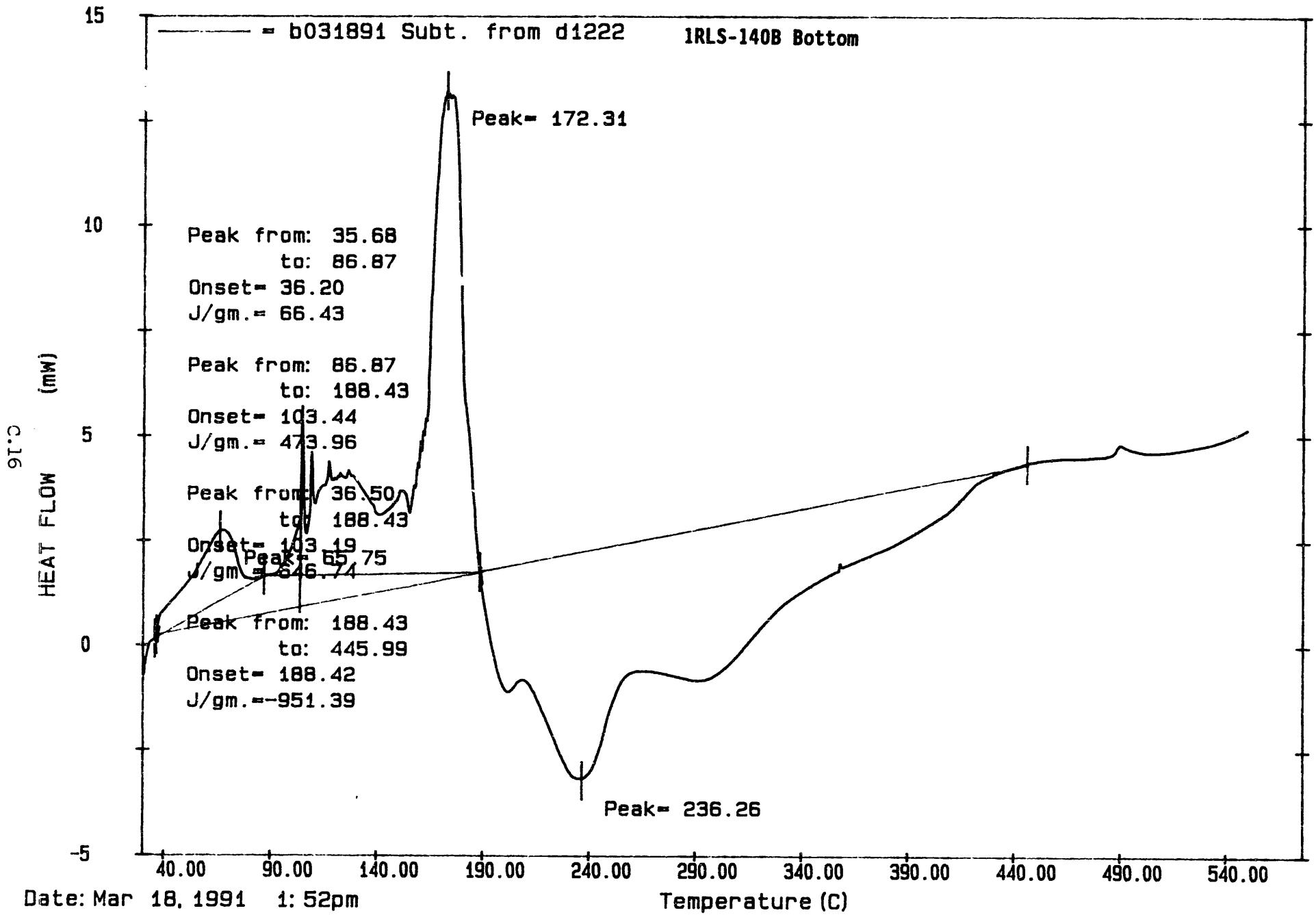

Date: Mar 18, 1991 1:52pm
Scanning Rate: 5.0 C/min
Sample Wt: 7.700 mg Path: d:\archive\

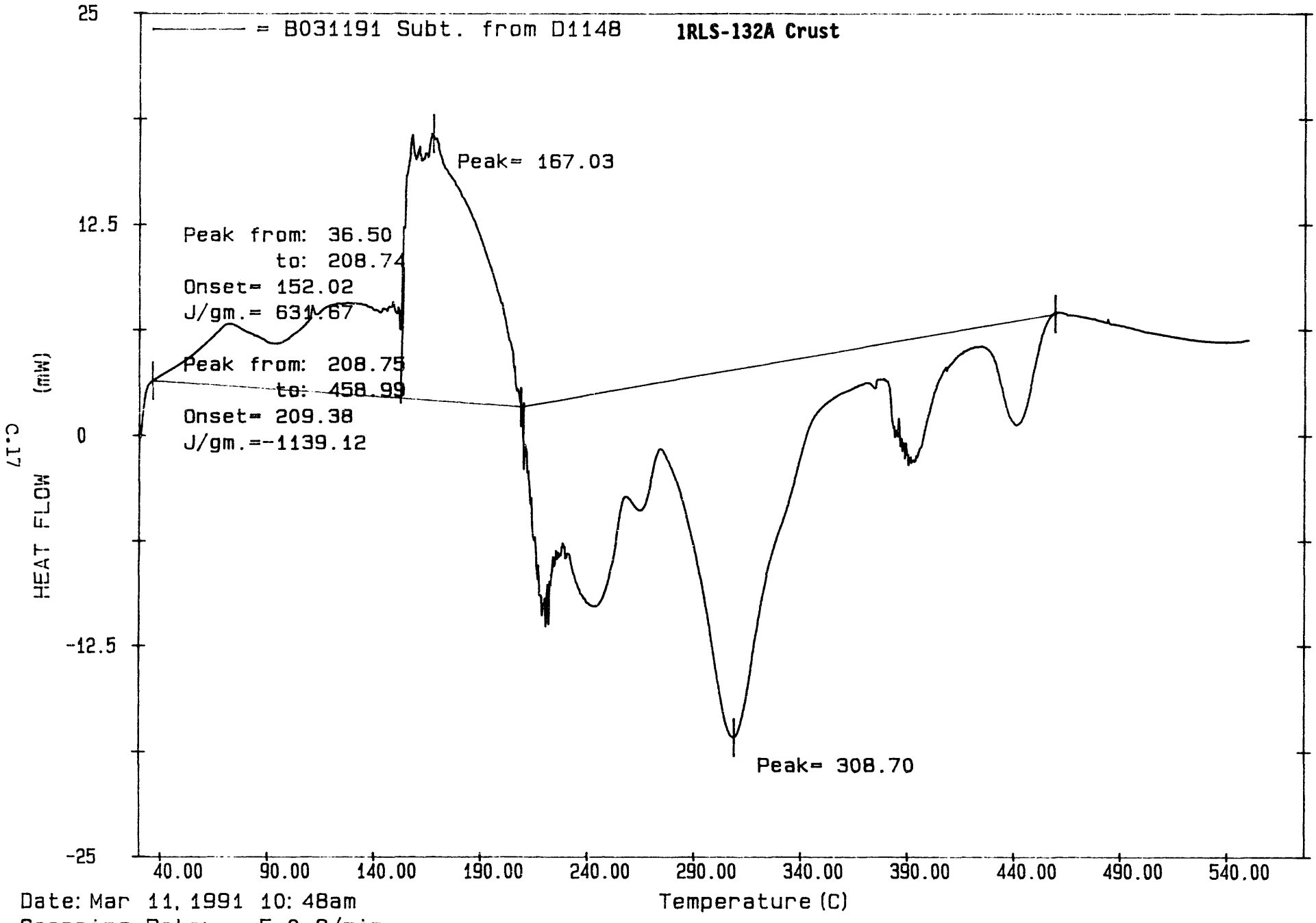

Date: Mar 11, 1991 10:48am
Scanning Rate: 5.0 C/min
Sample Wt: 19.000 mg Path: A:\
File: D1148 R L SELL

PE PC SERIES DSC7

High Aluminate / High Organic

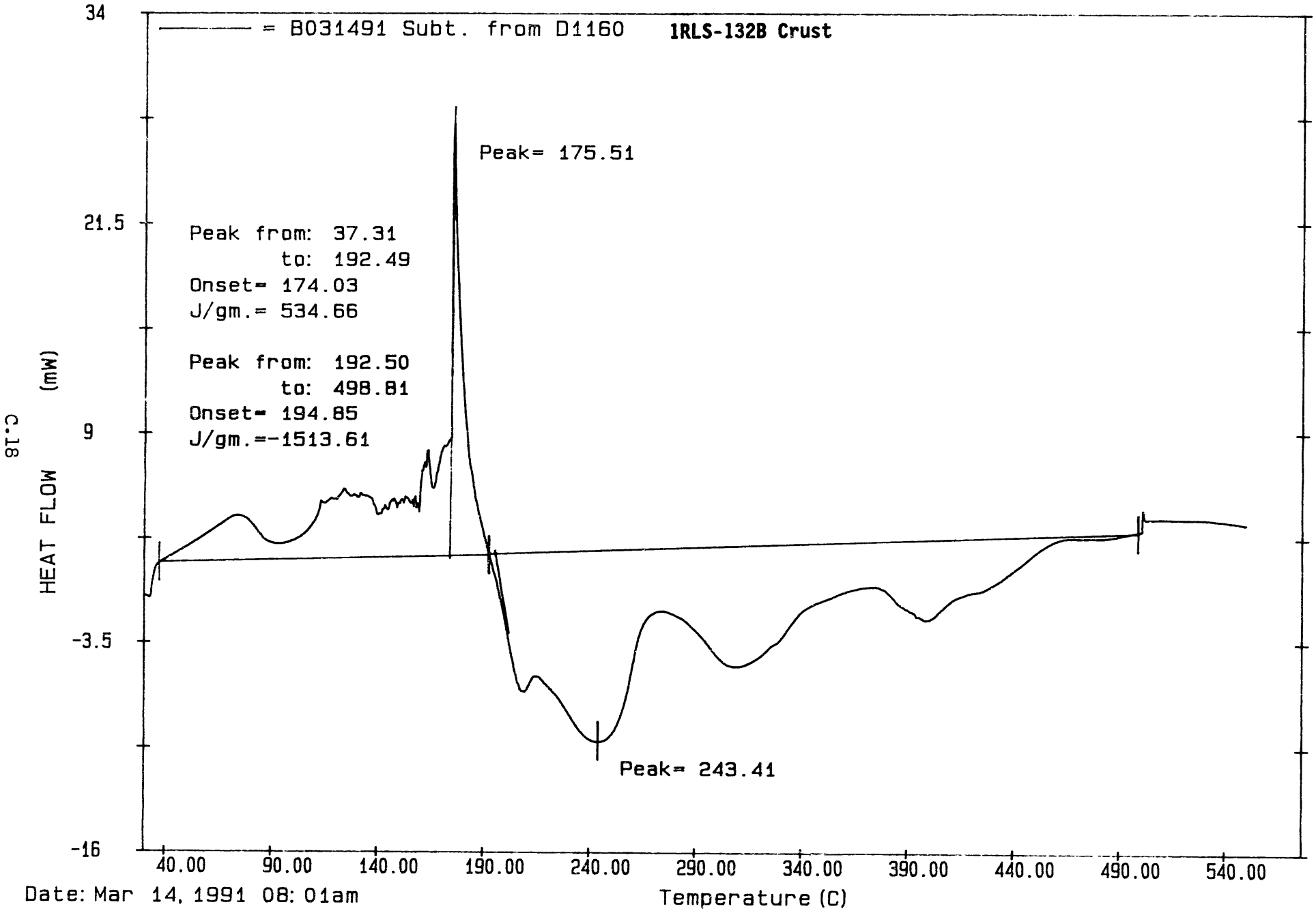

Date: Mar 14, 1991 08:01am
Scanning Rate: 5.0 C/min
Sample Wt: 11.000 mg Path: A:\

...gh Alumina ...gh Organic

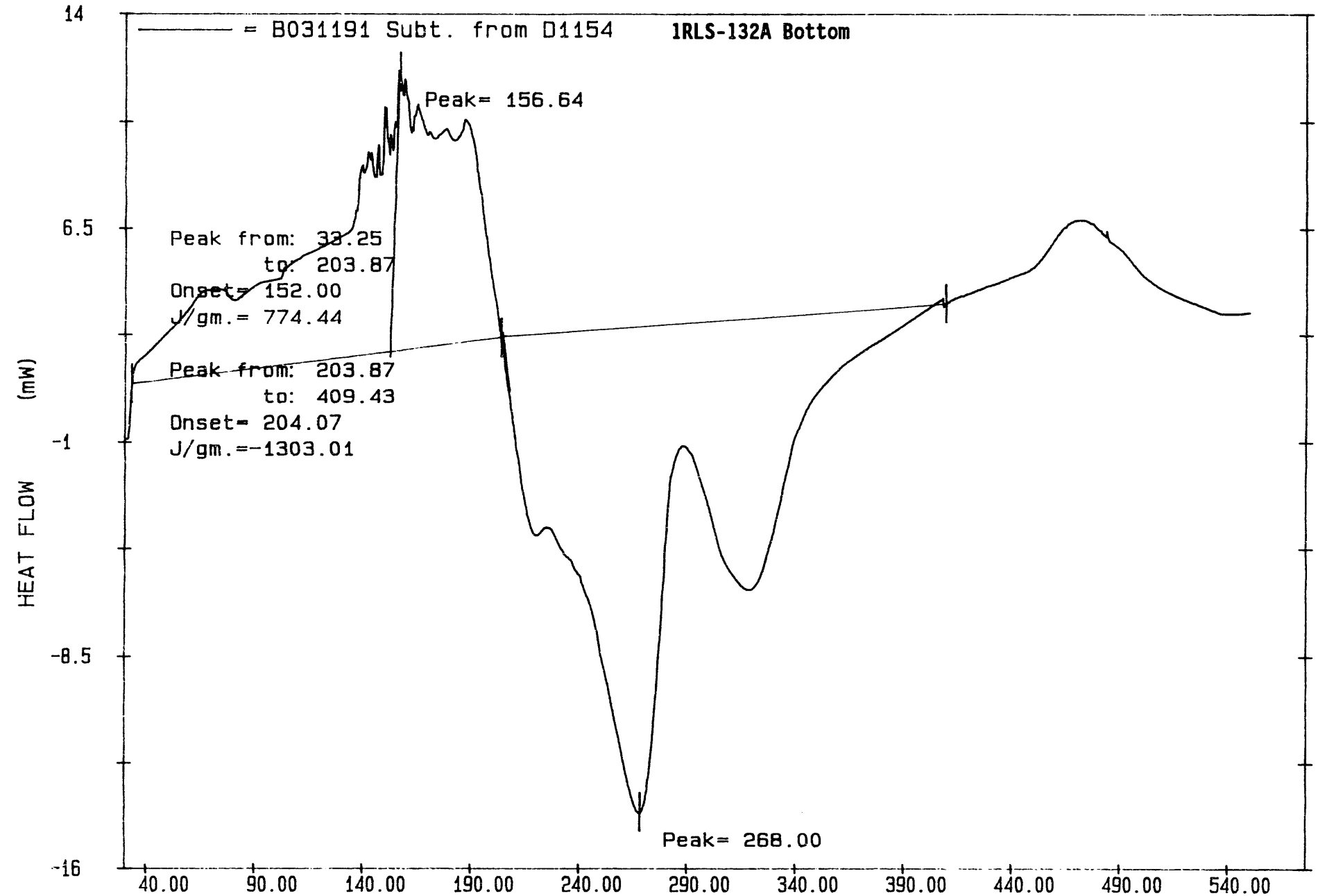

C.19

Date: Mar 11, 1991 2:36pm
Scanning Rate: 5.0 C/min
Sample Wt: 11.600 mg Path: A:\
File: D1154 R L SELL

PE PC SERIES DSC7

High Aluminate / High Organic

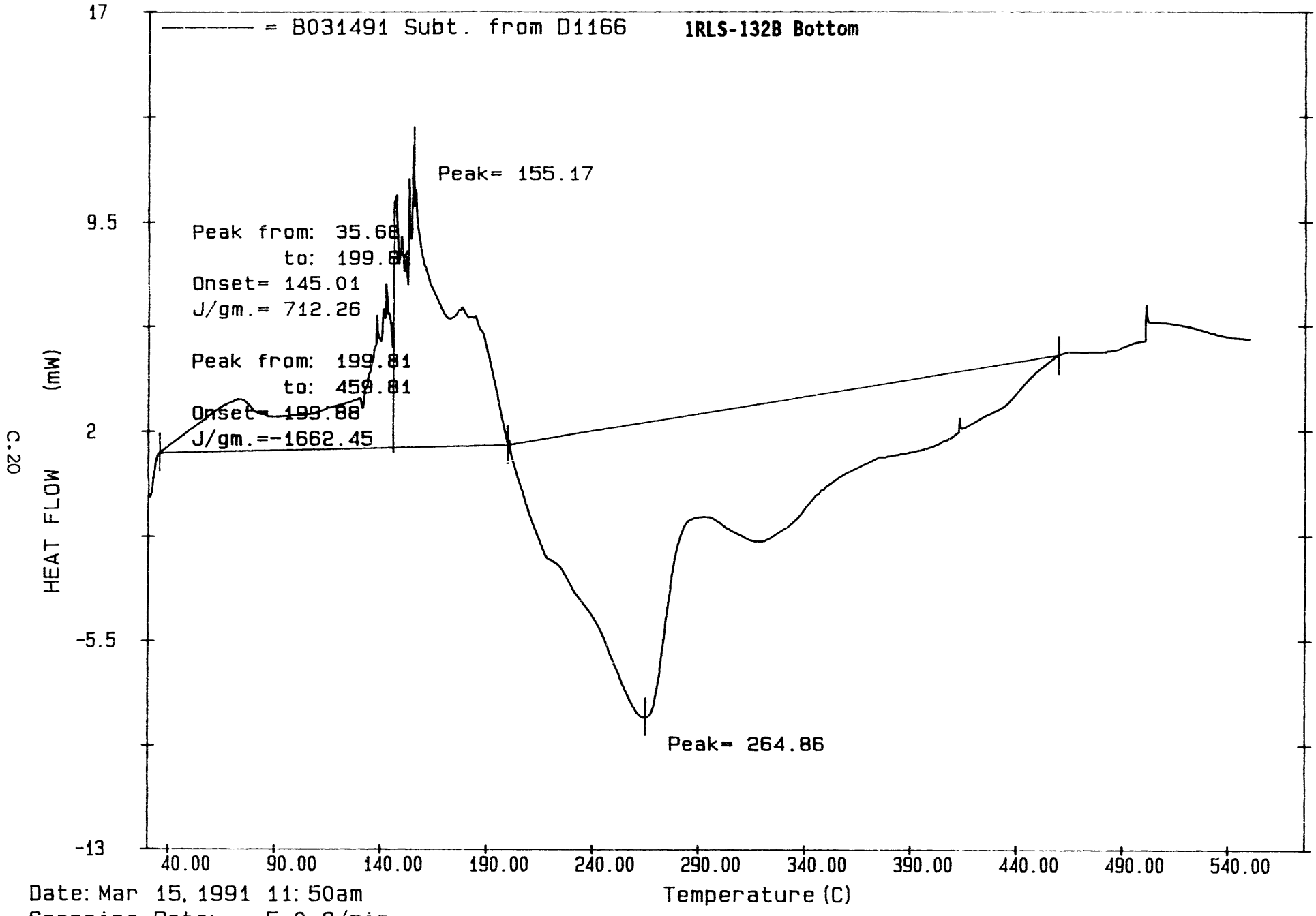

C.20

Date: Mar 15, 1991 11:50am
Scanning Rate: 5.0 C/min
Sample Wt: 7.400 mg Path: A:\

Reference

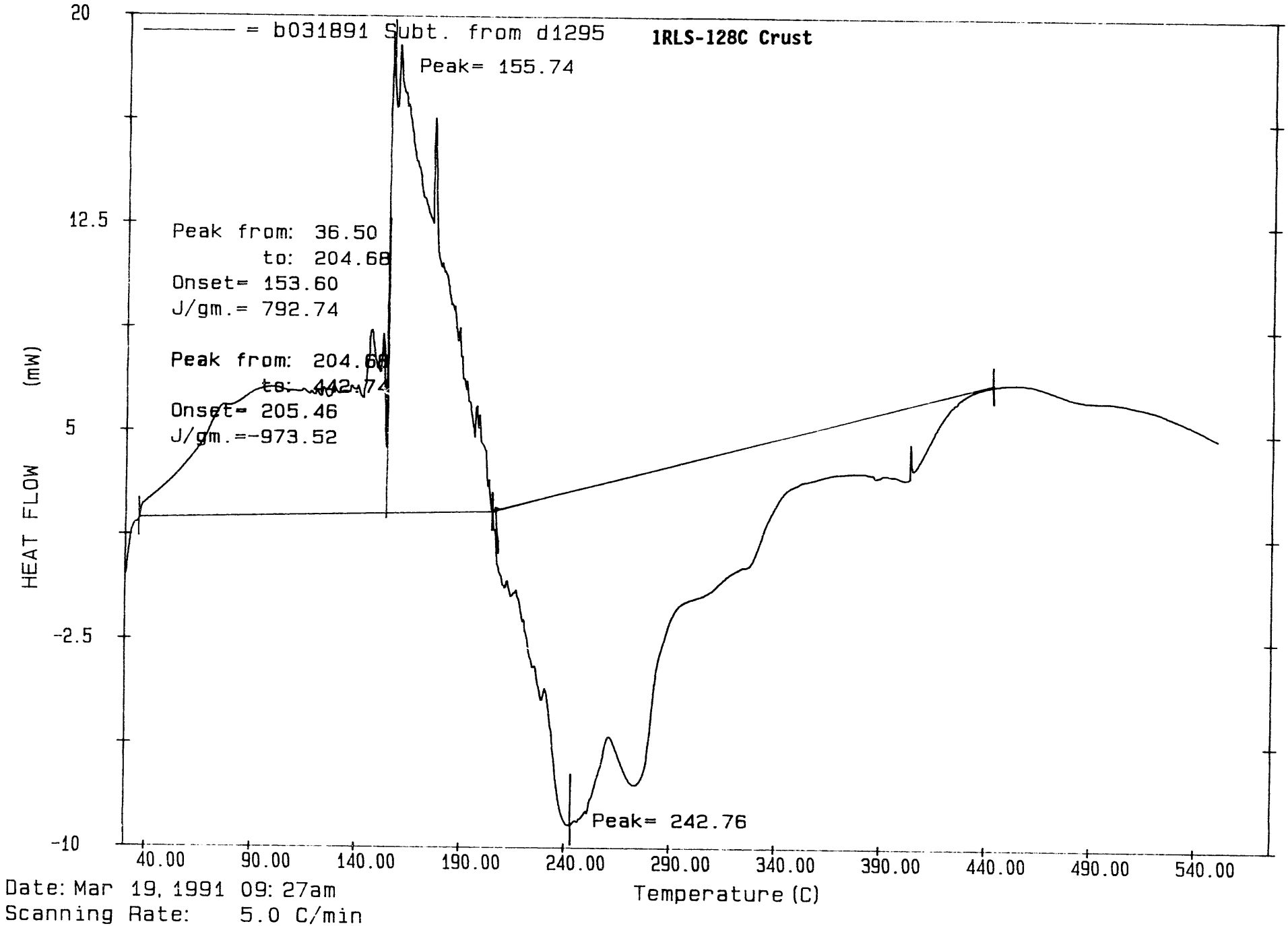

C.21

Date: Mar 19, 1991 09:27am
Scanning Rate: 5.0 C/min
Sample Wt: 13.300 mg Path: a:\
File: D1295 R L SELL

PE PC SERIES DSC7

Reference

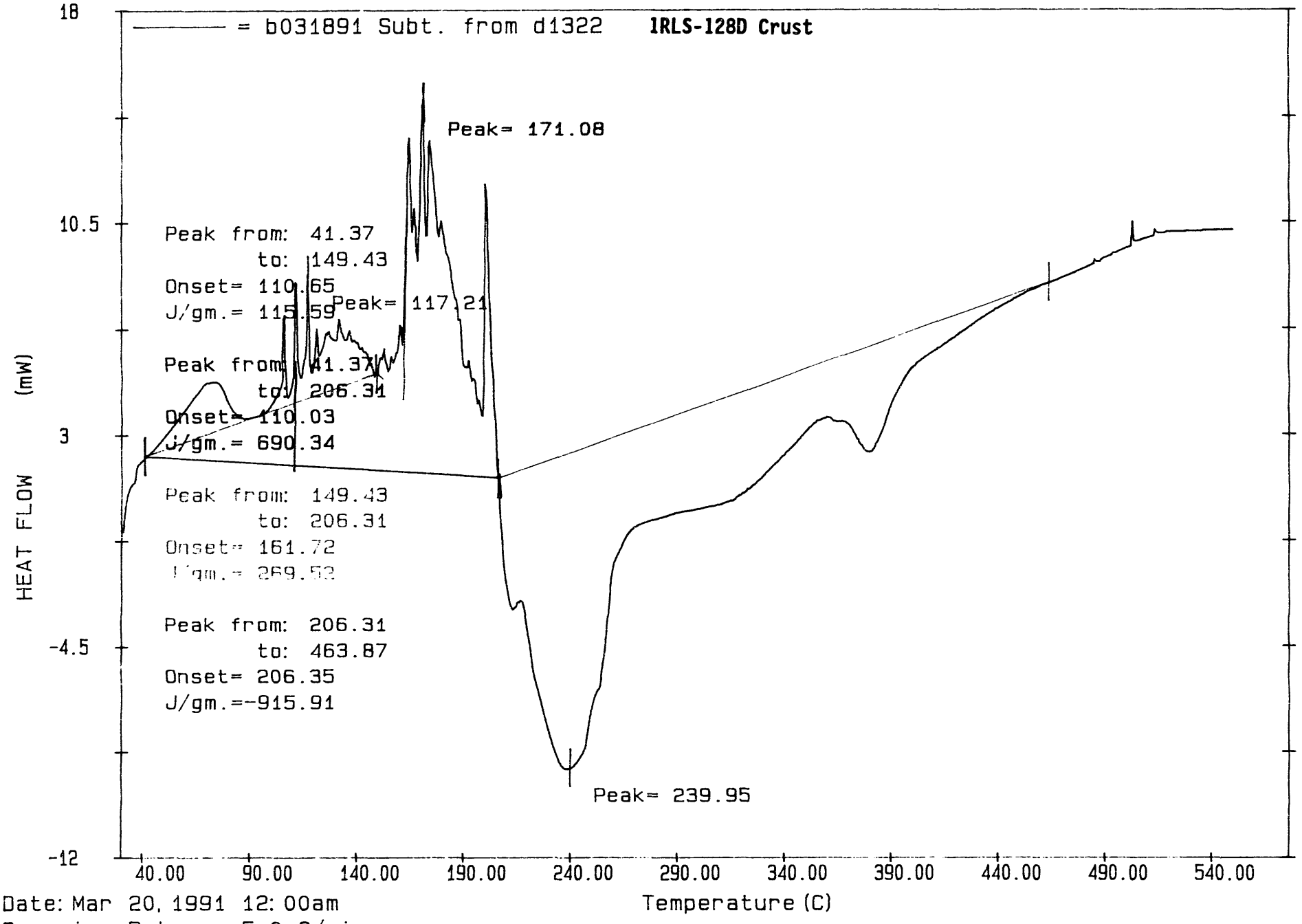

Date: Mar 20, 1991 12:00am
Scanning Rate: 5.0 C/min
Sample Wt: 11.500 mg Path: a:\

Reference

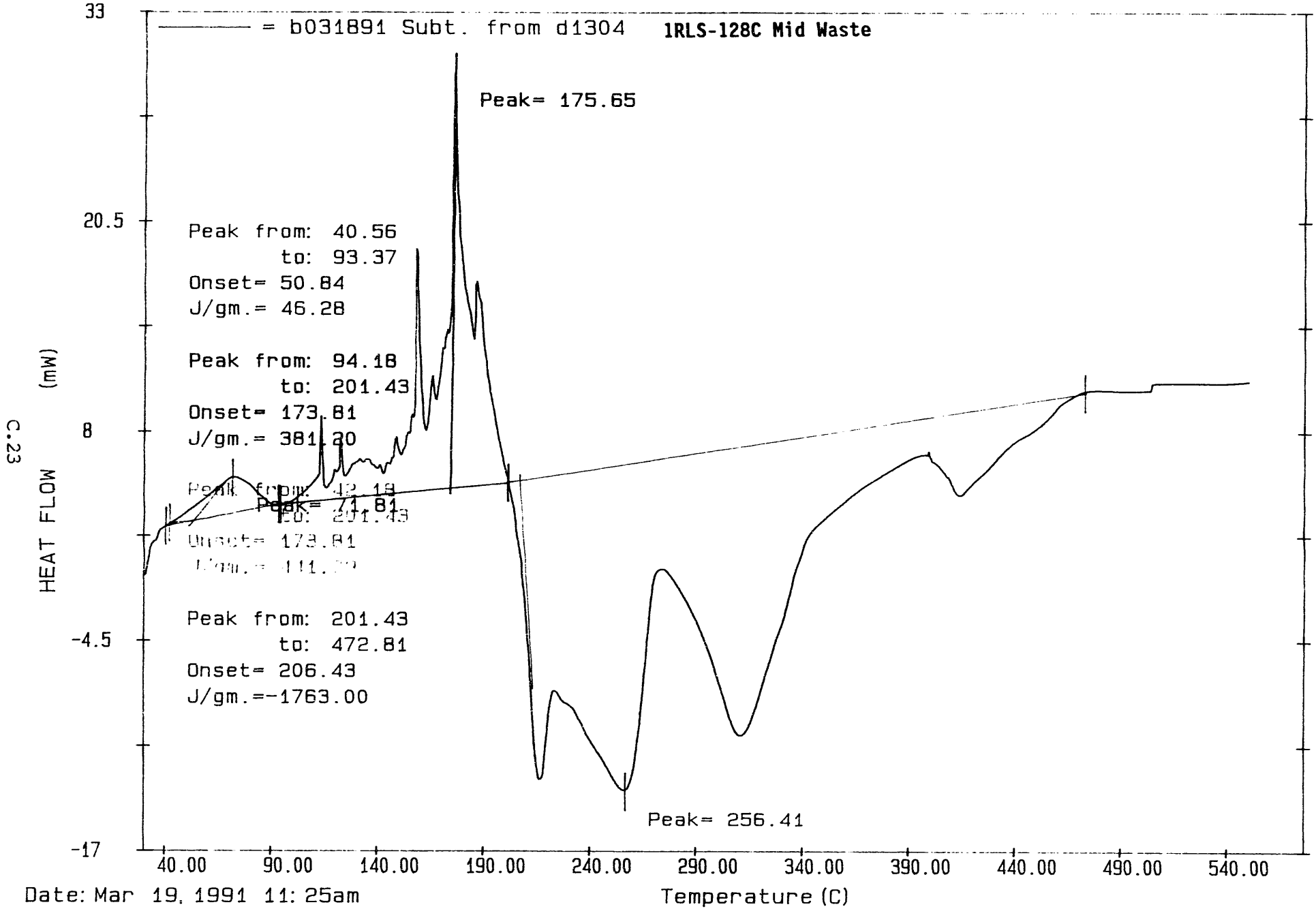

C.23

Date: Mar 19, 1991 11:25am
Scanning Rate: 5.0 C/min
Sample Wt: 14.900 mg Path: a:\
File: D1304 R L SELL

PE PC SERIES DSC7

Reference

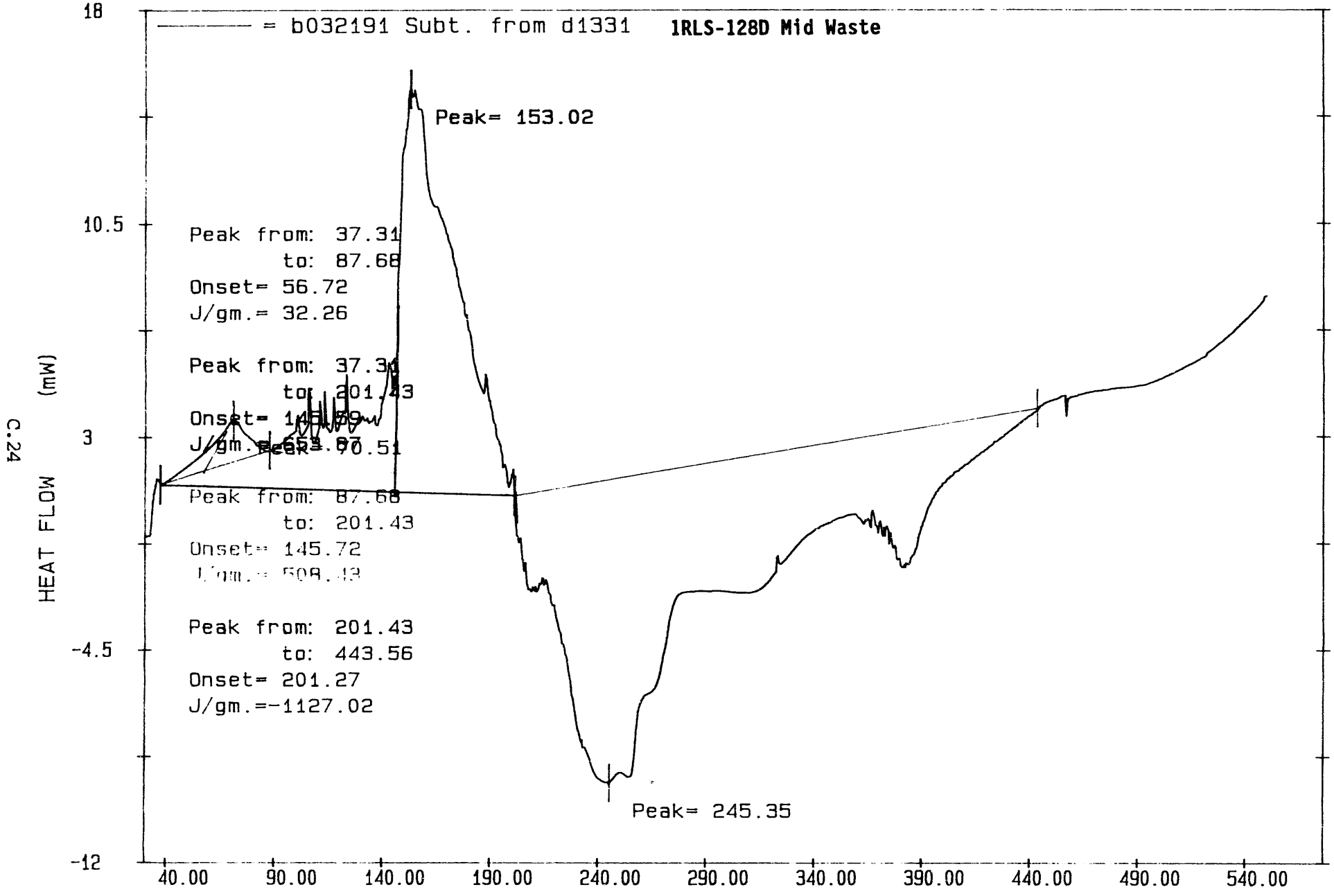

Date: Mar 21, 1991 09:19am
Scanning Rate: 5.0 C/min
Sample Wt: 11.000 mg Path: a:\

Reference

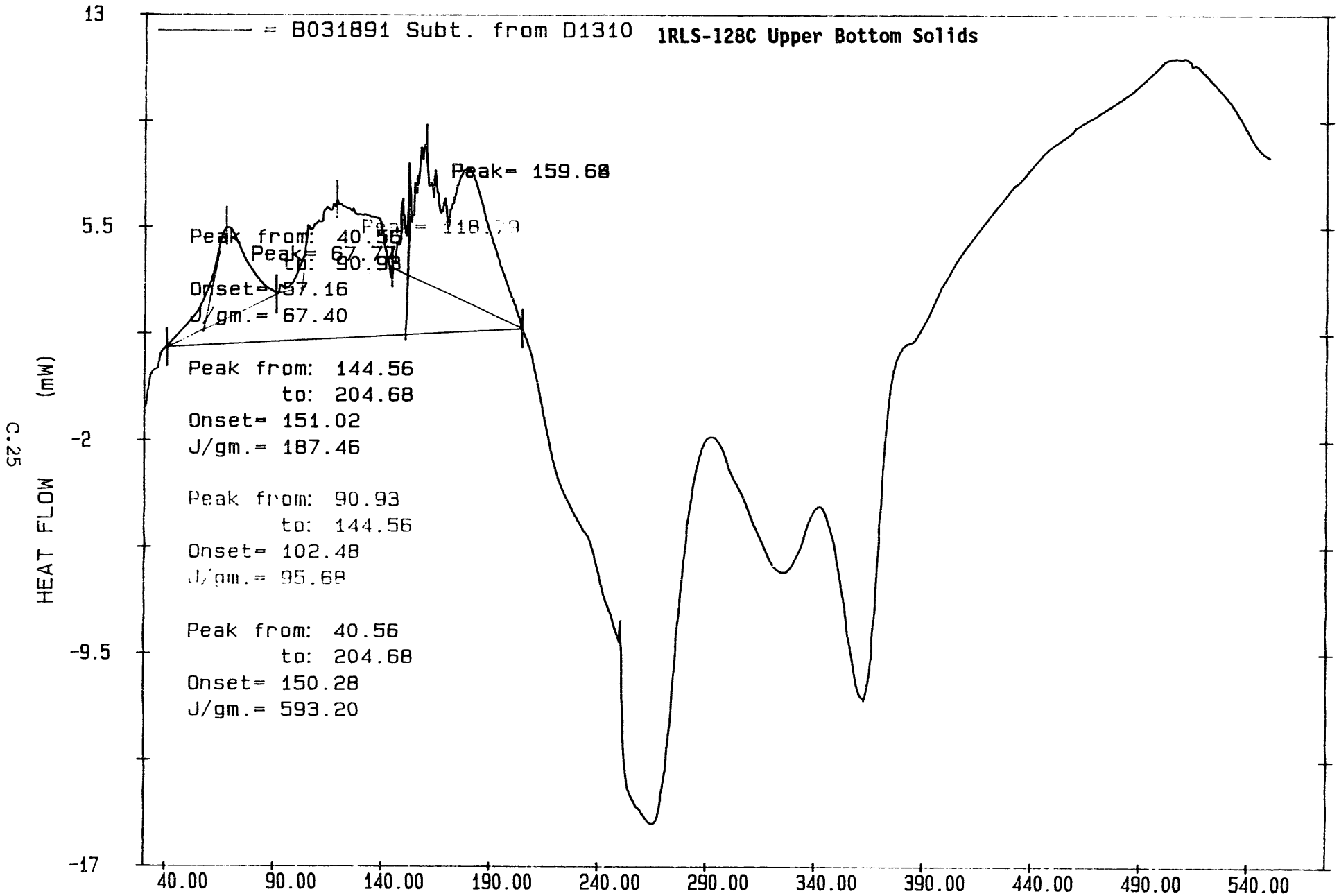

Date: Mar 19, 1991 1:26pm
Scanning Rate: 5.0 C/min
Sample Wt: 10.900 mg Path: a:\
File: D1310 R L SELL

PE PC SERIES DSC7

Reference

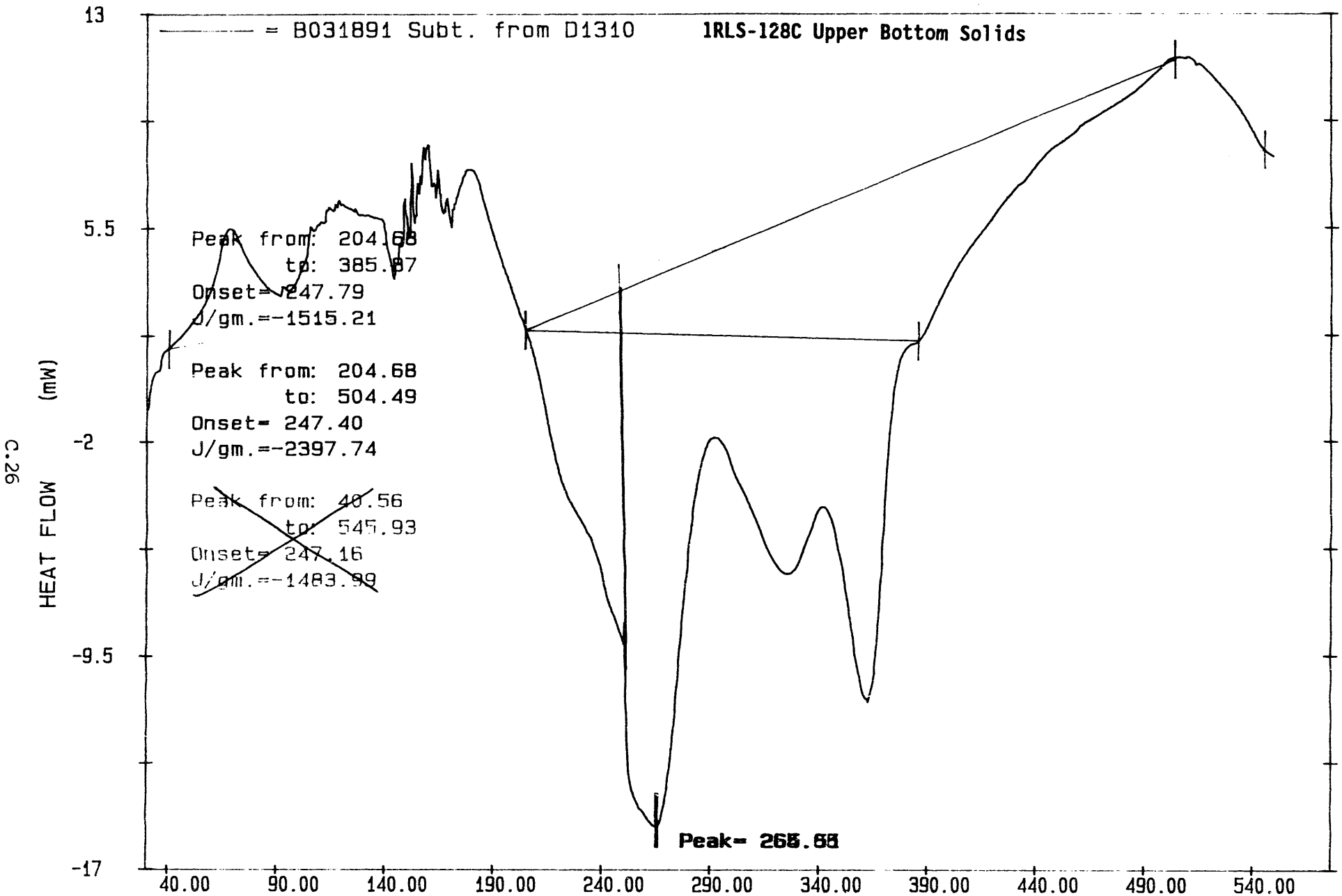

C:26

Date: Mar 19, 1991 1:26pm
Scanning Rate: 5.0 C/min
Sample Wt: 10.900 mg Path: A:\

Reference

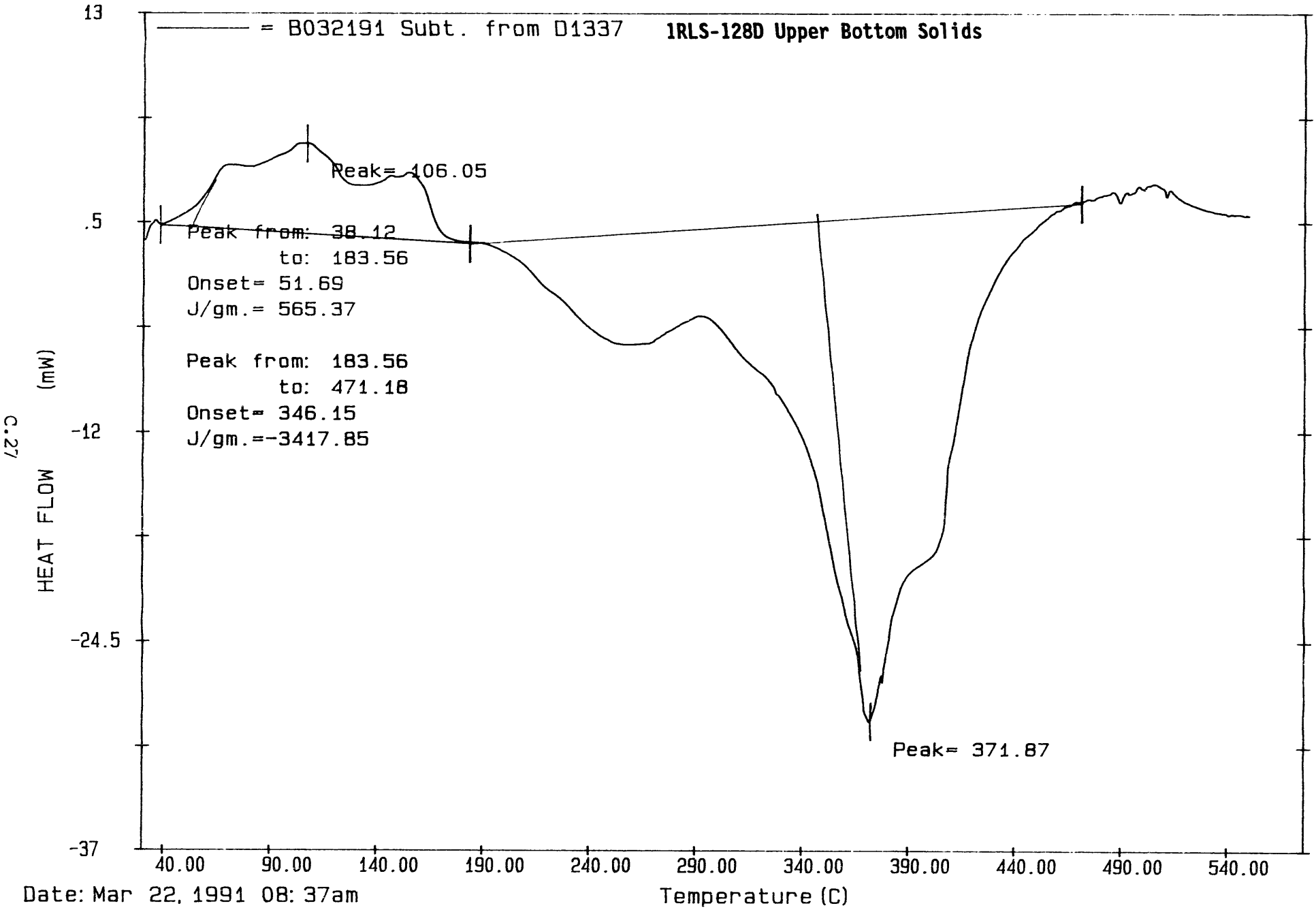

C.27

Date: Mar 22, 1991 08:37am
Scanning Rate: 5.0 C/min
Sample Wt: 9.200 mg Path: a:\
File: D1337 R L SELL

PE PC SERIES DSC7

Reference

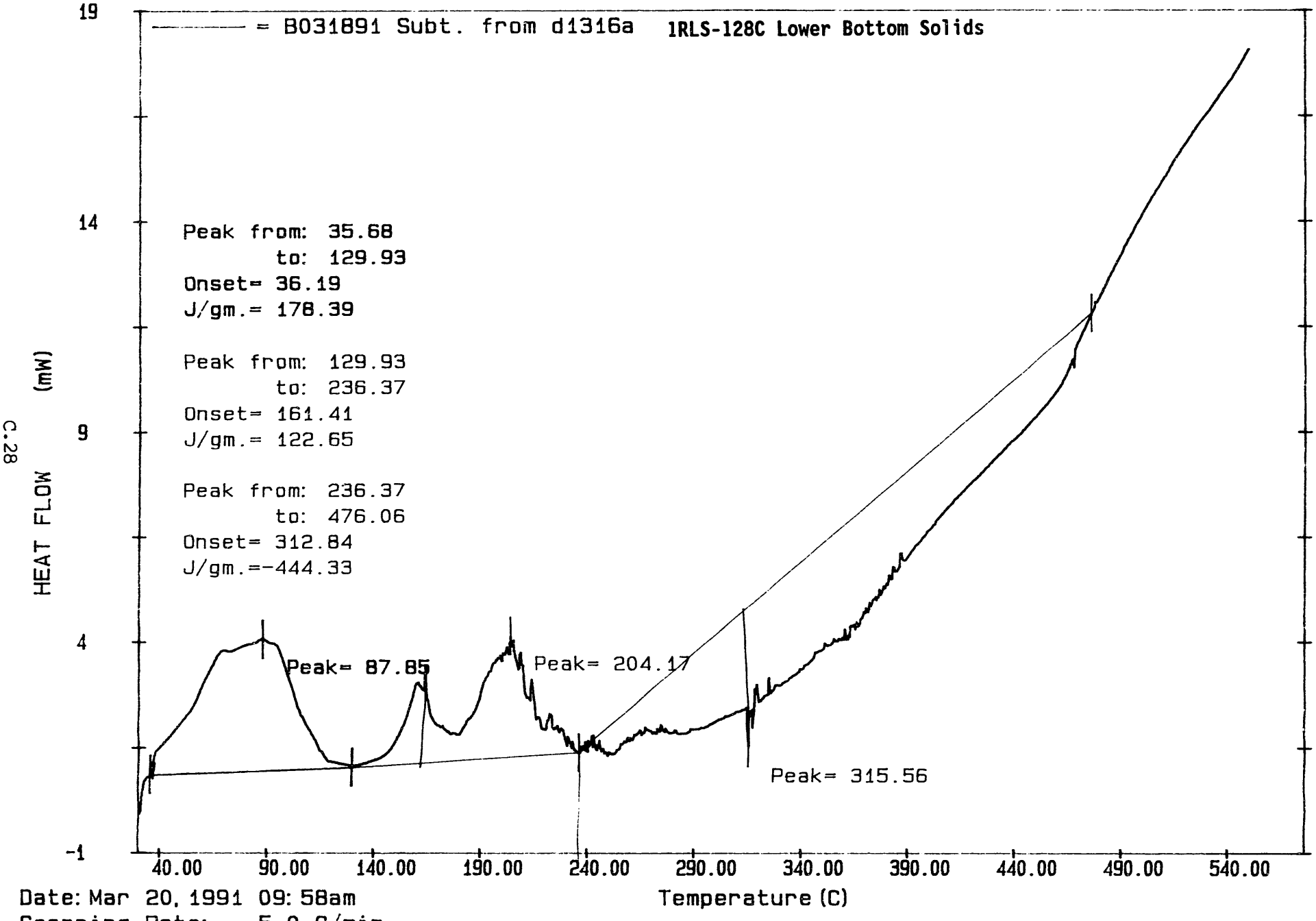

Date: Mar 20, 1991 09:58am
Scanning Rate: 5.0 C/min
Sample Wt: 10.700 mg Path: \pe\hyd\dsc

Reference

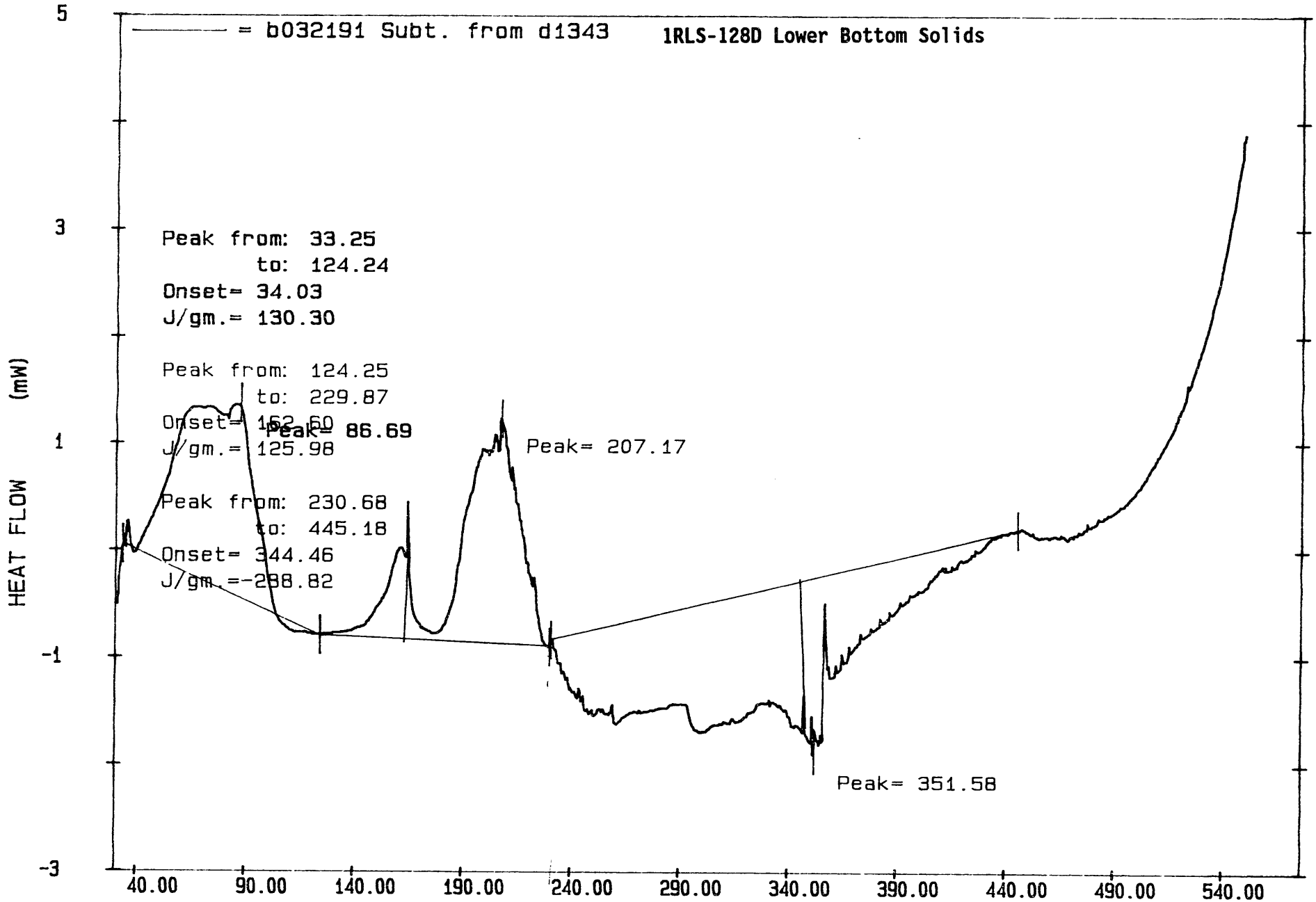

Date: Mar 22, 1991 10:50am
Scanning Rate: 5.0 C/min
Sample Wt: 6.400 mg Path: \pe\hyd\dsc
File: D1343 R L SELL

PE PC SERIES DSC7

Low Aluminate/Low Organic

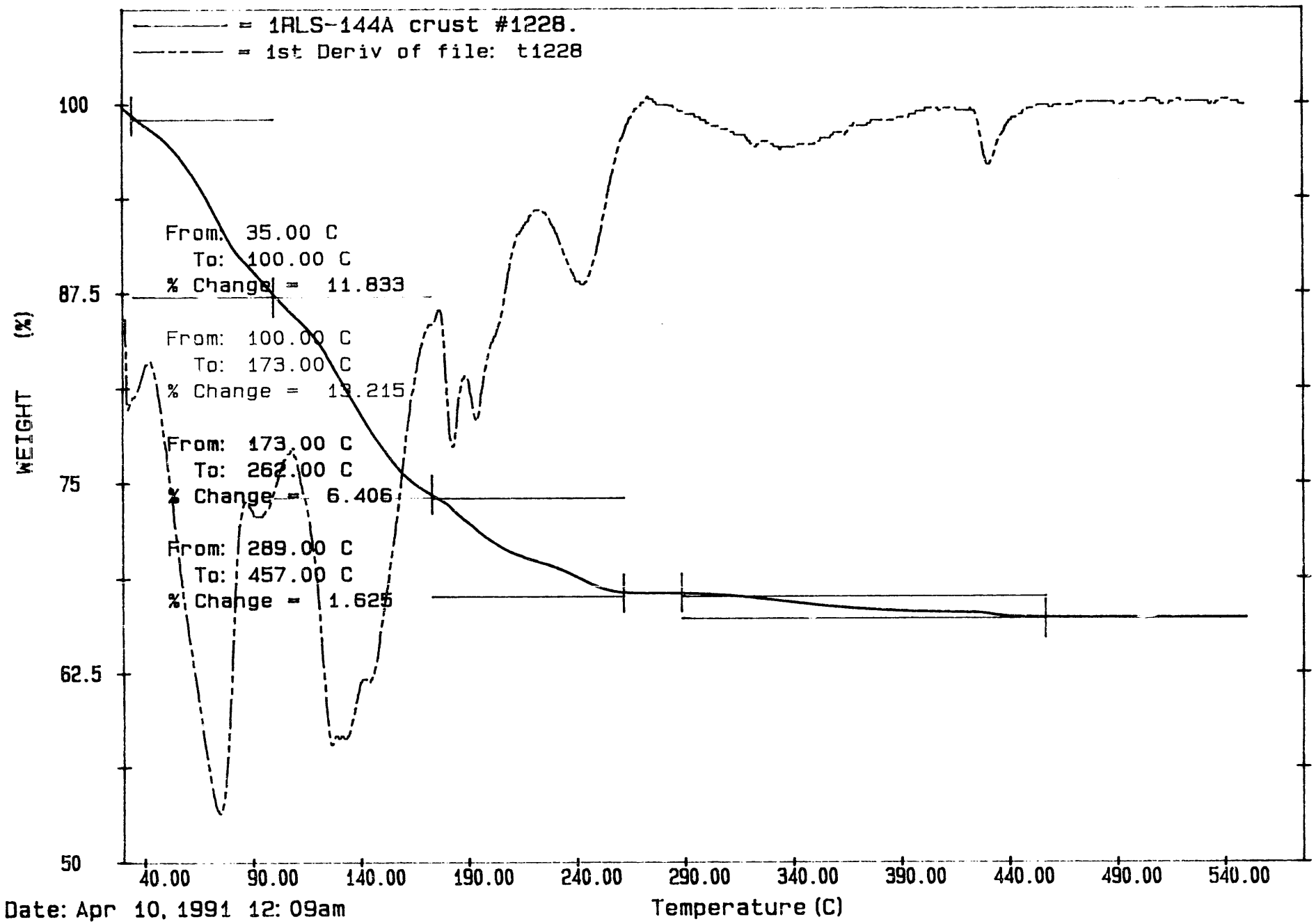

C.30

Date: Apr 10, 1991 12:09am
Scanning Rate: 5.0 C/min

Low Aluminate/Low Organic

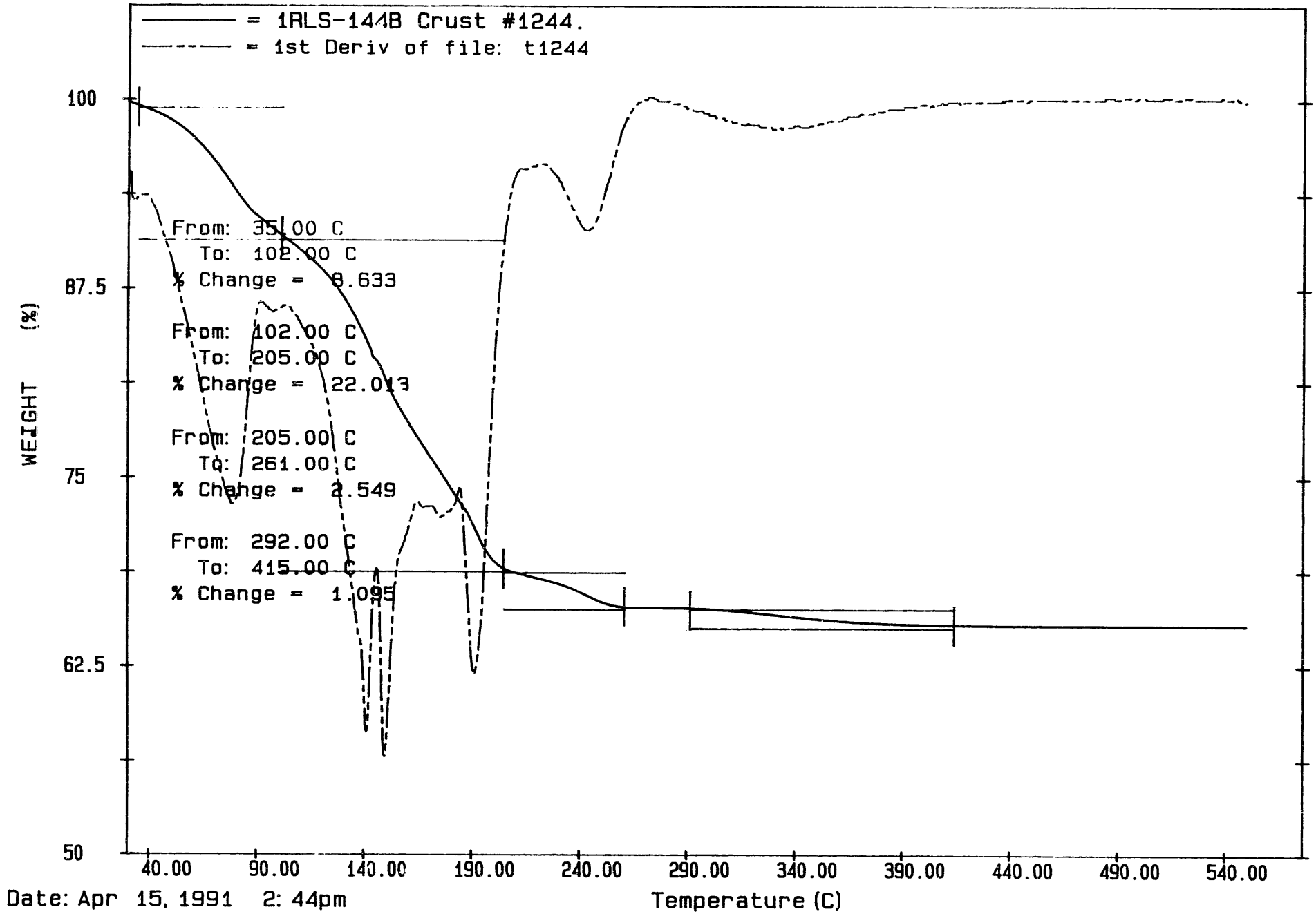

Date: Apr 15, 1991 2:44pm
Scanning Rate: 5.0 C/min
Sample Wt: 25.487 mg Path: d:\archive\h
File: T1244 *R L SELL*

PC SERIES TGA7

Low Aluminate/Low Organic

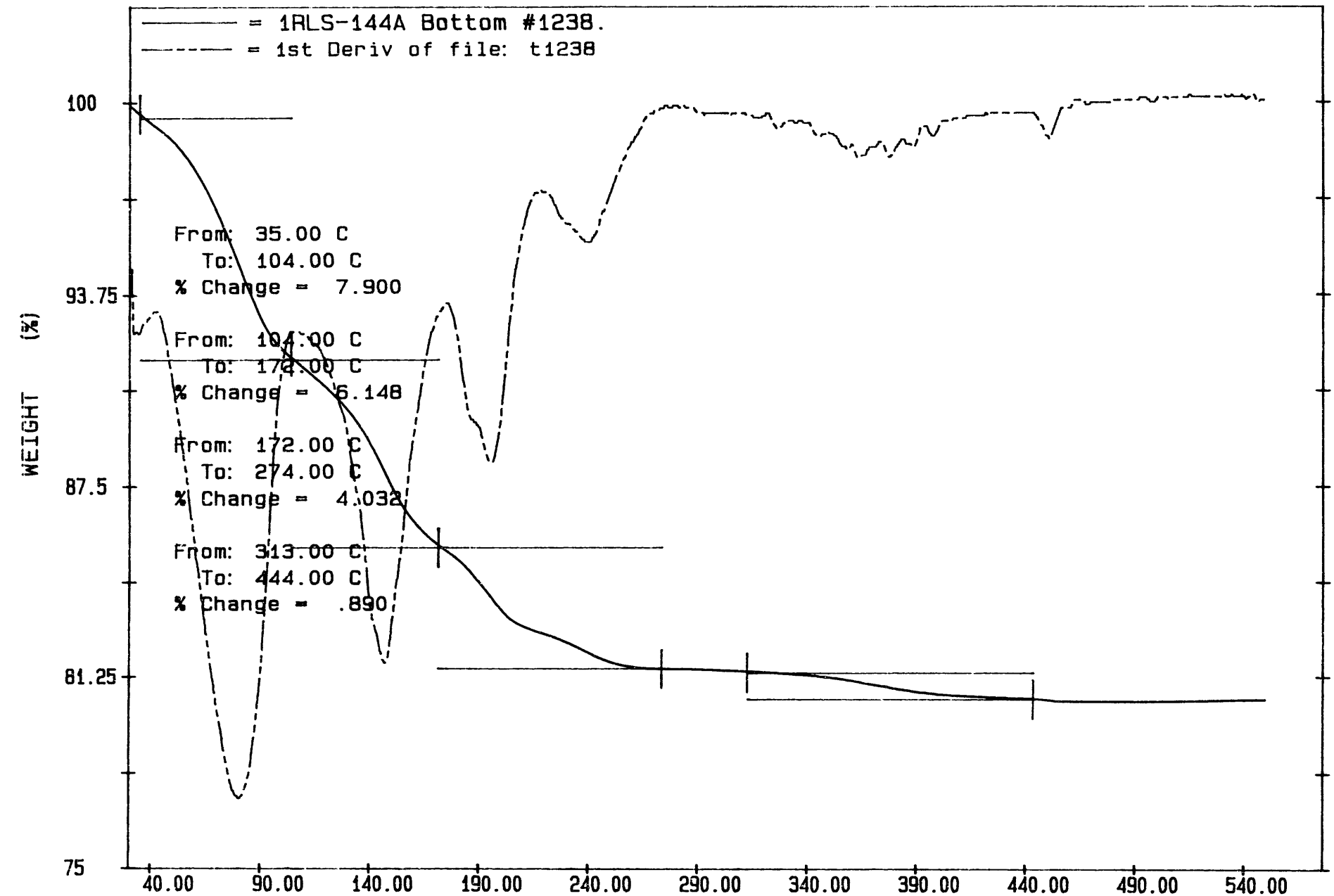

Date: Apr 10, 1991 2:16pm
Scanning Rate: 5.0 C/min
Sample Wt: 29.120 mg Path: d:\archive\

Low Aluminate/Low Organic

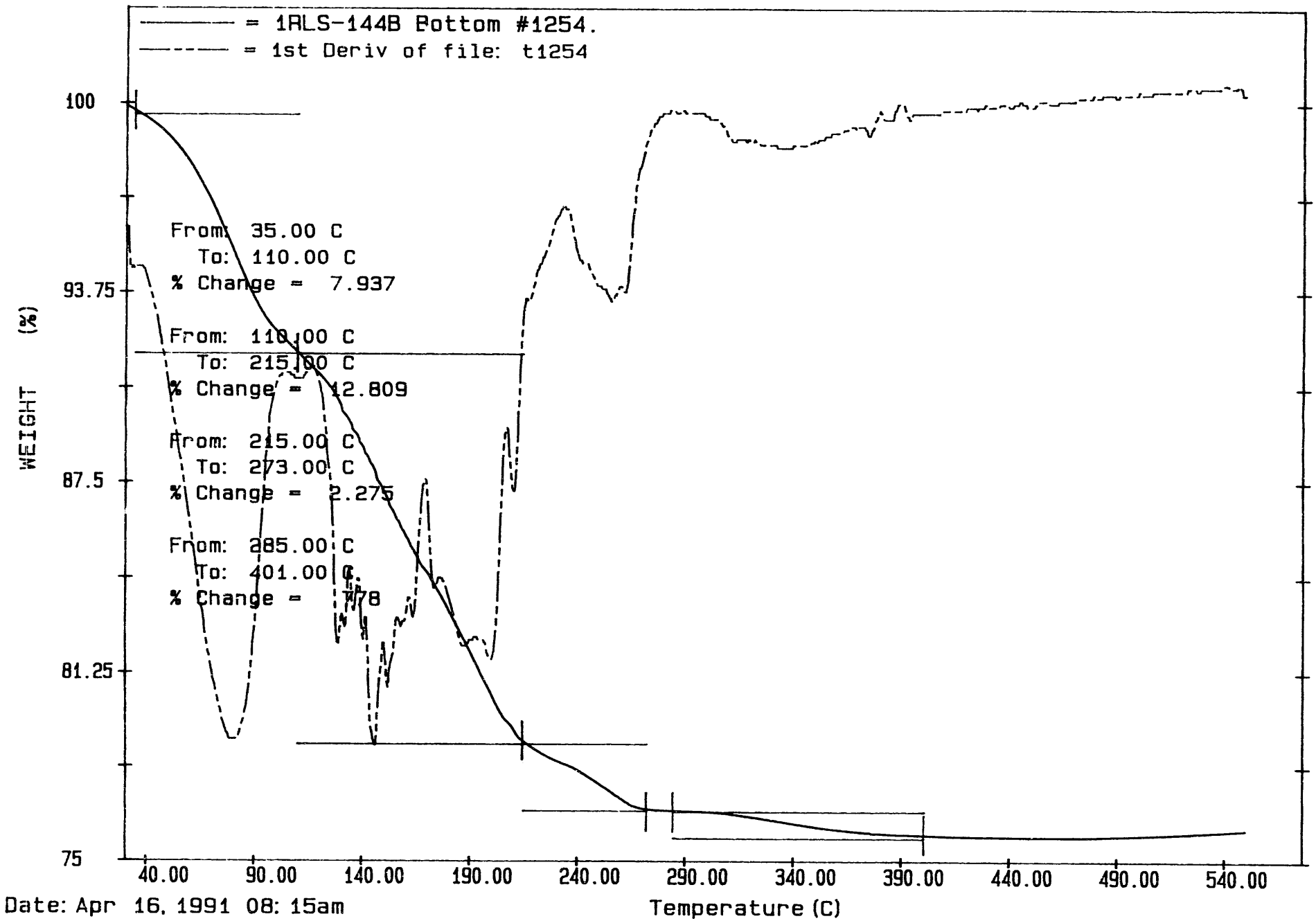

Date: Apr 16, 1991 08:15am
Scanning Rate: 5.0 C/min
Sample Wt: 31.934 mg Path: d:\archive\h
File: T1254 R L SFLL

PC SERIES TGA 7

Low Aluminate/High Organic

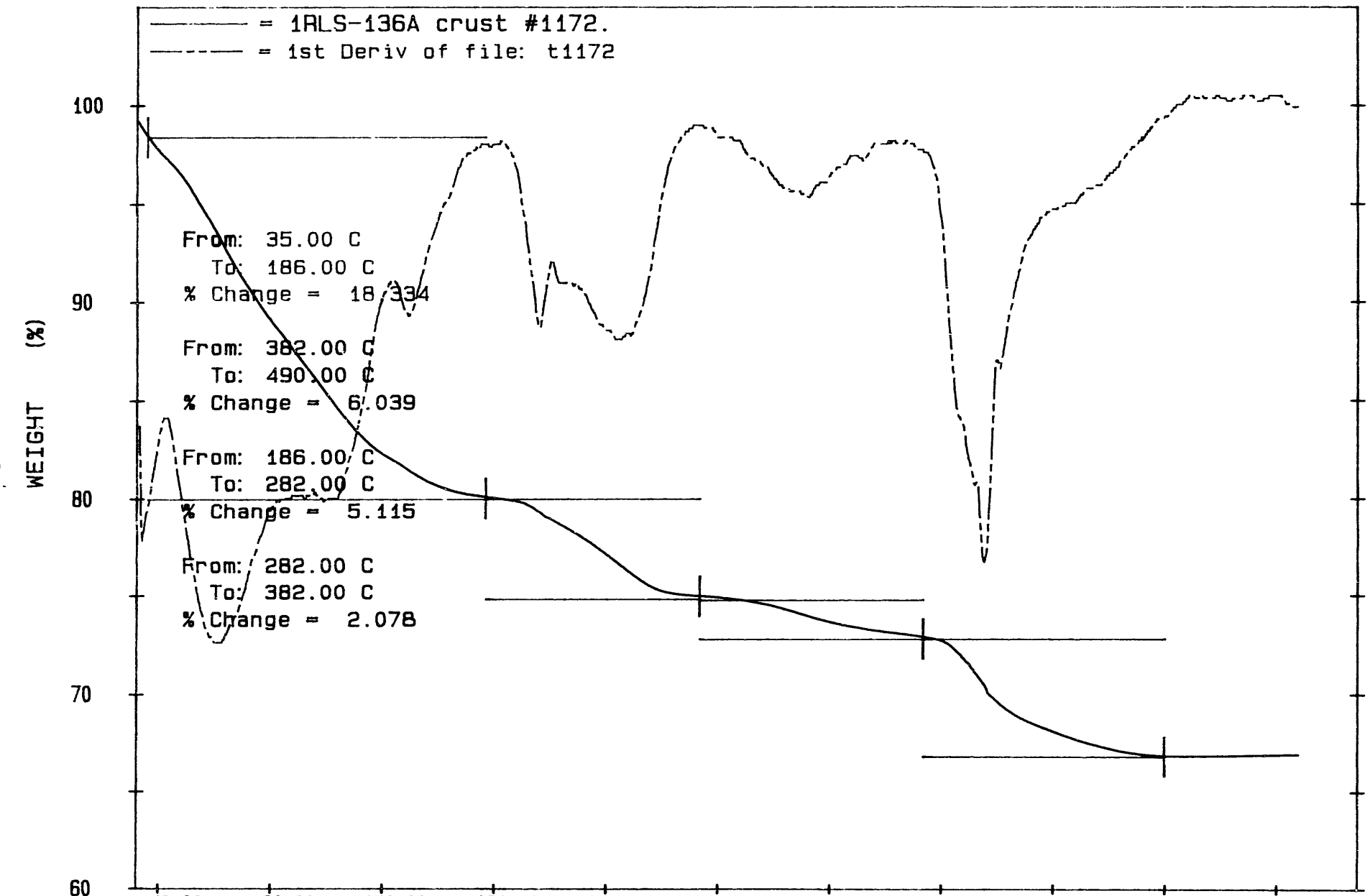

Date: Apr 09, 1991 11:23am
Scanning Rate: 5.0 C/min
Sample Wt: 7.077 mg Path: d:\analysis\

Low Aluminate/High Organic

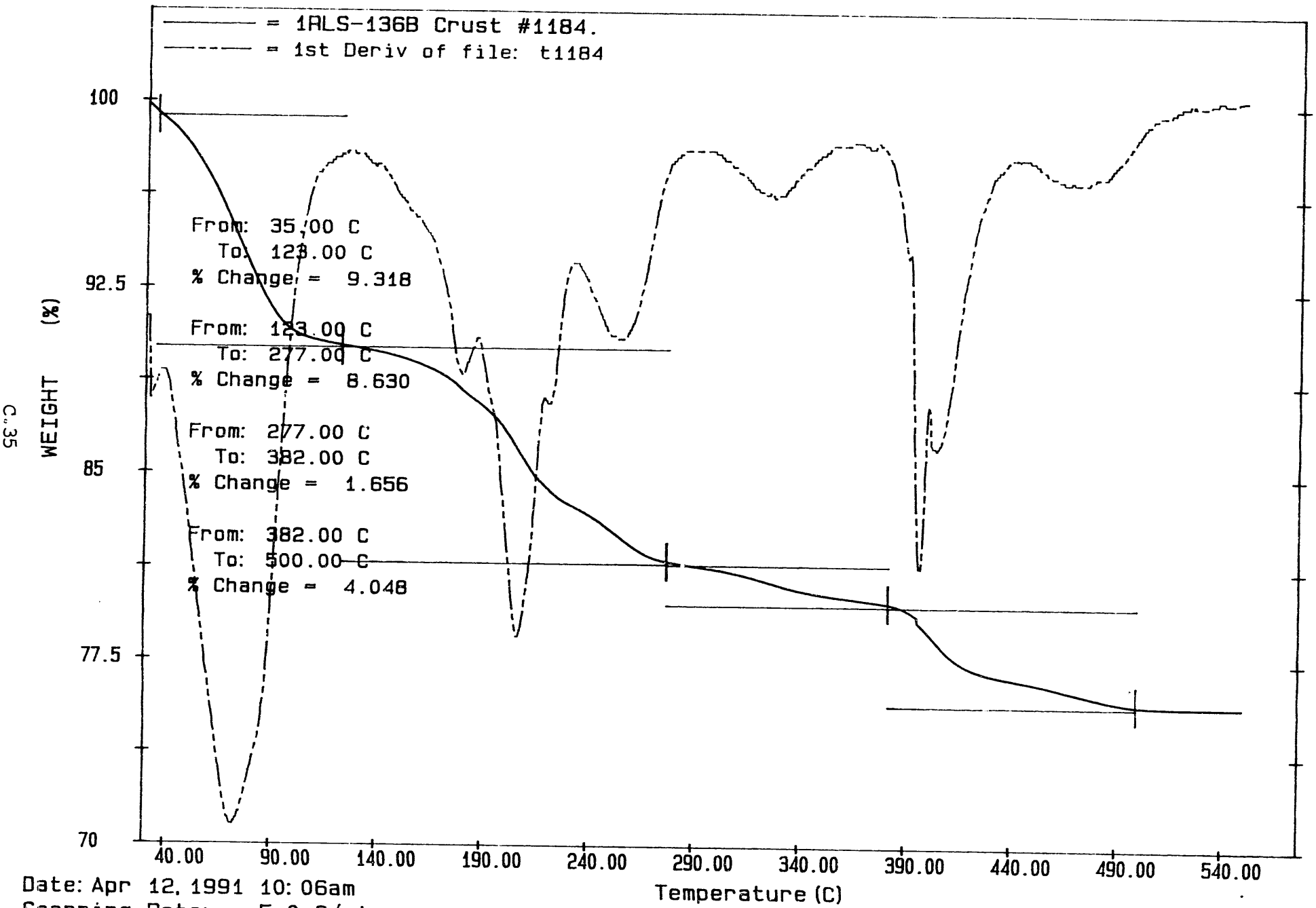

Date: Apr 12, 1991 10:06am
Scanning Rate: 5.0 C/min
Sample Wt: 14.848 mg Path: d:\archive\h
File: T1184 R L SELL

PC SERIES TGA7

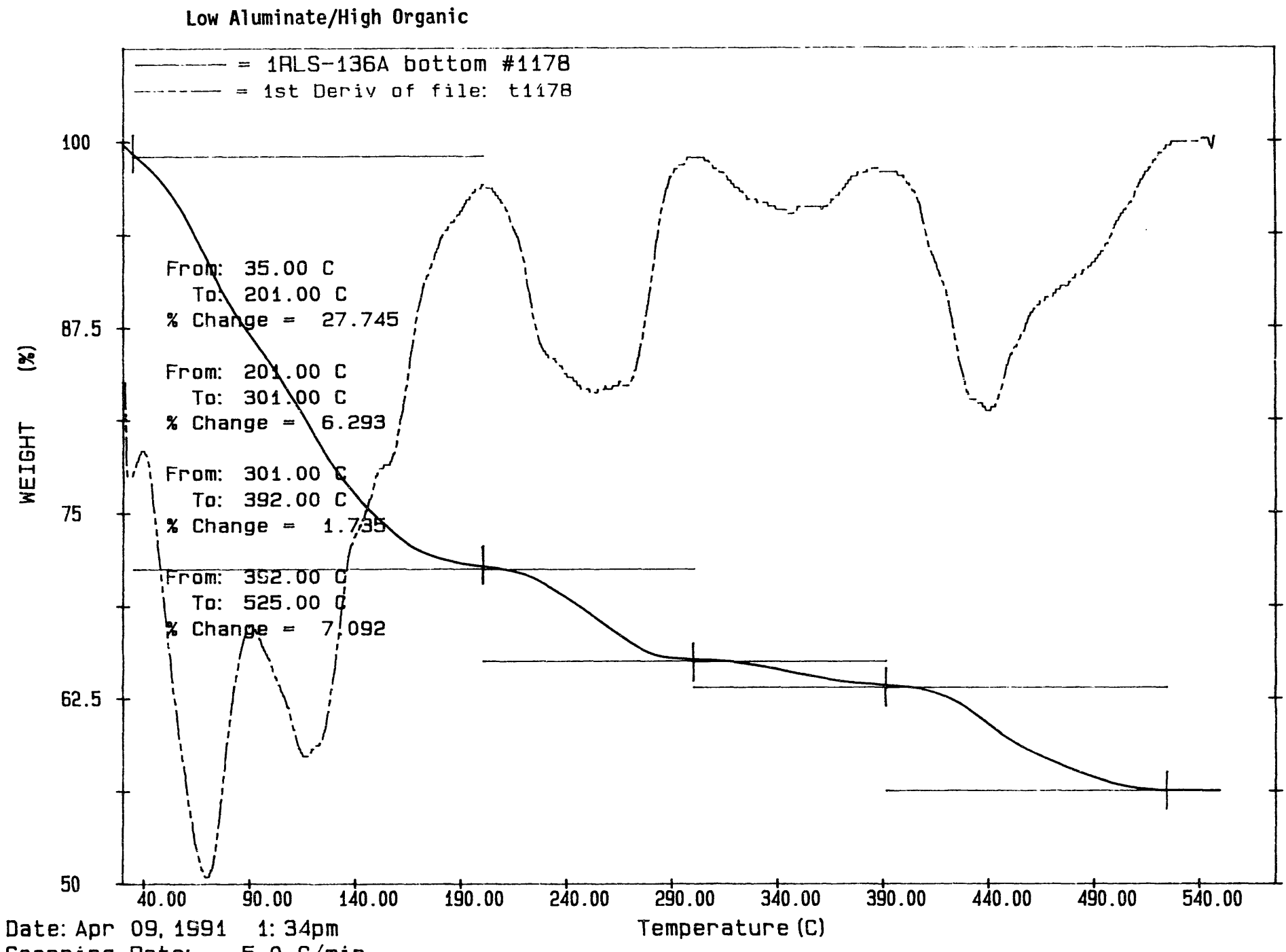
Low Aluminate/High Organic
1RLS-136A bottom #1178
1st Deriv of file: t1178
From: 35.00 C
To: 201.00 C
% Change = 27.745
From: 201.00 C
To: 301.00 C
% Change = 6.293
From: 301.00 C
To: 392.00 C
% Change = 1.735
From: 392.00 C
To: 525.00 C
% Change = 7.092
WEIGHT (%)
100
87.5
75
62.5
50
40.00
90.00
140.00
190.00
240.00
290.00
340.00
390.00
440.00
490.00
540.00
Temperature (C)
Date: Apr 09, 1991 1:34pm
Scanning Rate: 5.0 C/min
Sample Wt: 7.594 mg

Low Aluminate/High Organic

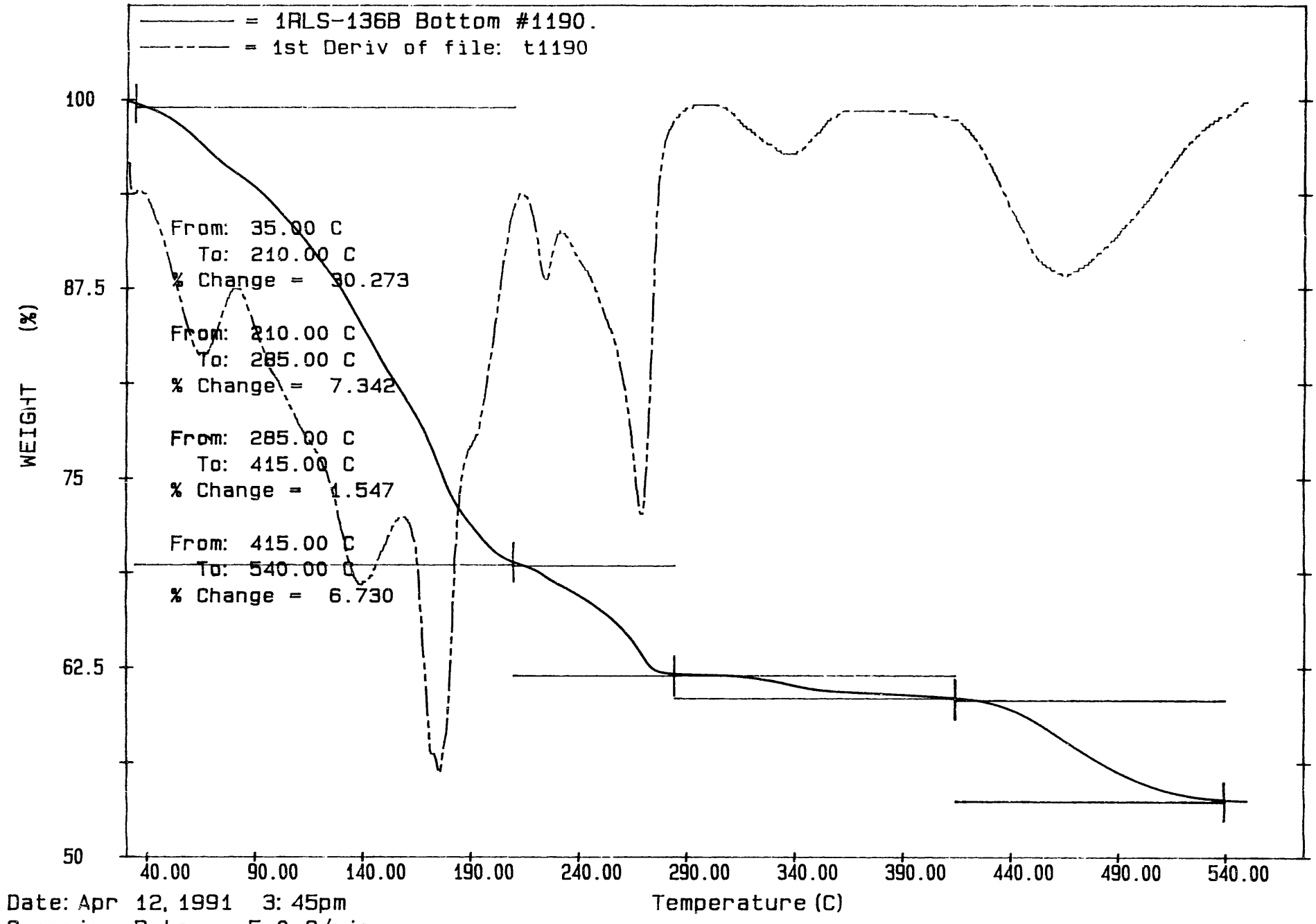

Date: Apr 12, 1991 3:45pm
Scanning Rate: 5.0 C/min
Sample Wt: 25.875 mg Path: d:\archive\h
File: T1190 R / SEC

PC SERIES TGA 7

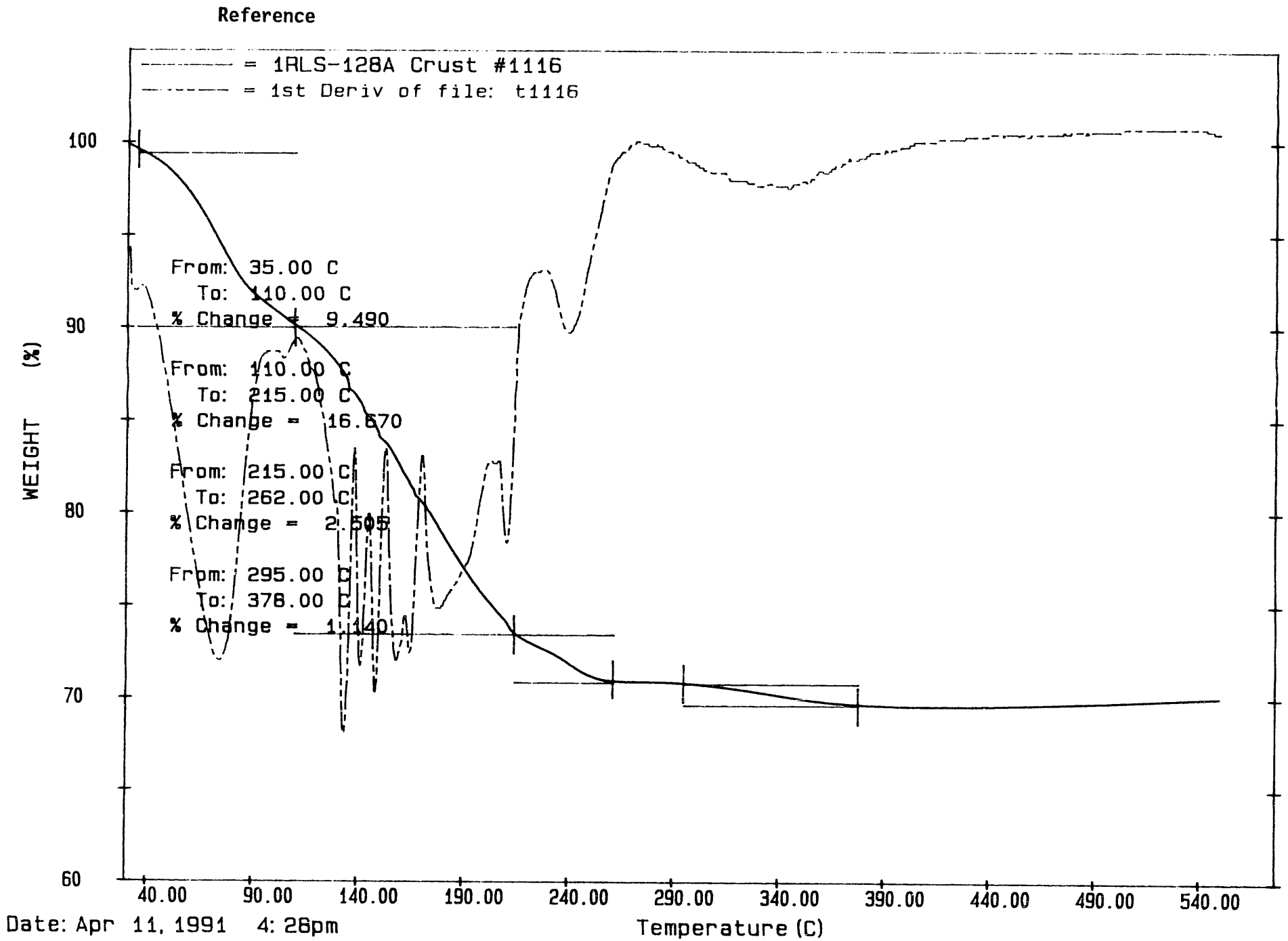
Reference
= 1RLS-128A Crust #1116
= 1st Deriv of file: t1116
From: 35.00 C
To: 110.00 C
% Change = 9.490
From: 110.00 C
To: 215.00 C
% Change = 16.670
From: 215.00 C
To: 262.00 C
% Change = 2.505
From: 295.00 C
To: 378.00 C
% Change = 1.140
WEIGHT (%)
100
90
80
70
60
40.00
90.00
140.00
190.00
240.00
290.00
340.00
390.00
440.00
490.00
540.00
Temperature (C)
Date: Apr 11, 1991 4:28pm
Scanning Rate: 5.0 C/min
Sample Wt: 19.758 mg Path: d:\archive\b

Reference

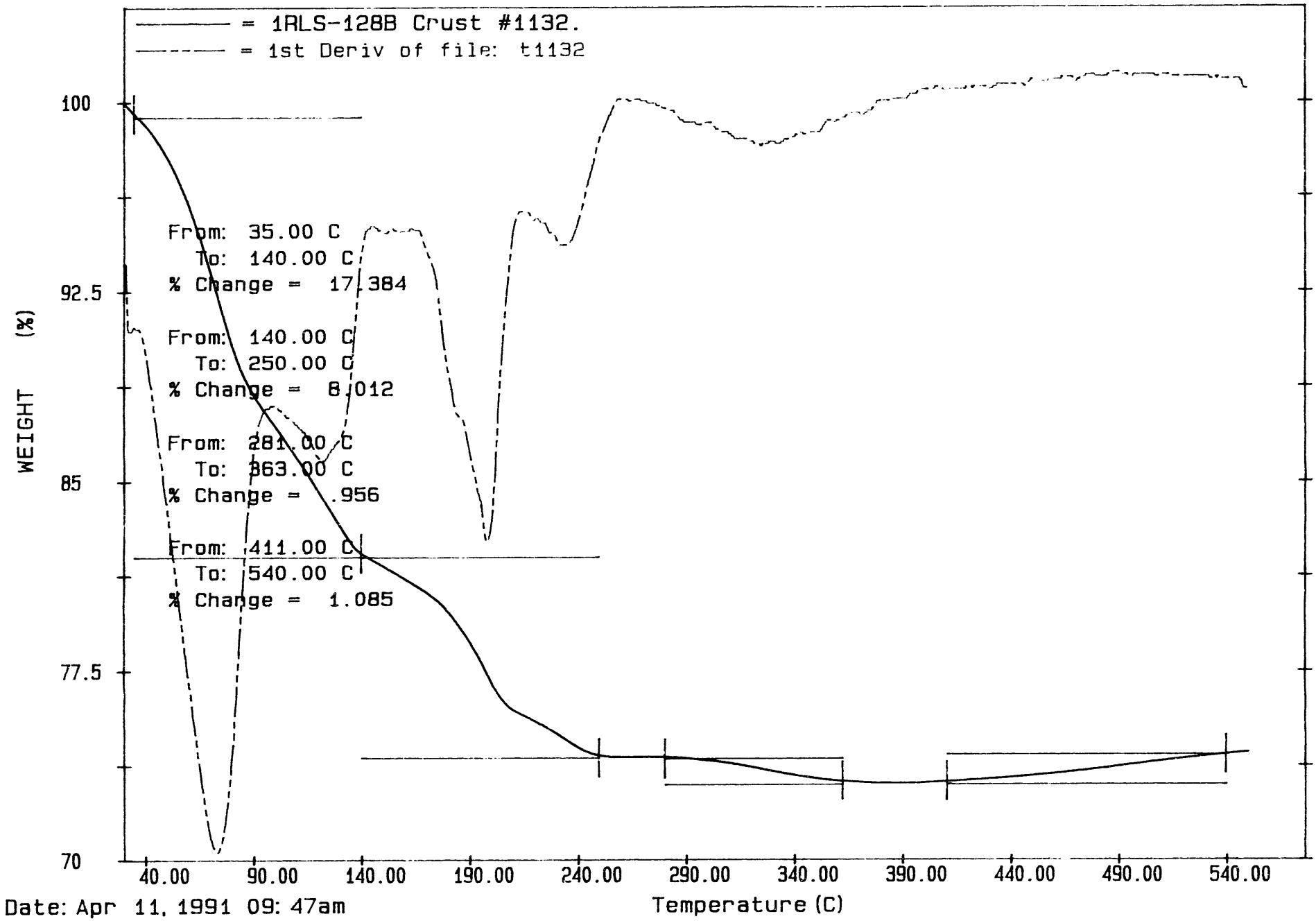

Date: Apr 11, 1991 09:47am
Scanning Rate: 5.0 C/min
Sample Wt: 10.508 mg Path: d:\archive\h
File: T1132 *R L SELL*

PC SERIES TGA7

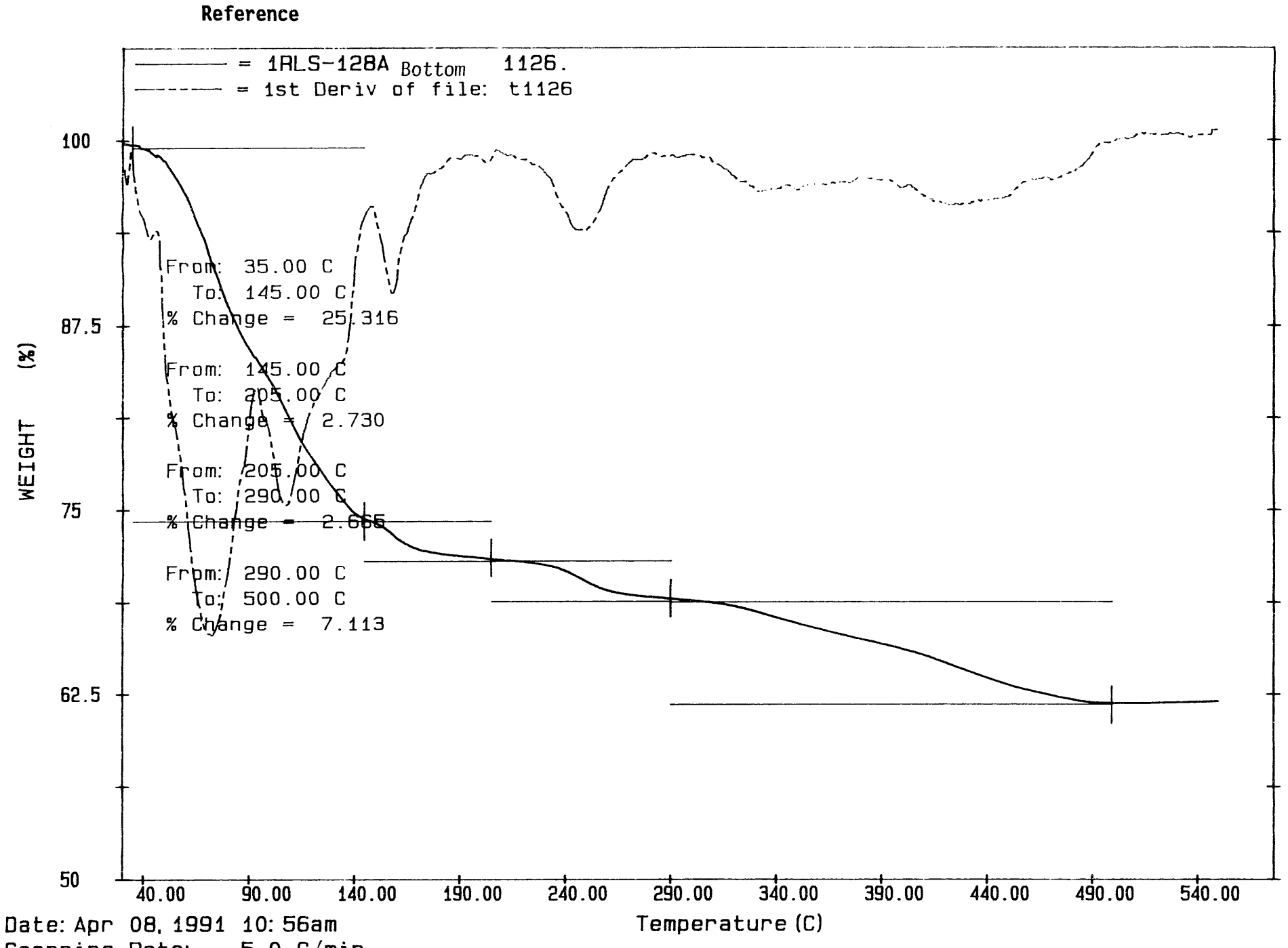
Reference
= 1RLS-128A Bottom 1126.
= 1st Deriv of file: t1126
100
87.5
75
62.5
50
WEIGHT (%)
From: 35.00 C
To: 145.00 C
% Change = 25.316
From: 145.00 C
To: 205.00 C
% Change = 2.730
From: 205.00 C
To: 290.00 C
% Change = 2.665
From: 290.00 C
To: 500.00 C
% Change = 7.113
40.00
90.00
140.00
190.00
240.00
290.00
340.00
390.00
440.00
490.00
540.00
Temperature (C)
Date: Apr 08, 1991 10:56am
Scanning Rate: 5.0 C/min
Sample Wt: 4.138 mg Path: d:\archive\h

Reference

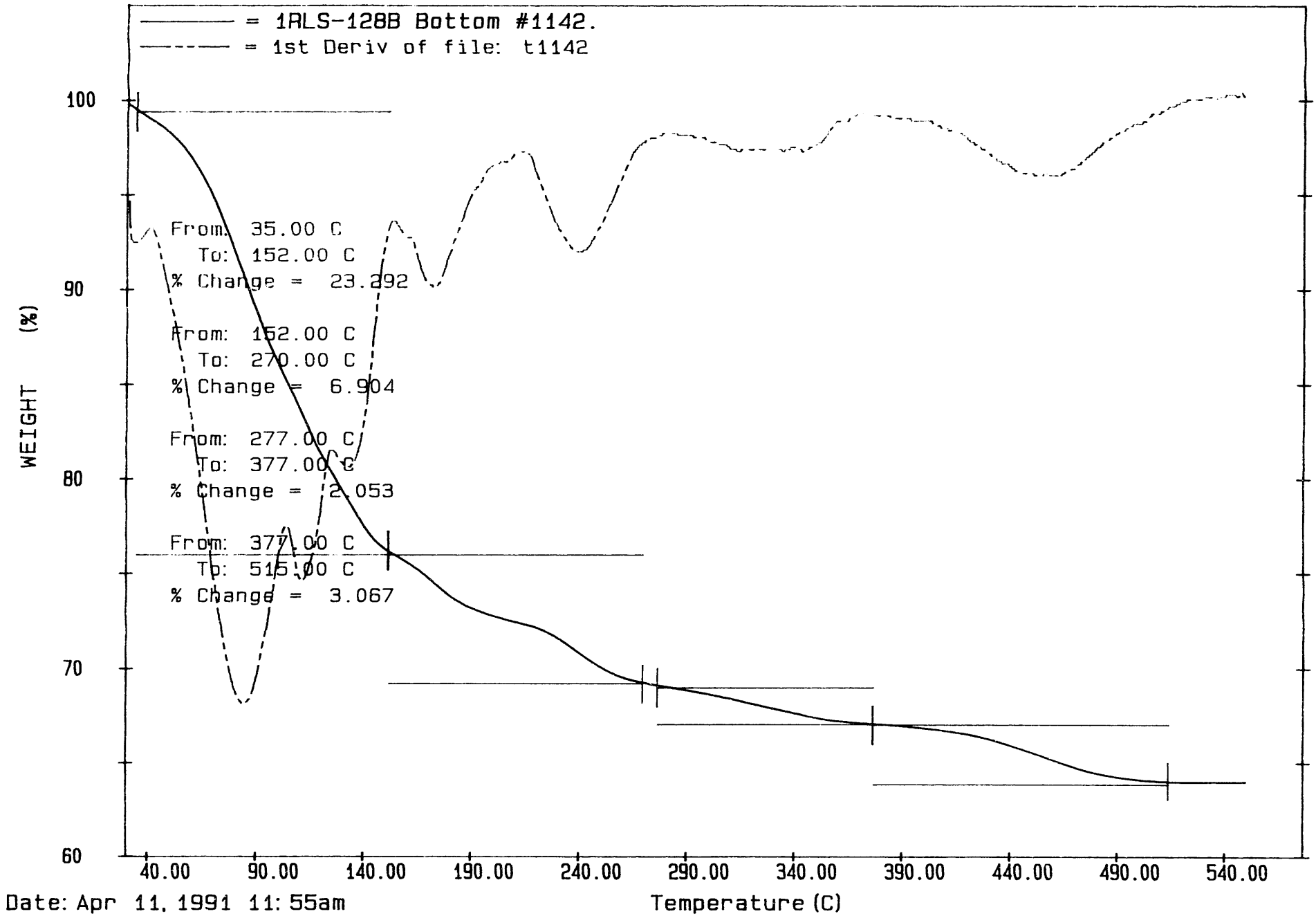

Date: Apr 11, 1991 11:55am
Scanning Rate: 5.0 C/min
Sample Wt: 14.550 mg Path: d:\archive\h
File: T1142 R L SELL

PC SERIES TGA7

High Aluminate/Low Organic

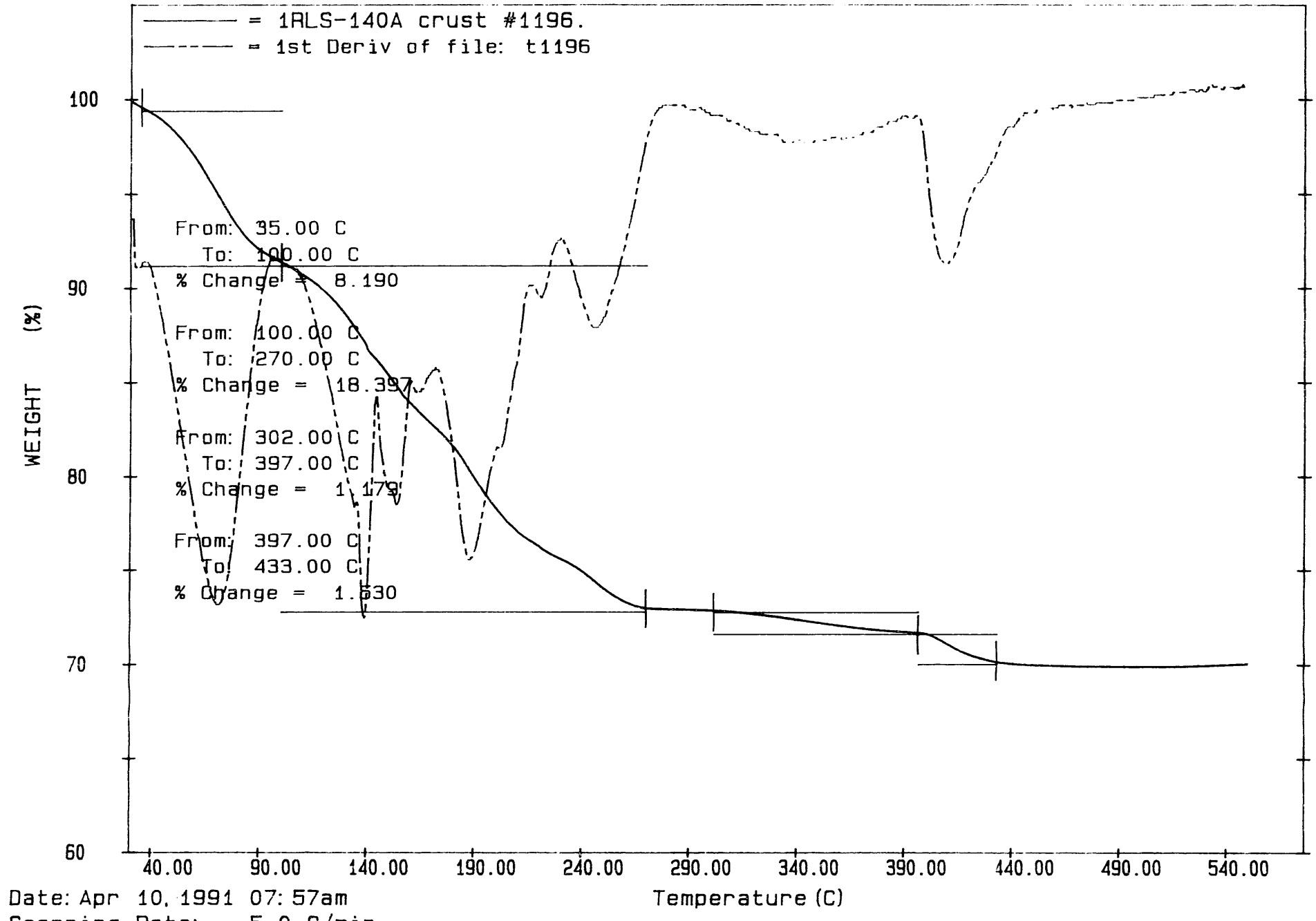

Date: Apr 10, 1991 07:57am
Scanning Rate: 5.0 C/min
Sample Wt: 15.367 mg Path: d:\archive\h

High Aluminate/Low Organic

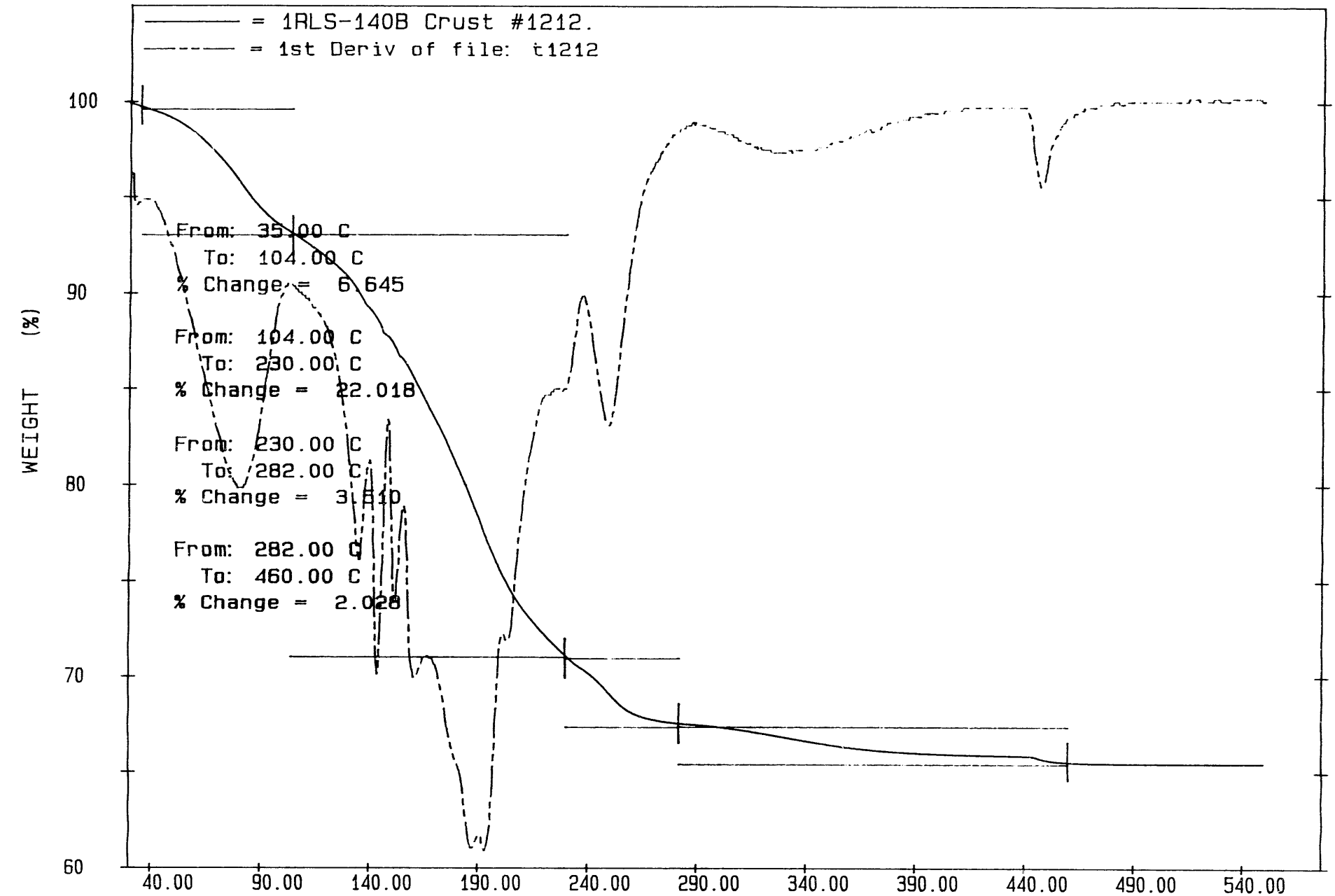

Date: Apr 15, 1991 10:16am
Scanning Rate: 5.0 C/min
Sample Wt: 33.991 mg Path: d:\archive\h
File: T1212 R / SFII

PC SERIES TGA 7

High Aluminate/Low Organic

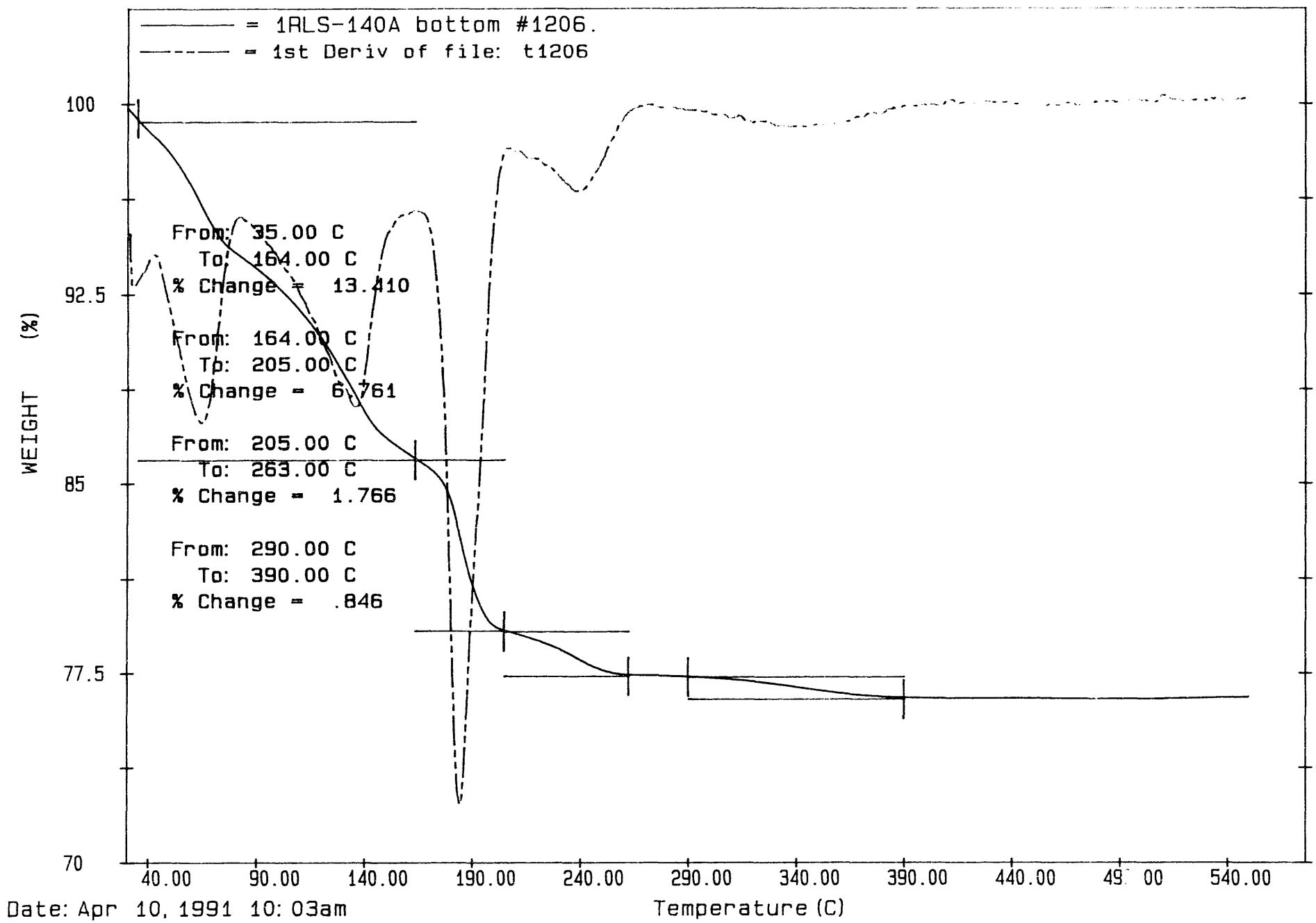

Date: Apr 10, 1991 10:03am
Scanning Rate: 5.0 C/min
Sample Wt: 11.440 mg Path: d:\archive\h

High Aluminate/Low Organic

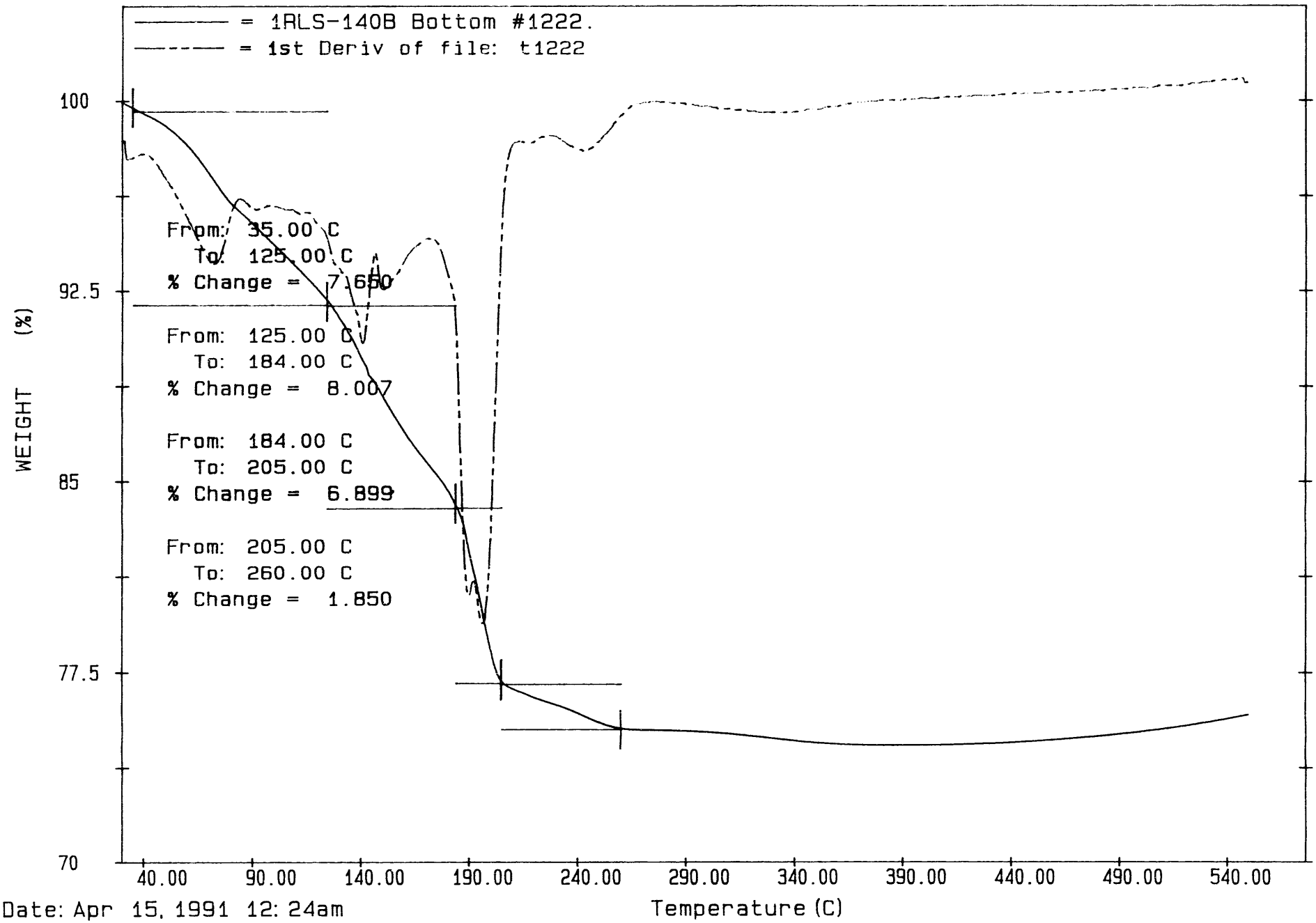

C.45

Date: Apr 15, 1991 12:24am
Scanning Rate: 5.0 C/min
Sample Wt: 28.911 mg Path: d:\archive\h
File: T1222 R1 SFII

PC SERIES TGA 7

High Aluminate/High Organic

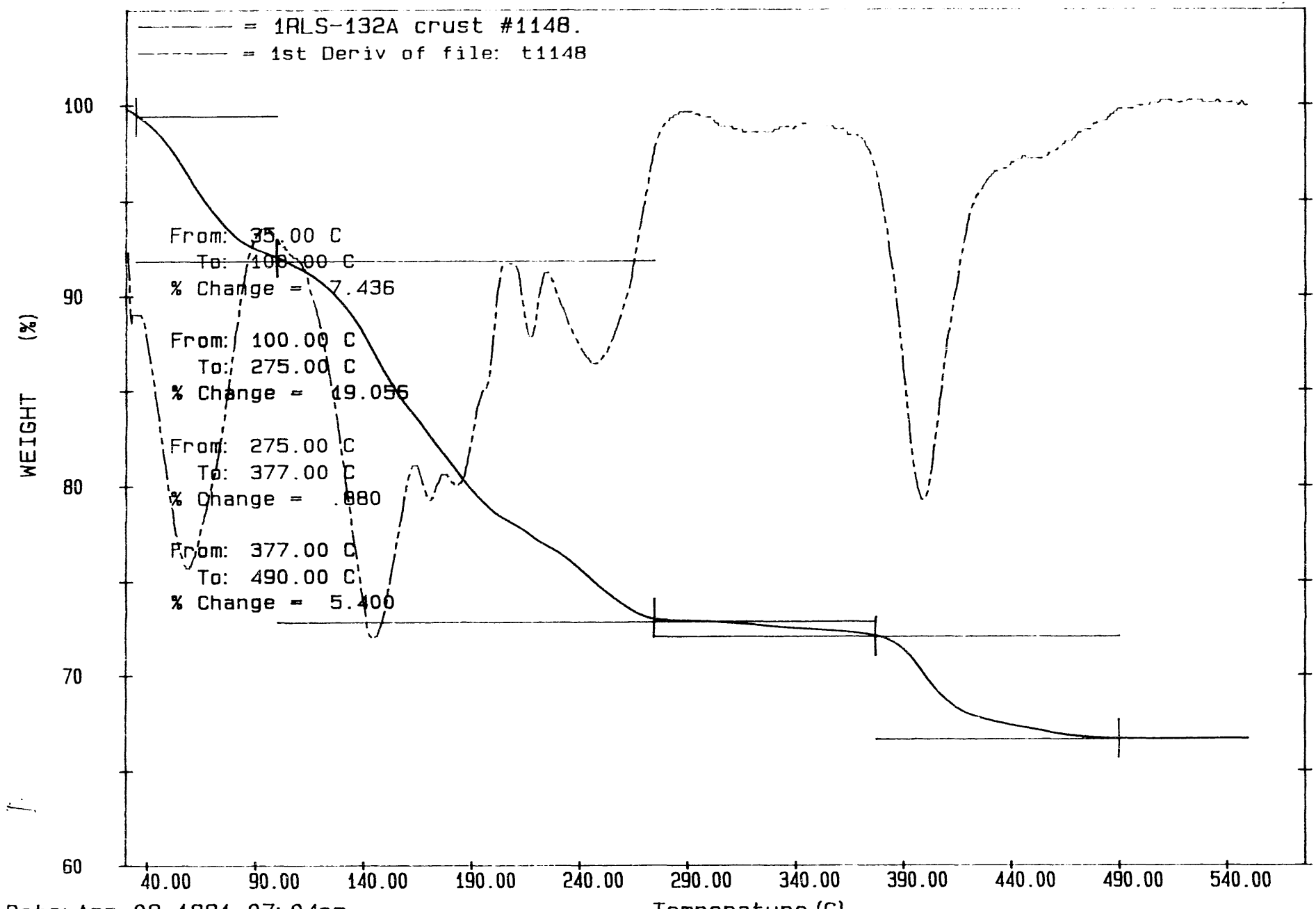

Date: Apr 09, 1991 07:04am
Scanning Rate: 5.0 C/min
Sample [illegible] C:\[illegible]

High Aluminate/High Organic

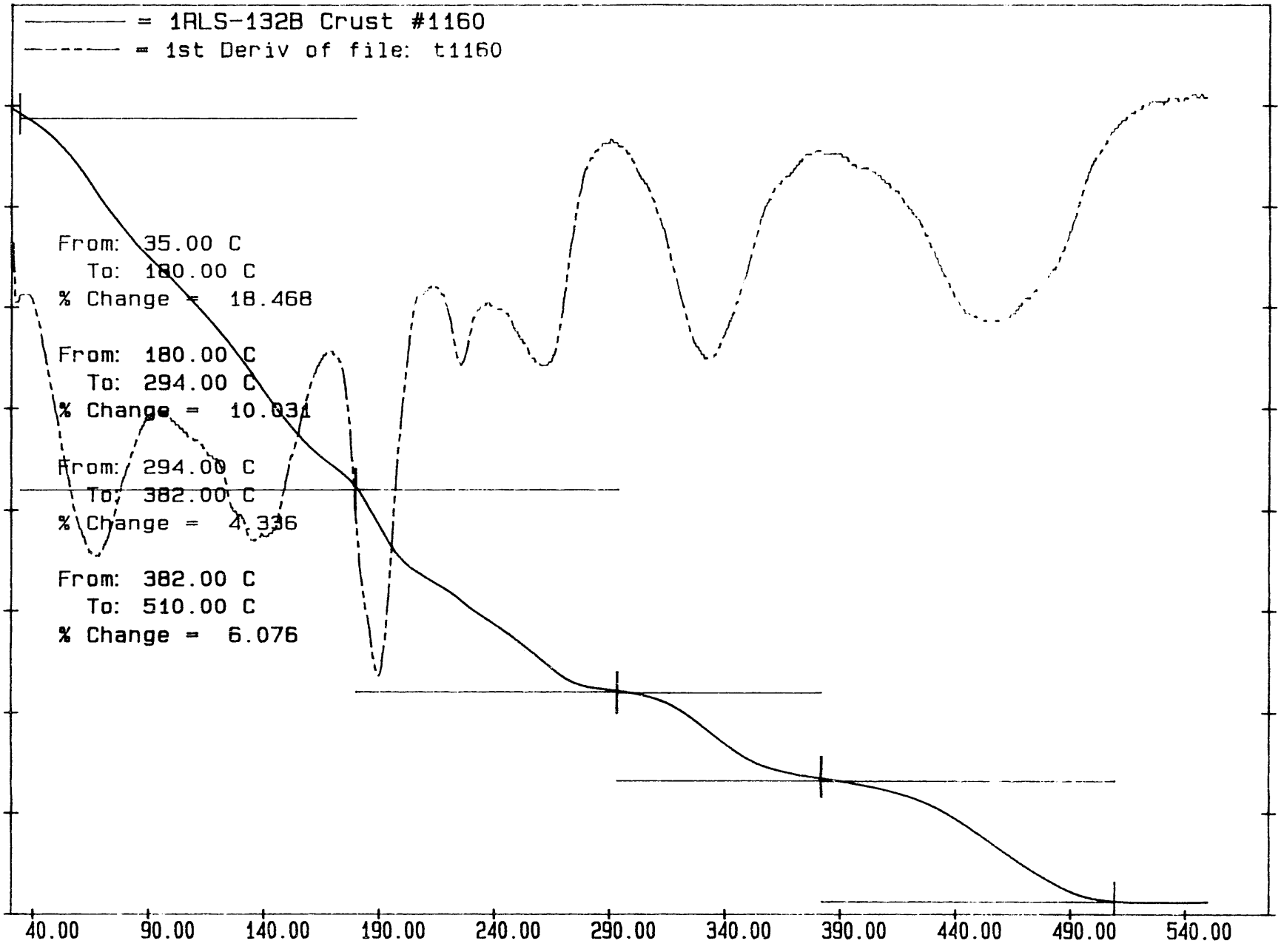

Date: Apr 11, 1991 4:05pm
Scanning Rate: 5.0 C/min
Sample Wt: 15.875 mg Path: d:\archive\h
File: T1160 R L SELL

PC SERIES TGA7

High Aluminate/High Organic

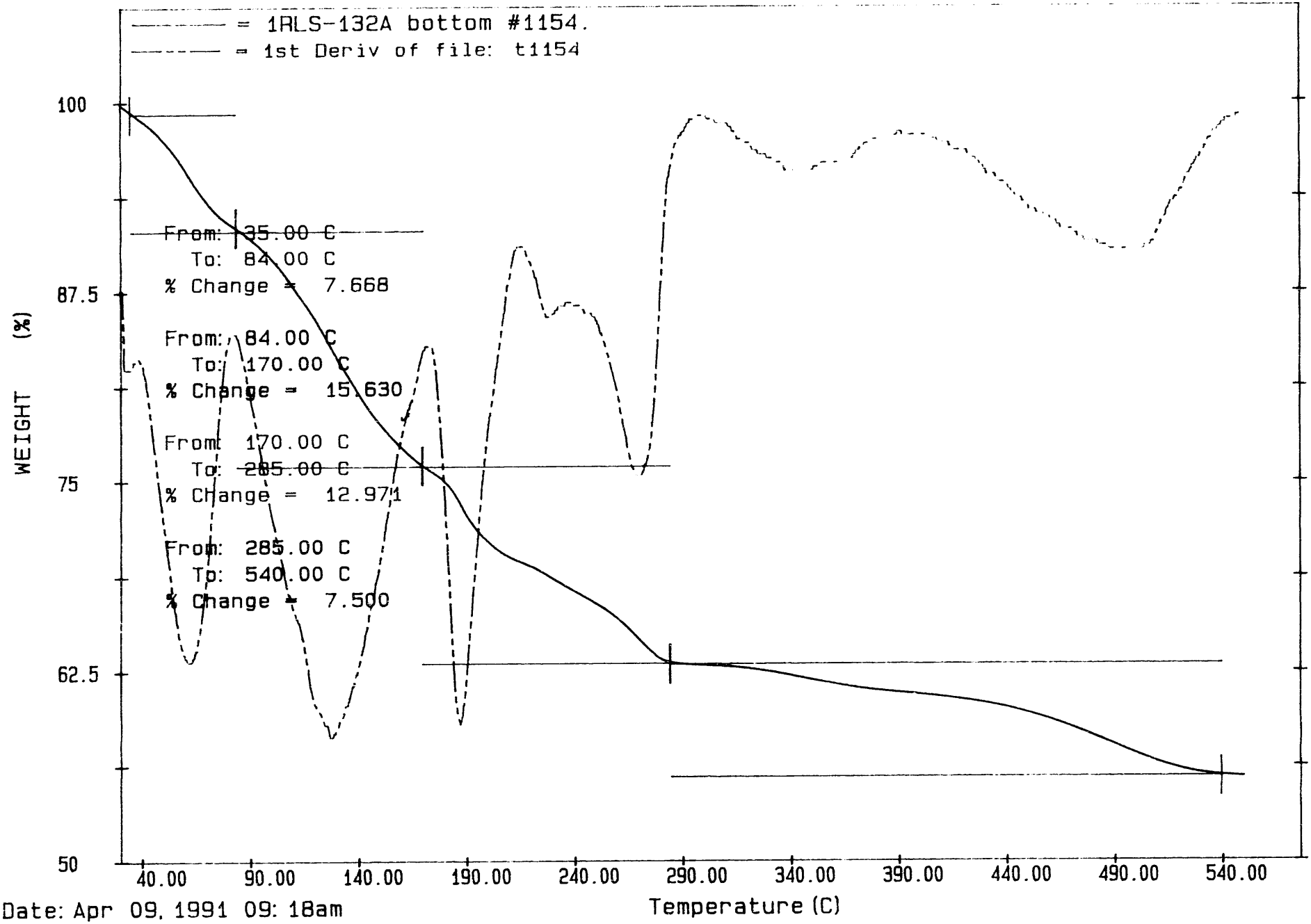

Date: Apr 09, 1991 09: 18am
Scanning Rate: 5.0 C/min

High Aluminate/High Organic

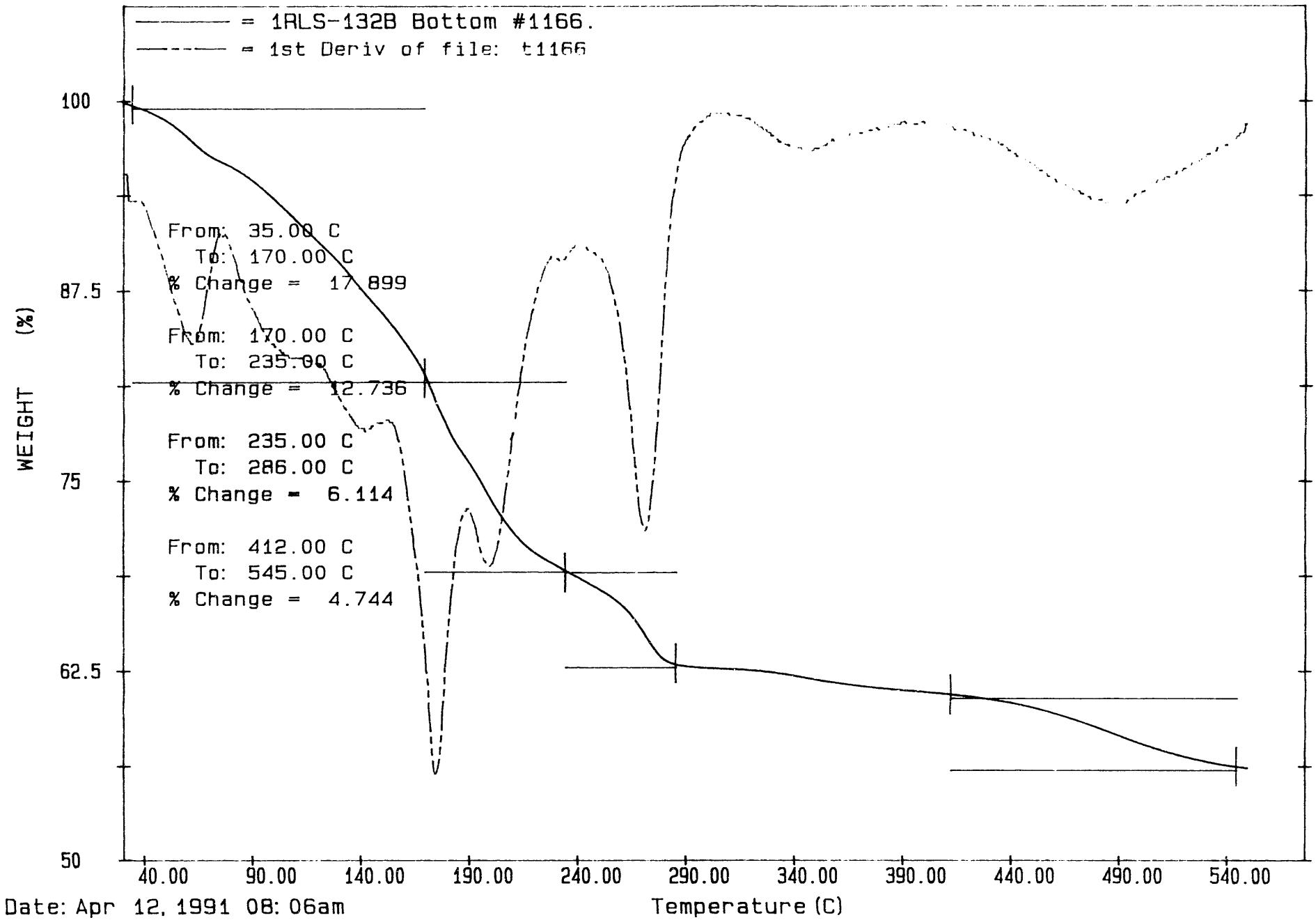

Date: Apr 12, 1991 08:06am
Scanning Rate: 5.0 C/min
Sample Wt: 21.064 mg Path: d:\archive\h
File: T1166 *R L SELL*

PC SERIES TGA7

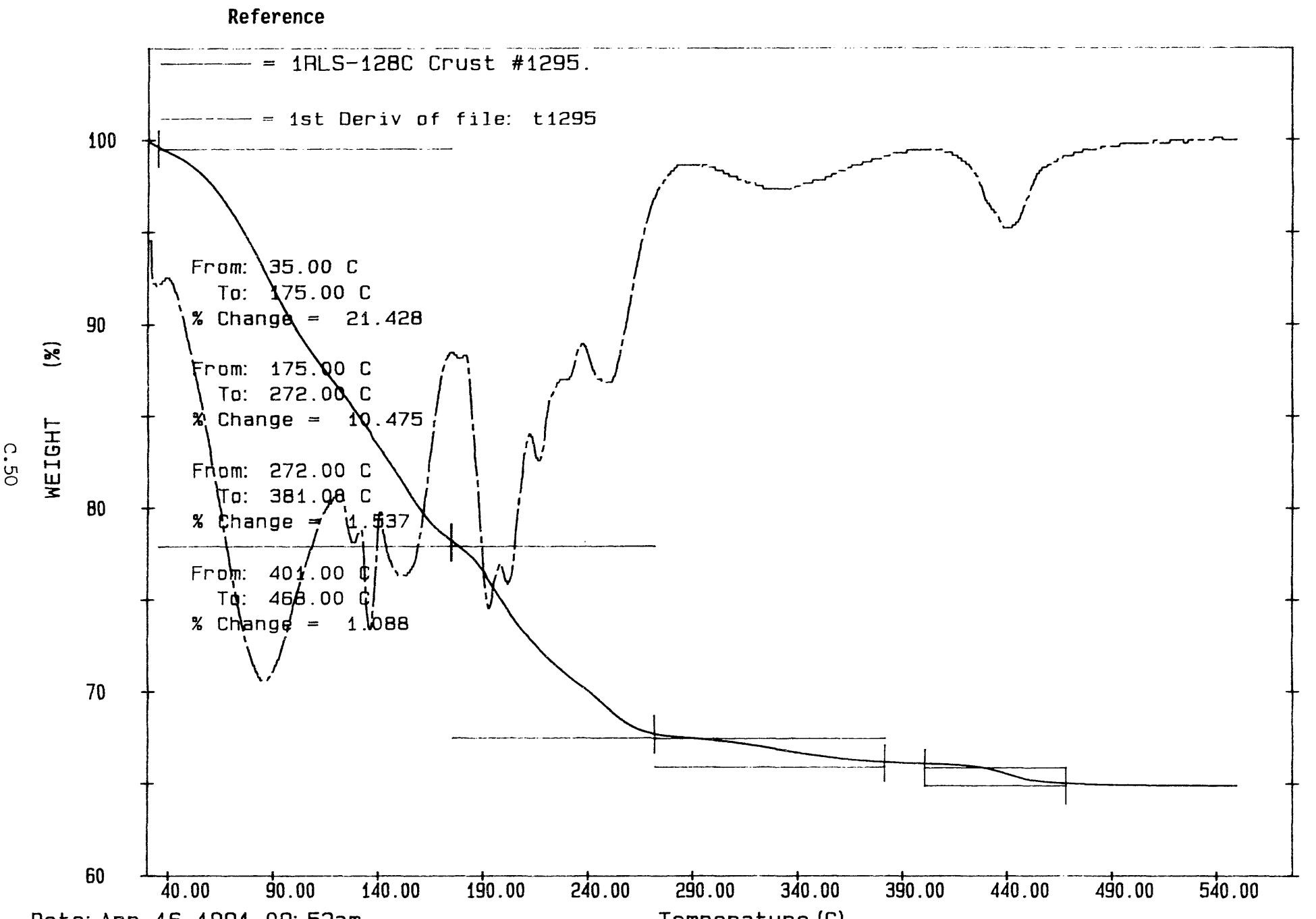
Reference
1RLS-128C Crust #1295.
1st Deriv of file: t1295
From: 35.00 C
To: 175.00 C
% Change = 21.428
From: 175.00 C
To: 272.00 C
% Change = 10.475
From: 272.00 C
To: 381.08 C
% Change = 1.537
From: 401.00 C
To: 468.00 C
% Change = 1.088
WEIGHT (%)
100
90
80
70
60
40.00
90.00
140.00
190.00
240.00
290.00
340.00
390.00
440.00
490.00
540.00
Temperature (C)
C.50
Date: Apr 16, 1991 09:52am
Scanning Rate: 5.0 C/min
Sample Wt: 24.628 mg Path: d:\archive\h

Reference

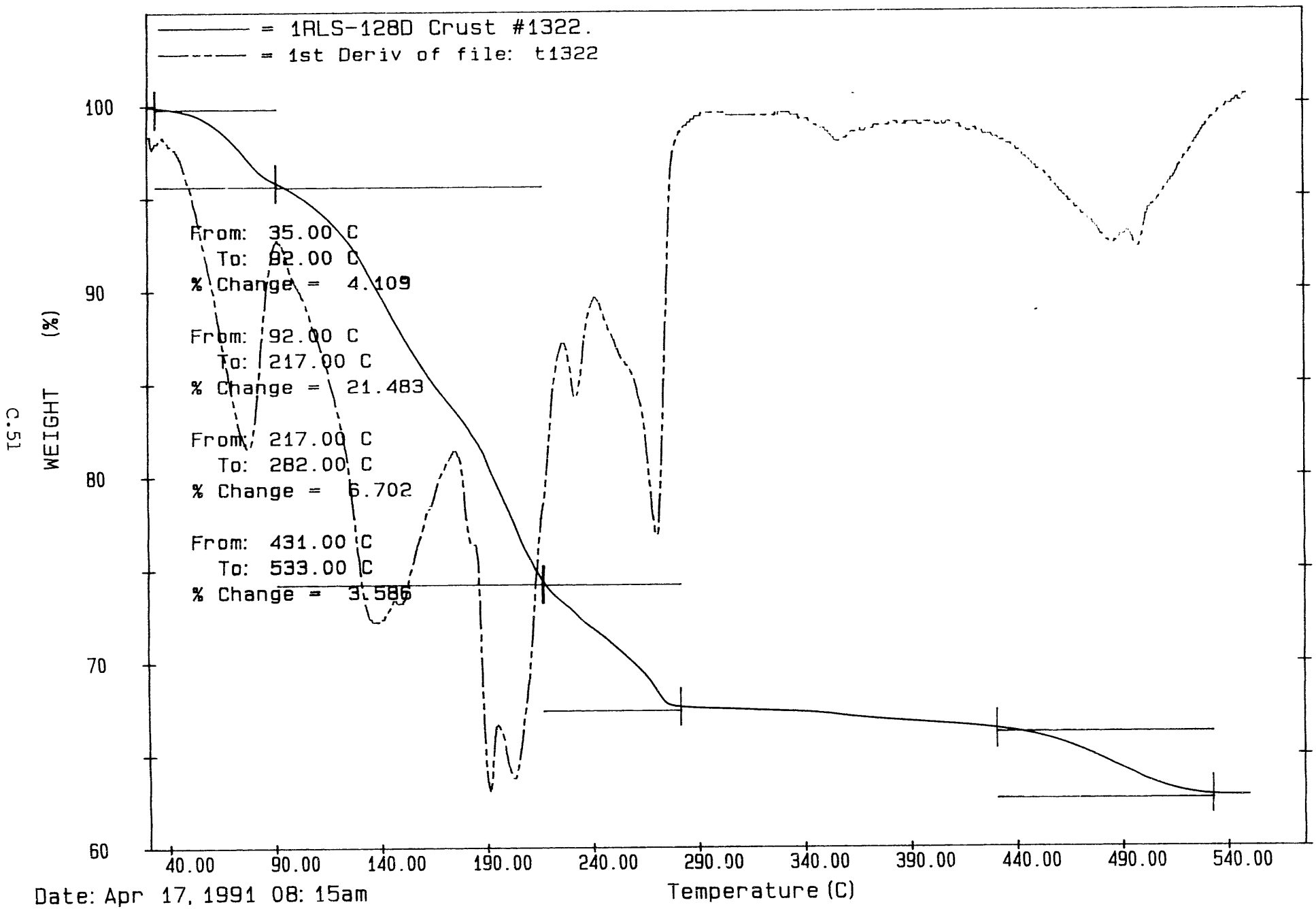

C.51

Date: Apr 17, 1991 08:15am
Scanning Rate: 5.0 C/min
Sample Wt: 31.614 mg Path: d:\archive\h
File: T1322 R I

TC SERIES 347

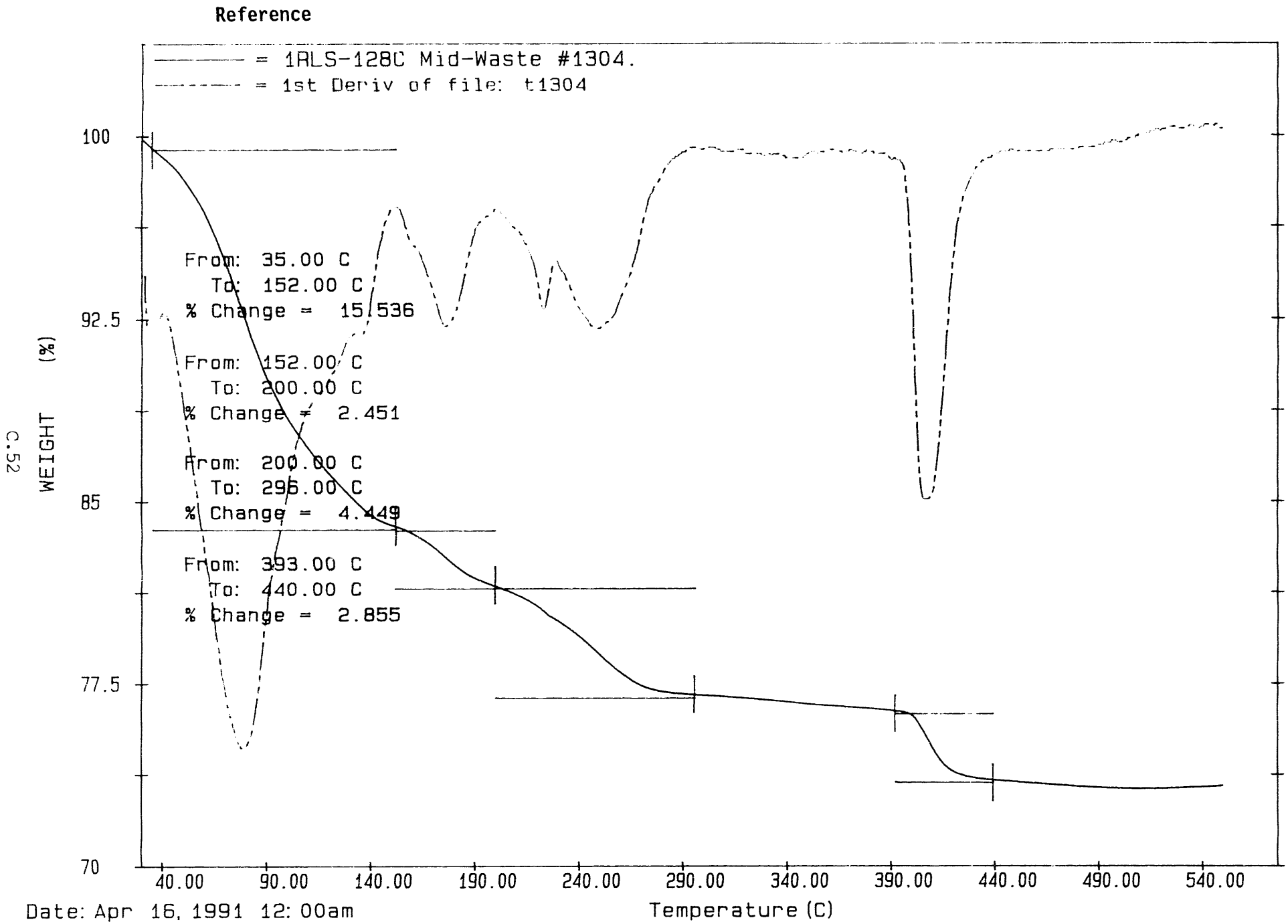
Reference
——— = 1RLS-128C Mid-Waste #1304.
------- = 1st Deriv of file: t1304
From: 35.00 C
To: 152.00 C
% Change = 15.536
From: 152.00 C
To: 200.00 C
% Change = 2.451
From: 200.00 C
To: 296.00 C
% Change = 4.449
From: 393.00 C
To: 440.00 C
% Change = 2.855
100
92.5
85
77.5
70
WEIGHT (%)
40.00
90.00
140.00
190.00
240.00
290.00
340.00
390.00
440.00
490.00
540.00
Temperature (C)
Date: Apr 16, 1991 12:00am
Scanning Rate: 5.0 C/min

Reference

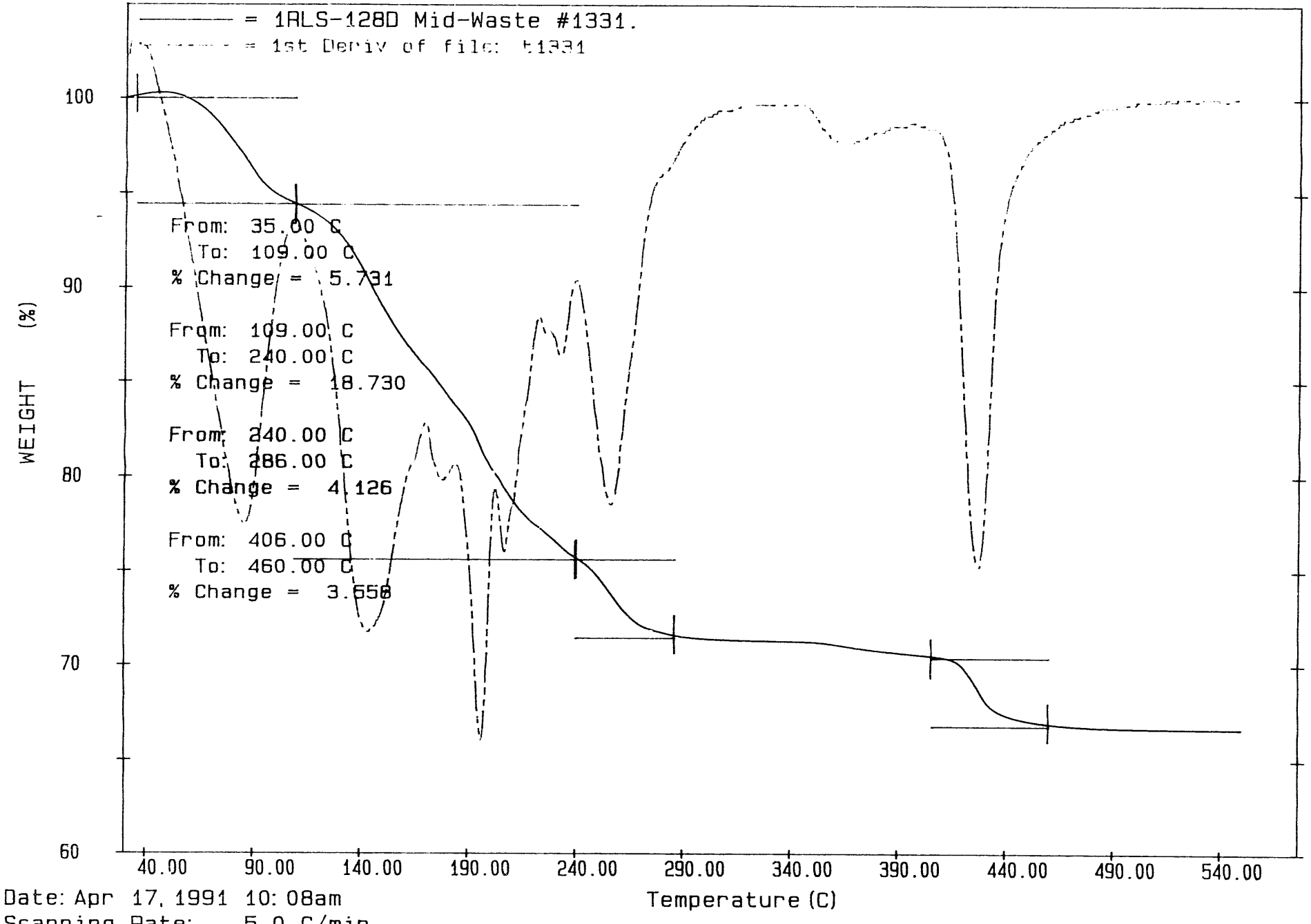

C.53

Date: Apr 17, 1991 10:08am
Scanning Rate: 5.0 C/min
Sample Wt: 34.012 mg Path: d:\archive\h
File: T1331 R L SELL

PC SERIES TGA7

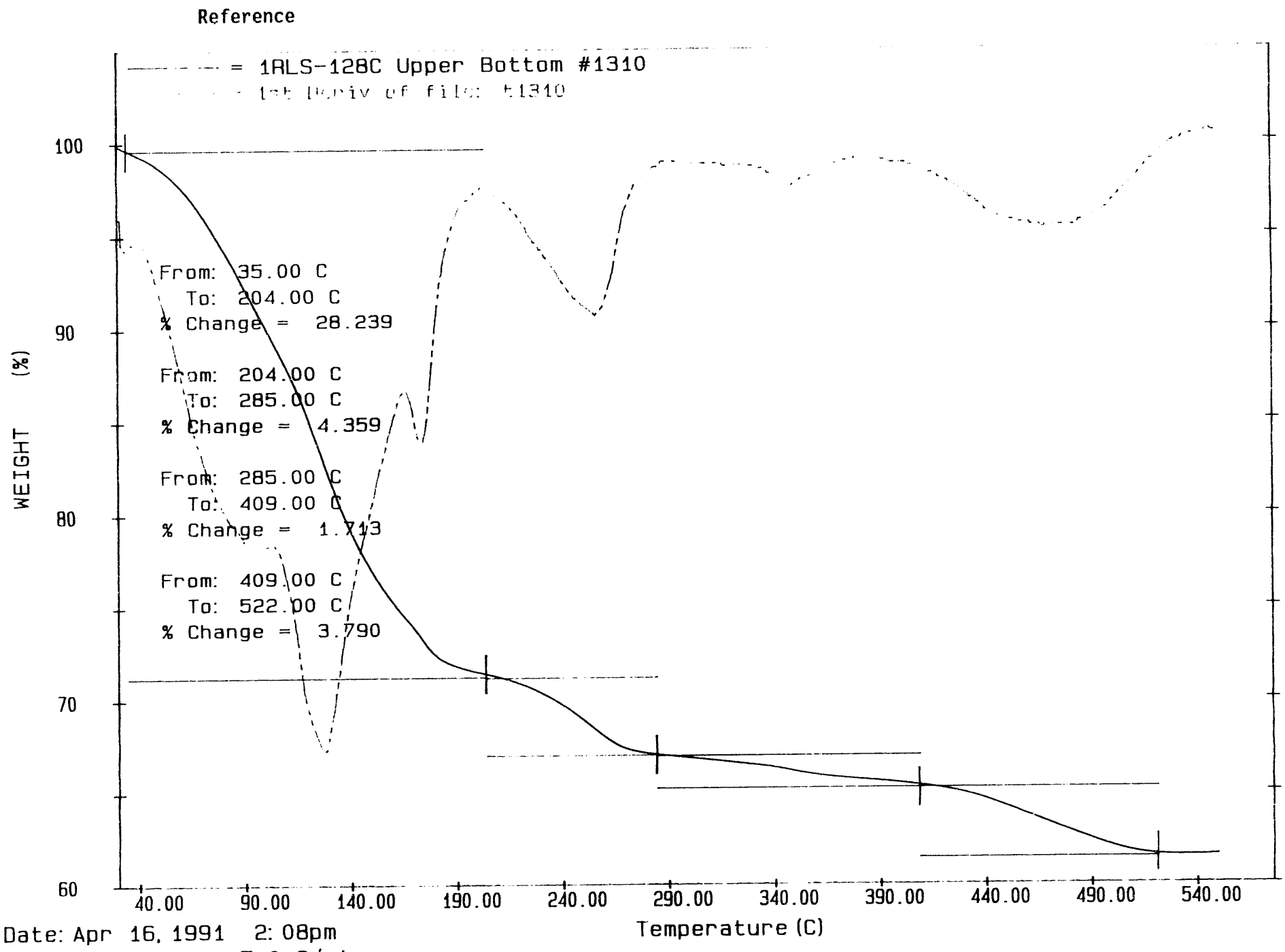
Reference
= 1RLS-128C Upper Bottom #1310
From: 35.00 C
To: 204.00 C
% Change = 28.239
From: 204.00 C
To: 285.00 C
% Change = 4.359
From: 285.00 C
To: 409.00 C
% Change = 1.713
From: 409.00 C
To: 522.00 C
% Change = 3.790
WEIGHT (%)
100
90
80
70
60
40.00
90.00
140.00
190.00
240.00
290.00
340.00
390.00
440.00
490.00
540.00
Temperature (C)
Date: Apr 16, 1991 2:08pm
Scanning Rate: 5.0 C/min

Reference

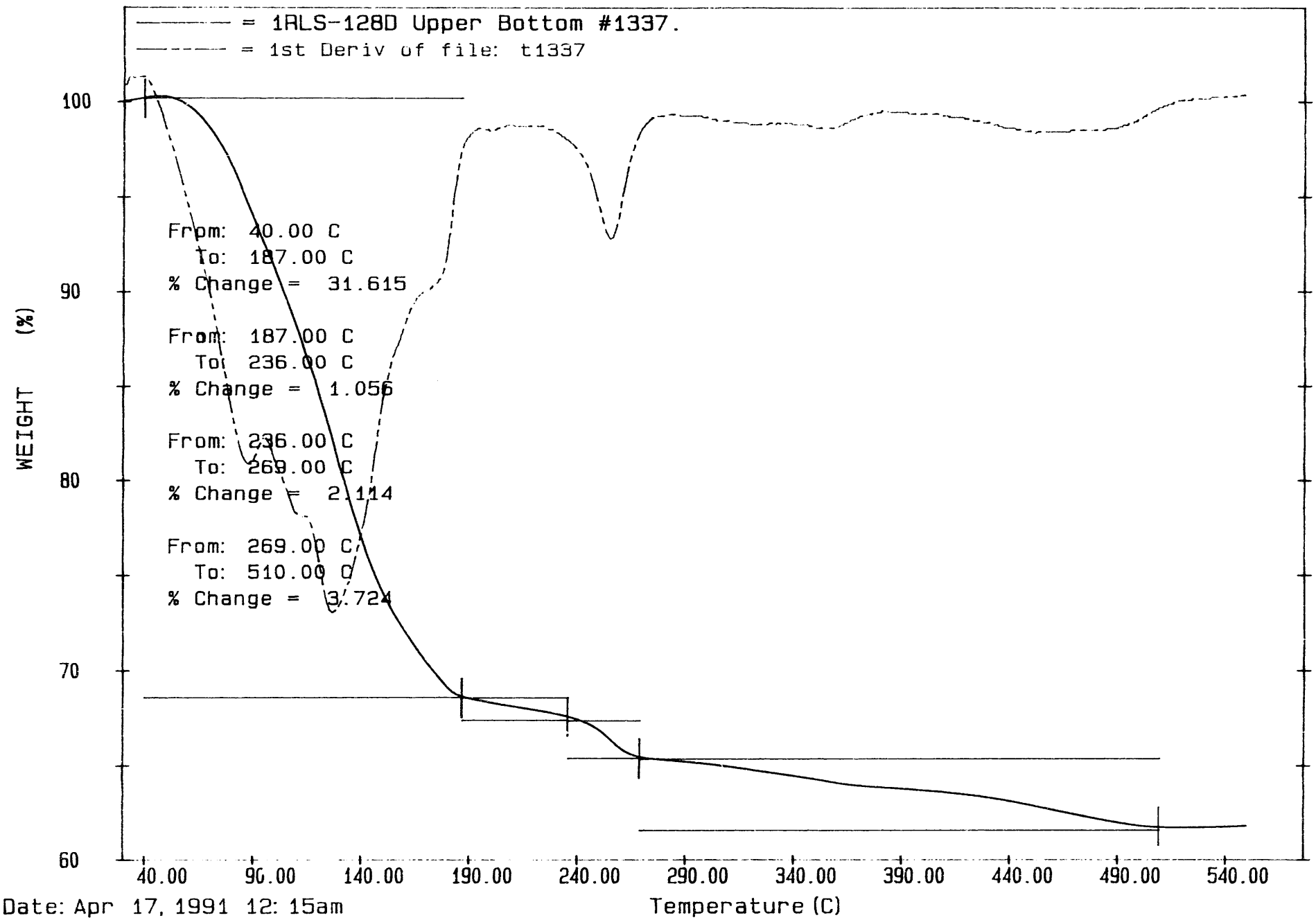

Date: Apr 17, 1991 12:15am
Scanning Rate: 5.0 C/min
Sample Wt: 22.389 mg Path: d:\archive\h
File: T1337 R L SELL

PC SERIES TGA

Reference

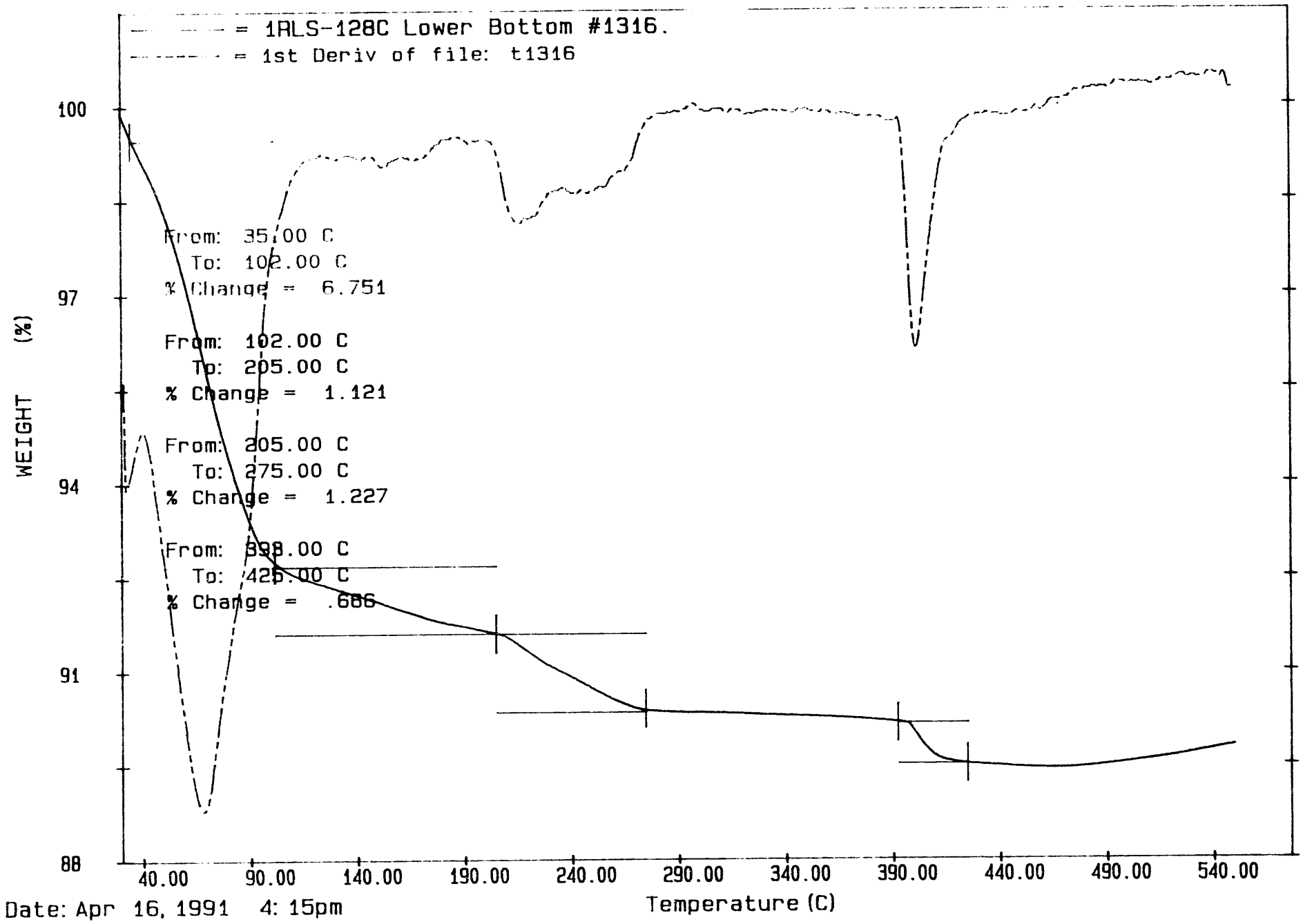

C.56

Date: Apr 16, 1991 4: 15pm
Scanning Rate: 5.0 C/min

Reference

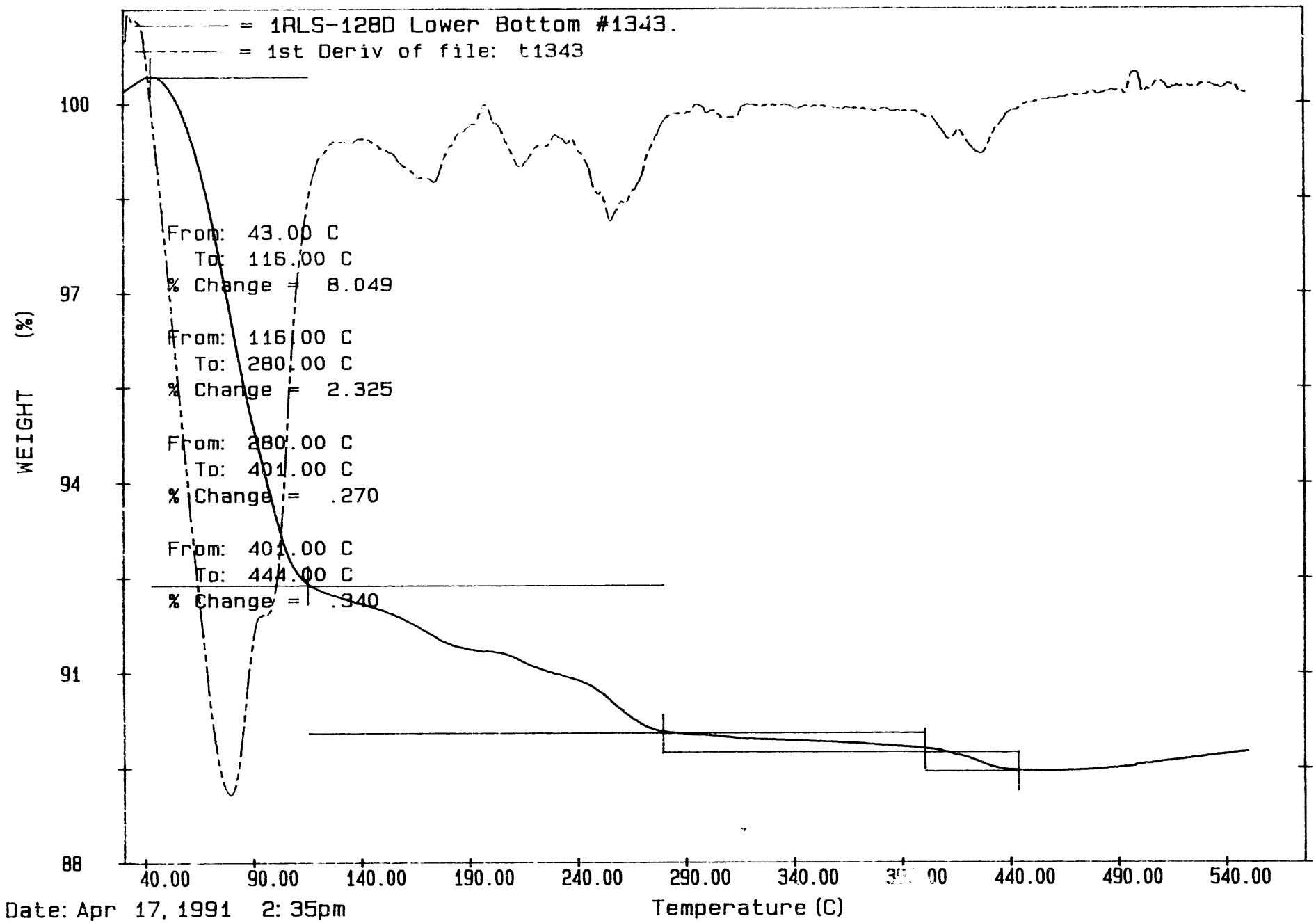

Date: Apr 17, 1991 2:35pm
Scanning Rate: 5.0 C/min
Sample Wt: 17.820 mg Path: d:\archive\h
File: T1343 *R.L. SELL*

PC SERIES TGA7

APPENDIX D

RAW DATA FOR SHEAR STRESS VERSUS SHEAR RATE ANALYSES

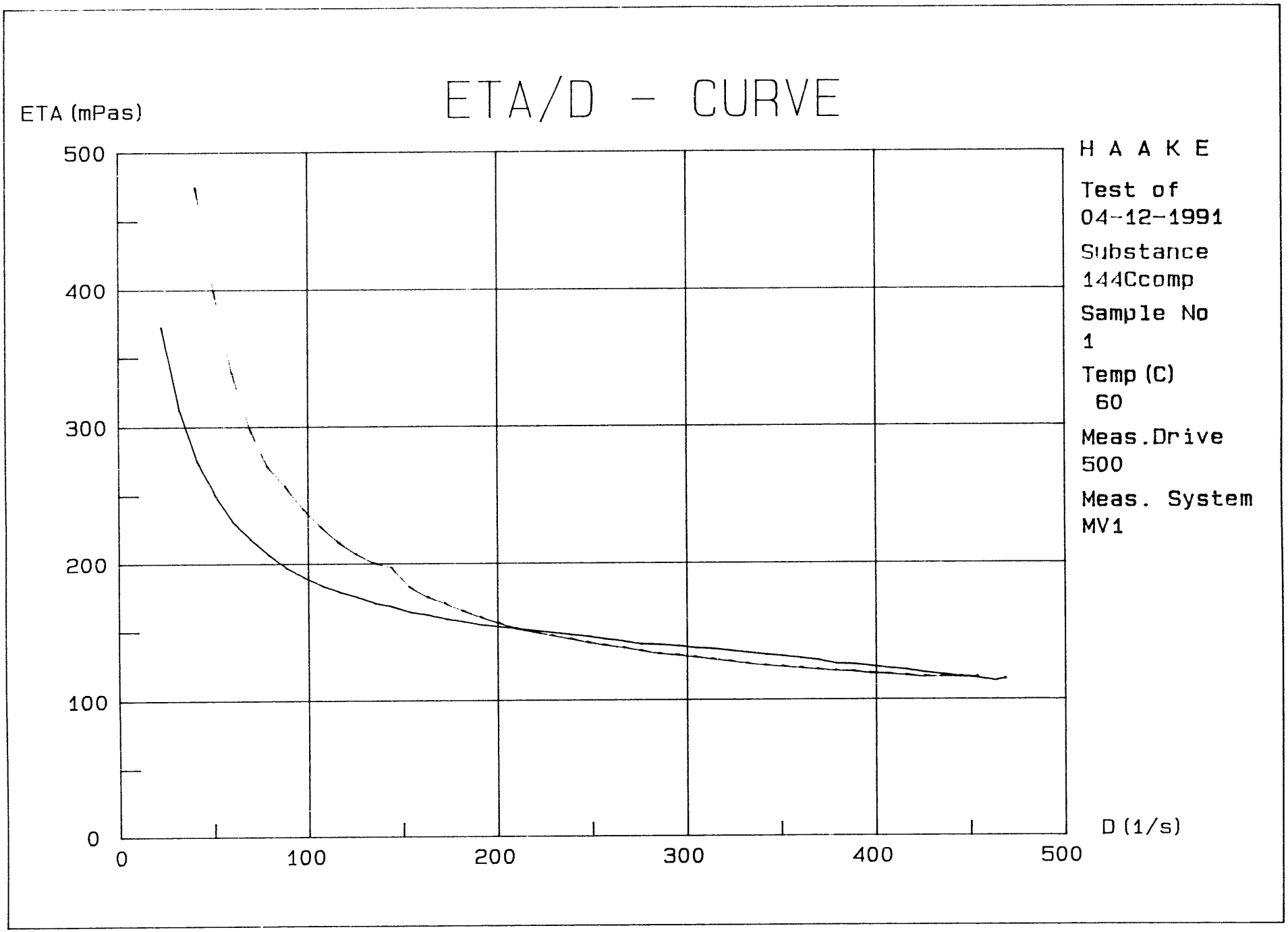
ETA/D - CURVE
ETA (mPas)
500
400
300
200
100
0
0
100
200
300
400
500
D (1/s)
H A A K E
Test of
04-12-1991
Substance
144Ccomp
Sample No
1
Temp (C)
60
Meas.Drive
500
Meas. System
MV1

Low Aluminate / Low Organic

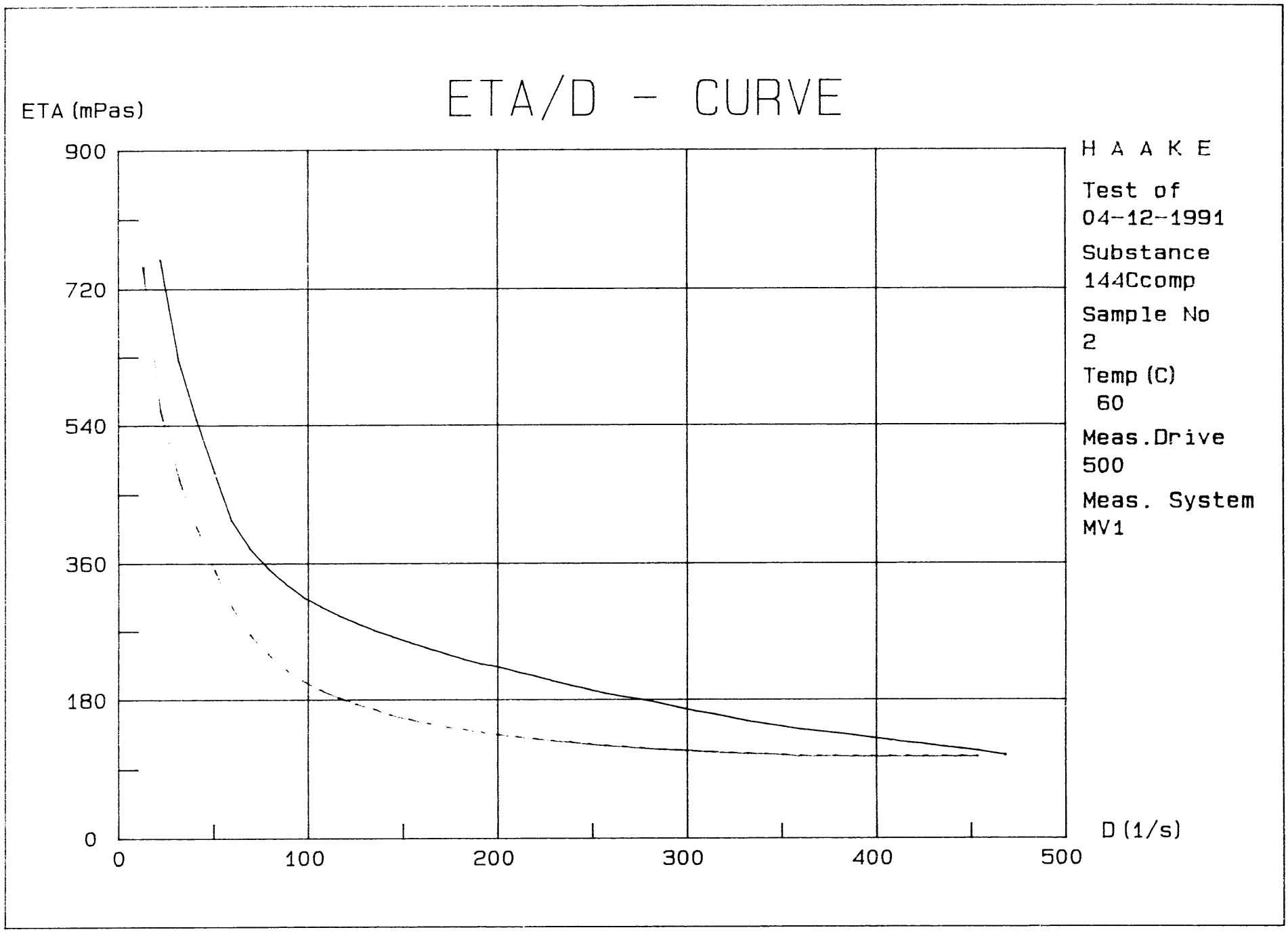

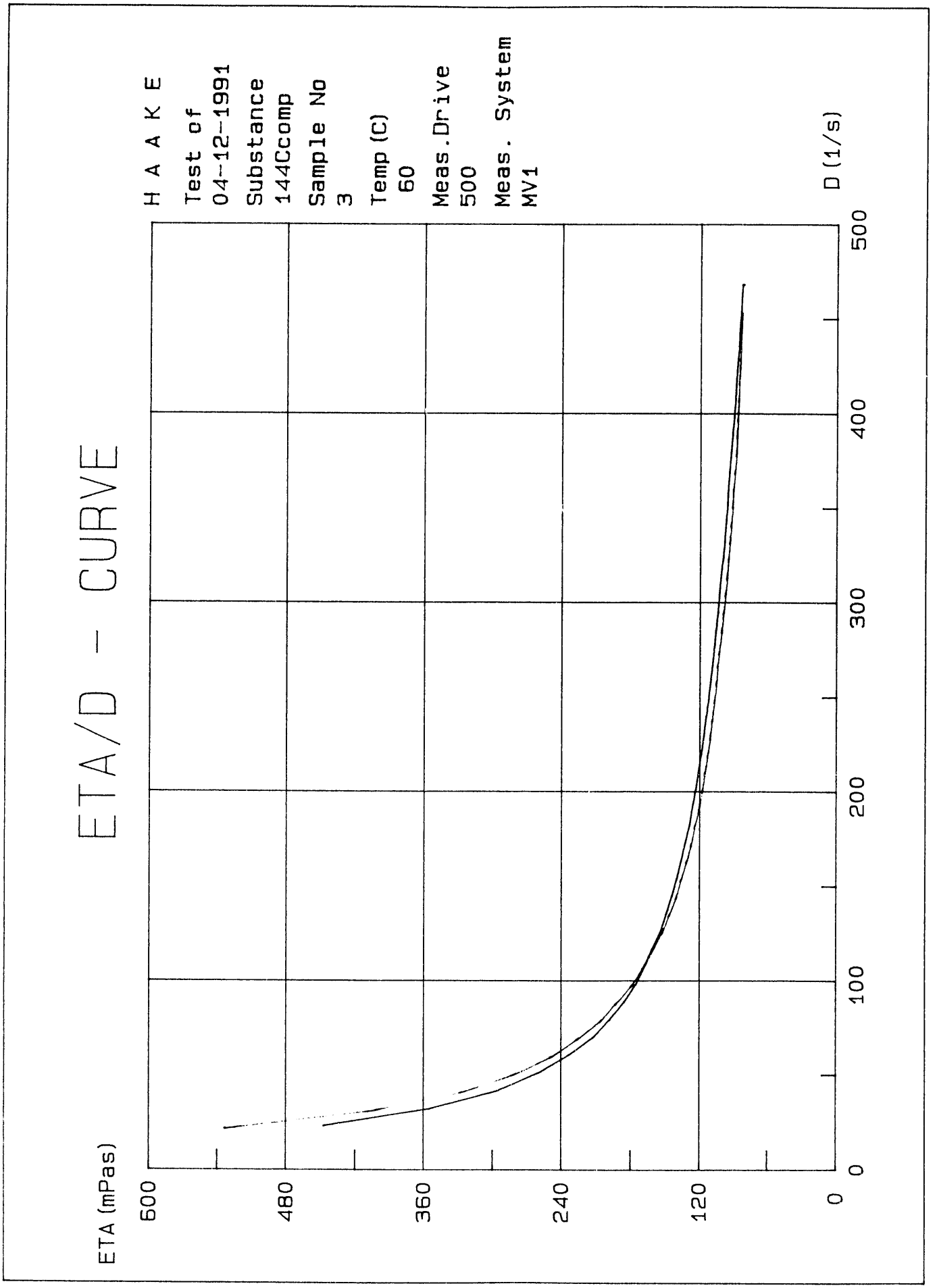
ETA/D - CURVE
H A A K E
Test of
04-12-1991
Substance
144Ccomp
Sample No
3
Temp (C)
60
Meas.Drive
500
Meas. System
MV1
ETA (mPas)
600
480
360
240
120
0
0
100
200
300
400
500
D (1/s)

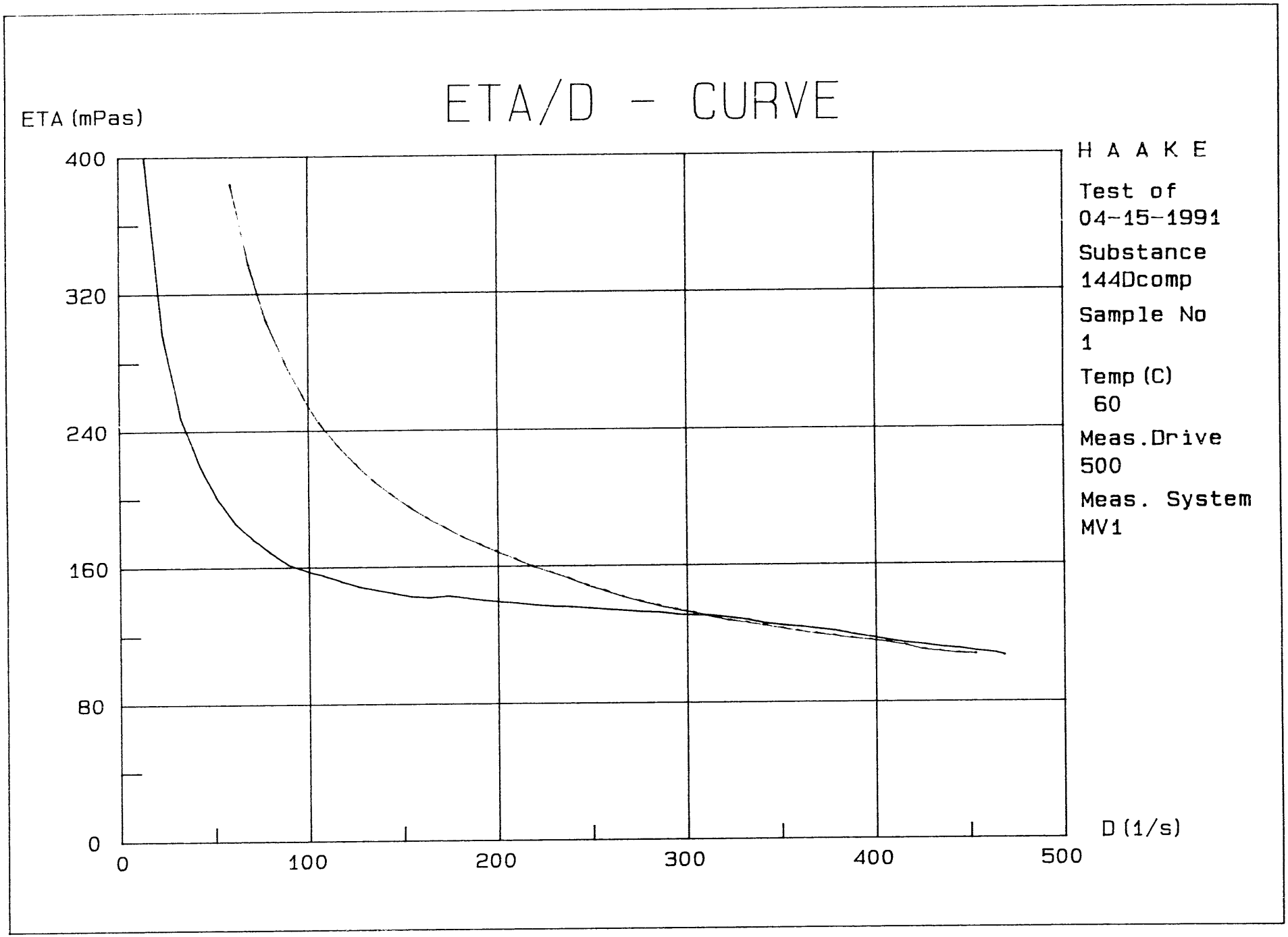
ETA/D - CURVE
ETA (mPas)
400
320
240
160
80
0
0
100
200
300
400
500
D (1/s)
H A A K E
Test of
04-15-1991
Substance
144Dcomp
Sample No
1
Temp (C)
60
Meas.Drive
500
Meas. System
MV1

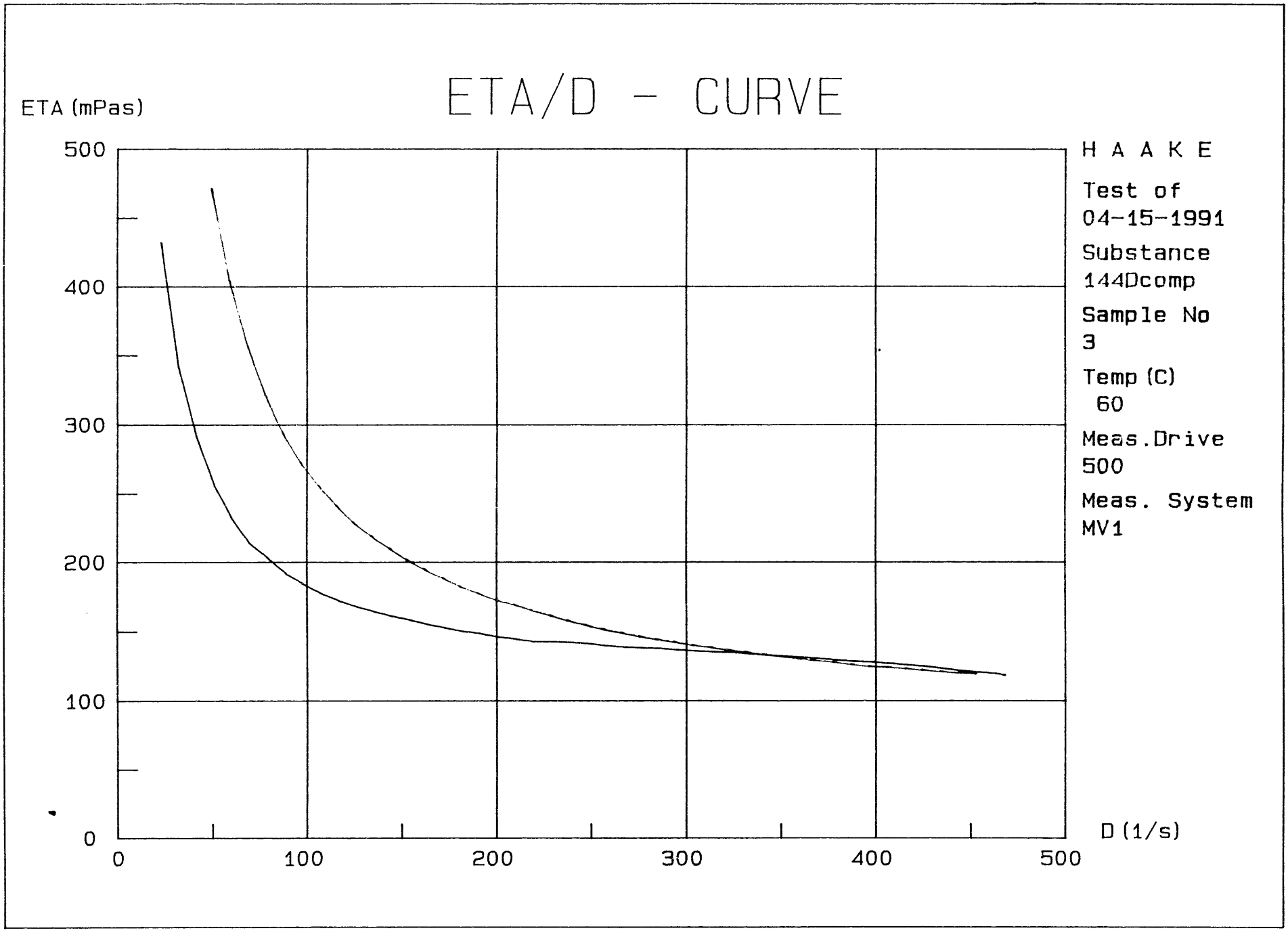
ETA/D - CURVE
ETA (mPas)
500
400
300
200
100
0
0
100
200
300
400
500
D (1/s)
H A A K E
Test of
04-15-1991
Substance
144Dcomp
Sample No
3
Temp (C)
60
Meas.Drive
500
Meas. System
MV1

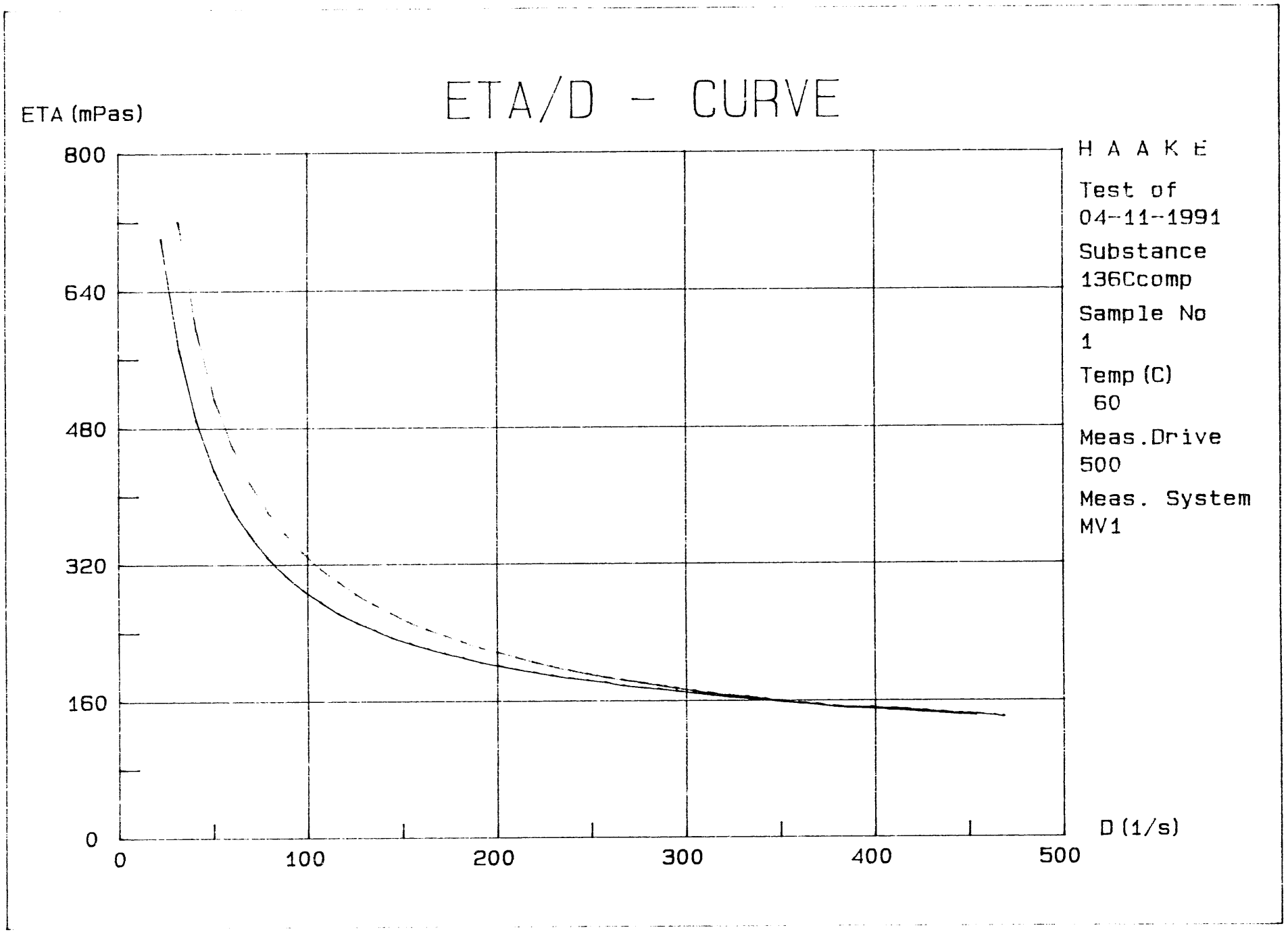
ETA/D - CURVE
ETA (mPas)
800
640
480
320
160
0
0
100
200
300
400
500
D (1/s)
H A A K E
Test of
04-11-1991
Substance
136Ccomp
Sample No
1
Temp (C)
60
Meas.Drive
500
Meas. System
MV1

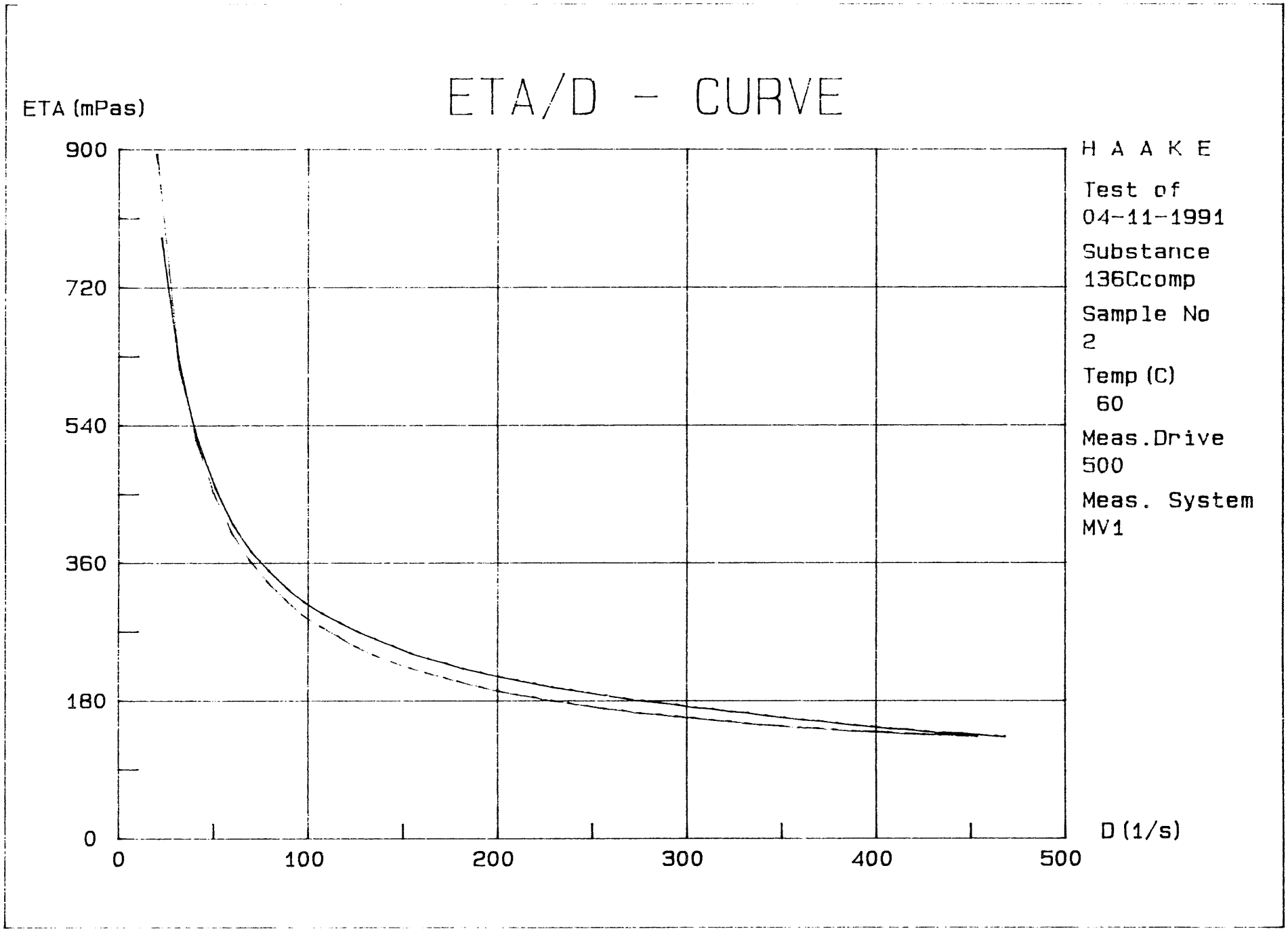
ETA/D - CURVE
ETA (mPas)
900
720
540
360
180
0
0
100
200
300
400
500
D (1/s)
H A A K E
Test of
04-11-1991
Substance
136Ccomp
Sample No
2
Temp (C)
60
Meas.Drive
500
Meas. System
MV1

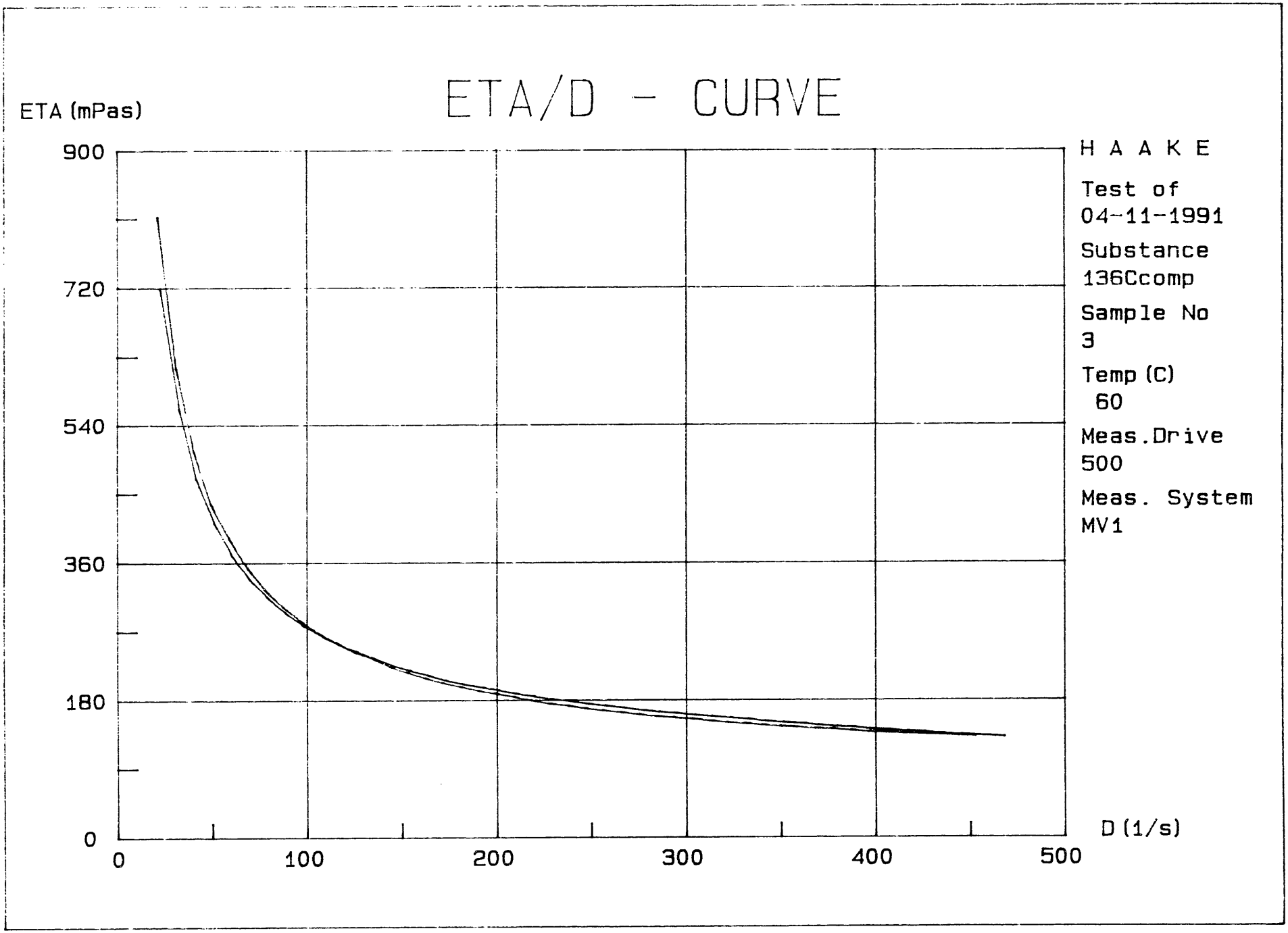
ETA/D - CURVE
ETA (mPas)
900
720
540
360
180
0
0
100
200
300
400
500
D (1/s)
H A A K E
Test of
04-11-1991
Substance
136Ccomp
Sample No
3
Temp (C)
60
Meas.Drive
500
Meas. System
MV1

Low Aluminate / High Organic

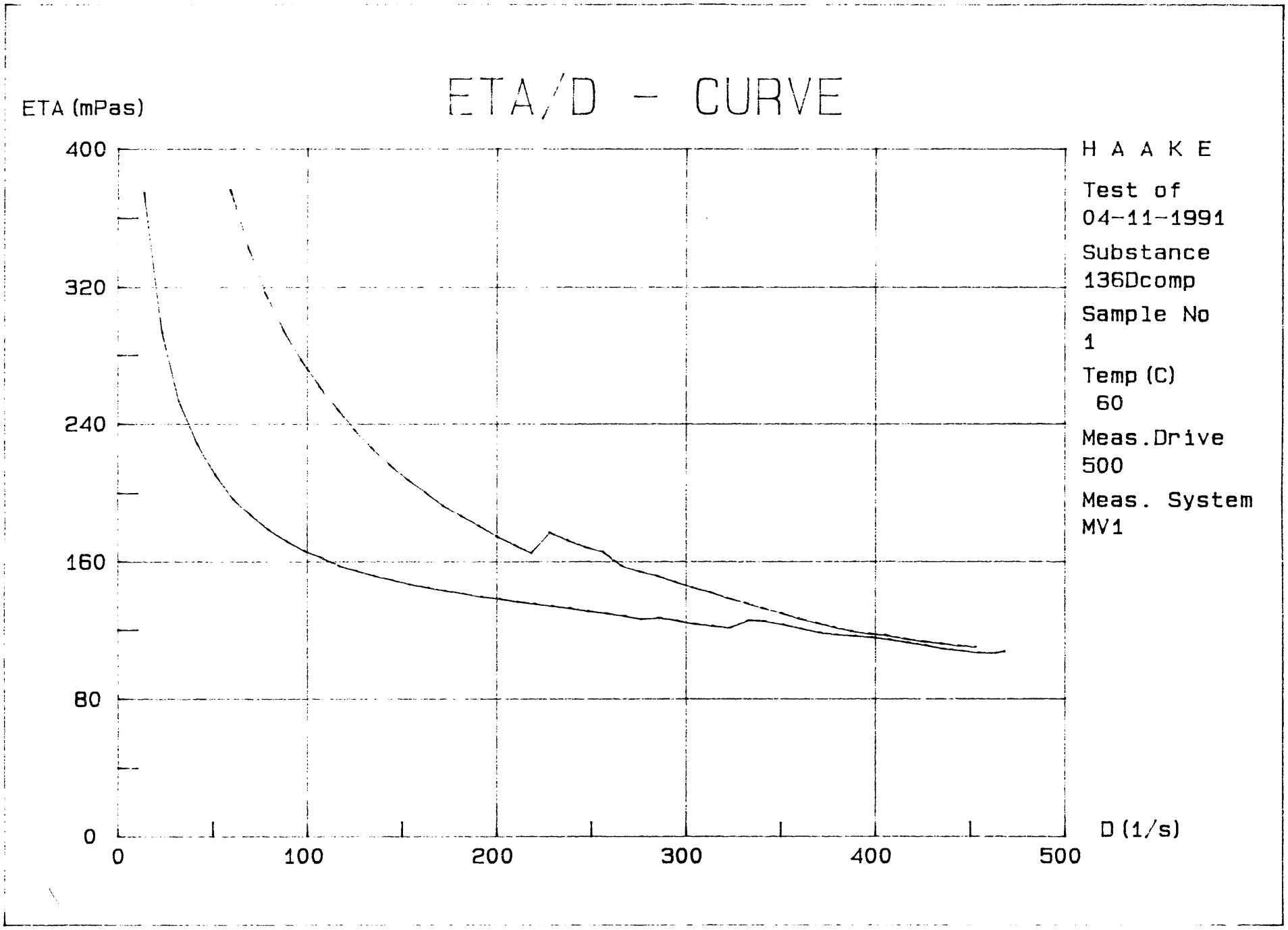

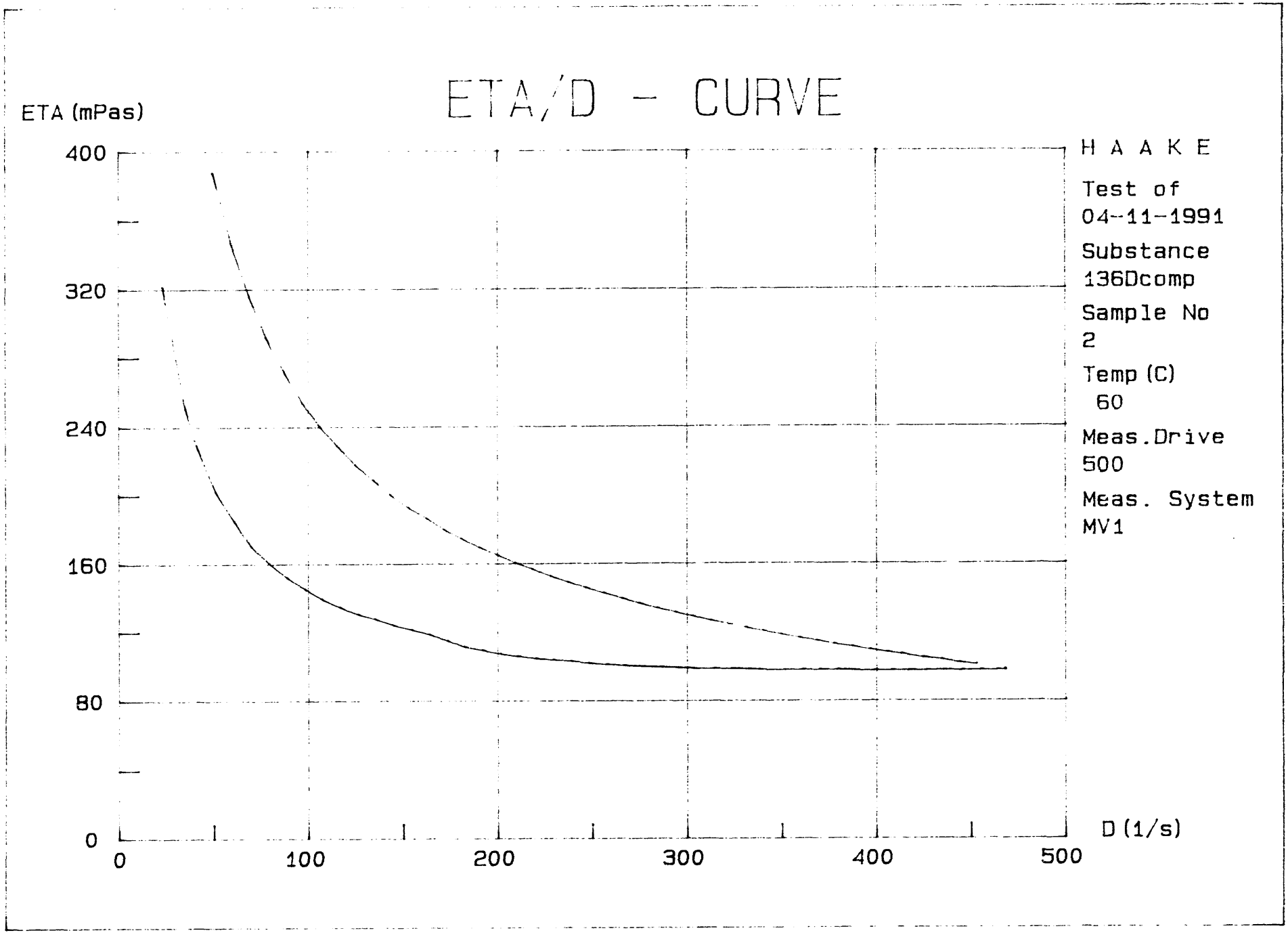
ETA/D - CURVE
ETA (mPas)
400
320
240
160
80
0
0
100
200
300
400
500
D (1/s)
H A A K E
Test of
04-11-1991
Substance
136Dcomp
Sample No
2
Temp (C)
60
Meas.Drive
500
Meas. System
MV1

Low Aluminate / High Organic

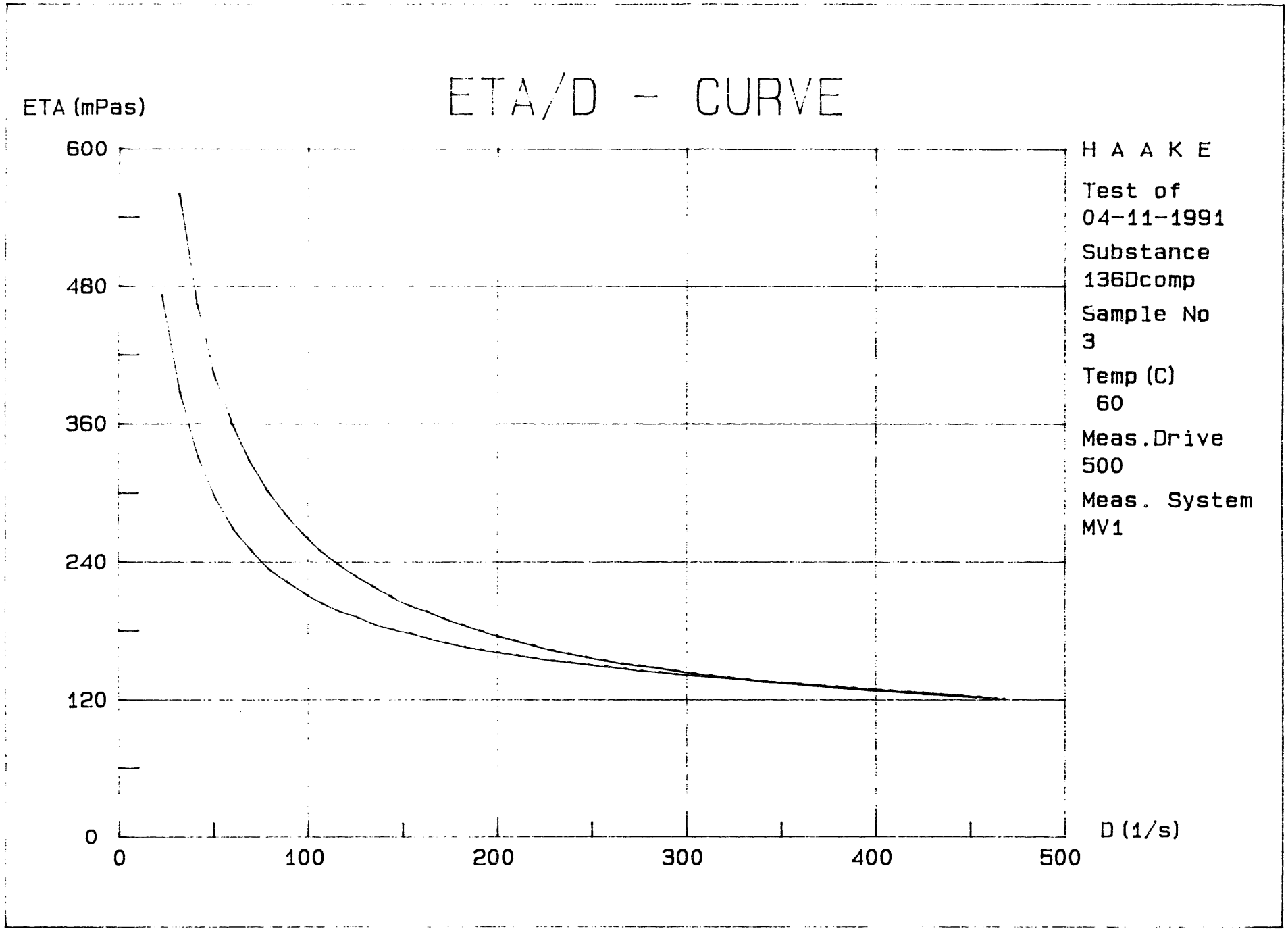

D.11

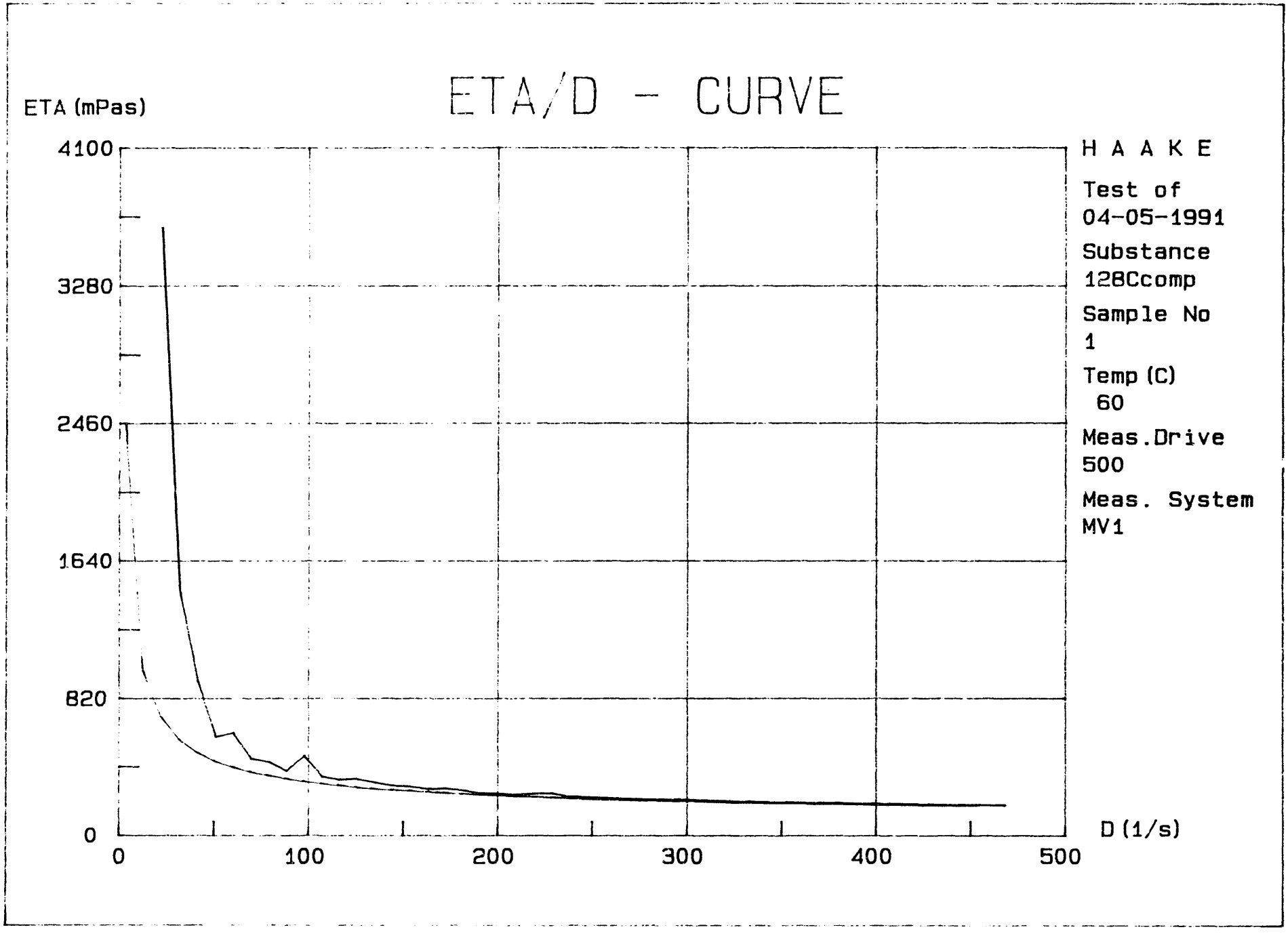
ETA/D - CURVE
ETA (mPas)
4100
3280
2460
1640
820
0
0
100
200
300
400
500
D (1/s)
H A A K E
Test of
04-05-1991
Substance
128Ccomp
Sample No
1
Temp (C)
60
Meas.Drive
500
Meas. System
MV1

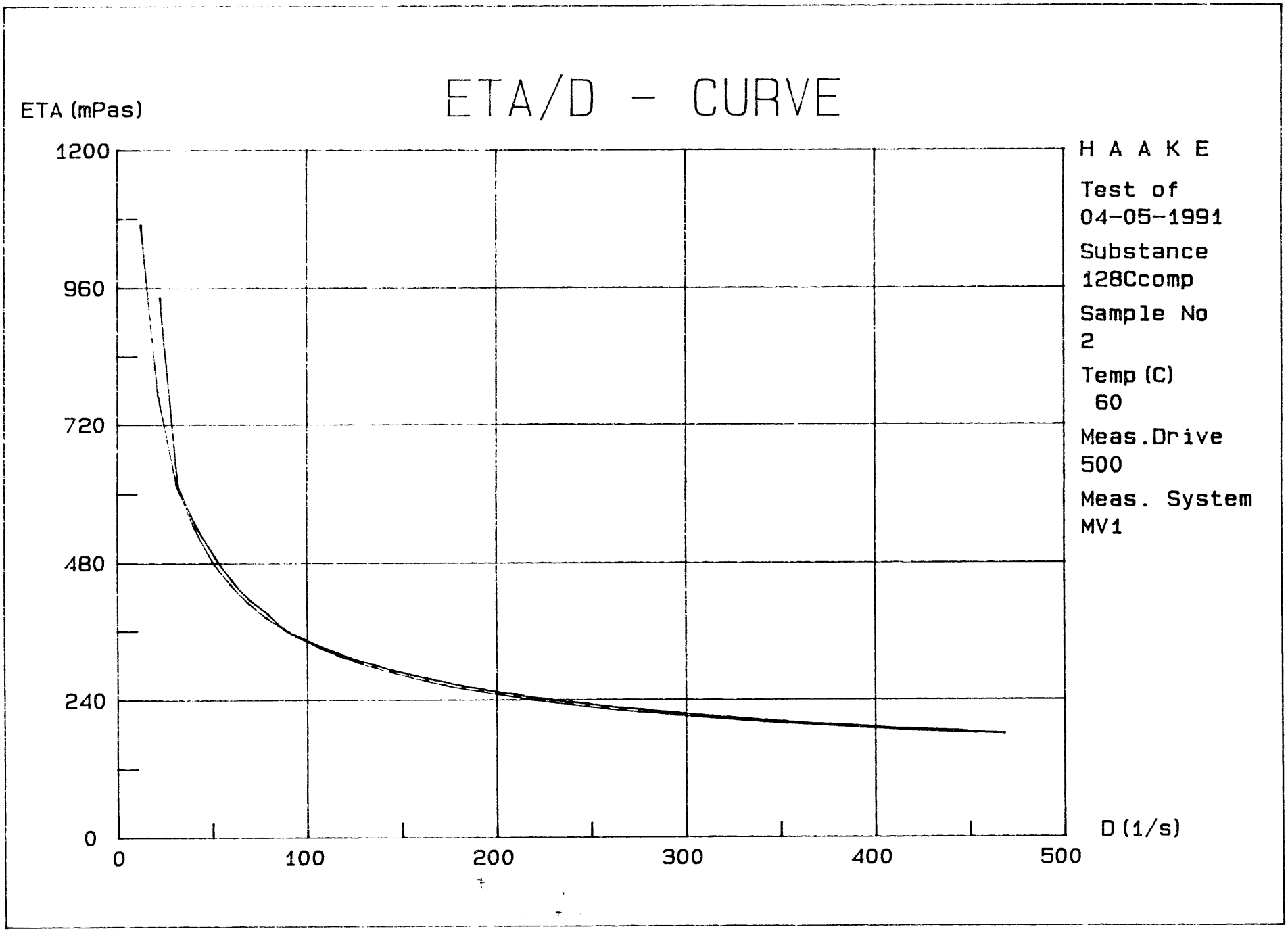
ETA/D - CURVE
ETA (mPas)
1200
960
720
480
240
0
0
100
200
300
400
500
D (1/s)
H A A K E
Test of
04-05-1991
Substance
128Ccomp
Sample No
2
Temp (C)
60
Meas.Drive
500
Meas. System
MV1

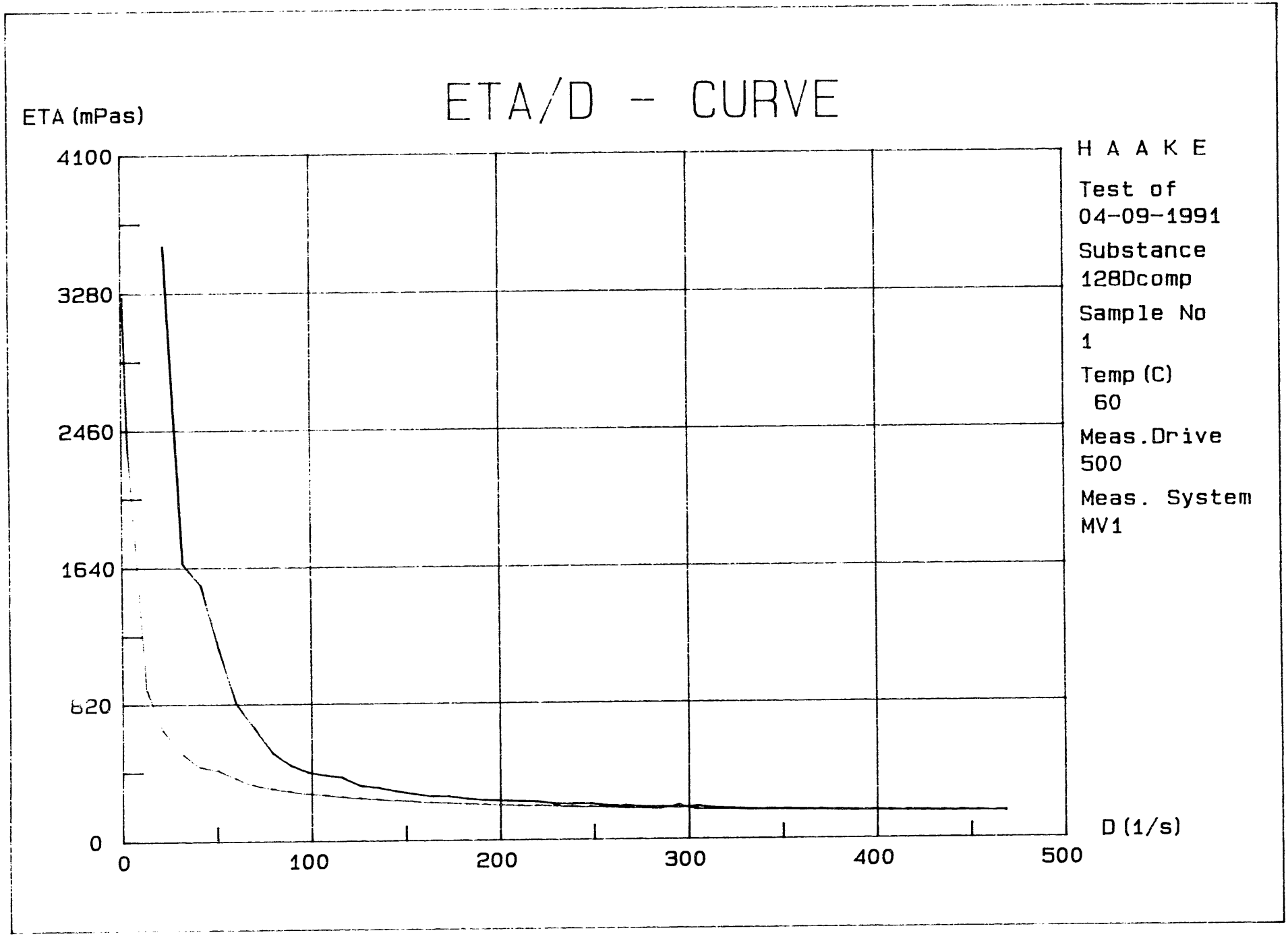
ETA/D - CURVE
ETA (mPas)
4100
3280
2460
1640
820
0
0
100
200
300
400
500
D (1/s)
H A A K E
Test of
04-09-1991
Substance
128Dcomp
Sample No
1
Temp (C)
60
Meas.Drive
500
Meas. System
MV1

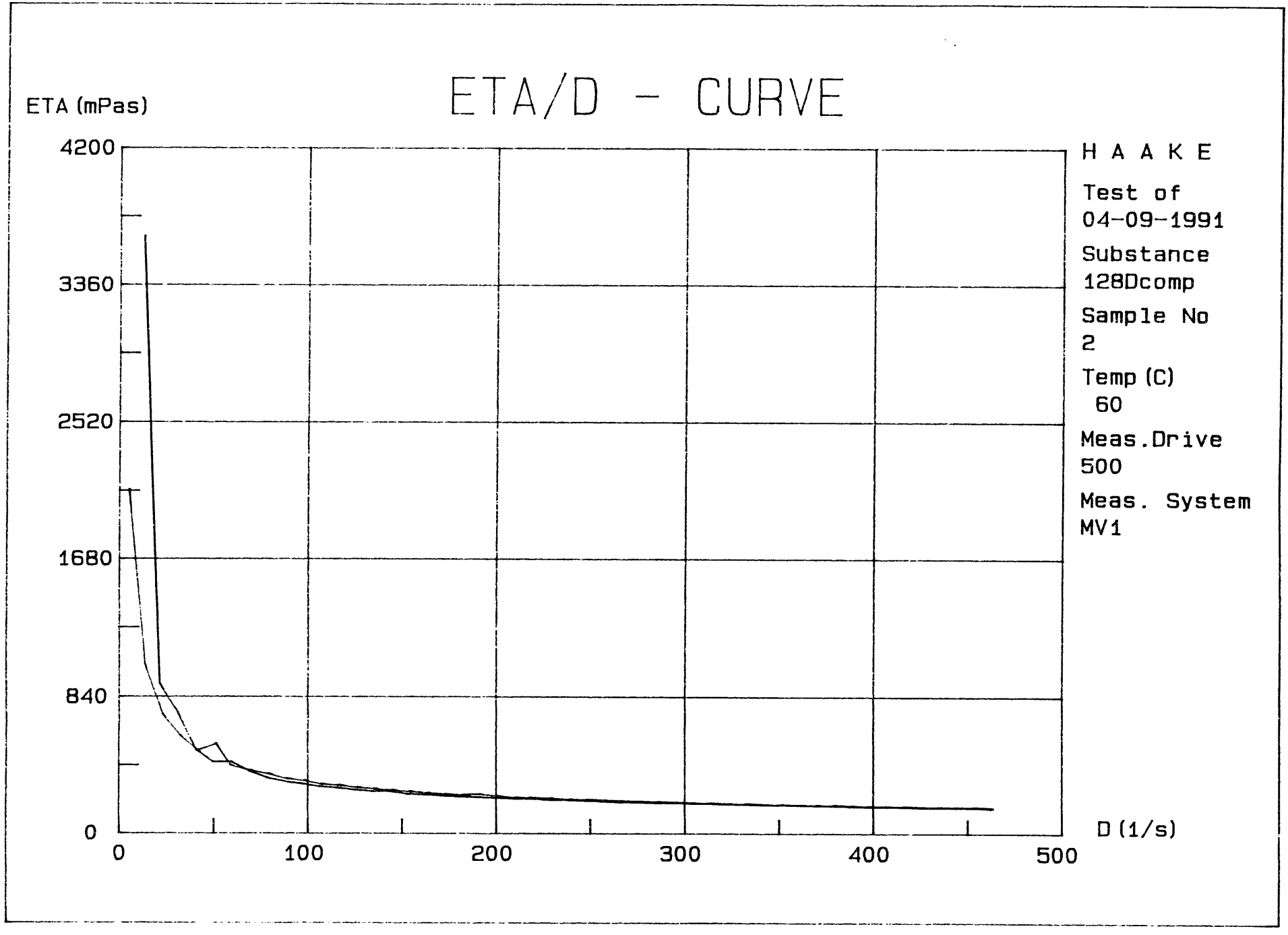
ETA/D - CURVE
ETA (mPas)
4200
3360
2520
1680
840
0
0
100
200
300
400
500
D (1/s)
H A A K E
Test of
04-09-1991
Substance
128Dcomp
Sample No
2
Temp (C)
60
Meas.Drive
500
Meas. System
MV1

High Aluminate / Low Organic

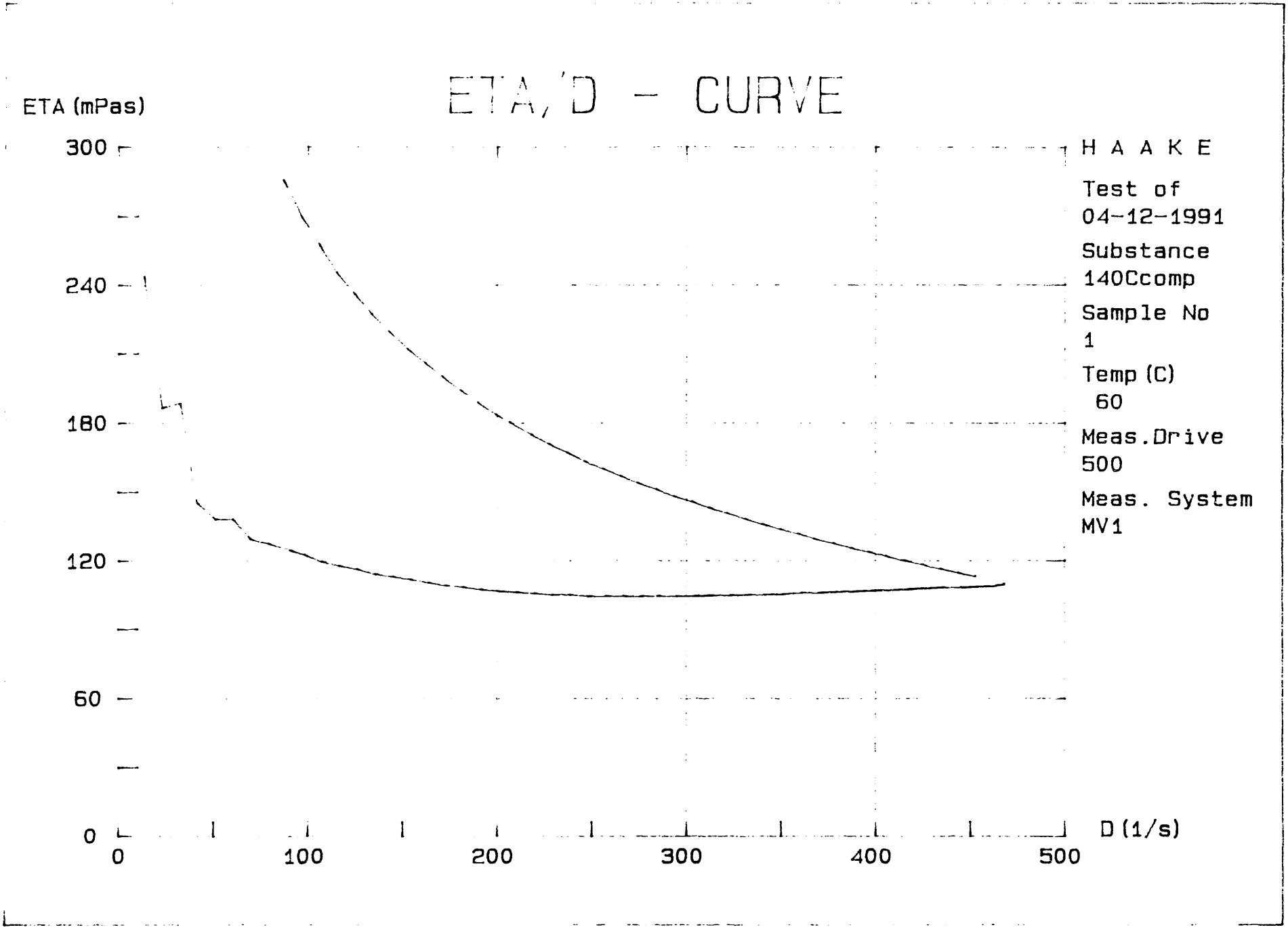

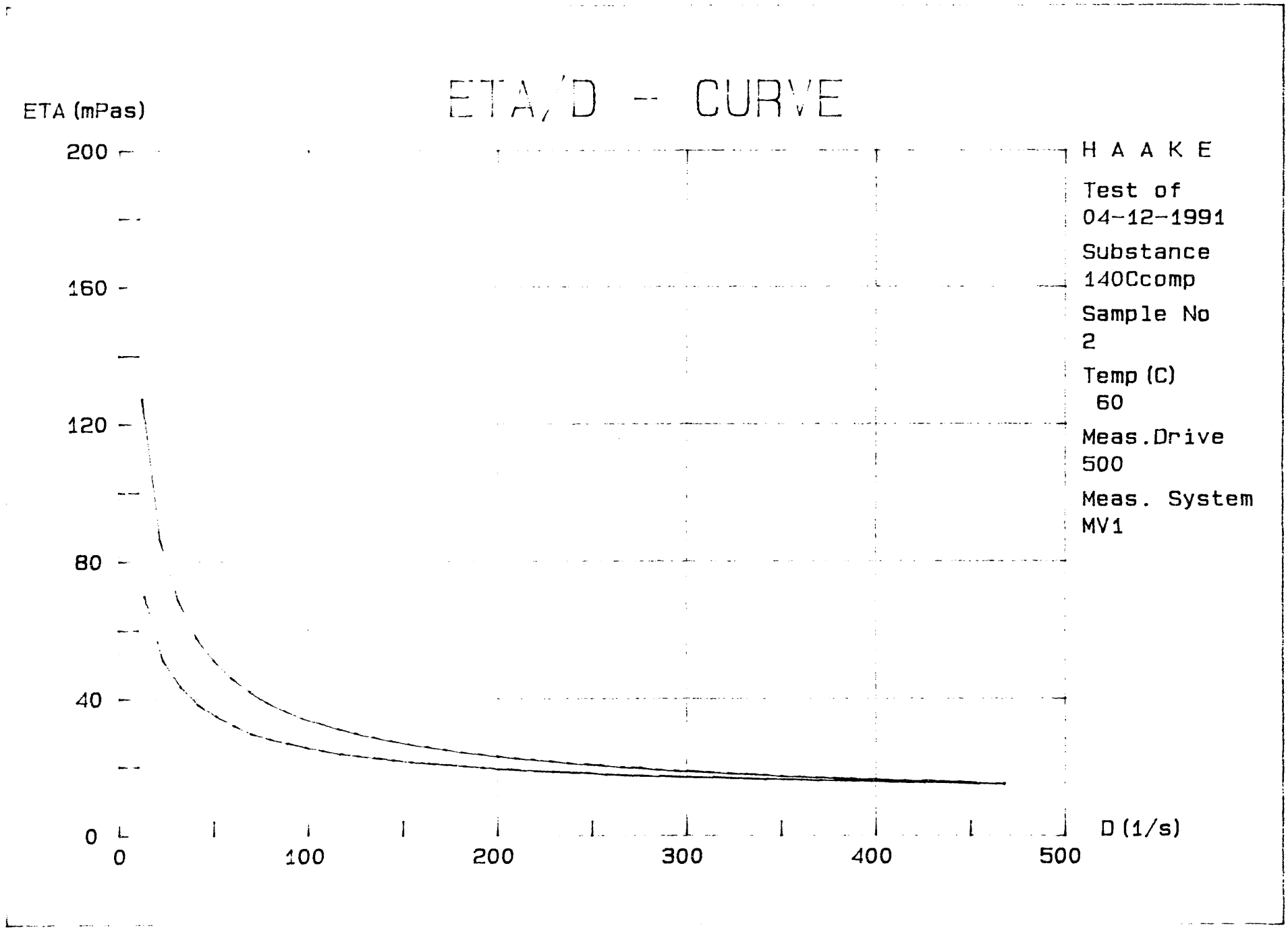
ETA/D - CURVE
ETA (mPas)
200
160
120
80
40
0
0
100
200
300
400
500
D (1/s)
H A A K E
Test of
04-12-1991
Substance
140Ccomp
Sample No
2
Temp (C)
60
Meas.Drive
500
Meas. System
MV1

High Aluminate / Low Organic

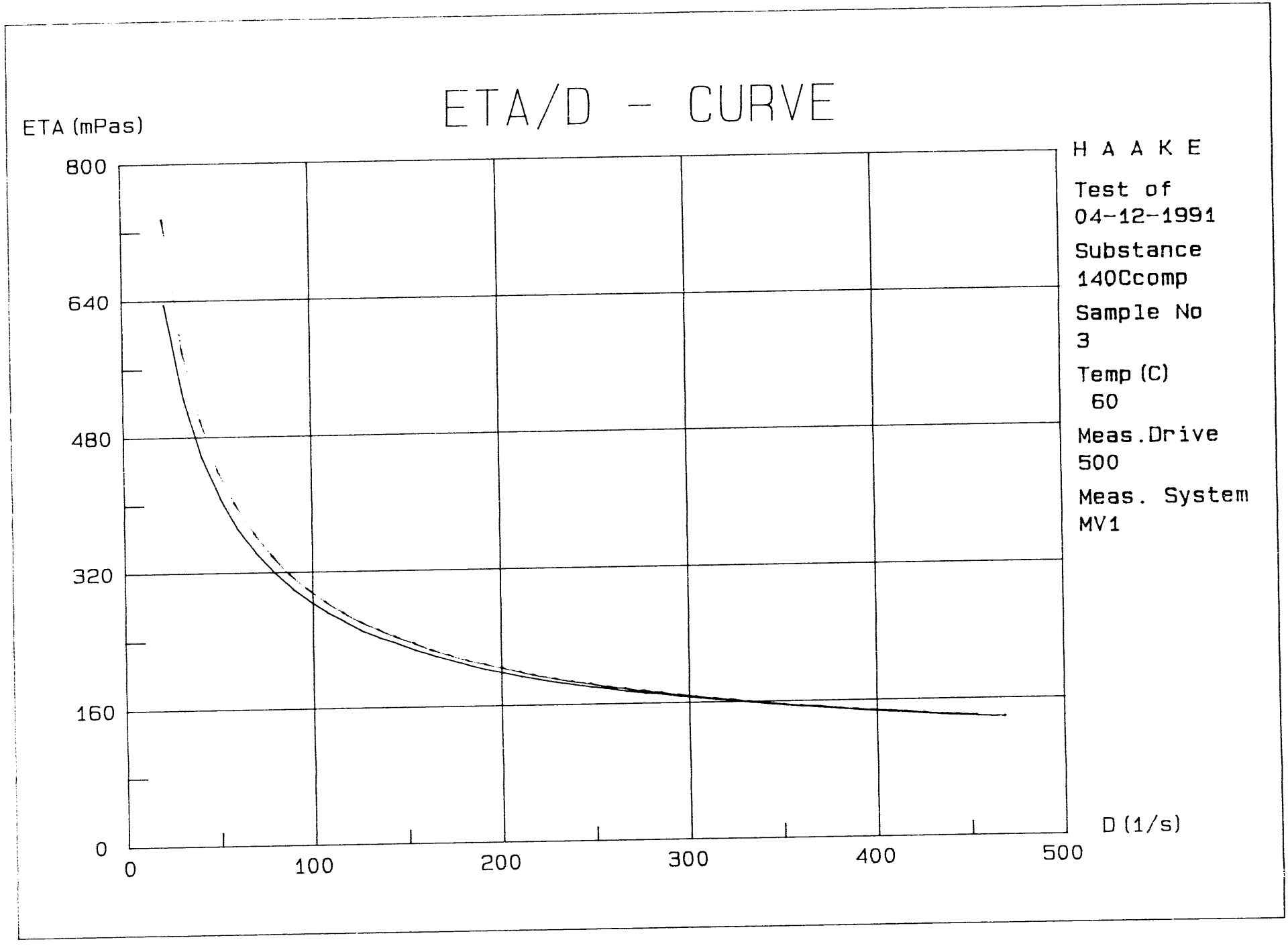

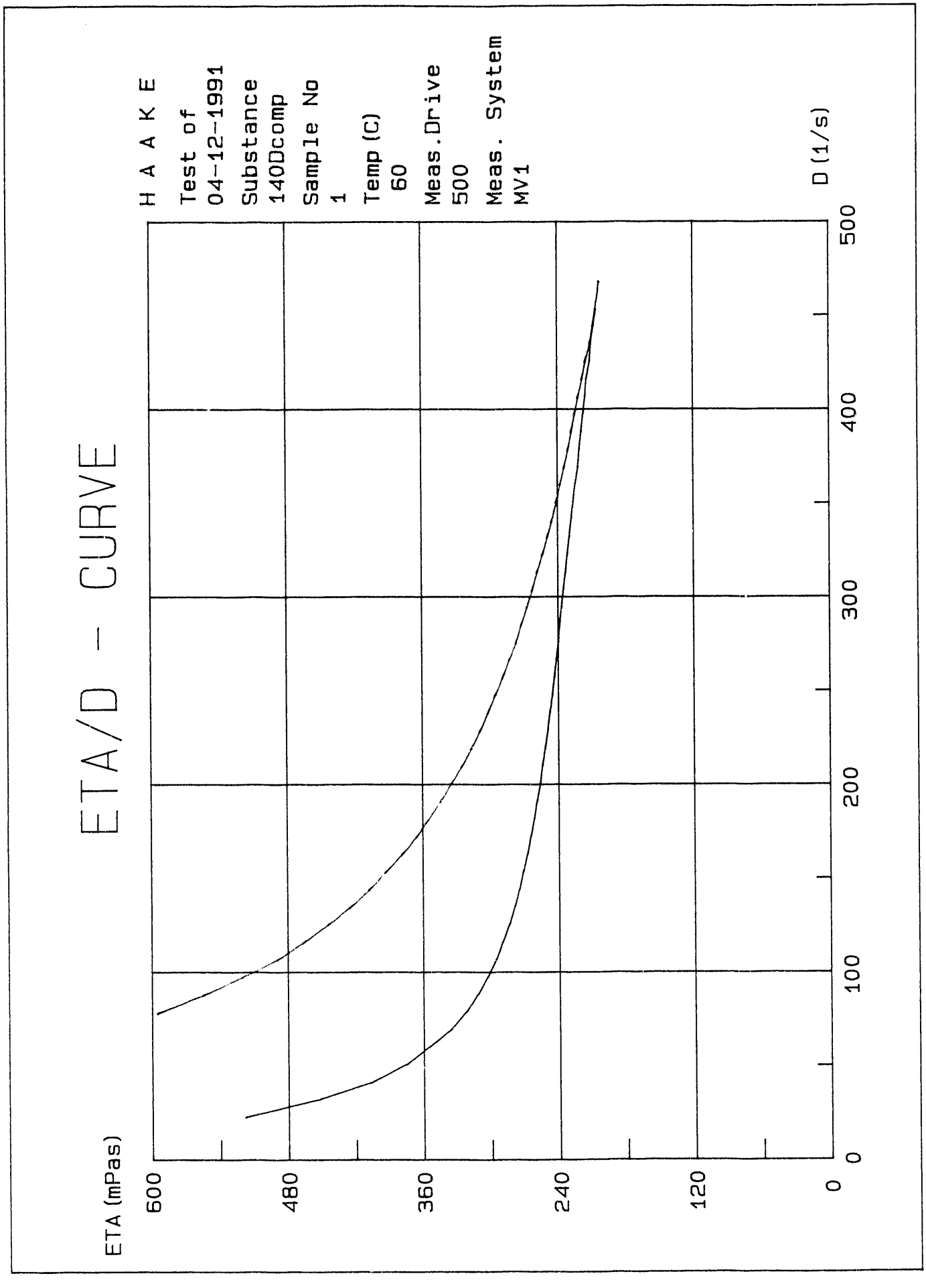
ETA/D - CURVE
H A A K E
Test of
04-12-1991
Substance
140Dcomp
Sample No
1
Temp (C)
60
Meas.Drive
500
Meas. System
MV1
ETA (mPas)
600
480
360
240
120
0
0
100
200
300
400
500
D (1/s)

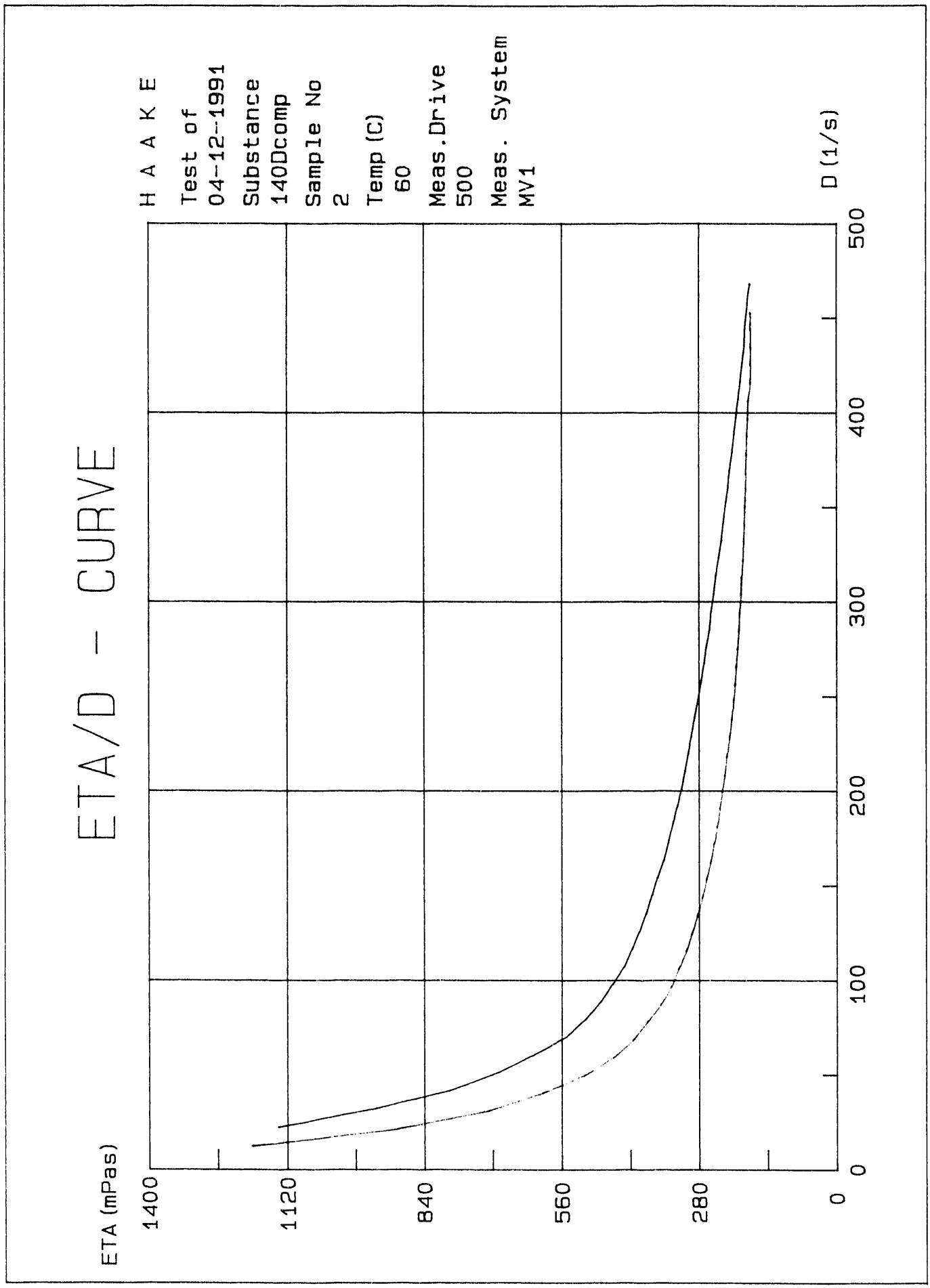
ETA/D - CURVE
H A A K E
Test of
04-12-1991
Substance
140Dcomp
Sample No
2
Temp (C)
60
Meas.Drive
500
Meas. System
MV1
ETA (mPas)
1400
1120
840
560
280
0
D (1/s)
0
100
200
300
400
500

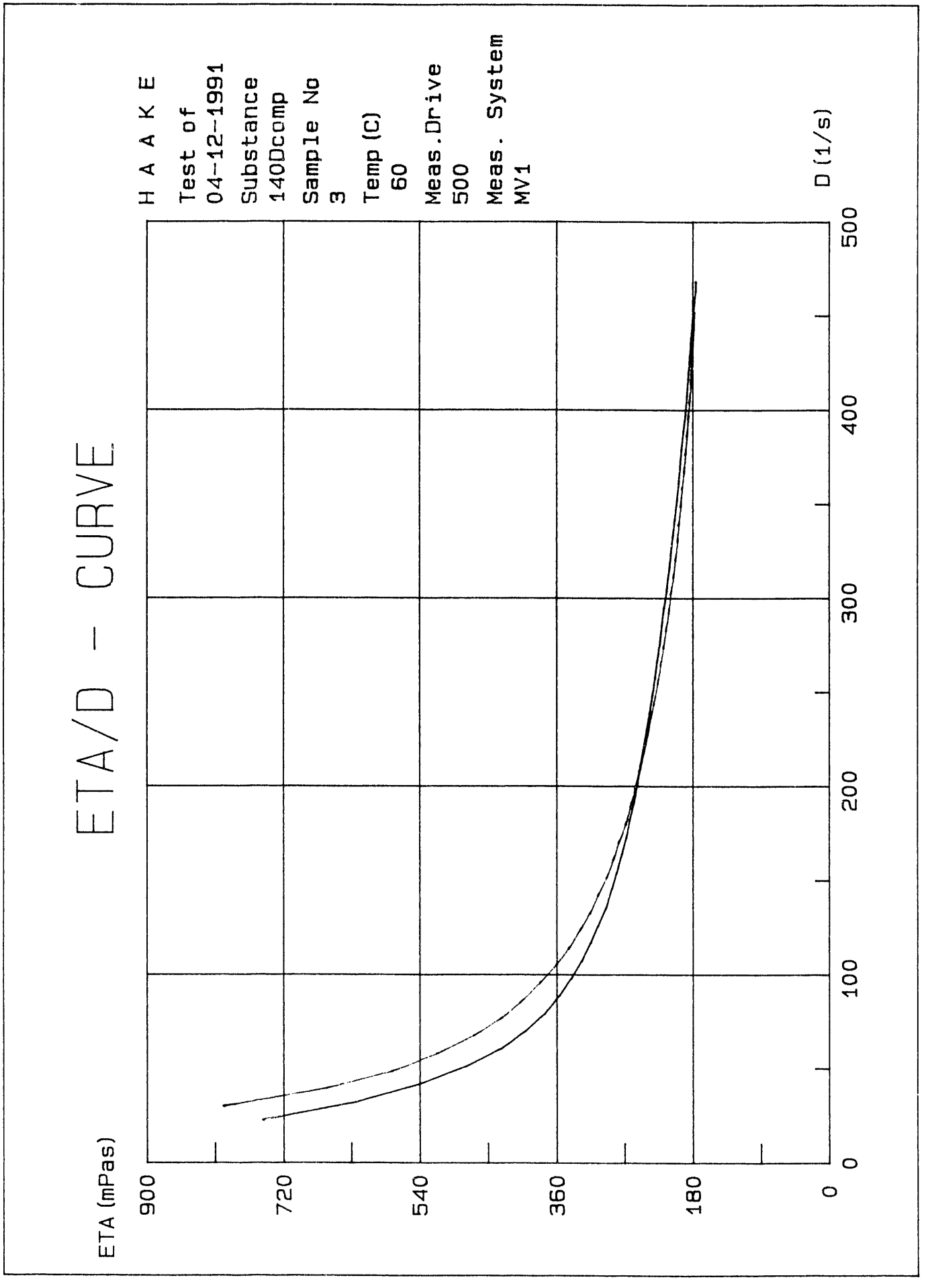
ETA/D - CURVE
H A A K E
Test of
04-12-1991
Substance
140Dcomp
Sample No
3
Temp (C)
60
Meas.Drive
500
Meas. System
MV1
ETA (mPas)
900
720
540
360
180
0
0
100
200
300
400
500
D (1/s)

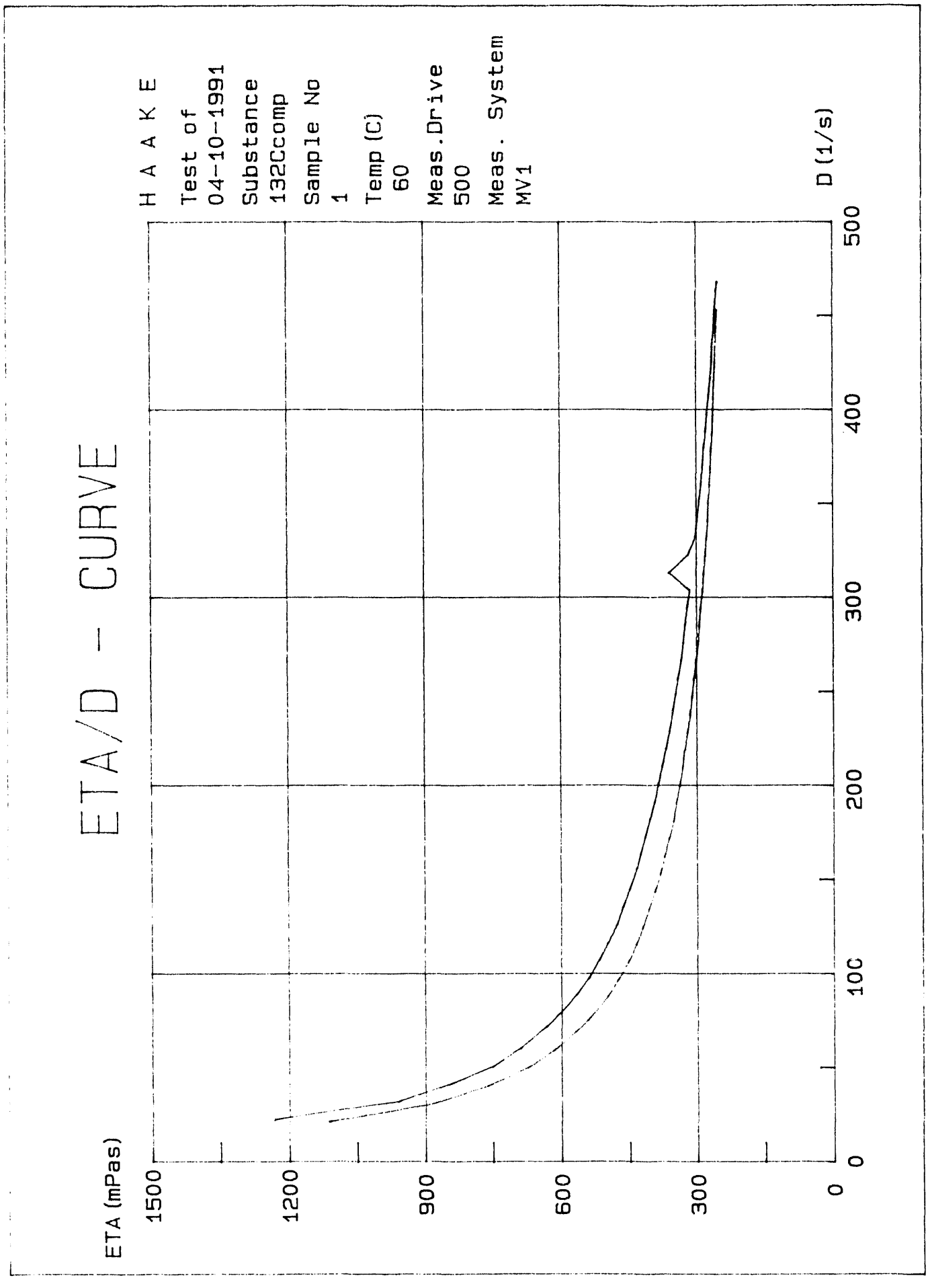
ETA/D - CURVE
H A A K E
Test of
04-10-1991
Substance
132Ccomp
Sample No
1
Temp (C)
60
Meas.Drive
500
Meas. System
MV1
ETA (mPas)
1500
1200
900
600
300
0
0
100
200
300
400
500
D (1/s)

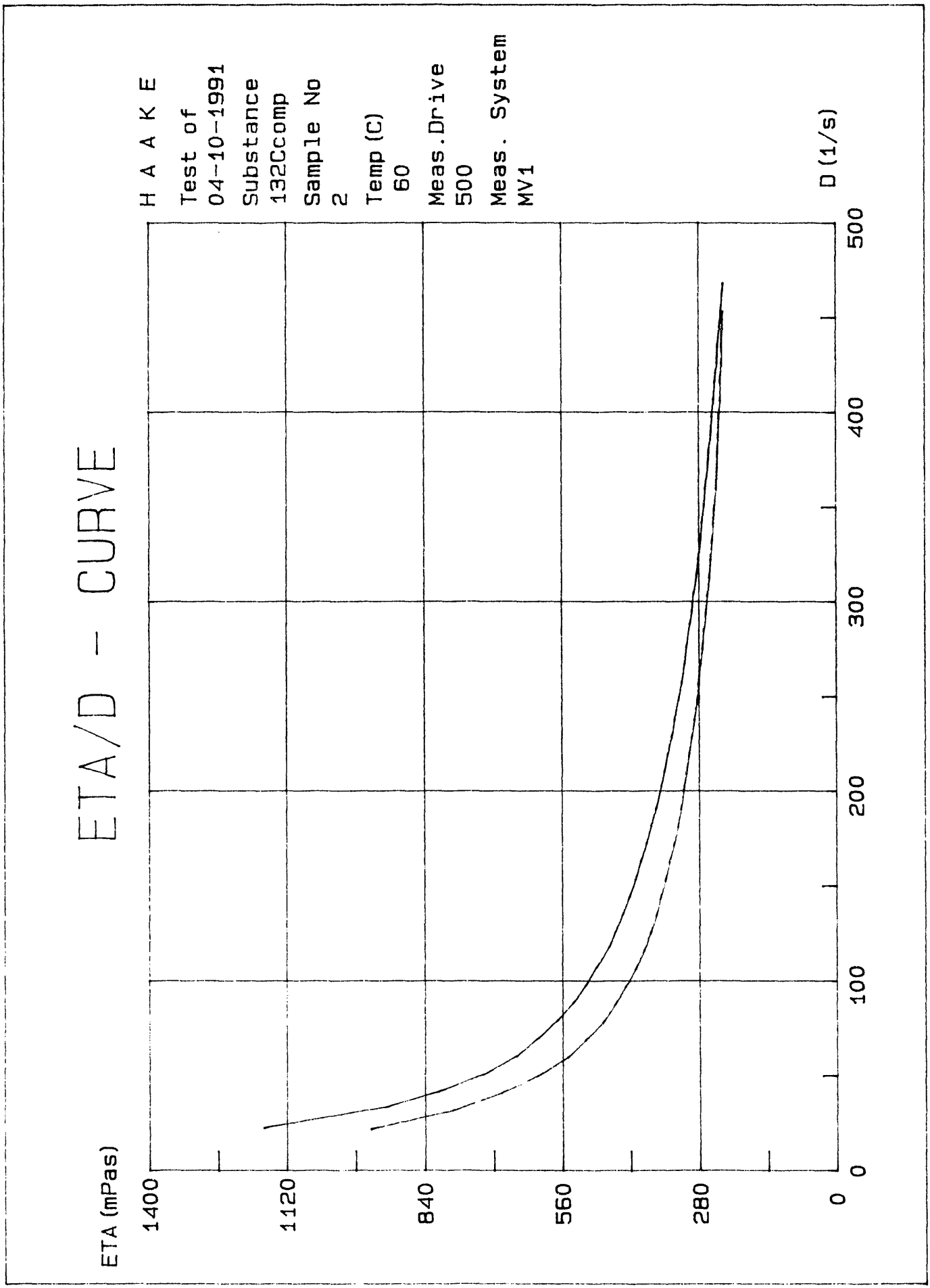
ETA/D - CURVE
H A A K E
Test of
04-10-1991
Substance
132Ccomp
Sample No
2
Temp (C)
60
Meas.Drive
500
Meas. System
MV1
ETA (mPas)
1400
1120
840
560
280
0
D (1/s)
0
100
200
300
400
500

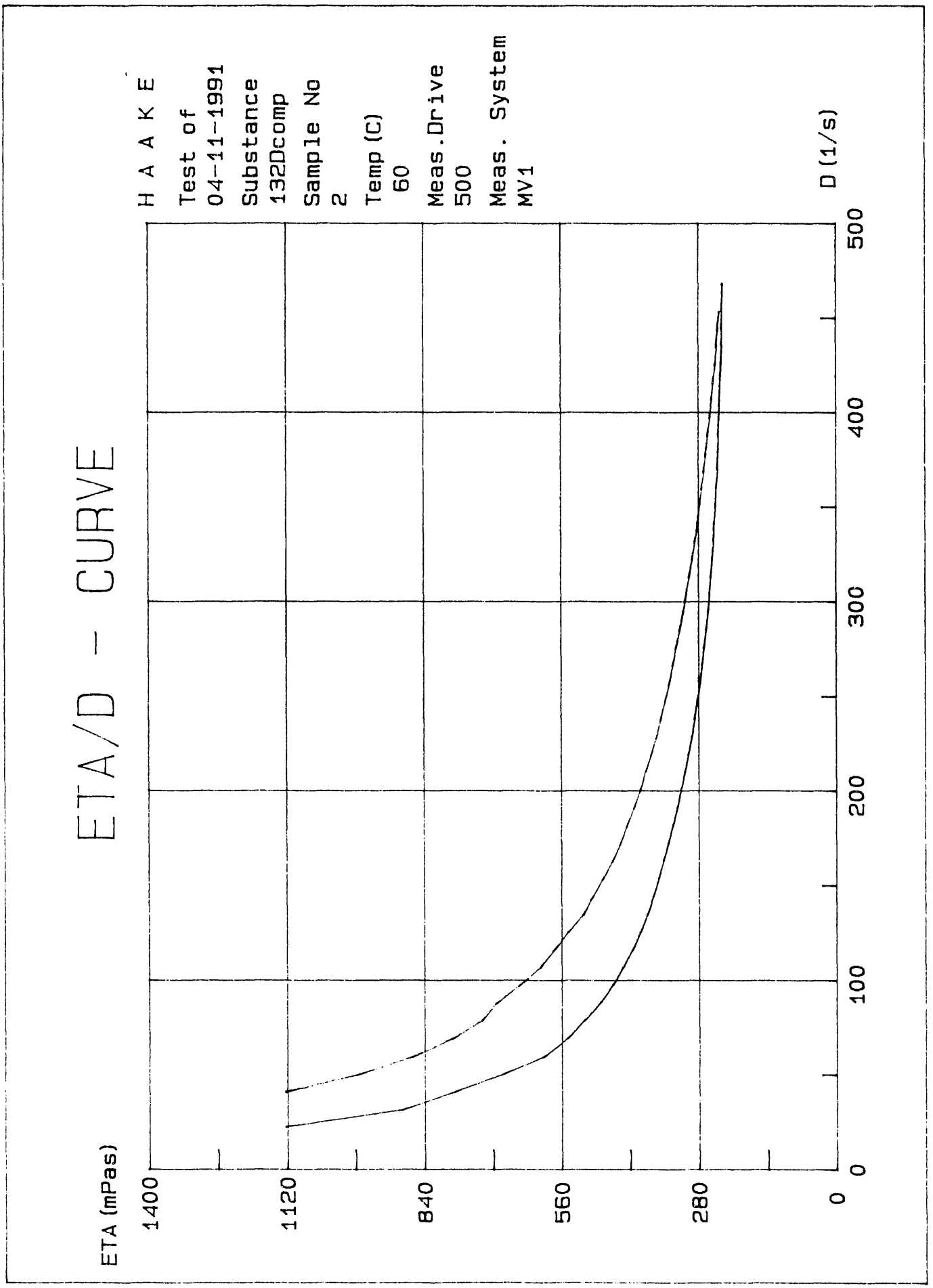
ETA/D - CURVE
H A A K E
Test of
04-11-1991
Substance
132Dcomp
Sample No
2
Temp (C)
60
Meas.Drive
500
Meas. System
MV1
ETA (mPas)
1400
1120
840
560
280
0
D (1/s)
0
100
200
300
400
500

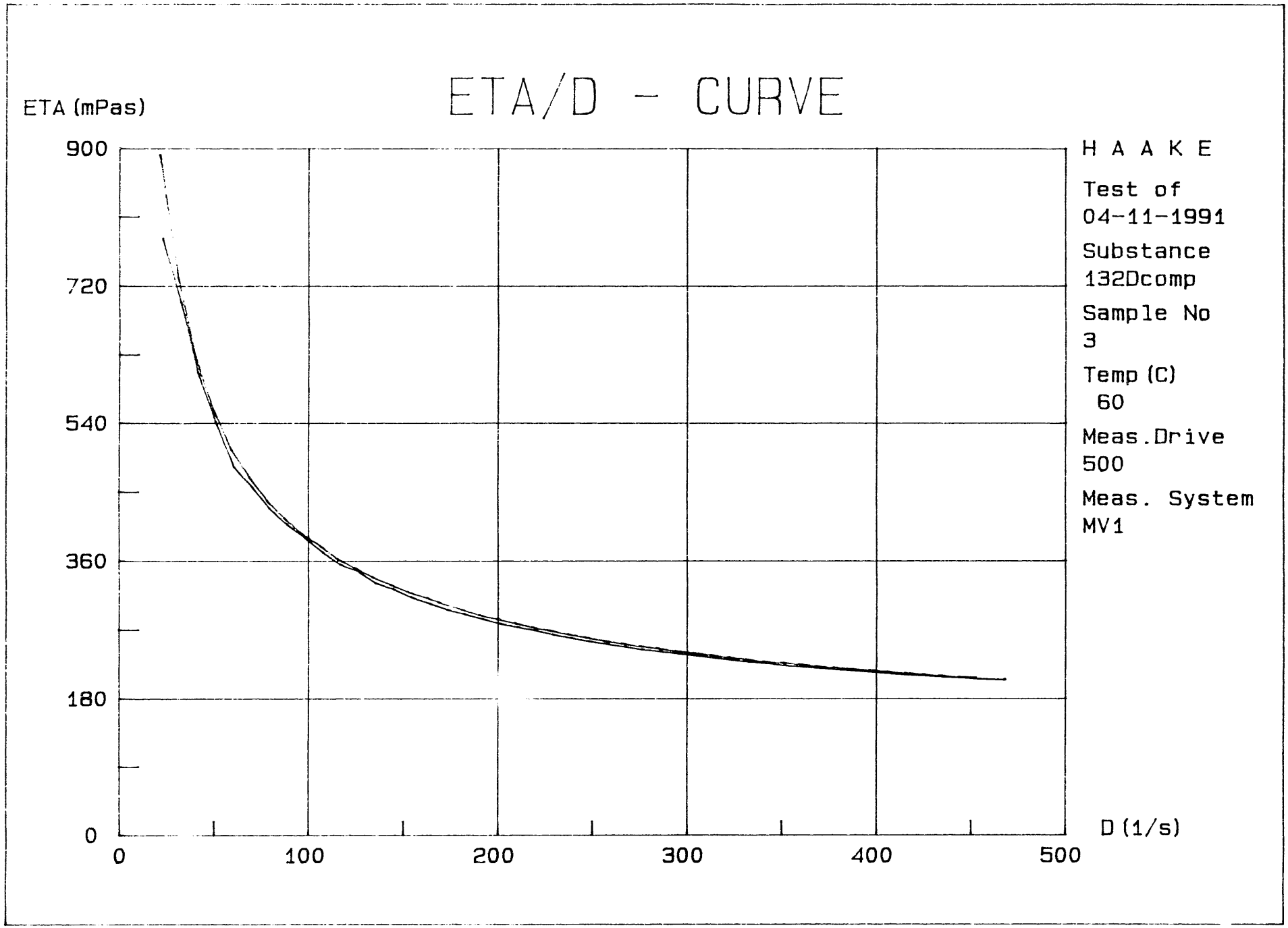
ETA/D - CURVE
ETA (mPas)
900
720
540
360
180
0
0
100
200
300
400
500
D (1/s)
H A A K E
Test of
04-11-1991
Substance
132Dcomp
Sample No
3
Temp (C)
60
Meas.Drive
500
Meas. System
MV1

APPENDIX E

RAW DATA FOR X-RAY DIFFRACTION ANALYSES

FN: 1232SWS.NI ID: 1232 SYNTHETIC WASTE STUDIES SCINTAG/USA
DATE: 3/14/91 TIME: 9: 1 PT: 0.600 STEP: 0.020 WL: 1.54059

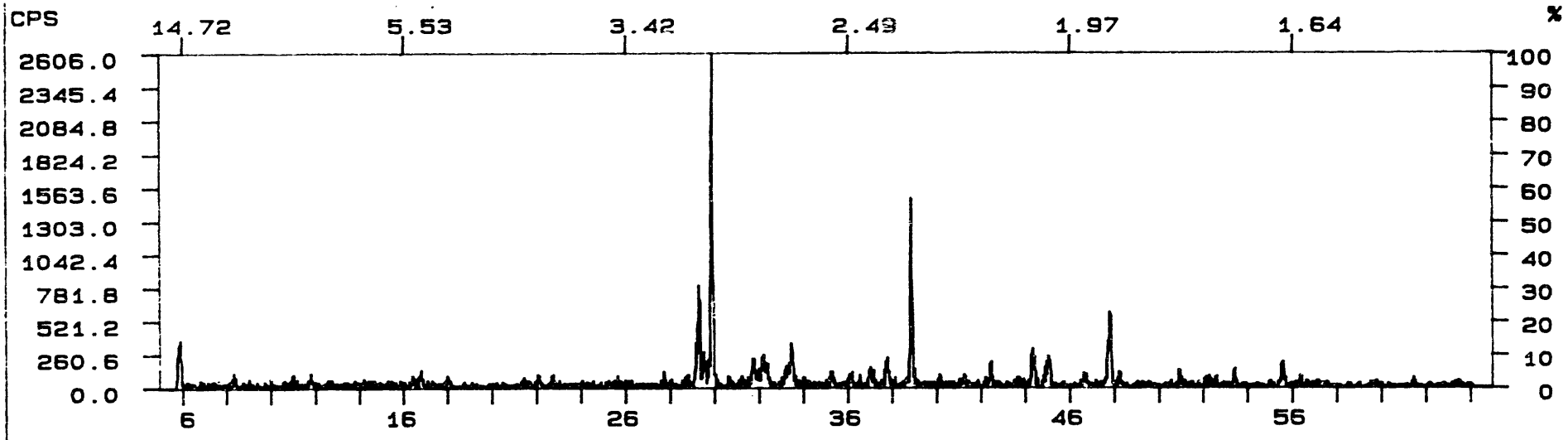

Low Aluminate / Low Organic SAMPLE 1232 CRUST

FN: 1248SWS.NI ID: 1248 SYNTHETIC WASTE STUDIES SCINTAG/USA
DATE: 3/14/91 TIME: 10:36 PT: 0.600 STEP: 0.020 WL: 1.54059

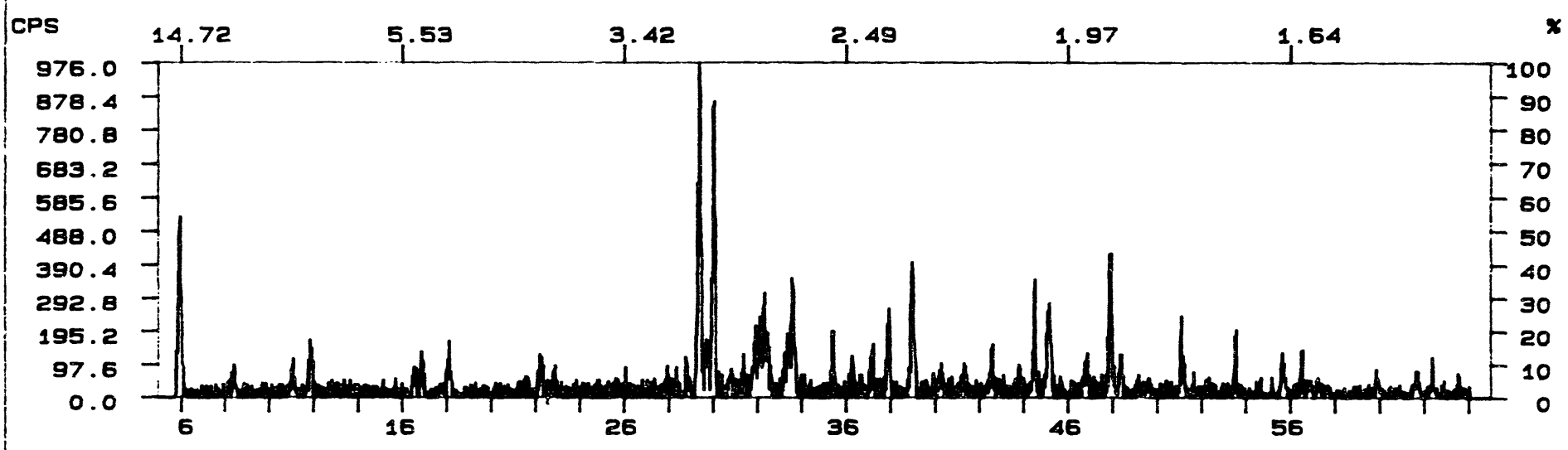

Low Aluminate / Low Organic SAMPLE 1248 CRUST

FN: 1242SWS.NI ID: 1242 SYNTHETIC WASTE STUDIES SCINTAG/USA
DATE: 3/14/91 TIME: 9:50 PT: 0.600 STEP: 0.020 WL: 1.54059

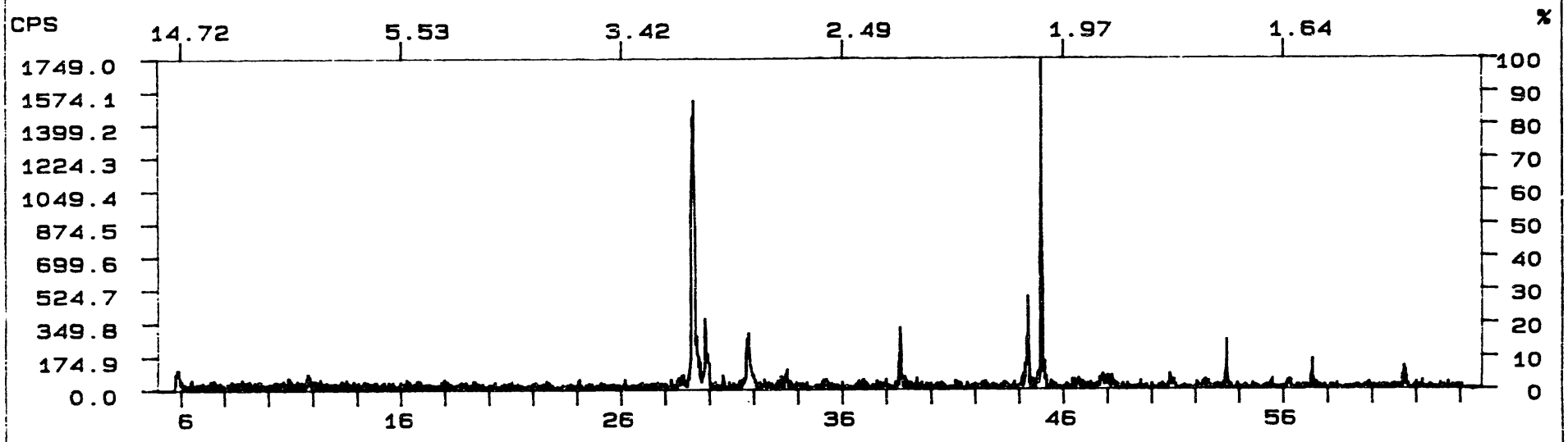

Low Aluminate / Low Organic SAMPLE 1242 IMMERSED

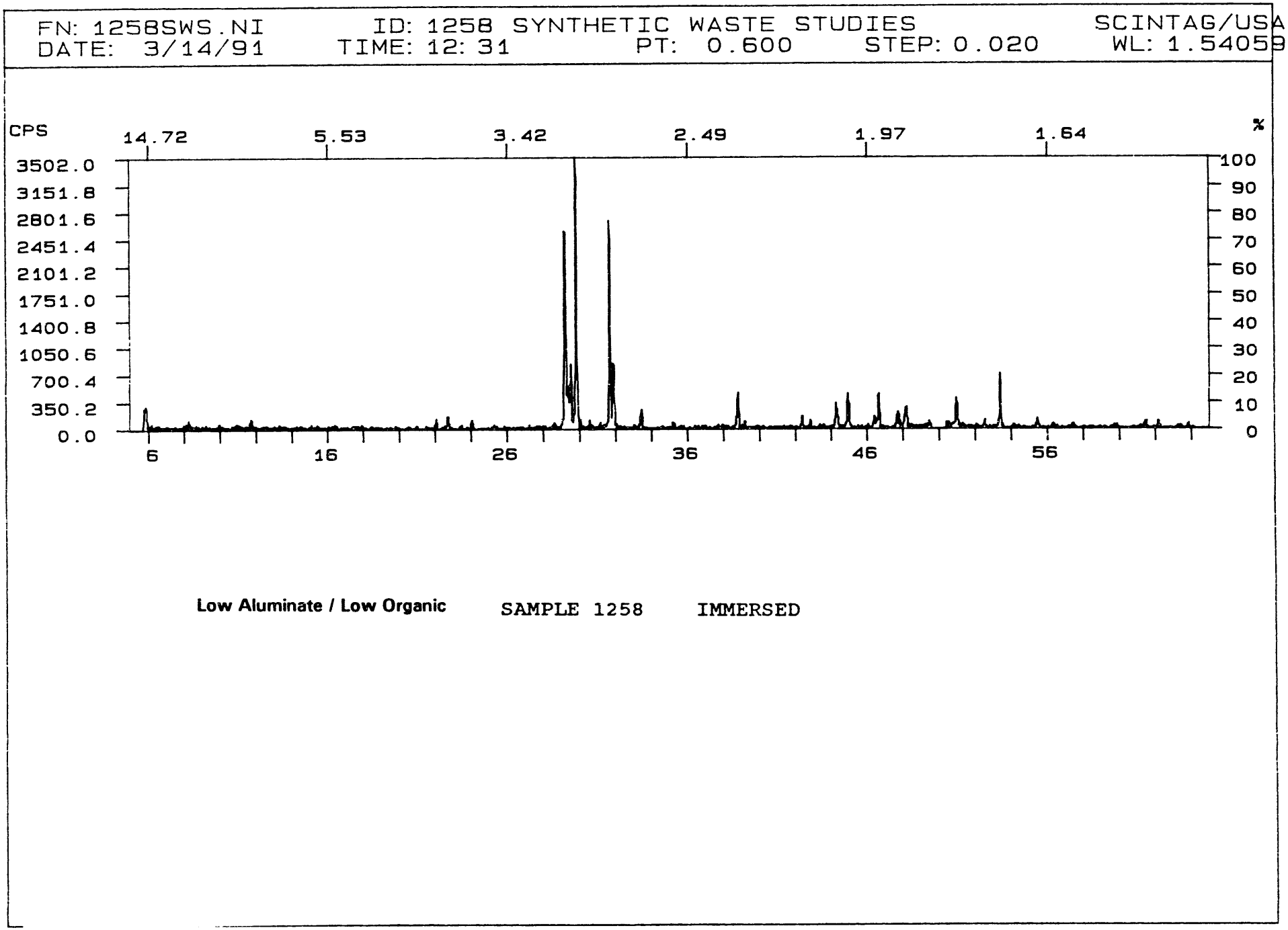
FN: 1258SWS.NI
ID: 1258 SYNTHETIC WASTE STUDIES
SCINTAG/USA
DATE: 3/14/91
TIME: 12:31
PT: 0.600
STEP: 0.020
WL: 1.54059
CPS
%
14.72
5.53
3.42
2.49
1.97
1.64
3502.0
3151.8
2801.6
2451.4
2101.2
1751.0
1400.8
1050.6
700.4
350.2
0.0
100
90
80
70
60
50
40
30
20
10
0
6
16
26
36
46
56
Low Aluminate / Low Organic
SAMPLE 1258
IMMERSED

FN: 1176SWS.NI ID: 1176 SYNTHETIC WASTE STUDIES SCINTAG/USA
DATE: 3/12/91 TIME: 12:54 PT: 0.600 STEP: 0.020 WL: 1.54059

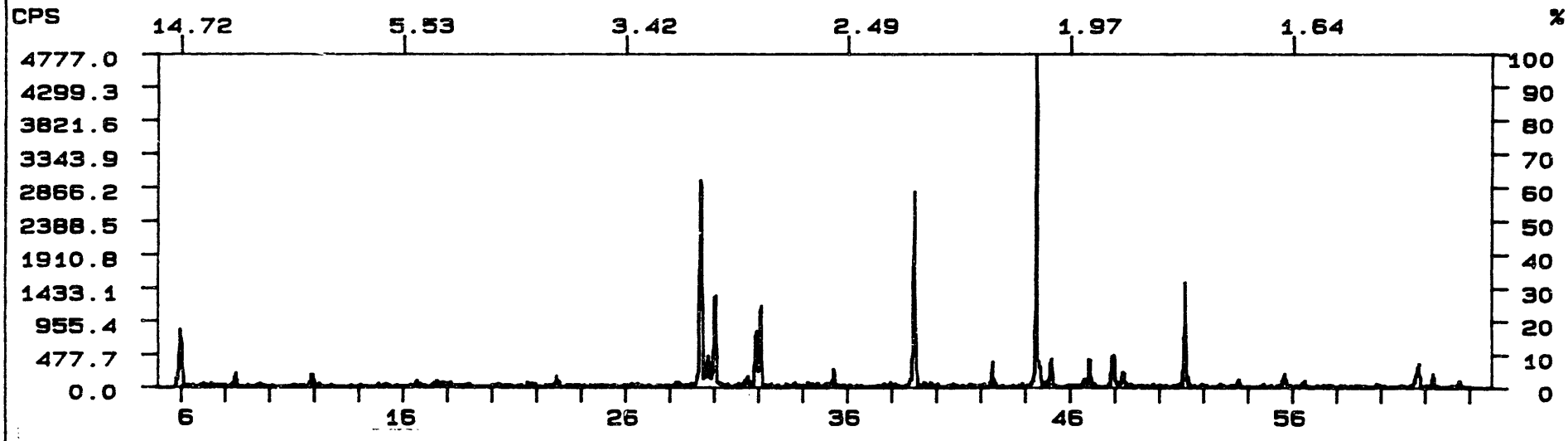

Low Aluminate / High Organic SAMPLE 1176 CRUST

FN: 1188SWS.NI ID: 1188 SYNTHETIC WASTE STUDIES CRUST SCINTAG/USA
DATE: 3/12/91 TIME: 14: 11 PT: 0.600 STEP: 0.020 WL: 1.54059

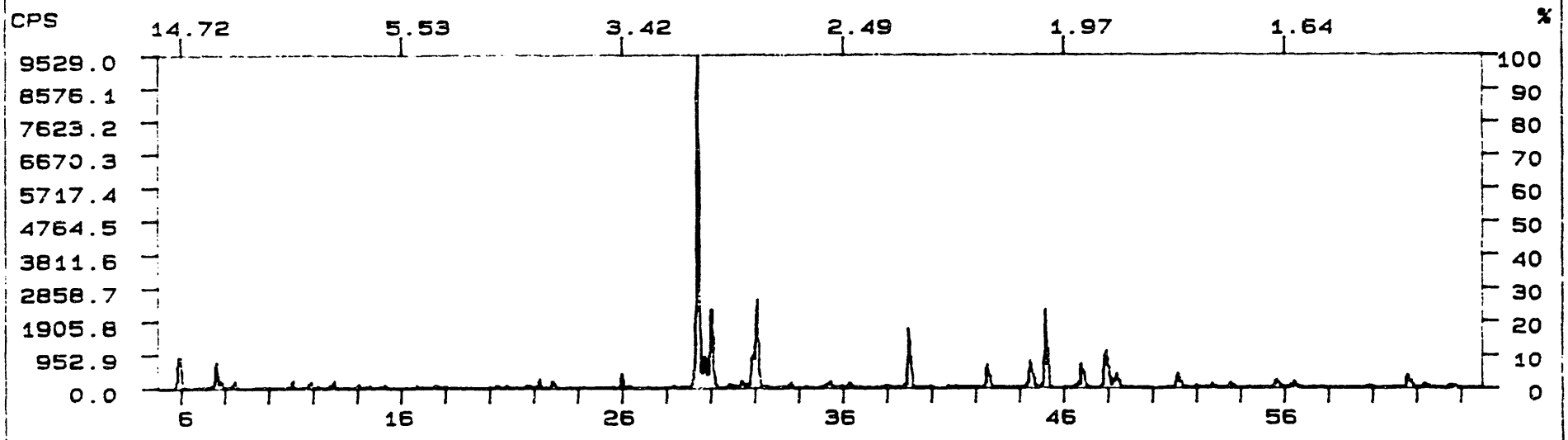

Low Aluminate / High Organic SAMPLE 1188 CRUST

FN: 1182SWS.NI ID: 1182 SYNTHETICV WASTE STUDIES BOTTOM SCINTAG/USA
DATE: 3/12/91 TIME: 13: 35 PT: 0.600 STEP: 0.020 WL: 1.54059

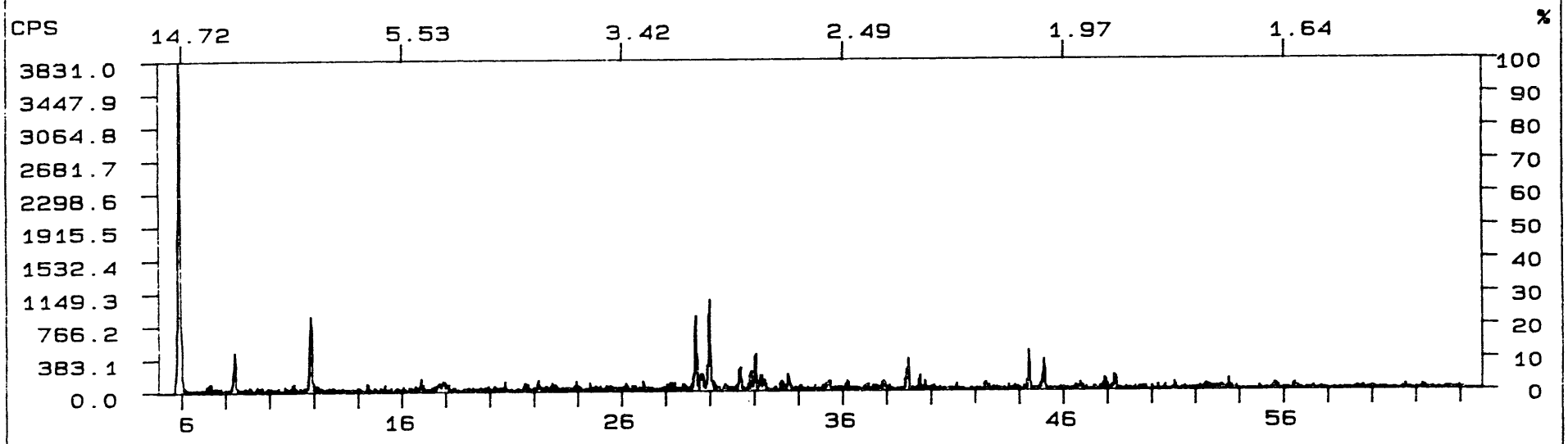

Low Aluminate / High Organic SAMPLE 1182 IMMERSED

FN: 1194SWS.NI ID: 1194 SYNTHETIC WASTE STUDIES SCINTAG/USA
DATE: 3/13/91 TIME: 9:23 PT: 0.600 STEP: 0.020 WL: 1.54059

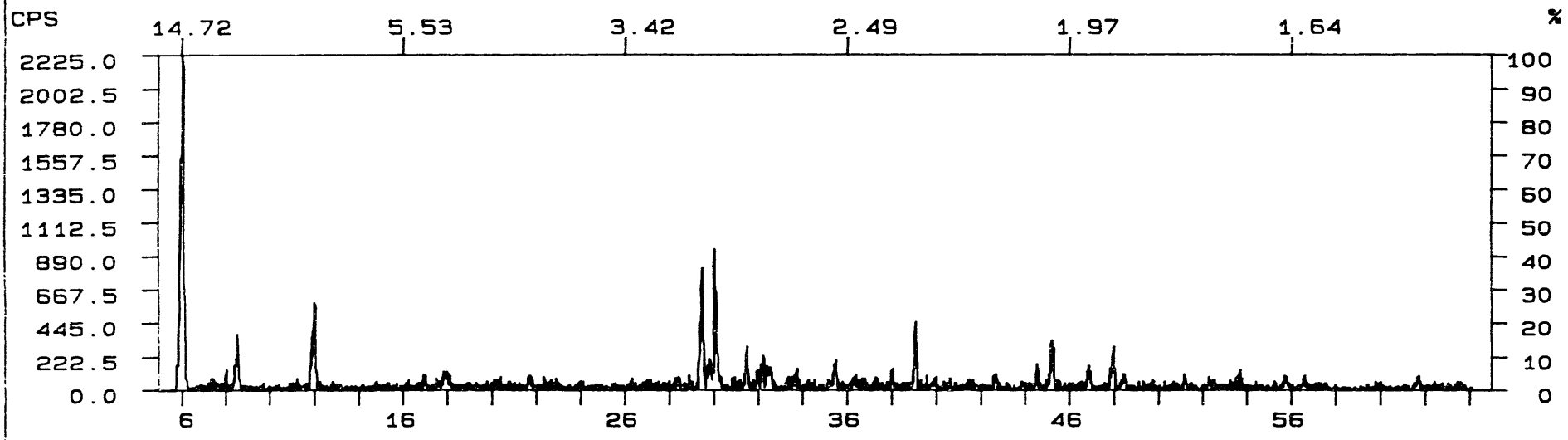

Low Aluminate / High Organic SAMPLE 1194 IMMERSED

FN: 1120SWS.NI ID: 1120 SYNTHETIC WASTE STUDIES SCINTAG/USA
DATE: 2/21/91 TIME: 10:25 PT: 0.600 STEP: 0.020 WL: 1.54059

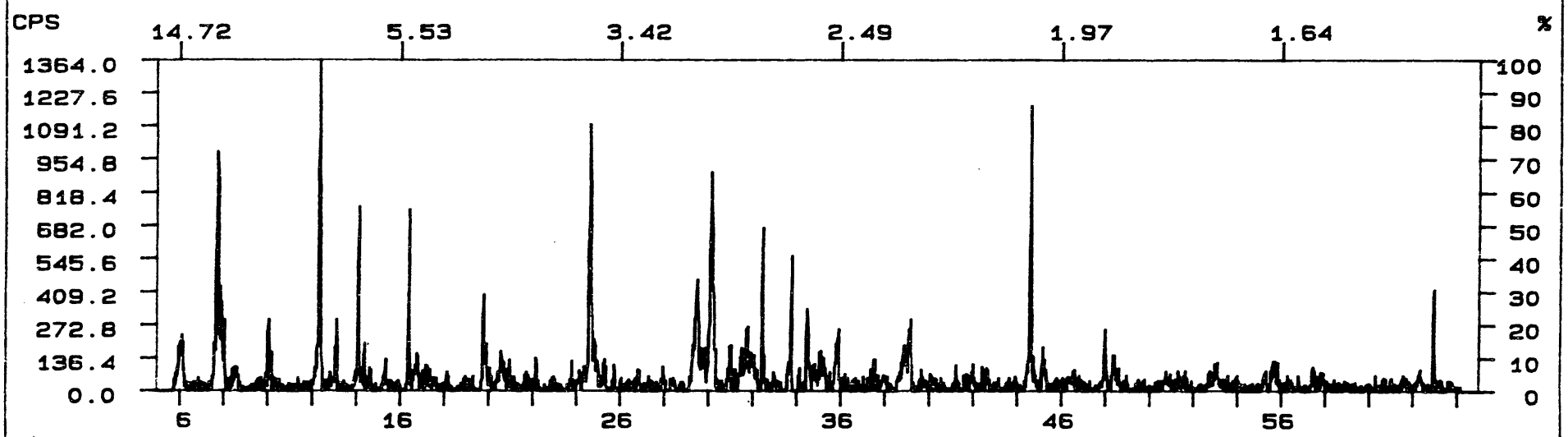

Reference SAMPLE 1120 CRUST

FN: 1136SWS.NI ID: 1136 SYNTHETIC WASTE STUDIES SCINTAG/USA
DATE: 3/11/91 TIME: 11:53 PT: 0.600 STEP: 0.020 WL: 1.54059

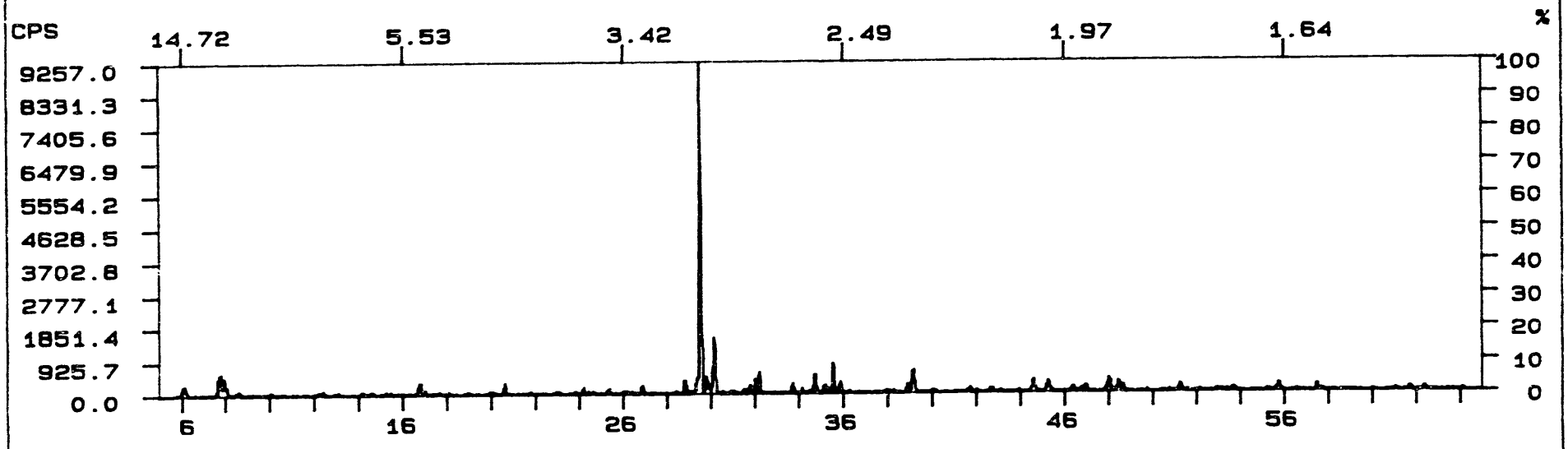

Reference SAMPLE 1136 CRUST

FN: 1130SWS.NI ID: 1130 SYNTHETIC WASTE STTUDIES SCINTAG/USA
DATE: 2/21/91 TIME: 11: 19 PT: 0.600 STEP: 0.020 WL: 1.54059

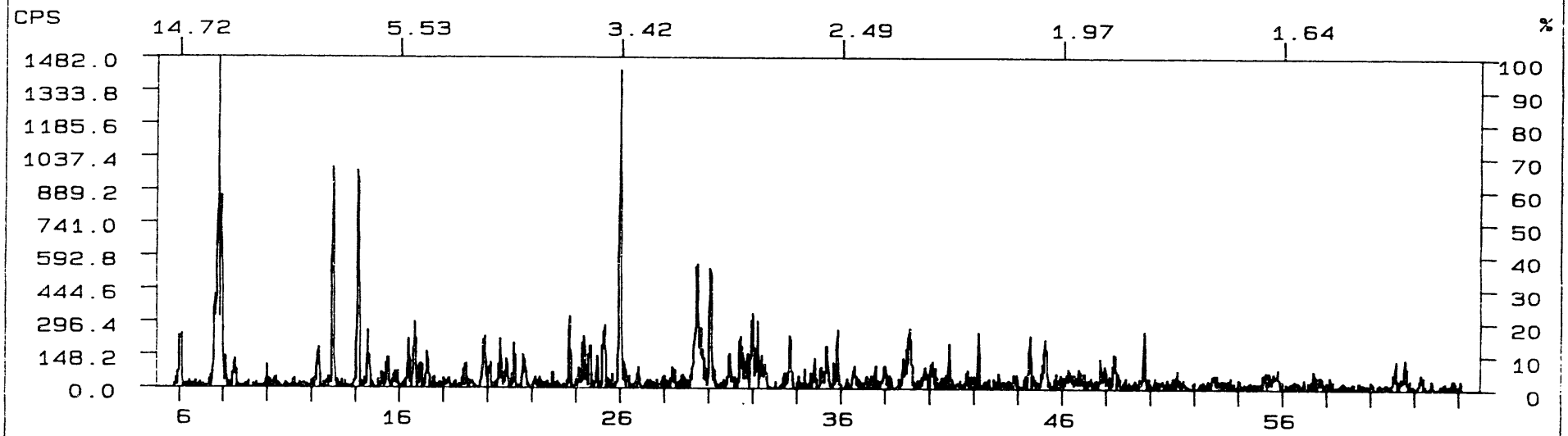

Reference SAMPLE 1130 IMMERSED

FN: 1146SWS.NI ID: 1146 SYNTHETIC WASTE STUDIES SCINTAG/USA
DATE: 3/11/91 TIME: 12:34 PT: 0.600 STEP: 0.020 WL: 1.54059

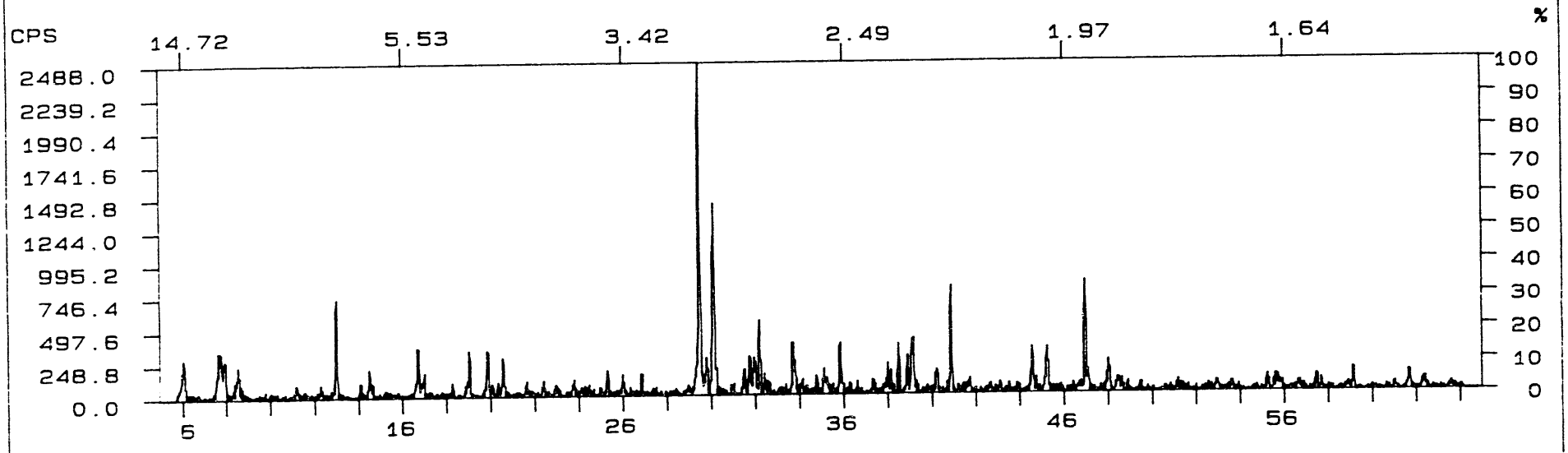

Reference SAMPLE 1146 IMMERSED

FN: 1200SWS.NI ID: 1200 SYNTHETIC WASTE STUDIES SCINTAG/USA
DATE: 3/13/91 TIME: 10: 6 PT: 0.600 STEP: 0.020 WL: 1.54059

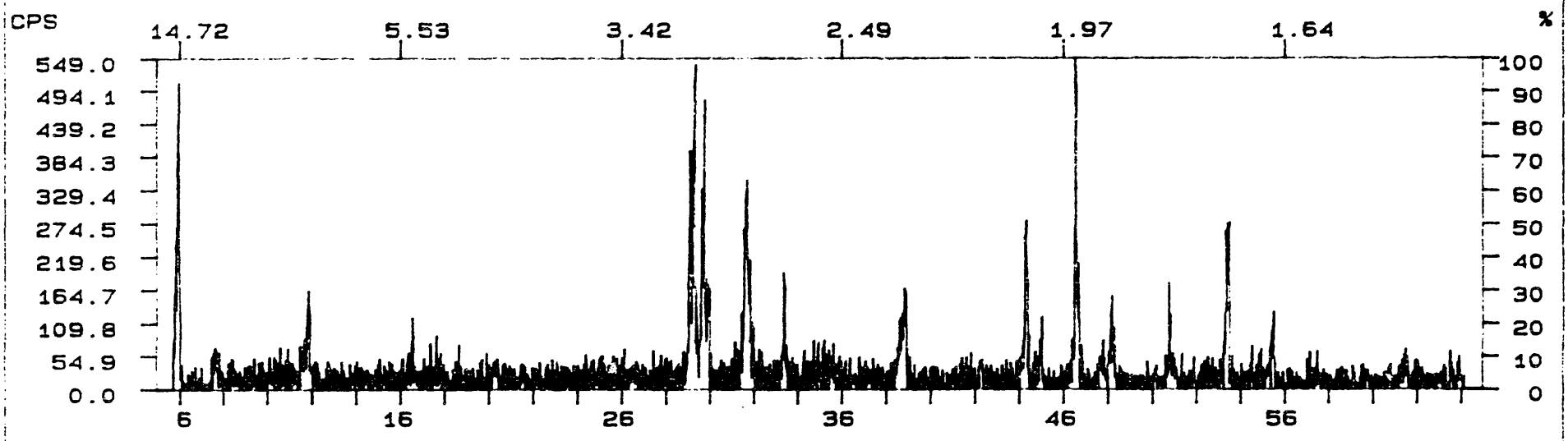

High Aluminate / Low Organic SAMPLE 1200 CRUST

FN: 1216SWS.NI ID: 1216 SYNTHETIC WASTE STUDIES SCINTAG/USA
DATE: 3/13/91 TIME: 11:29 PT: 0.600 STEP: 0.020 WL: 1.54059

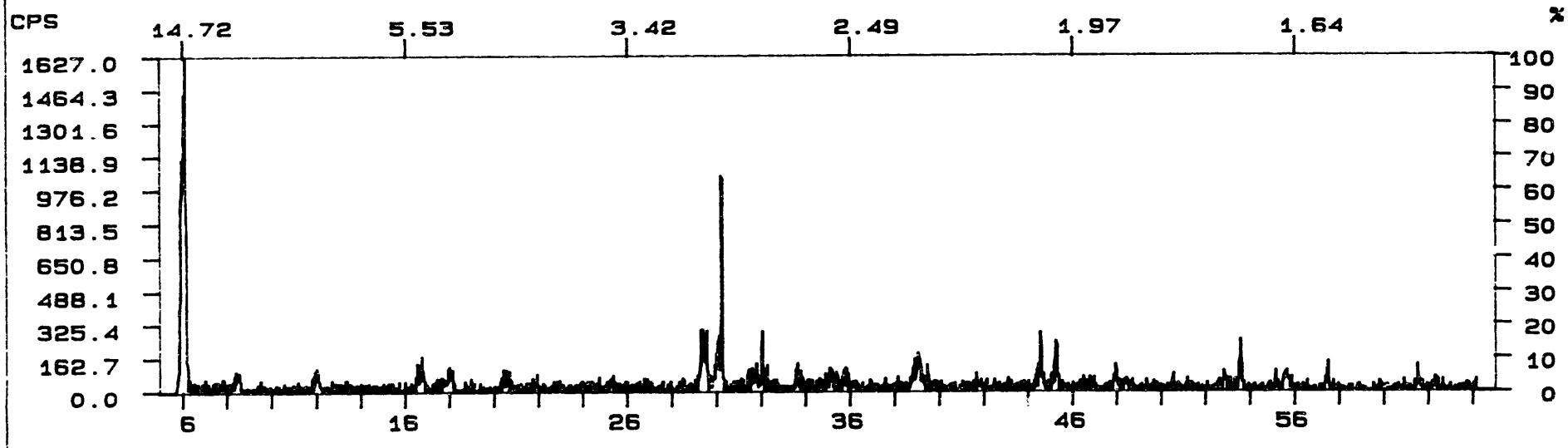

High Aluminate / Low Organic SAMPLE 1216 CRUST

FN: 1210SWS.NI ID: 1210 SYNTHETIC WASTE STUDIES SCINTAG/USA
DATE: 3/13/91 TIME: 10:42 PT: 0.600 STEP: 0.020 WL: 1.54059

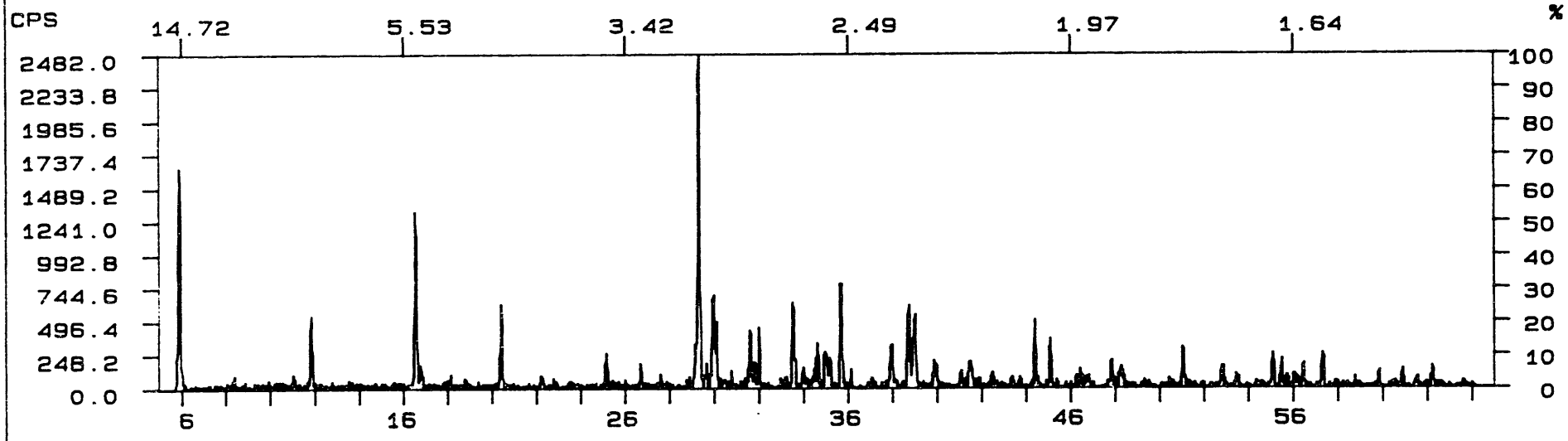

High Aluminate / Low Organic SAMPLE 1210 IMMERSED

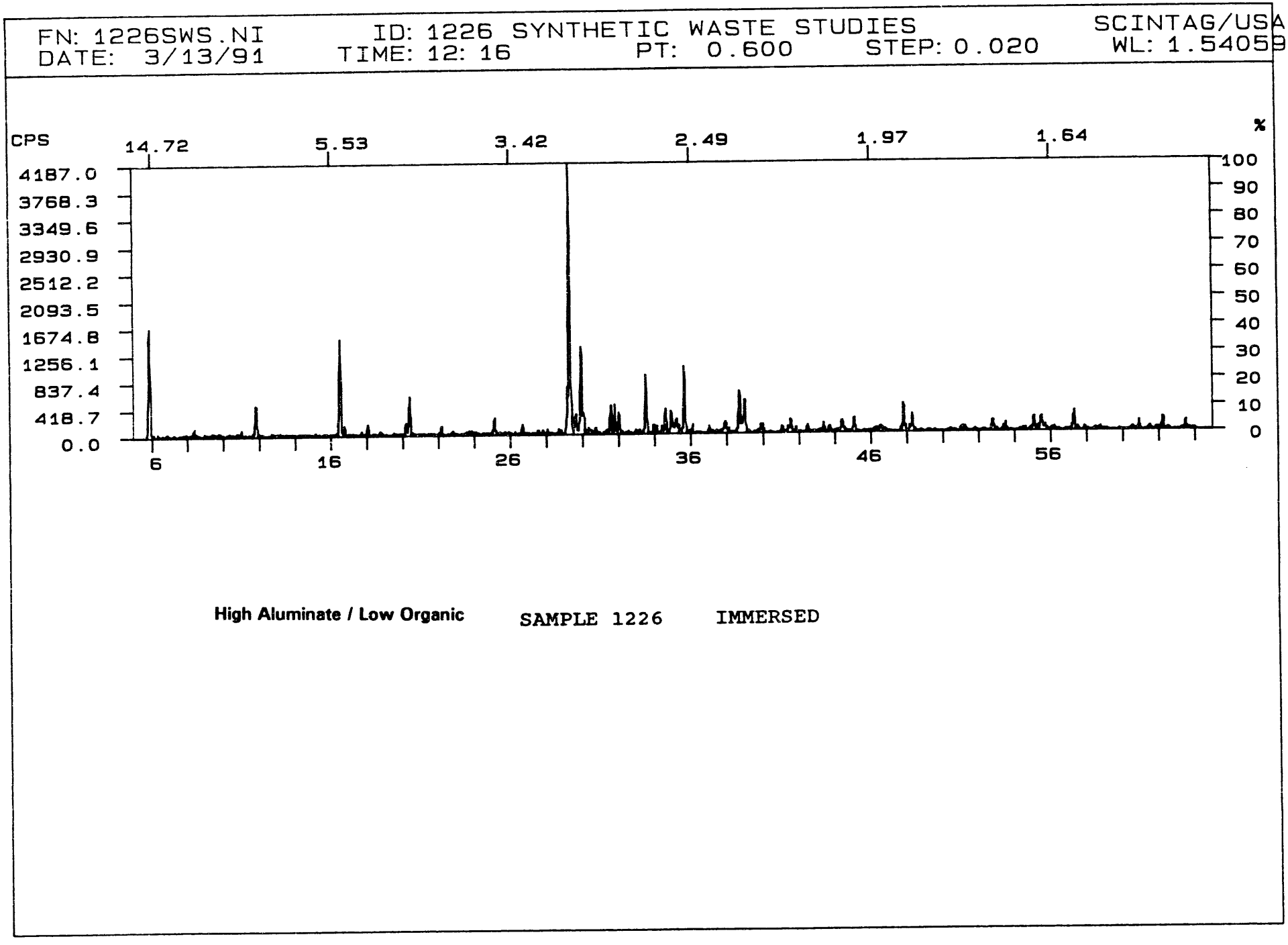
FN: 1226SWS.NI
DATE: 3/13/91
ID: 1226 SYNTHETIC WASTE STUDIES
TIME: 12: 16
PT: 0.600
STEP: 0.020
SCINTAG/USA
WL: 1.54059
CPS
%
14.72
5.53
3.42
2.49
1.97
1.64
4187.0
3768.3
3349.6
2930.9
2512.2
2093.5
1674.8
1256.1
837.4
418.7
0.0
100
90
80
70
60
50
40
30
20
10
0
6
16
26
36
46
56
High Aluminate / Low Organic
SAMPLE 1226
IMMERSED

FN: 1152SWS.NI ID: 1152 SIMULATED WASTE STUDIES SCINTAG/USA
DATE: 3/12/91 TIME: 9: 0 PT: 0.600 STEP: 0.020 WL: 1.54059

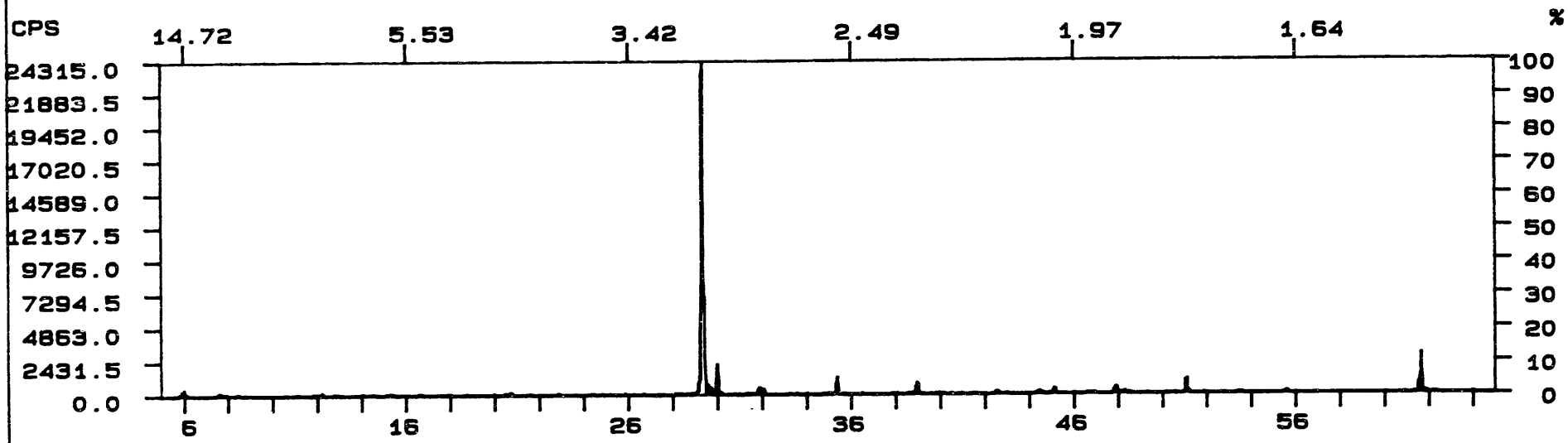

High Aluminate / High Organic SAMPLE 1152 CRUST

FN: 1164SWS.NI ID: 1164 SIMULATED WASTE STUDIES SCINTAG/USA
DATE: 3/12/91 TIME: 10:13 PT: 0.600 STEP: 0.020 WL: 1.54059

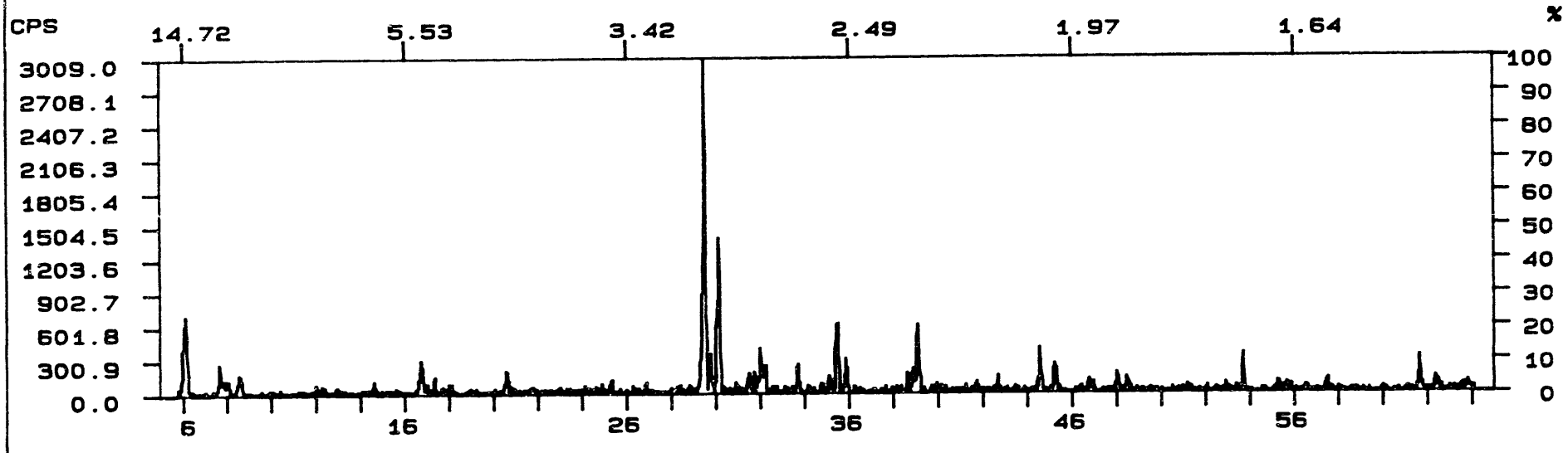

High Aluminate / High Organic SAMPLE 1164 CRUST

FN: 1158SWS.NI ID: 1158 SIMULATED WASTE STUDIES SCINTAG/USA
DATE: 3/12/91 TIME: 9:37 PT: 0.600 STEP: 0.020 WL: 1.54059

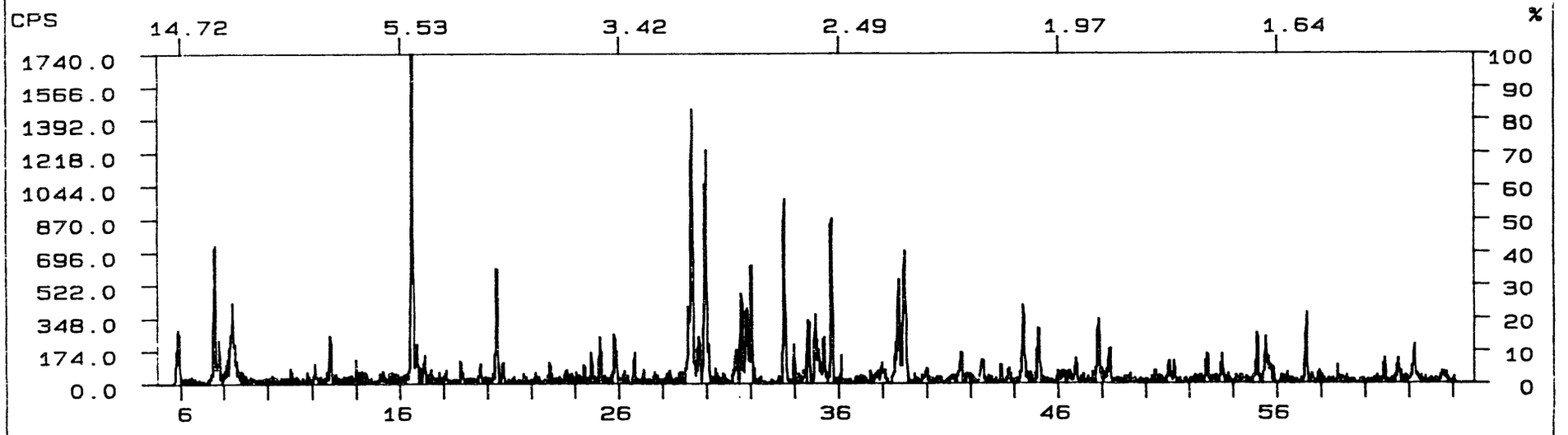

High Aluminate / High Organic SAMPLE 1158 IMMERSED

FN: 1170SWS.NI ID: 1170 SYNTHETIC WASTE STUDIES BOTTOM SCINTAG/USA
DATE: 3/12/91 TIME: 11:29 PT: 0.600 STEP: 0.020 WL: 1.5405B

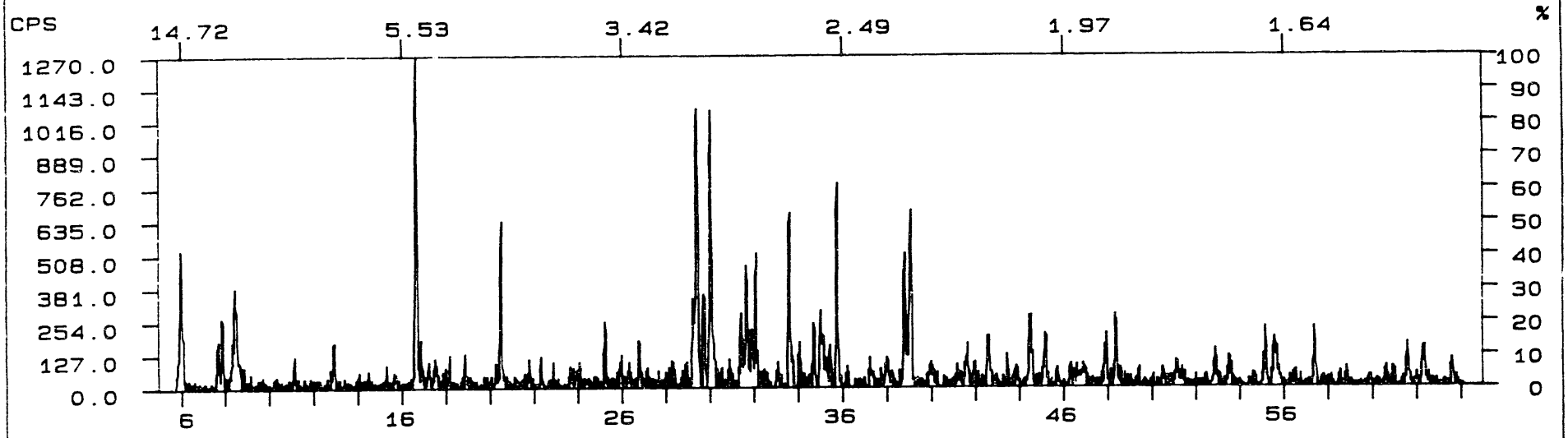

High Aluminate / High Organic

SAMPLE 1170 IMMERSED

FN: 1299SWS.NI ID: 1299 SYNTHETIC WASTE STUDIES SCINTAG/USA
DATE: 3/20/91 TIME: 8:58 PT: 0.600 STEP: 0.020 WL: 1.54059

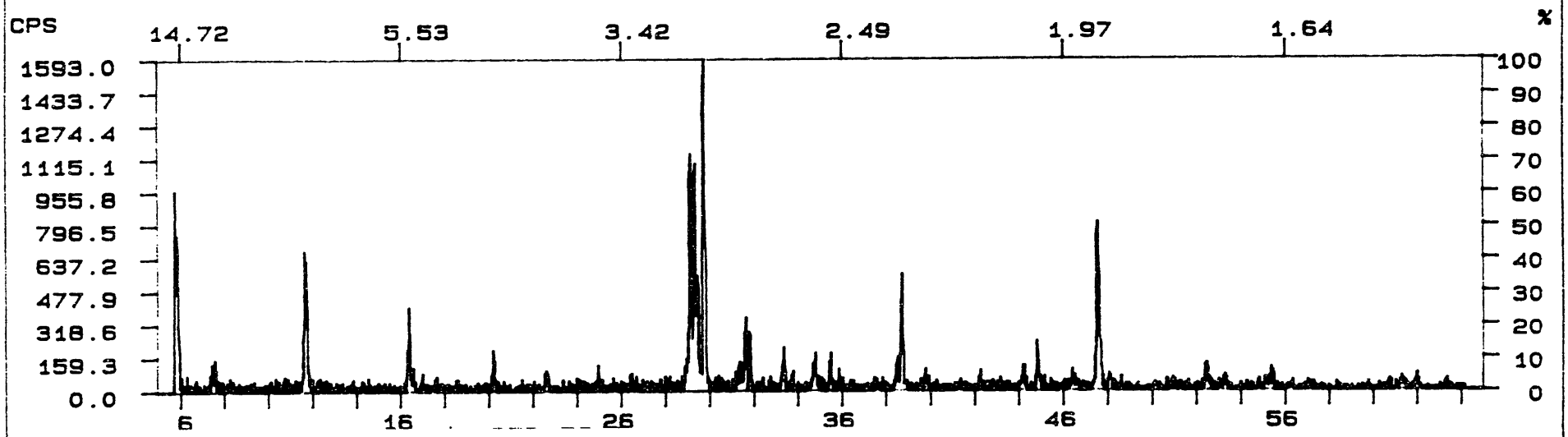

Reference SAMPLE 1299 CRUST

FN: 1326SWS.NI ID: 1326 SYNTHETIC WASTE STUDIES SCINTAG/USA
DATE: 3/20/91 TIME: 11:31 PT: 0.600 STEP: 0.020 WL: 1.54059

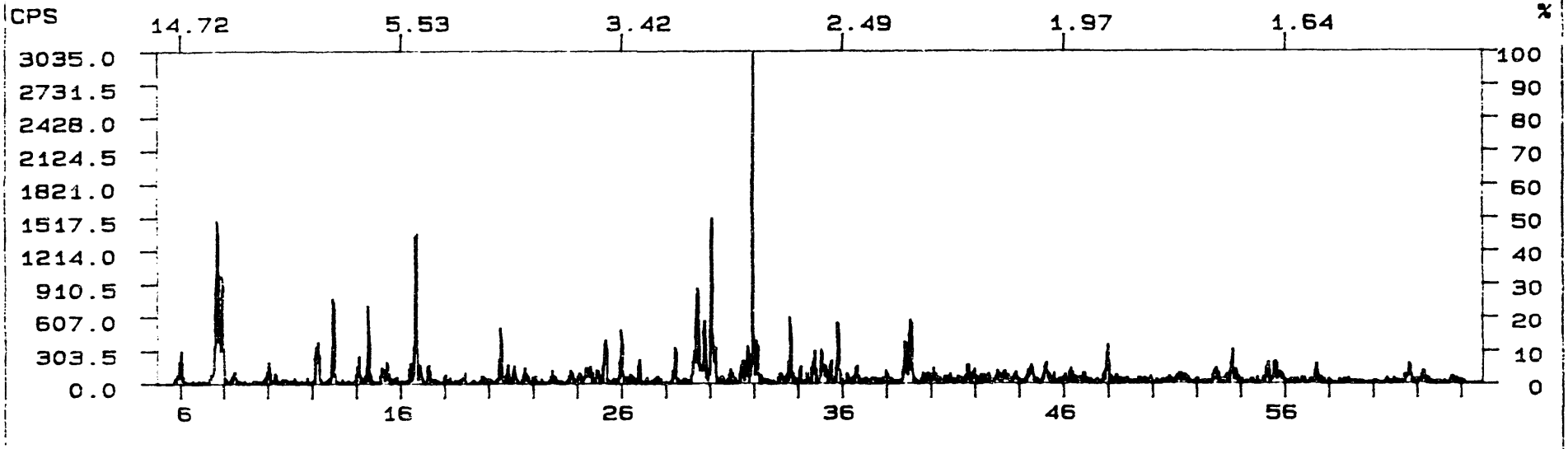

Reference SAMPLE 1326 CRUST

FN: 1308SWS.NI ID: 1308 SYNTHETIC WASTE STUDIES SCINTAG/USA
DATE: 3/20/91 TIME: 9:33 PT: 0.600 STEP: 0.020 WL: 1.54059

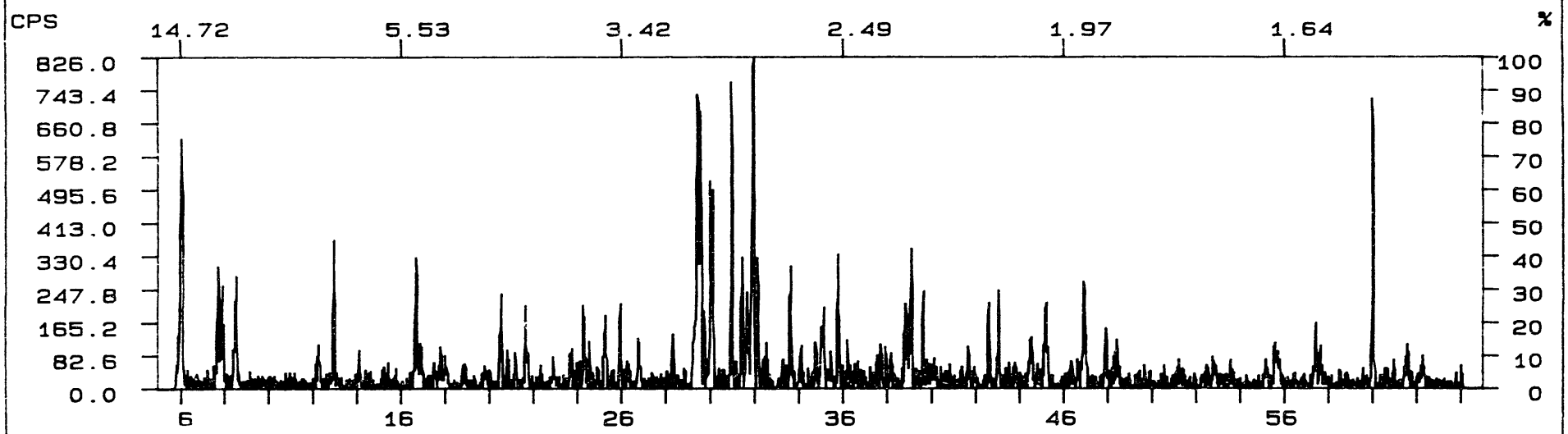

Reference SAMPLE 1308 IMMERSED

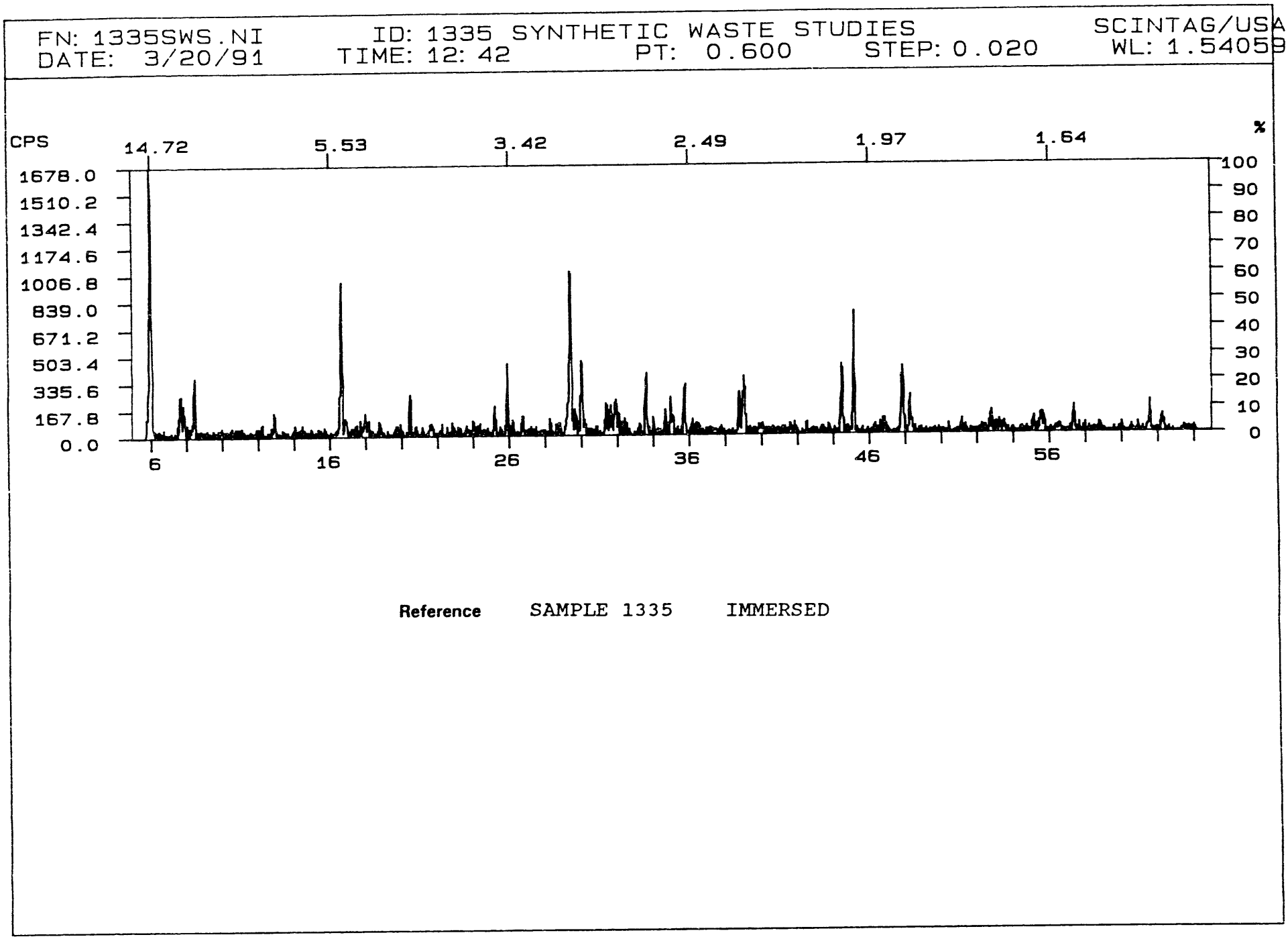
FN: 1335SWS.NI
DATE: 3/20/91
ID: 1335 SYNTHETIC WASTE STUDIES
TIME: 12:42
PT: 0.600
STEP: 0.020
SCINTAG/USA
WL: 1.54059
CPS
1678.0
1510.2
1342.4
1174.6
1006.8
839.0
671.2
503.4
335.6
167.8
0.0
14.72
5.53
3.42
2.49
1.97
1.64
%
100
90
80
70
60
50
40
30
20
10
0
6
16
26
36
46
56
Reference
SAMPLE 1335
IMMERSED

FN: 1314SWS.NI ID: 1314 SYNTHETIC WASTE STUDIES SCINTAG/USA
DATE: 3/20/91 TIME: 10: 8 PT: 0.600 STEP: 0.020 WL: 1.54059

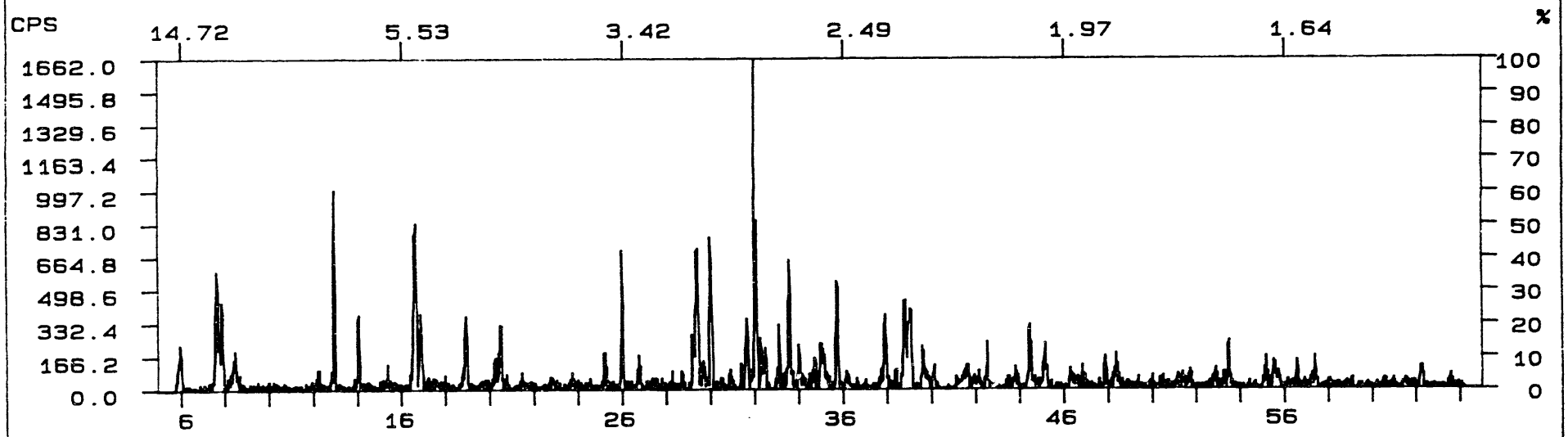

Reference SAMPLE 1314 IMMERSED

FN: 1341SWS.NI ID: 1341 SYNTHETIC WASTE STUDIES SCINTAG/USA
DATE: 3/20/91 TIME: 12: 6 PT: 0.600 STEP: 0.020 WL: 1.54059

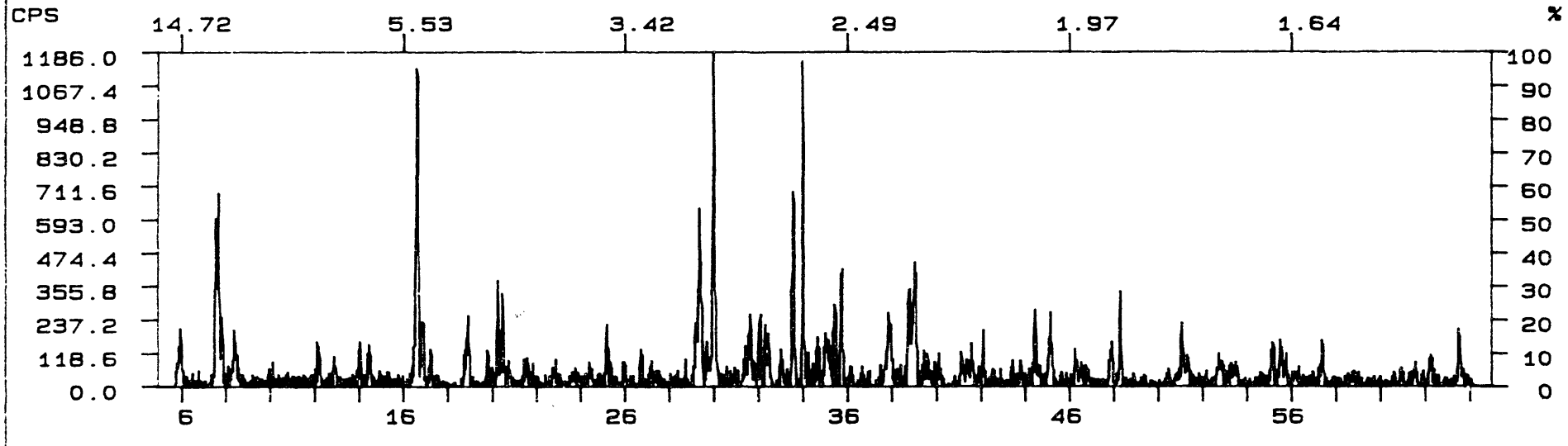

Reference SAMPLE 1341 IMMERSED

FN: 1320SWS.NI ID: 1320 SYNTHETIC WASTE STUDIES SCINTAG/USA
DATE: 3/20/91 TIME: 10:53 PT: 0.600 STEP: 0.020 WL: 1.54059

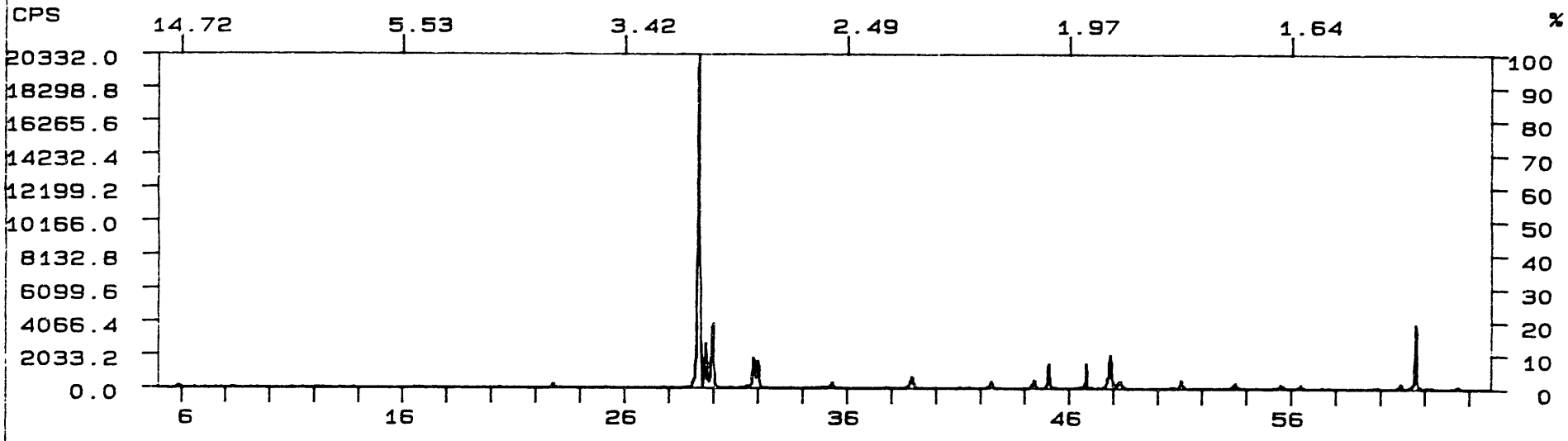

Reference SAMPLE 1320 IMMERSED

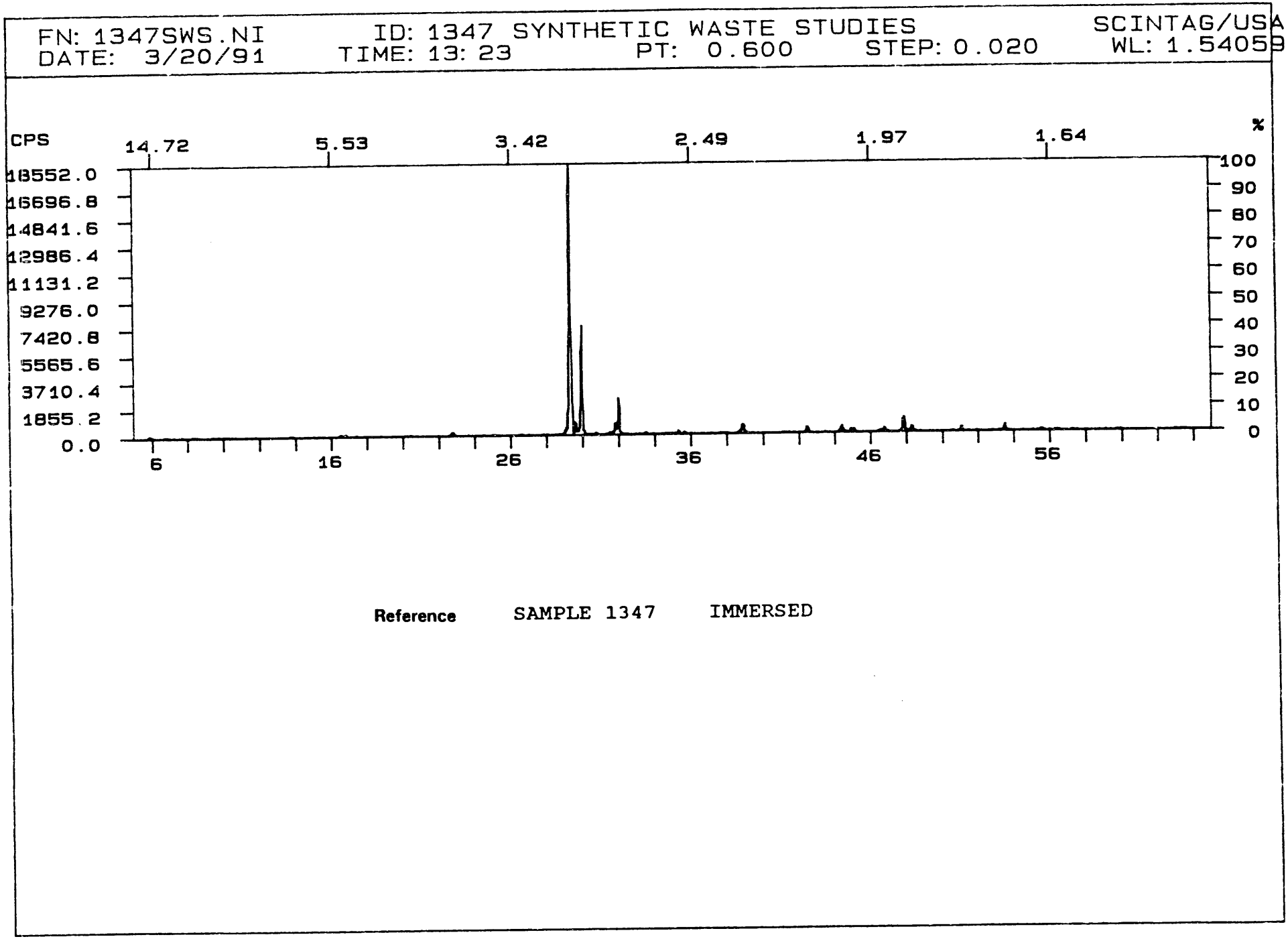
FN: 1347SWS.NI
DATE: 3/20/91
ID: 1347 SYNTHETIC WASTE STUDIES
TIME: 13:23
PT: 0.600
STEP: 0.020
SCINTAG/USA
WL: 1.54059
CPS
18552.0
16696.8
14841.6
12986.4
11131.2
9276.0
7420.8
5565.6
3710.4
1855.2
0.0
14.72
5.53
3.42
2.49
1.97
1.64
%
100
90
80
70
60
50
40
30
20
10
0
6
16
26
36
46
56
Reference
SAMPLE 1347
IMMERSED

DISTRIBUTION

No. of Copies

OFFSITE

12 DOE/Office of Scientific and Technical Information

J. Antizzo
U.S. Department of Energy
EM-351
Trevion II
Washington, DC 20585-0002

C. Terrell
U.S. Department of Energy,
Bldg. 704-S
P.O. Box A
Aiken, SC 29801

J. Tseng
U.S. Department of Energy
EM-35
Trevion II
Washington, DC 20585-0002

H. Walter
U.S. Department of Energy
EM-343
Trevion II
Washington, DC 20585-0002

M. Walter
U.S. Department of Energy
EM-35
Trevion II
Washington, DC 20845-0002

D. Wiffen
U.S. Department of Energy
EM-35
Trevion II
Washington, DC 20585-0002

No. of Copies

G. Woodall
U.S. Department of Energy,
MS-1139
785 DOE Place
Idaho Falls, ID 83402

C. Abrams
1987 Virginia
Idaho Falls, ID 83404

E. C. Ashby
225 North Avenue
Boggs Chemistry Building
Georgia Institute of
Technology
Atlanta, GA 30332

K. Bandyopadhyay
Building 129
Brookhaven National Laboratory
Upton, NY 11973

N. E. Bibler
Westinghouse Savannah River
Bldg. 773A, Room 108
Aiken, SC 29802

J. Bunting
SAIC
20030 Century Blvd.
Suite 201
Germantown, MD 20878

D. Campbell
Oak Ridge National Laboratory
P.O. Box 2008, MS 6268
Oak Ridge, TN 37831-6268

F. Carlson
6965 North, 5th West
Idaho Falls, ID 83401

No. of
Copies

P. d'Entremont
Westinghouse Savannah River
P.O. Box 616, Bldg. 703-H
Aiken, SC 29802

R. Daniels
SAIC
20030 Century Blvd.
Suite 201
Germantown, MD 20878

M. First
295 Upland Avenue
Newton Highlands, MA 02161

C. Forsberg
Room 24-109
77 Massachusetts Avenue
Cambridge, MA 02139

E. J. Hart
2115 Hart Road
Port Angeles, WA 98362

P. Hogroian
SAIC
20030 Century Blvd., Suite 201
Germantown, MD 20874

E. P. Horwitz
Chemistry Division
Argonne National Laboratory
Argonne, IL 60439

A. Hoskins
WINCO, MS-5217
P.O. Box 4000
Idaho Falls, ID 83403-4000

B. Hudson
Lawrence Livermore National
Laboratory, L-221
P.O. Box 808
Livermore, CA 94550

No. of
Copies

C. Jonah
Argonne National Laboratory
9700 South Cass Avenue
Argonne, IL 60439

M. Kazimi
Room 24-102
77 Massachusetts Avenue
Cambridge, MA 02139

P. Kiang
BDM, Trevion I, Suite 300
12850 Middlebrook Road
Germantown, MD 20874

T. Kress
P.O. Box 2009
MS 8088, Building 9108
Oak Ridge, TN 37381

T. Larson
Los Alamos National
Laboratory, M-1
MS C-920, P.O. Box 1663
Los Alamos, NM 87545

D. Meisel
Argonne National Laboratory
9700 South Cass Avenue
Argonne, IL 60439

D. Oakley
Los Alamos National
Laboratory
University of California,
Suite 310
409 12th Street, SW
Washington, DC 20024-2188

D. Ploetz
West Valley Nuclear
Services Co.
P.O. Box 191, MS 305
West Valley, NY 14171-0191

No. of Copies

M. Reich
Building 129
Brookhaven National Laboratory
Upton, NY 11973

G. A. Russell
Department of Chemistry
Iowa State University
Ames, Iowa 50011-3111

J. Saveland
20030 Century Blvd., Suite 201
Germantown, MD 20874

G. Schmauch
Air Products & Chemicals, Inc.
7201 Hamilton Blvd.
Allentown, PA 18195-1501

W. W. Schulz
727 Sweetleaf Drive
Wilmington, DE 19808

B. Schutte
EG&G Idaho, Inc.
P.O. Box 1625
Idaho Falls, ID 83415-3940

D. D. Siemer
WINCO
IRC, MS 2207
Idaho Falls, ID 83403

S. Slezak
Sandia National Laboratories,
Division 6463
P.O. Box 5800
Albuquerque, NM 87185

H. Sullivan
Los Alamos National
Laboratory, N-6, MS-K557
P.O. Box 1664
Los Alamos, NM 87545

No. of Copies

W. J. Thomson
Department of Chemical
Engineering
Washington State University
Pullman, WA 99164

A. S. Veletsos
5211 Paisley
Houston, TX 77096

G. B. Wallis
Thayer School of Engineering
Dartmouth College
Hanover, NH 03755

6 Waste Management External Advisory Committee Members

Dr. Greg R. Choppin
Professor of Chemistry
Florida State University
Department of Chemistry, B-164
Tallahassee, FL 32306

Dr. Chester Grelecki
President, Chief Scientist
Hazards Research Corporation
200 Valley Road
Mt. Arlington, NJ 07856

Dr. Bruce R. Kowalski
Professor of Chemistry,
Co-director of Center for
Process
Analytical Chemistry
University of Washington
Chemistry Department, Bldg. 10
Seattle, WA 98195

Dr. Frank L. Parker
Professor of Environmental and
Water Resources Engineering
Vanderbilt University
P.O. Box 1596, Station B
Nashville, TN 37235

No. of
Copies

Dr. Gary Powers
President
Design Science, Inc.
163 Witherow Road
Sewickley, PA 15143

Dr. Alfred Schneider
MIT Department of Nuclear
Engineering
Room 24-1098
77 Massachusetts Avenue
Cambridge, MA 02139

ONSITE

6 DOE Richland Field Office

R. F. Christensen, A4-02
R. E. Gerton, A4-02
N. G. McDuffie, R2-78
G. Rosenwald, A4-02
B. J. Tucker, B2-42
Reading Room, A1-65

40 Westinghouse Hanford Company

H. Babad, R2-08
D. G. Baide, G6-16
D. B. Bechtold, T6-50
M. L. Bell, T6-16
R. M. Black, R1-19
R. J. Bliss, B3-04
W. F. Brehm, H5-67
T. M. Burke, H0-34
R. J. Cash, R2-32
J. L. Deichman, G6-02
G. L. Dunford, R1-51
K. A. Gasper, R2-08
H. D. Harmon, R2-52
W. H. Hamilton, N3-10

No. of
Copies

D. L. Herting, T6-50
J. D. Hopkins, R2-08
G. D. Johnson, R2-78 (5)
N. W. Kirch, R2-11
W. L. Knecht, H0-34
W. D. Leggett, T6-07 (5)
J. W. Lentsch, R2-78
R. M. Marusich, H5-32
L. D. Muhlestein, N1-28
D. A. Reynolds, R2-11 (5)
W. G. Ruff, R3-50
M. H. Shannon, H5-30
D. D. Stepnewski, H5-32
D. D. Wodrich, L6-27

35 Pacific Northwest Laboratory

R. T. Allemann, K7-15
R. M. Bean, P8-08
S. A. Bryan, P7-25 (5)
J. A. Campbell, P8-08
J. B. Colson, K5-10
T. H. Dunning, K2-18
M. S. Hanson, K1-51
B. M. Johnson, Jr., K1-78
M. R. Kreiter, K7-90
D. K. Lemon, K7-02
G. B. Mellinger, K1-78
L. G. Morgan, P7-35
L. R. Pederson, K2-44 (5)
J.T.A. Roberts, K1-73
R. D. Scheele, P7-25
G. F. Schiefelbein, P8-38
J. C. Spanner, K2-05
D. M. Strachan, K2-38
R. W. Stromatt, P7-22
D. S. Trent, K7-15
H. H. Van Tuyl, P7-22
Publishing Coordination
Technical Report Files (5)

END

DATE
FILMED
5/3/93